The role of spindle pole body component Pcp1 in fission yeast

Chii Shyang Fong

Thesis submitted towards the degree of Doctor of Philosophy

University College London
Department of Biology
London WC1E 6BT

The program of research was carried out
under the supervision of Dr Takashi Toda at

Cancer Research UK London Research Institute
44 Lincoln's Inn Fields, London WC2A 3PX

September 2009

I, Chii Shyang Fong, confirm that the work presented in this thesis is my own. Where information has been derived from other sources, I confirm that this has been indicated in the thesis.

Acknowledgements

First and foremost, I would like to express my gratitude to my supervisor Takashi for his guidance, patience and inspiration. Also, special thanks to Masa for his supervision during the initial stage of the project and the constant encouragement beyond his time in the lab. My deepest appreciation to the members of the Cell Regulation Lab, past and present - Hiro, Mika, Chiho, Nathalie, Isabelle, Amy, Karen, Kuo-Shun, Peggy (Honorary member), Risa, Kathleen, Hannah and Susheela, for whose sharing and insight have inspired me in ways more than one; for the kindness, encouragement and friendships; and above all, for so willingly sharing their wisdom with me. The past four years have been a period of tremendous growth for me, both at professional and personal levels. A Big Thanks to you all!

I would also like to thank the Yeast Group – The Uhlmann Lab, Cooper Lab and Hayles Lab, for their encouragement and discussion. Thank you to Johanna Hoog, Claude Antony, Ken Blight, Hannah Armer and Lucy Collinson for their help with electron microscopy; to Duncan Smith for the mass spectrometry analysis; and to Muneyoshi Kanai and Dai Hirata for technical advice on centrifugal elutriation. I am also very grateful to my thesis committee – Neil McDonald and Jacky Hayles, for their input and support throughout.

Kuo-Shun, Peggy and Risa, thank you for the lift, you have made all the difference, and yes, I mean ALL the difference. Yatpeng, Liling, Ken and Jon, thank you for your friendship and believing in me more than I do myself. To Ofer, for sharing his world. To my parents, and Yann, Pyng, Joseph, Biao and Yen Lin for their unfailing support and love, without which I would not have made it through.

Abstract

The centrosomal pericentrin-related proteins play pivotal roles in various aspects of cell division, however their underlying mechanisms have remained largely elusive. Here we show that fission yeast Pcp1, a pericentrin-like protein, regulates multiple functions of the spindle pole body (SPB) by recruiting two crucial factors: γ-tubulin complex (γ-TuC) and polo kinase (Plo1).

We isolated two temperature-sensitive *pcp1* mutants, *pcp1-15* and *pcp1-18*, that display similar abnormal spindles but with remarkably different molecular defects. *pcp1-15* is defective in recruiting γ-TuC to the mitotic SPB, and crucially restoring γ-TuC localisation to the SPB suppresses the mutant. In contrast, *pcp1-18* fails to recruit Plo1, which results in defects in mitosis-specific reorganisation of the nuclear envelope (NE) and consequently, impairment of SPB insertion into the NE. Strikingly, *pcp1-18* is rescued by overproducing nuclear pore components or advancing mitotic onset. Consistent with these findings, Pcp1 forms a complex with both γ-TuC and Plo1 in the cell. Lastly, we also show that Pcp1 is phosphorylated by Plo1 during mitosis.

Our results therefore verify Pcp1's speculated role in γ-TuC-mediated spindle assembly and unveils its unanticipated function in Plo1-dependent mitotic entry and structural reorganisation of the NE. The central role of Pcp1 in orchestrating multiple SPB functions provides mechanistic insight into how centrosomes regulate multiple cellular pathways, and may be relevant to cancer development due to centrosomal aberrations.

Table of Contents

List of Figures

List of Tables

Abbreviations

Δ	gene deletion
5-FOA	5-fluoroorotic acid
aa	amino acid
ATR	ATM and Rad3-related
APC/C	anaphase-promoting complex/cyclosome
bp	base pair
CBZ/MBC	carbendazim
CDK	cyclin-dependent kinase
cDNA	complementary deoxyribonucleic acid
dGTP	deoxyguanosine triphosphate
DNA	deoxyribonucleic acid
dNTP	deoxynucleoside triphosphate
DTT	dithiothreitol
EMM	Edinburgh minimal medium
eMTOC	equatorial microtubule organising centre
GAP	GTPase activating protein
GDP	guanosine diphosphate
GFP	green fluorescent protein
GST	glutathione *S*-transferase
GTP	guanosine triphosphate
H_2O	water
HA	hemagglutinin epitope
hph^r	hygromycin B resistance
HU	hydroxyurea
IMAC	immobilised metal affinity chromatography
iMTOC	interphase microtubule organising centre
IP	immunoprecipitation
IPTG	isopropyl β-D-1-thiogalactopyranoside
kan^r	kanamycin/geneticin resistance
LB	Luria-Bertani

mCherry	monomeric Cherry
MPF	maturation promoting factor
mRFP	monomeric red fluorescent protein
MTOC	microtubule organising centre
NaOH	sodium hydroxide
nat^r	nourseothricin resistance
NE	nuclear envelope
NEBD	nuclear envelope breakdown
NPC	nuclear pore complex
OD_{600}	optical density at 600 nm
PAA	post-anaphase array
PBD	polo-box-domain
PBS	phosphate buffered saline
PCM	pericentriolar material
PCR	polymerase chain reaction
PEG	polyethylene glycol
Plk	polo-like kinase
PMSF	phenylmethylsulphonyl fluoride
pNPP	*p*-nitrophenyl phosphate
SCF	Skp1/Cul1/F-box
siRNA	small interfering RNA
SOC	spindle orientation checkpoint
SPB	spindle pole body
TBZ	thiabendazole
YE5S	yeast extract with supplements
γ-TuC	γ-tubulin complex
γ-TuRC	γ-tubulin ring complex
γ-TuSC	γ-tubulin small complex

1 Introduction

1.1 Cell division and life

All life forms, regardless of whether they are unicellular or multicellular organisms, were created from cellular divisions from single cells. In unicellular organisms like bacteria, each cell division is a reproduction, as the process creates an entirely new organism. In multicellular organisms like humans, many rounds of cell division are required for the organism to develop into a multi-organs functional entity. Cell division is also required for multicellular organisms to replenish dead cells that are being constantly removed from the system. Therefore, cell division is not only necessary for life perpetuation, it is also essential for the maintenance of life.

1.2 The cell cycle

The cell division cycle, or more commonly known just as the cell cycle, is the repeated process of cellular duplication and division. It involves accurate replication and segregation of the genetic information from a mother cell to the two genetically identical daughter cells. An equally important process that takes place during the cell cycle is the duplication of organelles and macromolecules in the cell, so that the cell mass can be maintained after each cell division. Although there is no one scheme that all cells conform to, the cell cycle has a general order and characteristic that all cells follow.

A typical eukaryotic cell cycle is divided into four sequential phases, namely the G1, S, G2 and M phases. During the G1 (Gap 1) phase, the cell increases in size and synthesises all the enzymes required for DNA replication. This is followed by DNA replication in the S (DNA synthesis) phase, and a further cellular growth in the G2 (Gap 2) phase. Finally, the cell enters the M phase, where mitosis and cytokinesis take place.

Mitosis can be further broken down into five distinct stages: **Prophase** – the period when the duplicated chromosomes condense; **Prometaphase** – marked by the breaking down of the nuclear envelope; **Metaphase** – the stage in which the sister chromatids are attached to the spindle microtubules through the kinetochores and become aligned at the centre of the cell; **Anaphase** – starts when the sister chromatids separate and move to the opposite poles of the cell; and **Telophase** – the final stage of mitosis when the spindle microtubules disassemble and the nuclear envelope re-forms around the segregated chromosomes. Cytokinesis then cleaves the cell in two, yielding two daughter cells each with one of the two nuclei generated from mitosis.

The daughter cells now re-enter G1 phase and may repeat the whole process of cell division again. However, depending on the environmental conditions and signals that control cell division, the daughter cells may now enter a quiescent state, in which the cells are metabolically active but are not proliferating. This is known as the G0 phase. Cells in G0 may re-enter the cell cycle if the signals to grow are present again. Alternatively, the daughter cells may also proceed into differentiation processes. The point where the decision is made to re-enter the cell cycle, G0 or to differentiate is termed START in budding yeast (Hartwell, 1974) and the Restriction Point in animal cells (Pardee, 1974).

1.3 The centrosome

Central to the regulation of the cell cycle is the non-membranous organelle known as the centrosome, which serves as the platform for crosstalk between numerous regulatory and structural proteins essential for cell division. The centrosome was first observed during late 1800s in the middle of a cell as a small phase-dense material surrounded by a larger less phase-dense region. The organelle was the focus of the thin cytoplasmic fibers in interphase cells, and the mitotic spindles in mitotic cells. For its central position in the cell, Theodor Boveri named the organelle the centrosome (Boveri, 1901). It is now known that what Boveri observed – the phase-dense structures, the region

surrounding it and the fibers, were the centrioles, pericentriolar material (PCM) and microtubules, respectively.

Centrosomes are usually positioned in close proximity to the nucleus. Each centrosome is comprised of a pair of centrioles that are surrounded by the PCM. The centriole is about 0.5 μm in length and 0.2 μm in diameter, and is made up of nine microtubule triplets of A, B and C tubules (Bornens, 2002; Paintrand et al., 1992). The centriole pair lies at right angles to one another and is in close proximity at the proximal ends. A series of interconnecting fibres that is distinct from PCM connect the centriole pair at their proximal ends. The mother centriole has distal and subdistal appendages, where the latter anchor cytoplasmic microtubules and might function to position centrioles in a cell (Figure 1.1)(Bornens, 2002).

The PCM is an interconnected matrix of fibres and protein complexes that serves as the site of microtubule nucleation (Gould and Borisy, 1977). It is a dynamic structure that increases in size in preparation for mitosis, in a process known as centrosome maturation (Kalt and Schliwa, 1993; Kimble and Kuriyama, 1992; Vorobjev and Nadezhdina, 1987). The PCM also acts as a scaffold for the recruitment of various proteins that are important for the functions of the centrosome. The assembly and organisation of PCM is dependent on the integrity of centrioles as centriole loss has been shown to result in PCM dispersal (Basto et al., 2006; Bettencourt-Dias et al., 2005; Bobinnec et al., 1998).

1.4 Microtubule organising centres

The classical function of centrosomes is its role in organising microtubules. The term microtubule organising centre (MTOC) was coined by Pickett-Heaps to collectively describe all the heterogeneous organelles that nucleate, release and anchor microtubules (Pickett-Heaps, 1969). Therefore, MTOCs include

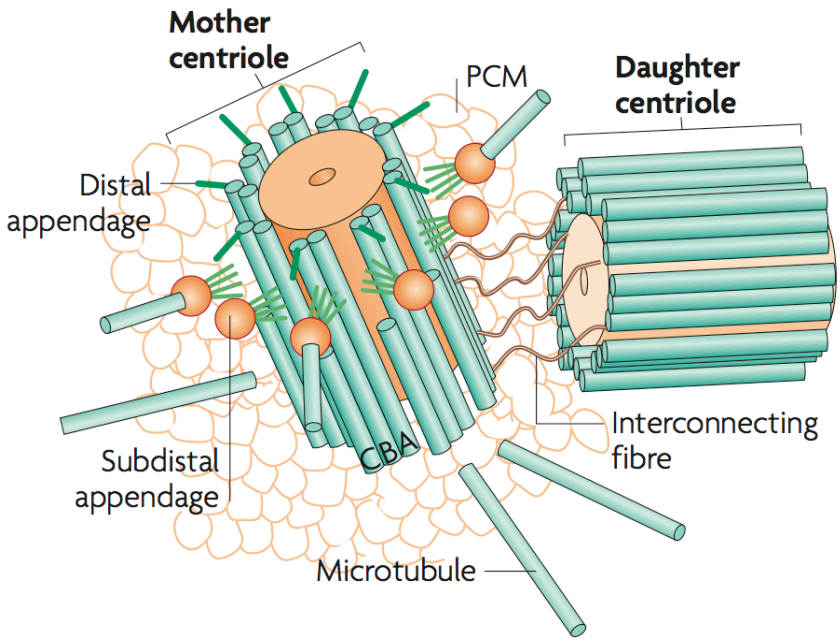

Figure 1.1 Centrosome structure.

A centrosome has a pair of centrioles, each with nine microtubule triplets of A, B and C tubules. The centriole pair is connected by interconnecting fibres. The mother centriole has distal and subdistal appendages, where the latter seems to anchor microtubules. PCM is the platform where microtubules are nucleated. Diagram is obtained from Bettencourt-Dias and Glover (2007).

centrosomal and non-centrosomal sites such as the nuclear envelope and the cytoplasm (Keating and Borisy, 1999).

In metazoan cells, centrosomes are the predominant sites of microtubule nucleation. Microtubules re-grow primarily from the centrosome when they are depolymerised and allowed to re-polymerise again. At the centrosome, microtubules are polarised with their slow-growing minus ends anchored to the centrosome, while the fast-growing plus ends projected away from the centrosome. Centrosomes are important for both cytoplasmic and spindle microtubule nucleation.

In budding yeasts, the spindle pole body (SPB), which is the functional equivalent of the centrosome, is the sole nucleation site for microtubules (further information on SPBs is presented in section 1.9). Budding yeast SPBs are embedded in the nuclear envelope throughout the cell cycle. The cells nucleate their cytoplasmic and spindle microtubules from the cytoplasmic and nucleoplasmic face of the SPB, respectively.

In contrast to budding yeasts, fission yeasts nucleate microtubules from three distinct types of MTOCs within a cell. During interphase, cytoplasmic microtubules not only nucleate from the SPB, but also from the nuclear surface, on existing microtubules, and within the cytoplasm (Drummond and Cross, 2000; Janson et al., 2005; Sawin et al., 2004; Tran et al., 2001). These non-SPB sites are known collectively as the interphase MTOC (iMTOC) (Figure 1.2). During mitosis, both astral and spindle microtubules are nucleated solely from the SPB. At mitotic exit, a distinct microtubule structure termed the post-anaphase array (PAA) is nucleated from the middle of the cell. This nucleation site is known as the equatorial MTOC (eMTOC) (Heitz et al., 2001).

1.5 Microtubules

Undoubtedly one of the most spectacular events that occurs during mitosis is the segregation of the duplicated chromosomes to the two daughter cells. The

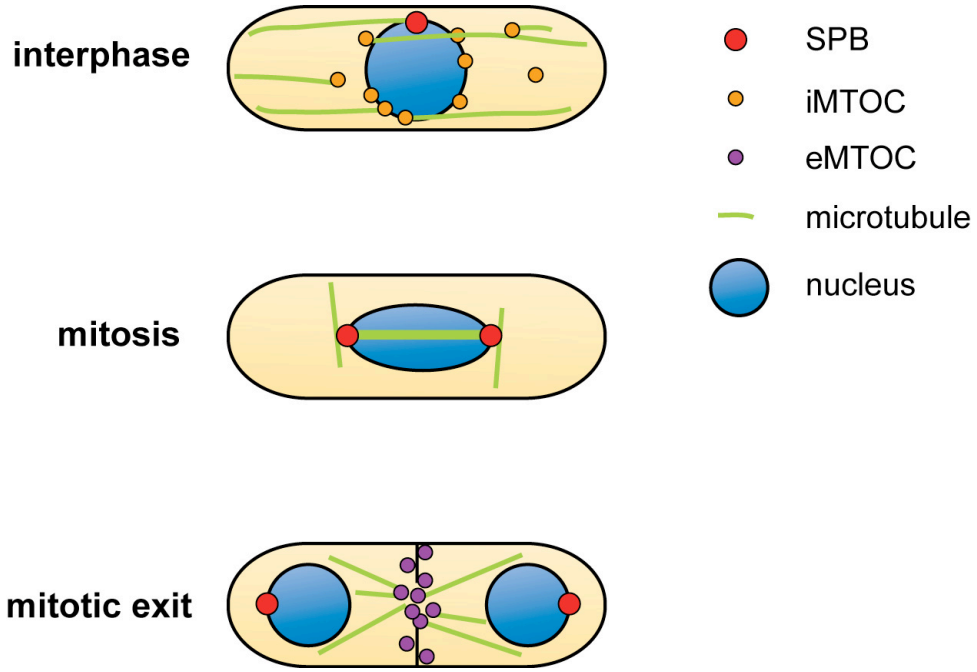

Figure 1.2 The three distinct types of MTOCs in fission yeasts.

(1) iMTOC. During interphase, apart from the SPB, cytoplasmic microtubules are nucleated from iMTOCs. These include the nuclear envelope, the existing microtubules themselves and the cytoplasm. (2) SPB. Microtubules are nucleated from the SPB during interphase and mitosis. During mitosis, the SPB nucleates both spindle and astral microtubules. (3) eMTOC. After disassembly of spindle microtubules, post-anaphase arrays are assembled from the eMTOC at the site of cell division.

dramatic movement of the chromosomes during the segregation process is achieved through dynamic changes to the property of the cytoskeletal component – the microtubules.

Microtubules are made up of αβ-tubulin heterodimers, which assemble uniformly in one direction to form linear protofilaments. The uni-directionality of the assembly confers the protofilaments an intrinsic molecular polarity, with the α-tubulin at the slower-polymerising minus end, and the β-tubulin at the faster-polymerising plus end (Mitchison, 1993; Nogales et al., 1999). When 13 protofilaments come together parallel to one another, a microtubule polymer is formed (Figure 1.3) (although variations have been observed in microtubules assembled *in vitro*).

Microtubules are hollow, yet rigid, cylindrical polymers with a diameter of about 25 nm, and are capable of polymerising longer than 20 μm in cells. The rigidity, length and polarity of microtubules render them valuable for structural support and as tracks for long-range transport of organelles by microtubule-associated motor proteins.

A highly dynamic structure, the microtubule constantly switches between stages of polymerisation and depolymerisation in a phenomenon referred to as dynamic instability (Mitchison and Kirschner, 1984). The dynamic nature of microtubules is important for their *in vivo* functions. It enables the microtubules to explore the cellular interior for structures that they bind to, such as the kinetochores on the chromosomes during early mitosis (Hayden et al., 1990; Kirschner and Mitchison, 1986).

Growth and shrinkage of microtubules is dependent on the GTP status of tubulin heterodimers. Free tubulin heterodimers exist in GTP-bound form. After their incorporation into a microtubule, the GTP-bound β-tubulin is converted to its GDP-bound form (Nogales et al., 1998). The GDP-bound β-tubulin destabilises the microtubule and facilitates depolymerisation. However, when the rate of tubulin heterodimer incorporation exceeds the rate of GTP

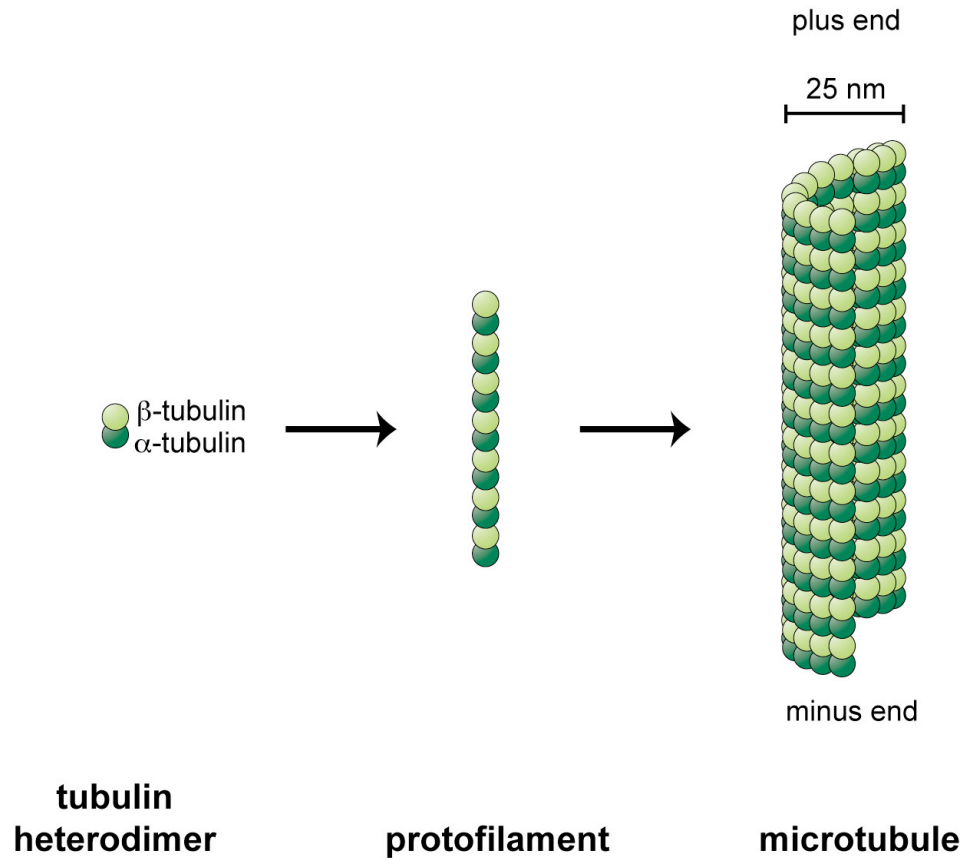

Figure 1.3 Microtubule assembly and structure.

αβ-tubulin heterodimers assemble into protofilaments, and 13 protofilaments associate laterally to form a microtubule that is 25 nm in diameter. The uni-directionality of tubulin heterodimers during polymer assembly confers the microtubules a polarity.

hydrolysis, the plus end of the microtubule is stabilised by a GTP-tubulin cap, which allows microtubule growth to continue (Drechsel and Kirschner, 1994). On the contrary, when tubulin heterodimers incorporation rate falls below the rate of GTP hydrolysis, the GTP-tubulin cap is lost from the plus end and the microtubule rapidly depolymerises. The switch from microtubule growth to rapid shrinkage is termed 'catastrophe'. Following a rapid shrinkage, the microtubule may switch back to growth and polymerisation, in a process known as 'rescue'.

1.6 γ-tubulin complex

Microtubules can self-assemble *in vitro* in the presence of high concentration of purified tubulin. *In vivo*, however, where tubulin concentration is much lower, the assembly of microtubules needs a nucleation factor known as the γ-tubulin complex (γ-TuC). The subunit γ-tubulin was identified about two decades ago, as the third member of the tubulin superfamily that is conserved in all eukaryotes (Horio et al., 1991; Marschall et al., 1996; Oakley and Oakley, 1989; Spang et al., 1996; Stearns et al., 1991; Zheng et al., 1991). Crucially, γ-TuC is not incorporated into the microtubule wall, but instead binds only to the microtubule minus end.

The γ-TuC exists in two distinct complexes of different size (Figure 1.4). The small complex, γ-tubulin small complex (γ-TuSC), is made up of two subunits of γ-tubulin and one subunit each of GCP2 (orthologue of Spc97/Alp4) and GCP3 (orthologue of Spc98/Alp6) (Geissler et al., 1996; Knop et al., 1997; Murphy et al., 1998; Vardy and Toda, 2000) (see Table 1.1 for a list of γ-TuC components in different species). The larger complex, γ-tubulin ring complex (γ-TuRC), is composed of multiple copies of γ-TuSC in association with the additional components GCP4 (orthologue of Gfh1), GCP5 (orthologue of Mod21) and GCP6 (orthologue of Alp16) (Figure 1.4) (Fava et al., 1999; Fujita et al., 2002; Murphy et al., 2001; Venkatram et al., 2004).

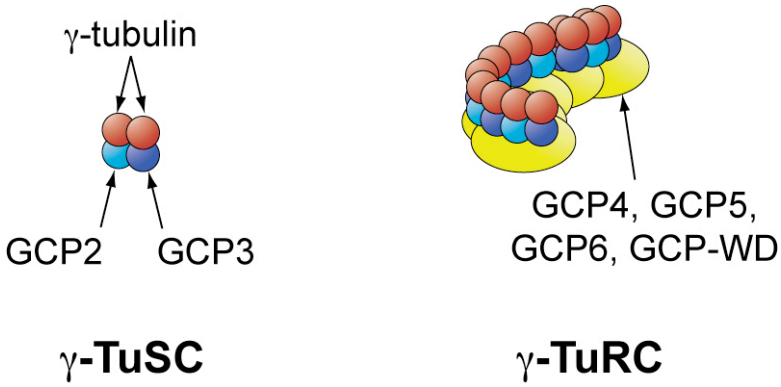

Figure 1.4 Schematic drawing of γ-tubulin small complex (γ-TuSC) and γ-tubulin ring complex (γ-TuRC).

The γ-TuSC contains two subunits of γ-tubulin, and one subunit each of GCP2 and GCP3. The γ-TuRC is made up of 6-7 γ-TuSC and additional subunits of GCP4, GCP5, GCP6 and GCP-WD, at an unknown stoichiometry. The γ-TuRC resembles a ring as seen by electron microscopy (Moritz et al., 2000; Moritz et al., 1995).

Human	Fission Yeast	Budding Yeast	*Drosophila melanogaster*	*Xenopus laevis*
γ-tubulin (two genes)	Gtb1	Tub4	γ-tubulin 23C γ-tubulin 37CD	γ-tubulin
GCP2	Alp4	Spc97	Dgrip84	Xgrip110
GCP3	Alp6	Spc98	Dgrip91	Xgrip109
GCP4	Gfh1	-	Dgrip75	Xgrip76
GCP5	Mod21	-	Dgrip128	Xgrip133
GCP6	Alp16	-	Dgrip163	Xgrip210
GCP-WD	?	-	Dgp71WD	X-Nedd1

Table 1.1 γ-tubulin complex components in various species.

A list of components that made up the γ-tubulin small complex and γ-tubulin ring complex. -: orthologue not present, ?: insufficient information to establish the presence or absence of an orthologue. Adapted from Wiese and Zheng (2006).

γ-TuSC components have been shown to be essential for spindle assembly in many systems. In contrast, the role of non-γ-TuSC components such as GCP4, GCP5 and GCP6 in γ-TuRC is not well understood. It has been shown that depletion or deletion of the non-γ-TuSC components does not seem to affect spindle assembly, but only slightly compromise microtubule nucleation activity or the fidelity of the process (Anders et al., 2006; Fujita et al., 2002; Schnorrer et al., 2002; Venkatram et al., 2004; Verollet et al., 2006; Vogt et al., 2006). However, it is known that purified γ-TuRC is 30x more active than purified γ-TuSC in microtubule nucleation *in vitro* (Oegema et al., 1999). Furthermore, γ-TuRC, instead of γ-TuSC, is often found at microtubule ends when examined using electron tomography (Moritz et al., 2000; Moritz et al., 1995). It is therefore postulated that GCP4, 5 and 6 may be responsible for the assembly of specific microtubules in certain differentiated cells (Oegema et al., 1999).

While some lower eukaryotes such as budding yeast contains only γ-TuSC, in fission yeast and higher eukaryotes such as humans, both γ-TuSC and γ-TuRC are present in the cell. For simplicity, we will refer to both γ-TuSC and γ-TuRC as γ-TuC hereafter, unless a distinction is to be made.

1.7 γ-tubulin-dependent microtubule nucleation

The molecular mechanism by which γ-TuC nucleates microtubules is currently unclear. Two models have been proposed, namely the template model and the protofilament model. In the template model, lateral association of γ-TuC forms a ring structure onto which αβ-tubulin heterodimers are assembled to form a microtubule (Zheng et al., 1995). With the protofilament model, γ-TuC forms a short protofilament where αβ-tubulin heterodimers are added. Lateral association of αβ-tubulin heterodimers then form the hollow tube of a microtubule (Erickson and Stoffler, 1996).

Data from electron microscopy studies seem to favour the template model, as γ-TuRC is often seen at the minus end of a microtubule (Keating and Borisy,

2000; Moritz et al., 2000; Wiese and Zheng, 2000). However, it is known that the minimum requirement for microtubule nucleation is the presence of γ-TuSC, but not γ-TuRC (Verollet et al., 2006). This raises questions regarding the essentiality of a ring structure and the validity of the template model. Although much insight into the mechanism of γ-tubulin-dependent microtubule nucleation has been gained from many recent studies, the controversy is yet to be resolved.

1.8 Centrosome and cell cycle progression

Apart from its classical role in organising microtubules, the centrosome also regulates many cellular processes during interphase and mitosis including cytokinesis (Hinchcliffe et al., 2001; Khodjakov et al., 2000), DNA damage response (Kramer et al., 2004; Loffler et al., 2007; Sibon et al., 2000; Tsvetkov et al., 2003), actin polymerisation (Stevenson et al., 2001), apoptosis (Preuss et al., 2003; Sandal et al., 2003), asymmetric cell division (Cheng et al., 2008) and cell-cycle progression (see below). For the purpose of this thesis, the role of centrosomes in the regulation of cell cycle progression is presented below in more detail.

1.8.1 G2 to M transition

The earliest evidence that the centrosome is involved in G2 to M transition came from the observation that injection of centrosomes into G2-arrested starfish oocytes could induce progression into mitosis (Picard et al., 1987). Later, it was shown that the centrosome could activate maturation promoting factor (MPF, now known as Cdk1-cycB) to trigger premature mitotic entry in *Xenopus* eggs (Perez-Mongiovi et al., 2000). In *C. elegans*, timely mitotic entry was also shown to be regulated by the centrosomes (Hachet et al., 2007; Portier et al., 2007).

Studies suggest that the centrosome is involved in the G2 to M transition in mammalian cells as well. During interphase, inactive cycB1 is diffuse in the cytoplasm. However, during prophase, active Cdk1-cycB1 is first detected at the centrosome, before the phosphorylation of histone H3 in the nucleus (note that Serine 10 phosphorylation of histone H3 is a marker for mitosis) (De Souza et al., 2000; Jackman et al., 2003). Furthermore, various mitotic kinases and cyclins are located at centrosomes prior to mitotic entry (Bailly et al., 1989; Dutertre et al., 2004; Golsteyn et al., 1995; Hirota et al., 2003; Pockwinse et al., 1997).

Another study demonstrates that mitotic entry is regulated by centrosomal localisation of Chk1 (Kramer et al., 2004), a modulator of Cdk1. Chk1 localises to the centrosome in interphase but is absent from the organelle in mitosis. Inhibiting Chk1 function promotes activation of Cdk1 and premature entry into mitosis. Importantly, artificial targeting of Chk1 to the centrosome inhibits Cdk1 activation at the centrosome and induces mitotic failure (Kramer et al., 2004).

Finally, localisation of Polo kinase to the centrosome is also known to regulate mitotic entry. Overexpression of the polo box, which interrupts the binding between Polo kinase and the centrosome, leads to cell cycle arrest with 4N DNA content (Jang et al., 2002b; Lee et al., 1998; Reynolds and Ohkura, 2003).

1.8.2 Metaphase to anaphase transition

The centrosome also plays a role in the metaphase to anaphase transition. The first evidence suggesting this came from the observation that cycB-GFP degradation at metaphase to anaphase transition was initiated at the centrosome in *Drosophila* embryos (Huang and Raff, 1999). Furthermore, a *Drosophila* mutant that loses centrosome attachment to the spindle experiences anaphase arrest (Wakefield et al., 2000). Other studies also showed that disruption of γ-tubulin function in *Aspergillus nidulans* delayed the metaphase to anaphase transition (Prigozhina et al., 2004).

1.8.3 G1 to S transition

Removal of centrosomes from cells by microsurgical cutting or laser ablation has been shown to induce G1 arrest (Hinchcliffe et al., 2001; Khodjakov et al., 2000). Cells also experience G1 arrest when centrosomal proteins such as centriolin (Gromley et al., 2003), AKAP450 (Keryer et al., 2003) and PCM-1 (Balczon et al., 2002) are depleted or delocalised from the centrosome. These studies demonstrate that the centrosome is important for the G1 to S transition, although how disruption of centrosome function leads to G1 arrest is not well understood.

1.9 The spindle pole body

The spindle pole body (SPB) is the centrosome equivalent in yeasts. Despite the differences in size, structure and composition, SPBs and centrosomes share many components and functions. Many proteins localised to the centrosome are conserved, and can also be found at the SPB. In fact, studies on SPB structure and functions have been instrumental in our current understanding of the function of the centrosome.

The structure of the budding yeast SPB is probably the best studied among all SPBs. It is a disc-shaped organelle with a diameter that changes proportionally with ploidy. The diameter of the SPB in a haploid cell is about 100 nm (Byers and Goetsch, 1974), whereas in diploid and tetraploid cells, it is about 200 and 400 nm, respectively (Byers and Goetsch, 1975b). The increase in the SPB size that correlates with DNA content is believed to be crucial for the increase in microtubule nucleation activity necessary for chromosome segregation.

Detailed electron microscopy analyses show that the SPB is made up of three plaques of electron-dense material. The outer plaque is the region that faces the cytoplasm and is in association with cytoplasmic microtubules. The inner plaque faces the nucleoplasm and is in contact with spindle microtubules. The central plaque spans the nuclear envelope and is believed to be the connecting

point between the SPB and the nuclear envelope (Byers and Goetsch, 1974, 1975a; Moens and Rapport, 1971; Robinow and Marak, 1966). The central plaque also has an appendage on one its end that is known as the half-bridge. This is the site where the daughter SPB is assembled (Adams and Kilmartin, 1999; Byers and Goetsch, 1974, 1975a).

Further studies on the SPB structure with cryo-electron microscopy and electron tomography revealed an even more refined organisation of its structure (Bullitt et al., 1997; O'Toole et al., 1999). Two additional layers termed the first and second intermediate layers (IL1 and IL2) were found between the outer and central plaques. The half-bridge was also found to be a multi-layered structure. It is composed of two continuous layers, similar to the double lipid bilayers, and is linked to the central plaque and the intermediate layers at the cytoplasmic side of the half-bridge.

The structure of the fission yeast SPB is comparatively less well studied. Nonetheless, it is clear that fission yeast SPB is also a disc-shaped organelle that is about the same size as the budding yeast SPB. It is also made up of three plaques of electron-dense material, with a half-bridge associated at the central plaque (Ding et al., 1997). A schematic diagram of both the budding and fission yeast SPBs is presented in Figure 1.5.

In fission yeast, a member of the STE11/MEKK family of kinases Cdc7 (Hanks et al., 1988; Petretti and Prigent, 2005; Smith, 1999; Smith et al., 1997) localises to both mitotic SPBs when the GTPase Spg1 becomes the active GTP-bound form at mitotic entry (Sohrmann et al., 1998). In late anaphase, Cdc7 is released from the mother SPB as Spg1 on the mother SPB is converted to the inactive GDP-bound form by the GTPase activating proteins (GAPs), Byr4 and Cdc16 (Furge et al., 1998). This leaves Cdc7 localised asymmetrically on the daughter SPB in late anaphase (Sohrmann et al., 1998).

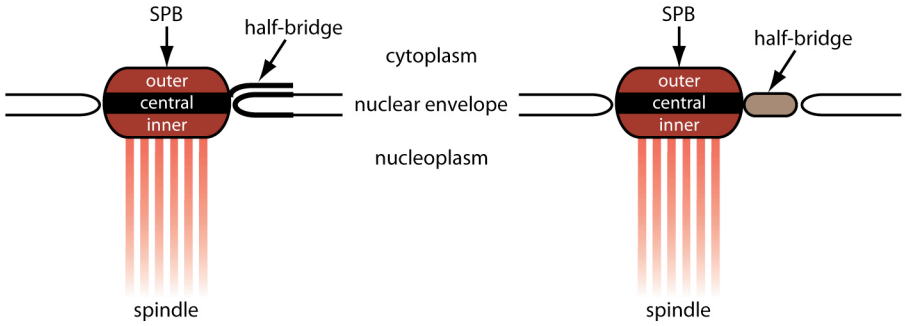

budding yeast SPB **fission yeast SPB**

Figure 1.5 The structure of the budding and fission yeast SPBs.

Both SPBs are disc-shaped, and consist of outer, central and inner plaques. Associated with the central plaque is the half-bridge that is essential for SPB duplication. Cytoplasmic microtubules are omitted from the diagram.

1.10 The pericentrin family

The pericentrin family of proteins are centrosomal or SPB proteins that are essential for microtubule assembly. They are usually large coiled-coil proteins with a calmodulin-binding domain at their C-terminus, and a centrosomin motif 1 at their N-terminus (Samejima et al., 2008; Zhang and Megraw, 2007). This family of proteins are found across species from yeasts to human. While there is only one pericentrin-like protein identified in budding yeast, in fission yeast and higher eukaryotes multiple centrosomal proteins are potential homologues/orthologues of pericentrin based on sequence conservation and functional overlaps (Figure 1.6).

1.10.1 Spc110

Budding yeast Spc110 (or Nuf1) is one of the most characterised pericentrin-like proteins. It was first identified by two independent phage display screens using antibodies generated against the SPB (Kilmartin et al., 1993; Mirzayan et al., 1992). It is 944 aa residues in length, and is comprised of a central coiled-coil domain, a centrosomin motif 1 and a calmodulin-binding motif at its N-terminus and C-terminus, respectively.

Spc110 is thought to exist mainly as homodimers, because immunoprecipitated Spc110 migrates with double its molecular size when subjected to non-reducing SDS-PAGE (Knop and Schiebel, 1997). The related coiled-coil protein tropomyosin also forms a parallel two-stranded homodimer (Whitby et al., 1992).

Spc110 is an essential SPB component. Temperature-sensitive mutants of *spc110* exhibit defects in spindle assembly, which consequently lead to chromosome missegregation (Kilmartin and Goh, 1996; Stirling et al., 1996; Sundberg and Davis, 1997; Sundberg et al., 1996). In these mutants, SPB integrity is disrupted, with the inner plaque of the SPB detaching from the SPB core. In some cases, an intranuclear structure capable of assembling

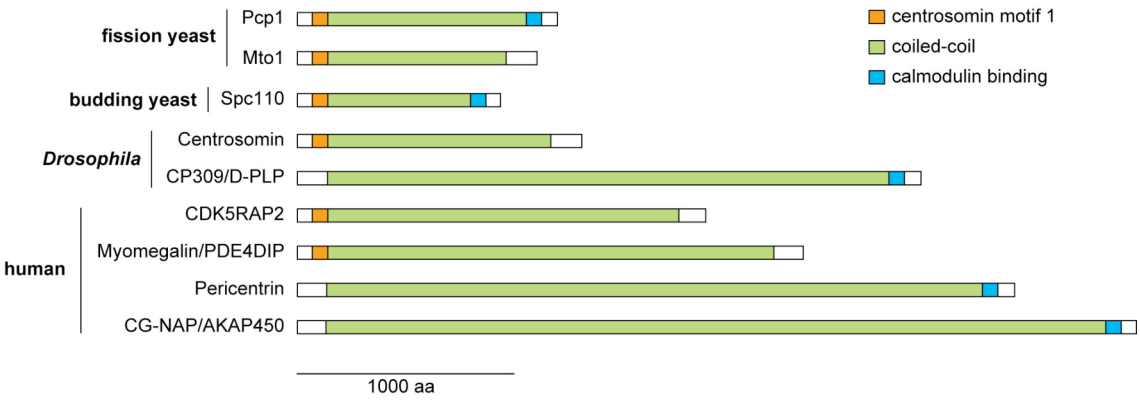

Figure 1.6 The pericentrin family of proteins.

All pericentrin-like proteins (except Myomegalin) have been shown to be involved in microtubule function (Fong et al., 2008; Kawaguchi and Zheng, 2004; Knop and Schiebel, 1997; Samejima et al., 2008; Sawin et al., 2004; Takahashi et al., 2002; Zhang and Megraw, 2007; Zimmerman et al., 2004). These proteins consist mainly of a central coiled-coil domain, and carry either or both centrosomin motif 1 and calmodulin-binding motif at their N-terminus and C-terminus, respectively.

microtubules is formed, which interferes with bipolar spindle formation. Altogether, these observations lead to the conclusion that Spc110 is required for the proper assembly of the SPB.

Deleting the coiled-coil domain of Spc110 did not affect viability, but decreased the distance between the central plaque and the spindle microtubules (Kilmartin et al., 1993). This indicates that the coil-coil domain is a non-essential spacer element of Spc110. The function of the coiled-coil domain in Spc110 is unclear currently, although it has been suggested to provide flexibility to the orientation of spindle microtubules (see section 1.10.3 for the role of coiled-coil domain of Pcp1).

Calmodulin plays a role in the stabilisation of Spc110 (Stirling et al., 1994). However, C-terminal truncation of Spc110, which removes the calmodulin-binding motif, has been shown to suppress the calmodulin mutant *cmd1-1* (Geiser et al., 1993). It is thus postulated that the calmodulin-binding motif is an auto-inhibitory domain that, when present, requires the binding of calmodulin to reverse its inhibitory effect. This is analogous to the auto-inhibitory domain of the myosin light chain kinase (Yano et al., 1993) or Ca^{2+}/calmodulin-dependent protein kinase (Schulman et al., 1992). Deleting the motif, however, relieves the requirement for calmodulin binding for the functioning of Spc110 (Stirling et al., 1994).

The N-terminal 1-204 aa residues of Spc110, which contains the centrosomin motif 1, has been shown to interact with γ-TuC components Spc98 and Spc97 in GST pull-down assays (Knop and Schiebel, 1997). This observation led to the postulation that Spc110 is the docking platform for γ-TuC to nucleate spindle microtubules at the nucleoplasmic side of the SPB. However, this has not been complemented with *in vivo* experiments that show the essentiality of Spc110 in γ-TuC recruitment to the SPB.

Spc110 is phosphorylated in mitosis (Friedman et al., 1996; Stirling and Stark, 1996). It was shown that the phosphorylation is dependent on Mps1, a protein

kinase required for spindle checkpoint signalling and SPB duplication (Weiss and Winey, 1996; Winey et al., 1991). However, the role of this post-translational modification is unclear, as a phosphomutant of *spc110* did not exhibit any growth defects (Friedman et al., 2001). Another study showed that Spc110 was phosphorylated by Cdc28-Clb5 kinase (Huisman et al., 2007). Again, the phosphomutant did not exhibit any growth defects. However, careful examination revealed that spindle dynamics in this mutant was affected, resulting in a metaphase delay. This suggests that phosphorylation of Spc110 is not essential for mitosis, but acts to increase the fidelity of the process.

1.10.2 Pericentrin

Pericentrin was originally identified as a centrosome protein through reactivity against serum from scleroderma patients (Doxsey et al., 1994). It is 3321 aa residues in length and consists mainly of coiled-coil domains. A calmodulin-binding motif was detected at its C-terminus (Flory et al., 2002). Fluorescence resonance energy transfer (FRET) analysis showed that pericentrin and γ-TuC are in close proximity, and that the two components form a lattice that nucleates microtubules (Dictenberg et al., 1998).

Antibody inhibition or immunodepletion analyses showed that pericentrin is required for microtubule nucleation (Doxsey et al., 1994; Takahashi et al., 2002). Consistent with this, knockdown of pericentrin by small interfering RNA (siRNA) caused delocalisation of γ-TuC from the centrosome and disrupted spindle formation, suggesting that pericentrin is the recruitment factor of γ-TuC at the centrosome (Zimmerman et al., 2004). Indeed, physical interaction between pericentrin and the γ-TuC components GCP2 and GCP3 was detected by yeast two-hybrid and immunoprecipitation (Zimmerman et al., 2004). Interestingly, pericentrin knockdown was also shown to induce G2 to M arrest in some cell lines (Zimmerman et al., 2004). The cell cycle arrest was believed to be due to activation of a centrosome maturation checkpoint that was elicited by

the centrosome's inability to recruit γ-TuC, though the molecular pathway remains to be determined.

Recent studies implicated pericentrin in dwarfism and microcephaly, a human disease with reduced brain size and a high rate of mental retardation (Griffith et al., 2008; Rauch et al., 2008). Two models have been proposed for the role of pericentrin in the development of the disease. Firstly, since pericentrin is known to regulate spindle formation, it is possible that loss of pericentrin function leads to loss of cellularity and growth restriction. Secondly, pericentrin was shown to be involved in ATR-dependent checkpoint signalling (Griffith et al., 2008; Tibelius et al., 2009). As defects in DNA damage response is one of the characteristic anomalies associated with the disease (Alderton et al., 2004; O'Driscoll et al., 2003), it is therefore possible that pericentrin mutations somehow disrupt the DNA damage response, which lead to the disease development.

1.10.3 Pcp1

Pcp1 (for pole target of calmodulin in *S. pombe*) was identified as the fission yeast orthologue of budding yeast Spc110 and human pericentrin based on their sequence homology (Flory et al., 2002). It is also a large coiled-coil protein that is 1208 aa residues in length that indeed binds to calmodulin at its C-terminus (Flory et al., 2002). Pcp1 also carries a centrosomin motif 1 at its N-terminus. Deletion of *pcp1*$^{+}$ is lethal to the cell.

Pcp1 localises to the SPB throughout the cell cycle, as confirmed by both endogenous GFP-tagging and immunofluorescence microscopy (Flory et al., 2002). Immuno-electron microscopy (immuno-EM) analysis further defined the localisation of Pcp1 to the inner plaque of the SPB (Flory et al., 2002). Pcp1 remains in the cytoplasm during interphase, but is immersed in the nucleoplasm during mitosis when the SPB is inserted into the nuclear envelope. Therefore, during interphase, Pcp1 is not in direct contact with the γ-TuC in the nucleoplasm. It is only when the SPB is inserted into the nuclear envelope

during mitosis that Pcp1 comes in close proximity to the γ-TuC (Figure 1.7). It is thus speculated that the contact between Pcp1 and γ-TuC at this stage initiates spindle microtubule assembly.

A crucial contribution to the establishment of this view was the observation that overexpression of Pcp1 causes the formation of ectopic SPB-like structures which, apart from Pcp1, also contained γ-tubulin and SPB components such as Sad1 (Flory et al., 2002; Jin et al., 2005). These ectopic structures were capable of nucleating spindle microtubules and, hence, resulted in the formation of multipolar spindles and, ultimately, chromosome missegregation.

Pcp1 has been implicated in the spindle orientation checkpoint (SOC) (Rajagopalan et al., 2004). When the central coiled-coil domain (400-900 aa) of Pcp1 is deleted, cells trigger the SOC despite the presence of oriented spindles and cause a metaphase delay (Rajagopalan et al., 2004). It has since been proposed that Pcp1 senses an increase in forces at the SPBs generated by astral microtubules when the spindles are properly oriented, leading to inactivation of SOC and initiation of anaphase progression.

1.11 The nuclear envelope

The nuclear envelope (NE) is a highly specialised membranous structure in eukaryotes that serves multiple functions. It is a selective barrier that regulates the trafficking of macromolecules between the nucleoplasm and the cytoplasm. It sequesters the chromosomes from the cytoplasm and, in doing so, temporally and spatially separates nuclear processes of chromosome replication and gene transcription from cytoplasmic events such as translation. The NE also anchors the chromatin at the nuclear periphery, thereby regulating gene expression. Indeed, eukaryotes achieve many complex gene regulations that are not found in prokaryotes through the NE.

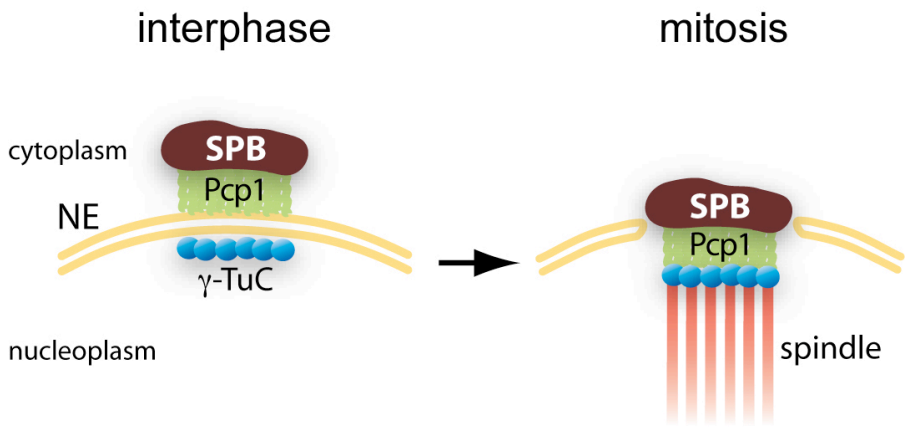

Figure 1.7 Pcp1 organisation during interphase and mitosis.

Pcp1 resides in the cytoplasm during interphase, and is separated from the γ-TuC in the nucleoplasm by the nuclear envelope. During mitosis, the SPB is inserted into the nuclear envelope, bringing Pcp1 into the nucleoplasm. This presumably allows interaction between Pcp1 and γ-TuC, and initiates spindle formation.

The NE is composed of a double lipid bilayer (inner and outer nuclear membranes) and nuclear pore complexes (NPCs), hollow cylinder structures that span across the inner and outer nuclear membranes, through which selective nucleocytoplasmic transport takes place (D'Angelo and Hetzer, 2008). In metazoans, the NE also consists of the nuclear lamina that is made up of type-V intermediate filaments (collectively called lamins), which form a peripheral fibrous meshwork that supports the inner nuclear membrane (Aebi et al., 1986; Gruenbaum et al., 2000).

1.12 Nuclear envelope breakdown

In metazoans, which undergo open mitosis, the NE is completely ruptured and disassembled during prometaphase in a process called nuclear envelope breakdown (NEBD). This allows spindle microtubules emanating from the centrosomes, which lie outside the nucleus before NEBD, to capture the duplicated chromosomes for segregation.

NEBD starts with partial disassembly of NPC in prophase (Hase and Cordes, 2003; Lenart et al., 2003; Terasaki et al., 2001). This is marked by the release of peripheral NPC components, while the scaffolding components remain stably associated (Lenart et al., 2003). The overall structure of the NE remains unchanged at this stage (Kiseleva et al., 2001; Lenart et al., 2003), but increased permeability of the NE is observed (Lenart et al., 2003; Terasaki et al., 2003). The partial disassembly of NPC is regulated by phosphorylation, and indeed some NPC components are phosphorylated in mitosis (Favreau et al., 1996; Kehlenbach and Gerace, 2000; Macaulay et al., 1995; Miller et al., 1999). The mitotic kinase Cdc2 has been shown to be responsible for this process (Favreau et al., 1996; Macaulay et al., 1995).

Following the partial disassembly of NPC, the NE structure is disrupted by phosphorylation of the nuclear lamins by Cdc2 (Collas, 1999; Gerace and Blobel, 1980). This leads to lamin depolymerisation, compromising the NE

integrity and contributing to NE disintegration. Further release of some scaffold proteins of the NPC occurs at this stage (Lenart et al., 2003).

In mammalian cells, live-cell imaging and electron microscopy studies showed that NEBD is also facilitated by microtubules and minus-end-directed motors including the dynein-dynactin complex (Beaudouin et al., 2002; Salina et al., 2002). The binding of these components to the outer surface of the NE generates tension in the NE, causing it to invaginate and eventually tearing the NE open. The NE fragments generated from the disintegration are then pulled away from the chromosomes and moved towards the centrosomes, clearing the chromosome surface for spindle microtubule attachment (Beaudouin et al., 2002; Salina et al., 2002).

1.13 SPB insertion

In lower eukaryotes such as budding and fission yeasts that undergo closed mitosis, the NE remains intact throughout the cell cycle. Whilst partial disassembly of NPC structures is also known to occur in prophase to regulate nuclear entry of cytoplasmic components (Bourett et al., 2002; Ovechkina et al., 2003; Wu et al., 1998), unlike in metazoan cells, this is not immediately followed by a general disruption to the NE structure. Instead, the SPB gains access to chromosomes in the nucleus by breaking down the NE locally to form a fenestra for its insertion into the NE (Araki et al., 2006; Schramm et al., 2000; West et al., 1998; Winey et al., 1991; Winey et al., 1993). In fission yeast, the processes of NE invagination and fenestration that occur during mitotic entry could be analogous to NEBD in metazoans (Figure 1.8) (Ding et al., 1997). Also, it was recently shown that the NE becomes highly permeable upon mitotic entry (Tallada et al., 2009). Therefore, understanding SPB insertion in yeasts could shed light on the complex process of NEBD in higher eukaryotes.

The SPB insertion in fission yeasts requires the activity of an essential NPC component, Cut11 (West et al., 1998). Cut11 is an evolutionarily conserved transmembrane protein with seven putative membrane-spanning domains at its

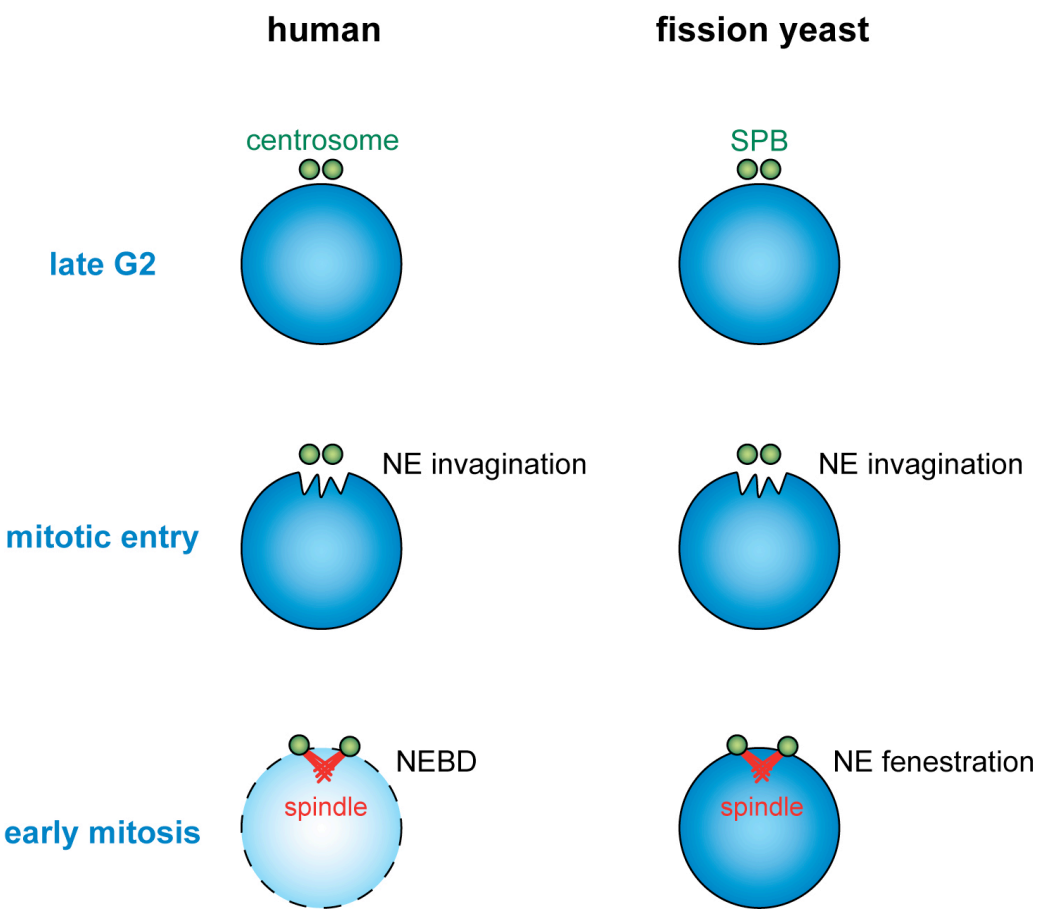

Figure 1.8 Comparison of NEBD in humans and SPB insertion in fission yeasts.

In both species, NE invagination is observed directly beneath the centrosomes or the SPBs at mitotic entry. In humans, this is followed by a complete breaking down of the NE in a process termed NEBD. On the contrary, in fission yeasts, the SPBs gain access to the nuclear content by breaking down the NE locally (NE fenestration) beneath the SPBs. Although the two events seem radically different, analogous processes are observed, which suggest conservation of the regulatory mechanisms.

N-terminus (Rost et al., 1995). It is the orthologue of Ndc1 in humans and budding yeasts (Stavru et al., 2006; Winey et al., 1993).

Cut11 localises to the NPC throughout the cell cycle and to the SPB during mitosis when the SPB is inserted into the NE (West et al., 1998). Electron microscopy shows that in the *cut11* mutants, the mother SPB is loosely attached to the NE and the daughter SPB completely fails to be inserted into the NE, resulting in the formation of monopolar spindles and chromosome missegregation (Tallada et al., 2009; West et al., 1998).

Budding yeast Ndc1 is also an essential NPC component (Thomas and Botstein, 1986; Winey et al., 1993). Combined proteomic and biophysical data revealed that Ndc1, together with Pom152 and Pom34, form the core membrane ring of the NPC (Alber et al., 2007). Apart from the NPC localisation, Ndc1 also localises to the SPB throughout the cell cycle (Chial et al., 1998; Winey et al., 1993). This is because, unlike the fission yeast SPB, the SPB in budding yeasts is inserted into the NE throughout the cell cycle, which account for the difference in the localisation pattern of these NPC components (Ding et al., 1997). Similar to the *cut11* mutants, *ndc1* mutants are able to duplicate their SPBs, but fail to insert the daughter SPBs into the NE (Lau et al., 2004; Winey et al., 1993).

1.14 Polo-like kinases

The Polo kinase was first identified through analyses of mutants with failed mitosis in *Drosophila melanogaster* (Llamazares et al., 1991; Sunkel and Glover, 1988). Orthologues in other organisms were subsequently identified, where in some of them multiple Polo-like kinases (Plks) were detected. In fission and budding yeasts, a single polo kinase was found in each of them, which are Plo1 (Ohkura et al., 1995) and Cdc5 (Kitada et al., 1993), respectively. On the contrary, humans carry four Plks that differ in structure and regulate distinct functions in the cell (Fode et al., 1994; Golsteyn et al., 1994;

Ma et al., 2003; Wang et al., 2002). Plk1 is most closely related to Polo, Plo1 and Cdc5, in terms of functional overlaps.

Plks play pivotal roles in many steps of cell division, including mitotic entry, spindle formation, chromosome segregation and cytokinesis (Archambault and Glover, 2009; Nigg, 2007; Takaki et al., 2008). In humans, abnormal expression of Plk1, both up and downregulation, has been implicated in cancer formation (Knecht et al., 1999; Simizu and Osada, 2000), indicating that cell division is exquisitely sensitive to Plk levels and activity.

1.14.1 Polo-like kinase structure and regulation

The Plk is a serine/threonine kinase with its kinase domain located at the N-terminus, and a regulatory domain known as the polo-box domain (PBD) at the C-terminus (Figure 1.9a)(Lowery et al., 2005).

Plk activity is regulated both temporally and spatially. Temporal regulation of Plks is achieved through transcriptional regulation (Alvarez et al., 2001; Buck et al., 2004; Laoukili et al., 2005), proteolysis (Ferris et al., 1998; Shirayama et al., 1998) and phoshphorylation (Jang et al., 2002b; Petersen and Hagan, 2005; Qian et al., 1999); whereas spatial regulation is achieved through protein binding that localises Plks to specific sites in a cell (see below). Although these regulatory mechanisms are highly conserved, there are some variations between species. For instance, while human Plk1 is degraded in late mitosis and G1 via the Skp1/Cullin1/Cdc53-F-box (SCF) ubiquitin ligase (Ferris et al., 1998), and budding yeast Cdc5 is degraded via the anaphase-promoting complex/cyclosome (APC/C) (Shirayama et al., 1998), fission yeast Plo1 does not exhibit fluctuation in protein levels throughout the cell cycle (Mulvihill et al., 1999).

Binding of Plks to a specific target protein requires the PBD, which is a phosphopeptide-binding motif (Cheng et al., 2003; Elia et al., 2003a; Elia et al., 2003b). Therefore, for Plks to interact with their target proteins, the target

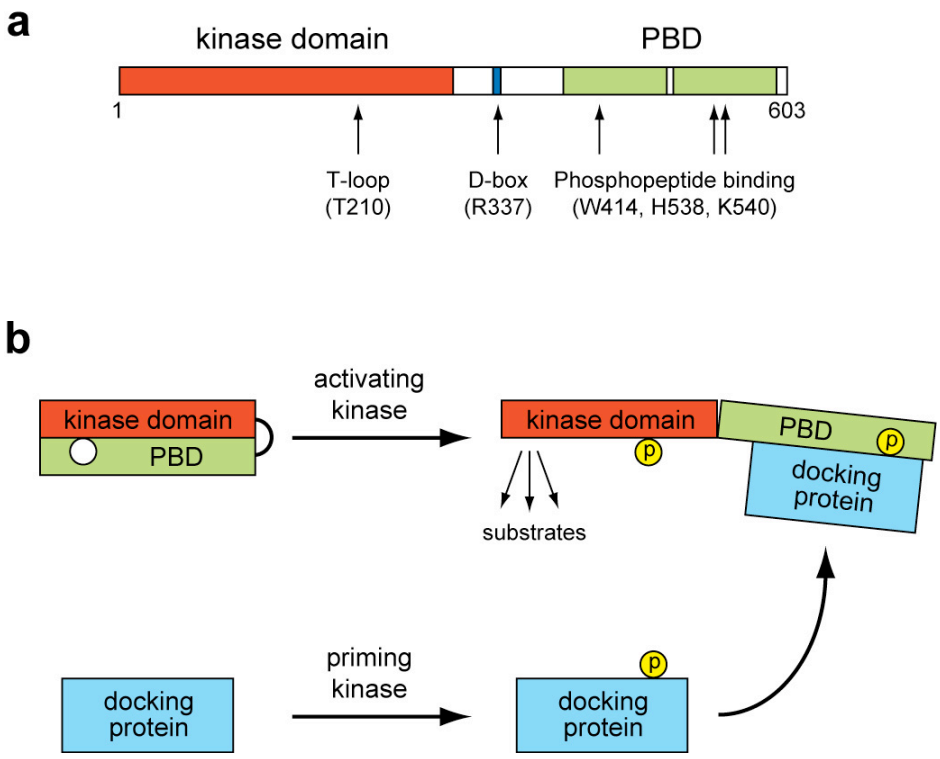

Figure 1.9 Plks structure and regulation.

(a) Key structural features of Plks. The kinase domain of Plks is located at the N-terminus, and the polo-box domain (PBD) is located at the C-terminus. T-loop is the kinase-activating phosphorylation site. Three phosphopeptide-binding residues are found in the PBD. Also indicated is a D-box that regulates degradation through the anaphase-promoting complex/cyclosome (APC/C). Note that the existence of a D-box in fission yeast Plo1 has never been shown. Amino acid numbering is based on human Plk1. (b) Activation of Plks requires two steps. First, binding of a phosphorylated docking protein (by priming kinases) to the PBD releases the T-loop in the kinase domain. Then, phosphorylation of the T-loop by upstream activating kinases activates the kinase activity. Figure is adapted from Barr et al. (2004).

proteins need to be phosphorylated at the PBD recognition motif S-[SpTp]-P by a priming kinase (Elia et al., 2003a), although there are exceptions to this (Bassermann et al., 2008; Lee et al., 1998; Seki et al., 2008). There are data pointing to Cdk1-cyclin-B and proline-directed kinases acting as the priming kinase (Elia et al., 2003a; Elia et al., 2003b). The polo kinase Plk1 might also prime its target proteins for binding (Neef et al., 2003), perhaps in a positive-feedback loop that would enhance recruitment of Plks to the specific sites.

The PBD-containing C-terminus of Plks has been shown to negatively regulate Plks activity (Jang et al., 2002a). It is believed that without binding of the PBD to the target protein, the PBD folds back onto the kinase domain and thereby inhibits the kinase activity. Only when the PBD interacts with phophopeptides, which releases the kinase domain for phosphorylation (at the T-loop) by upstream activating kinases, Plks can be converted to the active forms (Figure 1.9b)(Jang et al., 2002b; Kelm et al., 2002; Macurek et al., 2008; Qian et al., 1998; Seki et al., 2008). In cases where the phosphorylated target proteins are localised to specific sites, this confers a mechanism for temporal and spatial control of the Plks activity.

1.14.2 Polo-like kinase and spindle assembly

One of the important roles of Plks at the centrosomes and SPBs is to increase their microtubule nucleation activity during mitosis, in a process known as centrosome maturation in metazoans. In human cells, Plk1 has been shown to be required for the recruitment of γ-tubulin to the centrosomes (Lane and Nigg, 1996). In Plk1-depleted cells, the centrosomes are reduced in size and recruitment of γ-tubulin is impaired, leading to the formation of monopolar spindles (Lane and Nigg, 1996). Plk1 is also known to phosphorylate Nlp (ninenin-like protein) to inhibit the dynein-dynactin-dependent localisation of Nlp to the centrosomes, which presumably allows the recruitment of other centrosomal proteins to serve as a scaffold for γ-tubulin recruitment during mitosis (Casenghi et al., 2005; Casenghi et al., 2003).

Other substrates of Plks that are implicated in spindle assembly include the microtubule-severing protein katanin (McNally and Vale, 1993), the microtubule-destabilising protein stathmin/Op18 (Budde et al., 2001), the microtubule-stabilising protein TCTP (Yarm, 2002), the microtubule-associated protein Asp (do Carmo Avides and Glover, 1999; do Carmo Avides et al., 2001; Donaldson et al., 2001), the centrosome integrity protein Kizuna (Oshimori et al., 2006) and the Aurora A kinase (De Luca et al., 2006). The involvement of Plks at multiple steps of spindle assembly highlights the importance of Plks function during this process.

1.14.3 Polo-like kinase and G2 to M transition

The Cdk1-cyclin B complex is the master regulator of mitotic entry. In its inactive form, Cdk1 is phosphorylated at residues threonine 14 and tyrosine 15 in the ATP-binding site, which is achieved through the activity of Wee1 and Myt1 kinases. At the G2 to M transition, these inhibitory phosphates are removed by the dual-specificity phosphatase Cdc25, allowing the Cdk1-cyclin B complex to activate mitotic entry by promoting chromosome condensation and nuclear envelope breakdown. Both Wee1 and Cdc25 are in turn phosphorylated by Cdk1, which inactivates Wee1 and activates Cdc25, thus further activating Cdk1 activity in a positive-feedback loop.

Plks were linked to mitotic entry control when *Xenopus laevis* Plx1 was isolated as an activator of Cdc25 phosphatase (Kumagai and Dunphy, 1996). Recent data also indicate that phosphorylated Cdc25 is a target protein of Plk1 (Elia et al., 2003a). Furthermore, Myt1, Wee1 and Cyclin B are also phosphorylated and regulated by Plks (Inoue and Sagata, 2005; Nakajima et al., 2003; Okano-Uchida et al., 2003; Toyoshima-Morimoto et al., 2001; Watanabe et al., 2004). These observations suggest that Plks are the ‘trigger’ kinases for Cdk1 activation. However, data indicating that Plks are activated after Cdk1 activation also exist (Abrieu et al., 1998; Tanaka et al., 2001), in which case Plks are proposed to be involved only in feedback loops that further activate Cdk1. It is believed that the differences are dependent on species, cell type or

developmental context. A summary of the role of Plk1 in the control of mitotic entry is presented in Figure 1.10.

1.15 Cut12

Cut12 is an essential SPB component that localises to the fission yeast SPB throughout the cell cycle (Bridge et al., 1998). Immuno-electron microscopy analysis shows that Cut12 resides at the inner plaque of the SPB (Bridge et al., 1998). It is 548 aa residues in length and carries two predicted coiled-coil domains. No obvious orthologues have been identified in other organisms.

The temperature-sensitive *cut12* mutant, *cut12.1*, was isolated in a screen for mutants that undergo asymmetrical chromosome segregation (Bridge et al., 1998). The mutant fails to nucleate spindle microtubules from one of the SPBs, resulting in the formation of monopolar spindles (Bridge et al., 1998). Further analysis shows that the monopolar spindle phenotype of the mutant is due to a failure in activation and integration of the daughter SPB into the nuclear envelope (Tallada et al., 2009).

Interestingly, the gain-of-function mutation of *cut12*, *cut12.s11*, was shown to promote localisation of Plo1 to the SPB, resulting in increased levels of Plo1 activity during interphase and mitosis (MacIver et al., 2003; Petersen and Hagan, 2005). Consistent with the role of Plo1 in driving mitotic entry, the *cut12.s11* allele (first named *stf1.1*), was indeed isolated originally as a suppressor of the mitotic commitment mutant of *cdc25.22* (Hudson et al., 1990).

However, it is important to note that Cut12 is not required for Plo1 recruitment to the SPB during late G2 or mitosis per se, as Plo1 recruitment to the SPB is not affected in the *cut12Δ* mutant (Mulvihill et al., 1999). It is therefore postulated that the effect of Cut12.s11 on Plo1 recruitment is not mediated through a direct recruitment of Plo1. Rather, Cut12.s11 could be recruiting an activator of Plo1, for instance a polo kinase kinase, which enhances Plo1 recruitment to the SPB.

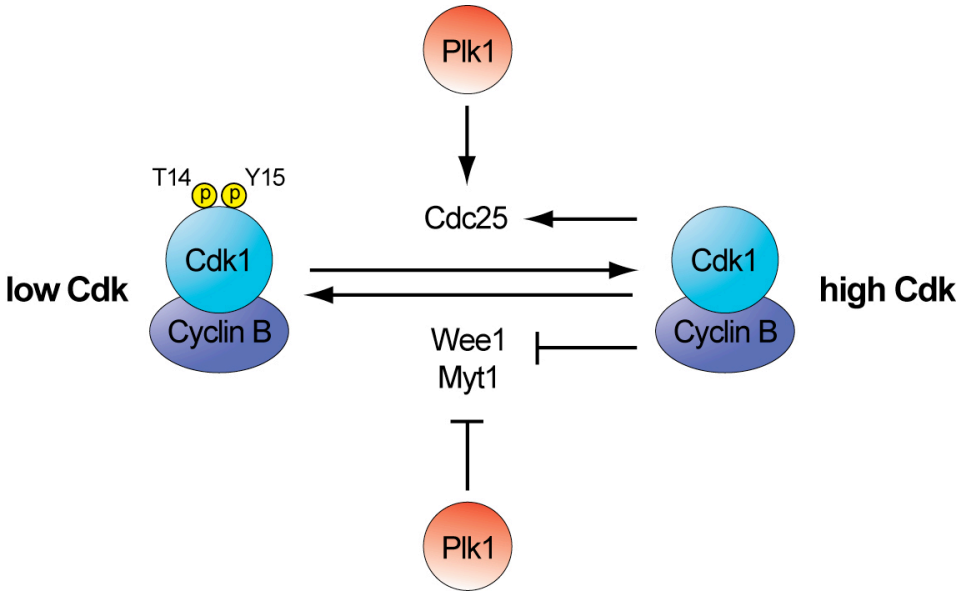

Figure 1.10 Regulation of G2 to M transition by Plk1.

Cdk1-cyclin B complex is kept in its inactive form by inhibitory phosphorylation at threonine 14 and tyrosine 15, by Wee1 kinase and membrane-associated Cdk1-inhibitory kinase Myt1. When the activity of Cdc25 phosphatase rises at G2 to M transition, the inhibitory phosphates on Cdk1 are removed, thus activating Cdk1. Once activated, Cdk1 phosphorylates Cdc25, Wee1 and Myt1 in a positive-feedback loop. Plk1 also phosphorylates Cdc25, Wee1 and Myt1 to regulate their activity (boosting Cdc25 function while repressing Wee1 and Myt1 function), which allows further activation of Cdk1.

The normal localisation of Plo1 in the *cut12Δ* mutant could also be explained by the fact that Plo1 interacts with multiple SPB components. Nonetheless, it is clearly established that the role of Cut12 during cell division is to promote Plo1 activity at the SPB to drive mitotic entry (MacIver et al., 2003).

1.16 Fission yeast as a model system

The fission yeast *Schizosaccharomyces pombe* is a unicellular eukaryote, a member of the ascomycete fungi. It is ordinarily a haploid organism, carrying three large chromosomes of 5.7, 4.7 and 3.5 megabases in size. Genome sequencing revealed that fission yeasts have 4824 genes (Wood et al., 2002). Fission yeast cells have a rigid cell wall and are rod-shaped. They are 3.5 μm in diameter (in haploids) and grow exclusively at the cell tips.

Similar to higher eukaryotes, the fission yeast cell cycle is divided into four sequential phases: the G1, S, G2 and M phases. In an exponentially growing culture, fission yeasts spend three-quarters of their time in G2 phase. G1 phase is almost not noticeable in exponentially growing fission yeast cells. After the completion of chromosome segregation in mitosis, cytokinesis and septation divide the cells into two. As S phase takes place concurrently with septation, the two daughter cells generated from medial fission are in early G2 phase, and already contain two copies of the genetic material (Figure 1.11).

In wild-type fission yeast, cells attain different sizes at different stages of the cell cycle. Starting from early G2 cells, the smallest cells (7 μm) in the life cycle of fission yeasts, they continue to increase in size until entry into mitosis where they acquired their maximum length (14 μm). At the end of mitosis, cytokinesis and septation divide the long cells (14 μm) in half, generating two small daughter cells of equal size (Figure 1.11).

The fission yeast serves as an excellent eukaryotic model for several reasons. Foremost is the ease of genetic manipulation, as it readily undergoes

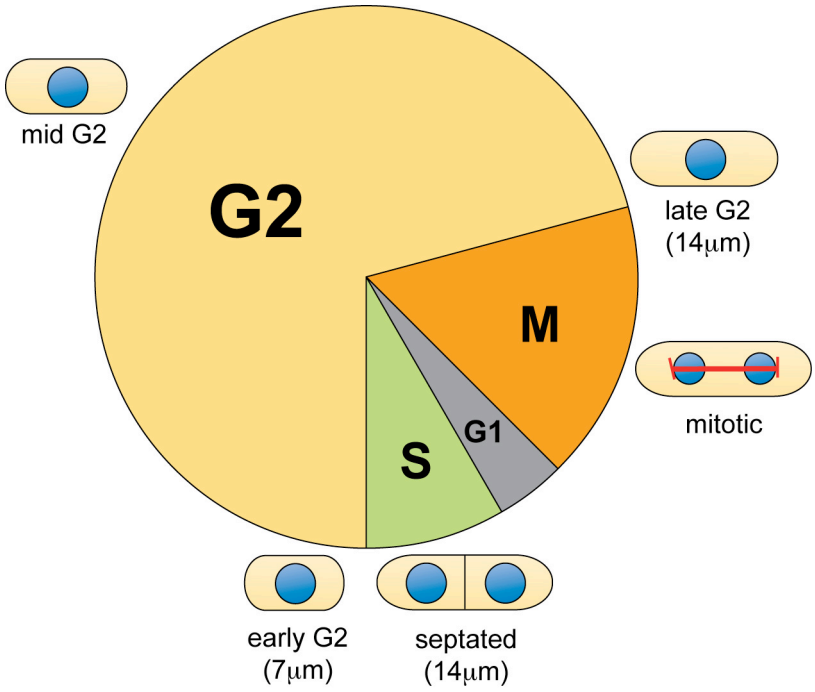

Figure 1.11 The fission yeast cell cycle.

In a nutrient-rich environment, fission yeast cells spend most of their time in G2 phase. Septation takes place concomitantly with S phase, which eventually gives rise to two daughter cells of equal size in early G2 phase. Note that early G2 cells are the smallest cells in the cell cycle of fission yeasts.

homologous recombination, which facilitates endogenous gene tagging, deletion and replacement. In addition, many functions carried out by fission yeasts bear similarity to higher eukaryotes such as humans at the molecular level, particularly with regards to the mechanisms controlling cell division. Indeed, multiple fission yeast genes were found to have human orthologues. The best-known example is the functional cloning of human Cdc2 gene by complementation of a fission yeast *cdc2* mutant (Lee and Nurse, 1987). Lastly, the well-studied genetics and physiology of fission yeast, together with its fast growth rate that greatly expedites experimentation, have made fission yeast an ideal model organism to work with.

1.17 Aim of study

The centrosome plays pivotal roles in many cellular processes (as presented in section 1.8), it is therefore not surprising that it is implicated in multiple human genetic diseases including cancer (Badano et al., 2005). Despite the importance of the centrosome, the molecular mechanisms by which it executes its diverse roles have remained unclear.

Pcp1 is an essential SPB component that was postulated to be the γ-TuC recruitment factor, based on its sequence homology to the budding yeast Spc110 and human pericentrin. Indeed, overexpression of Pcp1 was shown to affect spindle assembly (Flory et al., 2002). Furthermore, Pcp1 is a large coiled-coil protein that is positioned at the SPB periphery, suggesting that it could be a recruitment platform for multiple regulatory or structural proteins essential for SPB function. The aim of this study was to characterise the function of Pcp1. I would like to verify its postulated role in γ-TuC recruitment, by investigating localisation of γ-TuC at the SPB in *pcp1* mutants, and by examining whether restoring γ-TuC localisation to the SPB could rescue the growth defects of γ-TuC delocalisation mutants. I also aim to uncover any additional roles Pcp1 may play during cell division, by performing a multicopy suppressor screen on *pcp1* mutants that do not show γ-TuC delocalisation from the SPB. The isolation

of nuclear pore complex components as suppressors of *pcp1* mutants led to the examination whether *pcp1* mutants were defective in nuclear envelope reorganisation and SPB insertion using electron microscopy. Furthermore, the identification of Cut12 – the regulator of Plo1, as one of the suppressors of *pcp1* mutants prompted for the investigation whether Pcp1 is required for Plo1 recruitment to the SPB to promote mitotic entry using fluorescence microscopy and genetic suppressor analysis. Our study might provide insight into the molecular mechanisms by which the centrosome orchestrates multiple cellular pathways.

2 Isolation and initial characterisation of *pcp1* mutants

2.1 Overview

I describe in this chapter the screen undertaken to isolate temperature sensitive mutant alleles of *pcp1*. Mutation sites in the mutant alleles were identified by DNA sequencing. Initial characterisation of the mutants was performed, including examination of proteins levels and localisation of the mutant Pcp1 proteins and growth sensitivity to the microtubule destabilising drug thiabendazole (TBZ). The timing when the *pcp1* mutants experience lethality at the restrictive temperature of 36^{o}C was also established. Finally, the spindle and mitotic defects in the mutants were closely examined. These analyses show that Pcp1 is required for spindle microtubule nucleation and chromosome segregation.

2.2 Isolation of the temperature-sensitive mutants of *pcp1*$^{+}$

Pcp1 is an essential protein (Flory et al., 2002). In order to delineate Pcp1's roles precisely, I screened for conditional mutants of *pcp1* that grew at the permissive temperature of 27^{o}C, but not at the restrictive temperature of 36^{o}C. One of the advantages of using temperature-sensitive mutants to analyse the function of essential proteins is that it made isolation of separation-of-function alleles possible. This is because mutation(s) introduced into the gene could have no effect on the protein stability or localisation, and inactivate only one, but not all, of the functions of the protein. This is not achievable with gene deletion or shut-off mutants, which are expected to impair all the functions of the essential proteins of interest.

Using a polymerase chain reaction (PCR) based one-step gene tagging procedure, I endogenously tagged *pcp1*$^{+}$ at its C-terminus with a 3HA epitope

(*HA*) and a hygromycin drug resistance cassette (*hph*^{r}). The *HA-hph*^{r} tagging module was firstly PCR amplified from a plasmid with a pair of 100-mer primers. These primers carry 80 bp 5'-overhangs that match the 3'-end of *pcp1*$^+$ (not including the stop codon) and 3' untranslated region of *pcp1*$^+$. The amplified DNA fragment was transformed into a wild-type strain for homologous recombination to occur so that the tagging module can be incorporated into the genomic DNA at the 3'-terminus of *pcp1*$^+$. Transformants were then selected on hygromycin plates. Finally, PCR was performed to confirm proper integration of the tagging module.

After the successful tagging of *pcp1*$^+$ to create a strain with *pcp1*$^+$*-HA-hph*^{r}, genomic DNA was purified from the cells and *pcp1*$^+$*-HA-hph*^{r} was PCR amplified with a primer set that annealed to 406 bp upstream and 168 bp downstream of *pcp1*$^+$. This created a bigger region of homology for recombination and hence increased the chance of obtaining transformants. The purpose of this PCR amplification step was to generate sufficient amount of DNA template for the subsequent error-prone PCR that was usually very low in amplification efficiency.

Using the *pcp1-HA-hph*^{r} fragments as a template, I randomly mutagenised *pcp1*$^+$ through the combined use of the Vent DNA polymerase (New England Biolabs) and 2.5 mM deoxyguanosine triphosphate (dGTP), while the concentration of the other three dNTPs was kept at 0.25 mM. I also tried three other DNA polymerases – in-house produced Taq, LA Taq (Takara Bio) and Z Taq (Takara Bio), but only the Vent DNA polymerase yielded a specific band of the right molecular weight. The 10X increase in the usual amount of dGTP used caused a bias in nucleotide incorporation during the PCR amplification, and consequently introduced random mutation(s) in *pcp1*$^+$. The mutagenised *pcp1* fragments were transformed into a wild-type strain, and the transformants were selected on yeast extract with supplements (YE5S) plates containing hygromycin at 27^{o}C. Colonies were then replicated onto plates containing phloxin B, a red dye that stains dead cells. Replicated plates were then incubated at 27^{o}C and 36^{o}C for 1 to 2 days. Temperature-sensitive (ts) mutants

were identified on the basis of the ability to form a colony at 27°C, but not at 36°C. Dead cells were confirmed by the phloxin B staining. A summary of the ts mutant isolation strategy is depicted in Figure 2.1.

From a screen of about 5,000 transformants, 11 ts mutants of *pcp1*$^{+}$ were isolated. These mutants grew normally at 27°C, but showed severely compromised growth at 36°C (Figure 2.2). The mutants were backcrossed with *pcp1*$^{+}$*-mRFP-kan*^{r} to ensure proper integration and to remove potential second-site mutations. None of the segregants derived from this cross showed co-resistance to hygromycin and kanamycin. Furthermore, all of the mutants showed co-segregation of temperature sensitivity and hygromycin resistance. These results indicate that the mutation(s) responsible for the ts phenotype reside within the *pcp1* locus. A serial dilution assay was performed to assess the subtle differences between the mutants in terms of their temperature sensitivity (Figure 2.2).

Cold-sensitive mutants are another class of conditional mutants that are useful for protein function analysis. These mutants grow at the permissive temperature of 27°C, but not the restrictive temperature of 20°C. This creates flexibility for using the mutant in combination with other cold-sensitive mutants, such as the *nda3-311* β-tubulin mutant that is routinely used for arresting cells in mid mitosis (Hiraoka et al., 1984; Toda et al., 1983). Furthermore, it is known that some proteins are preferably inactivated at low, but not high temperature, thus making isolation of temperature-sensitive mutants not ideal. For those reasons, I also attempted to isolate cold-sensitive mutants of *pcp1*. However, as I did not manage to identify such mutants in my first screen, the isolation of cold-sensitive mutants was not pursued further.

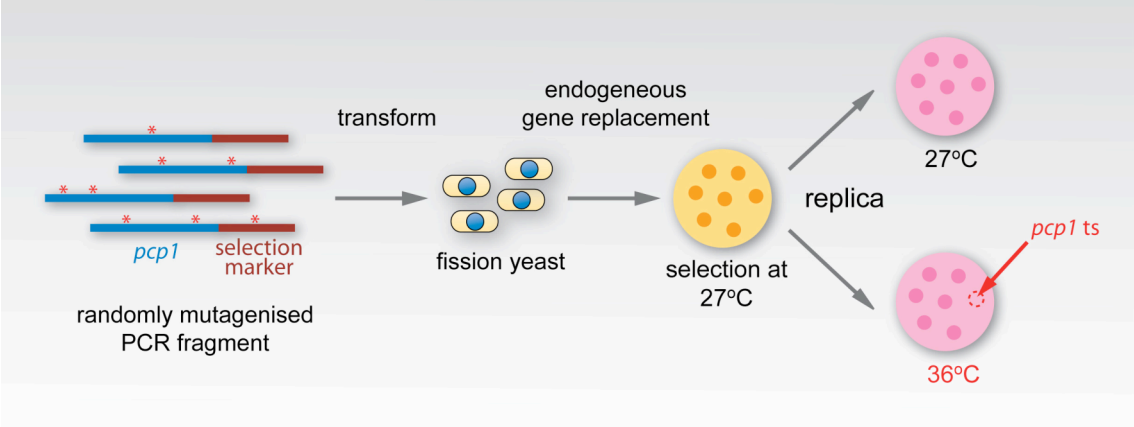

Figure 2.1 A schematic diagram of the temperature-sensitive mutant isolation strategy.

Randomly mutagenised PCR fragments of *pcp1* were transformed into a wild-type fission yeast strain. Cells were allowed to grow on non-selective medium overnight for endogenous gene replacement to occur. Transformants were then selected on plates containing hygromycin at 27°C for 3 to 4 days. Replicated colonies were incubated at 27°C and 36°C. Temperature-sensitive mutants were those that did not grow at 36°C, but grew normally at 27°C. Phloxin B was used to confirm dead cells.

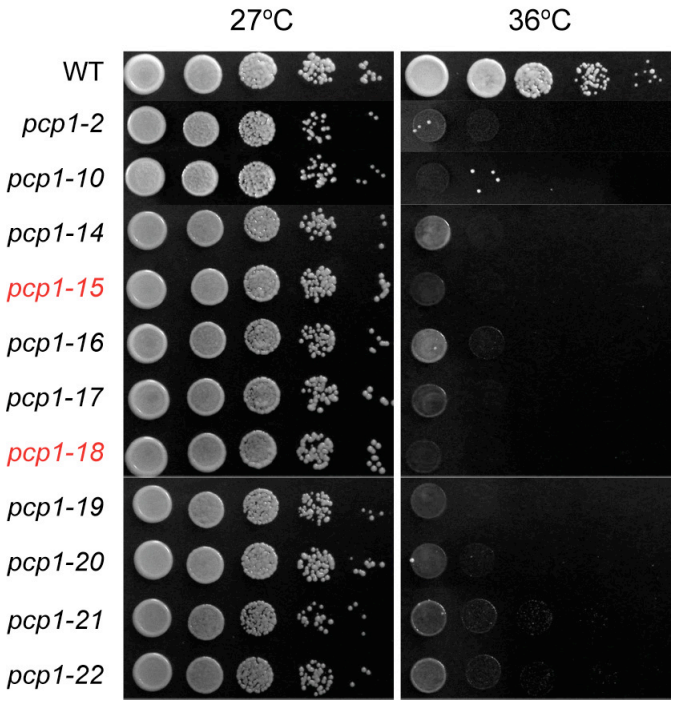

Figure 2.2 Temperature-sensitive mutants of *pcp1*.

Ten-fold serial dilution assays on rich YE5S media. $5x10^4$ cells were applied in the first spot and plates were incubated at 27°C or 36°C for 3 to 4 d. Highlighted in red are the *pcp1* mutants that I focused my analysis on for this study.

2.3 Mutations in the *pcp1* mutants

To get an insight into the molecular defect of the *pcp1* mutants, I sequenced four of the *pcp1* mutant alleles (selected for the strongest growth defects at 36^{o}C) and found that 57% (8 out of 14) of the missense mutations affected leucine and isoleucine residues (Figure 2.3). These are not random, but biased mutations considering that leucine and isoleucine residues constitute only 18% of the protein sequence. Leucine and isoleucine are important hydrophobic amino acid residues for coiled-coil structure. These data therefore suggest that the mutations found in the *pcp1* mutants affect coiled-coil function.

To investigate this, I analysed coiled-coil score of the *pcp1* mutants alleles using the PAIRCOIL prediction software. A score of 1 represents a high probability of the protein sequence in forming a coiled-coil structure, while a score of 0 represents the lowest probability. As predicted, 79% (12 out of 14) of the mutations in the *pcp1* mutants lowered the coiled-coil prediction score, confirming that coiled-coil function in the mutants were disrupted (Figure 2.4). Although it has been shown that the majority of the coiled-coil domain (400-900 aa) of *pcp1*$^{+}$ can be deleted and is not essential (Rajagopalan et al., 2004), my data show that mutations affecting coiled-coil function can have a detrimental effect on Pcp1's function. I envision that the mutations interfere with the proper folding of Pcp1.

I also noticed an interesting mutation in the *pcp1-15* mutant that causes an isoleucine to threonine change at residue 172. This mutation sits within the 17 amino acid residues of the centrosomin motif 1 that has been shown to be essential for the interaction between γ-TuC and Mto1 (Figure 2.5)(Samejima et al., 2008), and hence suggesting the possibility of disruption of the function of the centrosomin motif 1 in Pcp1.

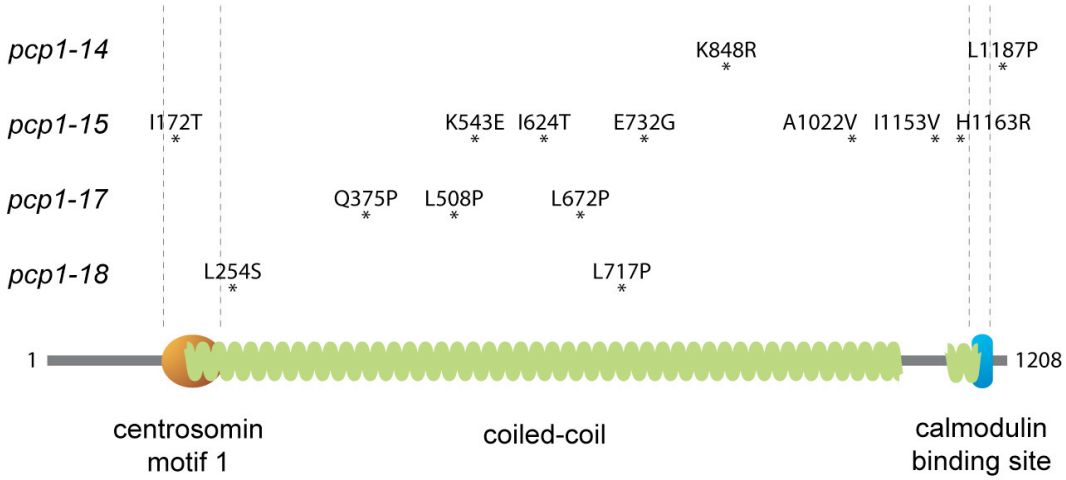

centrosomin motif 1: 147-210 aa
coiled-coil: 187-1085 aa, 1159-1171 aa
calmodulin binding site: 1165-1182 aa

Figure 2.3 Mutation sites in the *pcp1* mutants.

The majority of the mutations (8 out of 14) affect either leucine or isoleucine, which are important amino acid (aa) residues for coiled-coil function. Notably, *pcp1-15* also carries a mutation in centrosomin motif 1. Centrosomin motif 1, the coiled-coil domain and the calmodulin binding site are shown in orange (oval), green (wavy box) and blue (rectangular box) respectively.

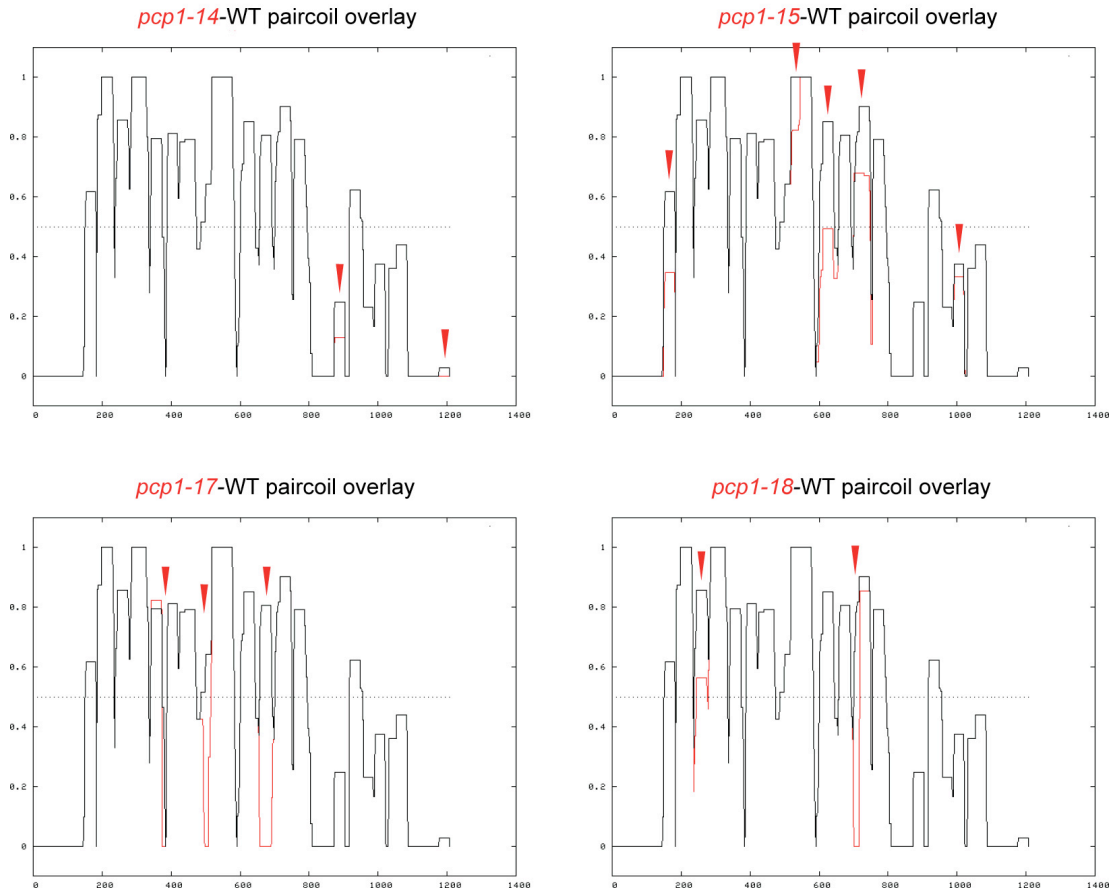

Figure 2.4 Mutations in the *pcp1* mutants interfere with coiled-coil function.

PAIRCOIL prediction score of the *pcp1* mutants. The wild-type profile is presented in black, and is overlaid onto the profile of the *pcp1* mutants that is presented in red. Red arrowheads highlight the regions where the coiled-coil prediction scores were different between the wild-type and the *pcp1* mutants.

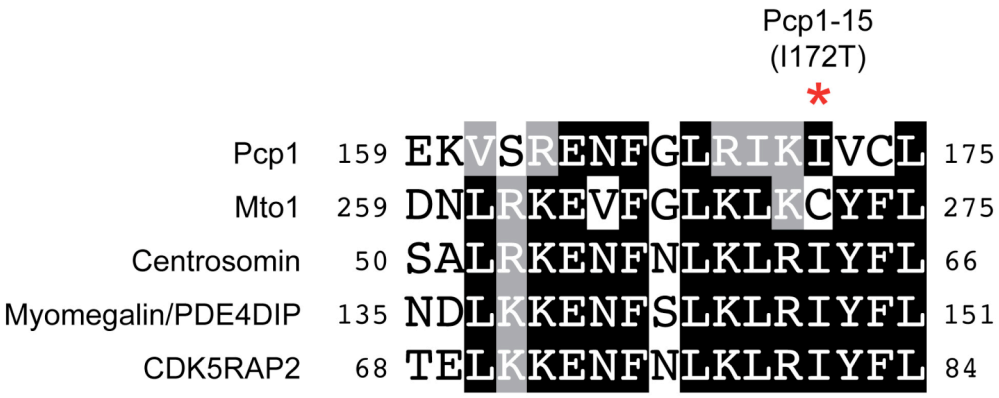

Figure 2.5 *pcp1-15* harbours a mutation within centrosomin motif 1.

Multiple sequence alignment of the highly conserved 17 amino acid residues of centrosomin motif 1 essential for interaction between γ-TuC and Mto1. Asterisk marks isoleucine 172 in Pcp1 that is mutated to threonine in the *pcp1-15* mutant. Accession numbers of sequences used: Pcp1, Q92351; Mto1, NP_588284; Centrosomin, NP_725298; Myomegalin/PDE4DIP, BAA32299; and CDK5RAP2, Q96SN8.

2.4 Mutant Pcp1 protein levels and SPB localisation

Proteins that are not in their native conformation may be targeted to the proteasome for degradation. I next asked whether mutant Pcp1 proteins are degraded at 36^{o}C, by examining protein levels of Pcp1 by immunoblot analysis. From an analysis of six *pcp1* mutants (again selected for the strongest growth defects at 36^{o}C), *pcp1-2* and *pcp1-14* showed significantly lower amount of Pcp1 at both permissive and restrictive temperatures (Figure 2.6a).

However, I observed no significant reduction in Pcp1 protein levels in *pcp1-10*, *pcp1-15*, *pcp1-17* and *pcp1-18* after 4 h incubation at 36^{o}C (Figure 2.6a), indicating that Pcp1 proteins are not degraded in these *pcp1* mutants. Although Pcp1 levels are normal in these mutants, there is a possibility that proper localisation of the mutant proteins to the SPB are disrupted at the restrictive temperature. To address this, I used an anti-Pcp1 antibody to detect localisation of Pcp1 in *pcp1-15* and *pcp1-18* in immunofluorescence microscopy experiments (see section 2.9 for details on the antibody generation). Cut12-GFP was used as an SPB marker. I found that Pcp1 localised properly to the SPB even after 4 h at 36^{o}C, indicating that Pcp1 localisation was not affected in the *pcp1-15* and *pcp1-18* mutants (Figure 2.6b). Collectively, these data demonstrate that the two alleles of *pcp1*, *pcp1-15* and *pcp1-18*, are not knockdown or delocalisation mutants of *pcp1*.

2.5 Thiabendazole sensitivity of the *pcp1* mutants

Many mutants that disrupt microtubule functions are sensitive to the microtubule destabilising drug thiabendazole (TBZ). Sine Pcp1 has been associated with a role in spindle microtubule assembly (Flory et al., 2002), I consequently tested the effect of TBZ on the *pcp1* mutants at 27^{o}C using serial dilution assays. Although the *pcp1* mutants did not show obvious growth defects at 27^{o}C, many temperature-sensitive mutants are hypomorphic, or have reduced gene activity, at their permissive temperature. Indeed, I observed that 5 out of 11 of the *pcp1*

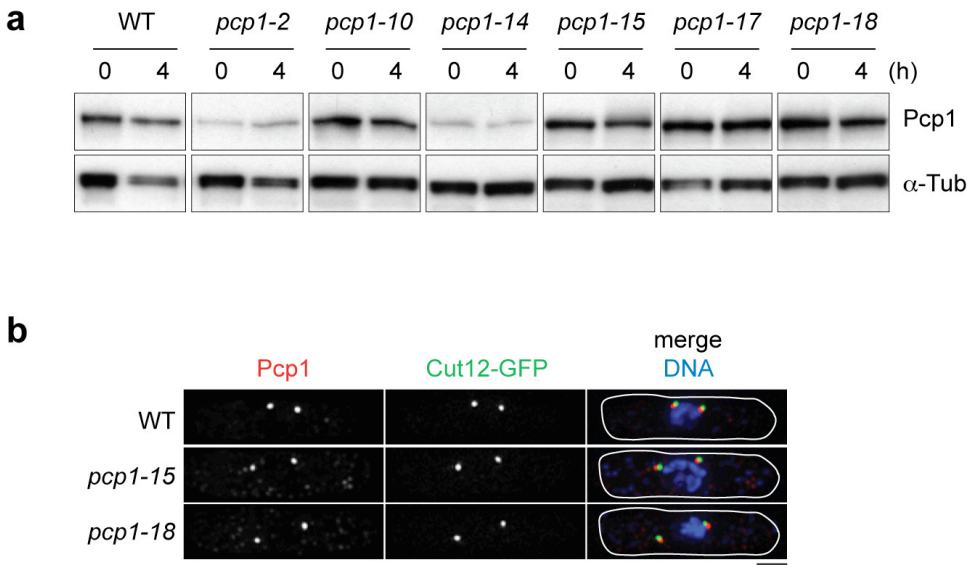

Figure 2.6 Pcp1 protein levels and SPB localisation in the *pcp1* mutants.

(a) Immunoblotting analyses of Pcp1 levels. Cells were shifted up to 36°C and samples were harvested at time 0 and 4 h. Strains carry Pcp1-HA and anti-HA antibody was used for immunoblotting. Tubulin (anti-α-tubulin antibody) acts as a loading control. (b) Immunofluorescence microscopy images showing localisation of Pcp1 after 4 h incubation at 36°C. Anti-Pcp1 antibody (see section 2.9) was used. Cut12-GFP is a marker of the SPB. *n* > 100. Scale bar, 2 μm.

mutants displayed compromised growth in the presence of TBZ at 27^{o}C, suggesting that Pcp1 is involved in microtubule functions (Figure 2.7).

2.6 Pcp1's function is essential for mitosis

To define the cell cycle stage for which Pcp1 function is essential, I performed a synchronous culture analysis using centrifugal elutriation. Centrifugal elutriation is a technique used to achieve size-based cell separation, through the opposing forces of centrifugation and flow velocity in an elutriator. Because early G2 cells are the smallest cells in the life cycle of fission yeasts, they are slow sedimenting under centrifugation and hence will be the first population to flow out from an elutriator once the flow velocity is increased.

The advantage of preparing a synchronous culture by centrifugal elutriation is that it does not involve genetic or chemical intervention, thus allowing subsequent analysis to be performed in cells that closely resemble their physiological conditions.

For the experiment, 3 L of YE5S broth was inoculated to 3x10^{5} cells/ml with an overnight starter culture, and was incubated at 27^{o}C for 16 h until a cell density of 1x10^{7} cells/ml was reached. The culture was then subjected to centrifugal elutriation and 1 L of early G2 cells at 1x10^{6} cells/ml was harvested at the end of the process. The cells were concentrated to 200 ml of 5x10^{6} cells/ml by filtration and the culture was shifted up to 36^{o}C. Cell viability was monitored at fixed intervals as cells proceeded synchronously through the cell cycle. Septation index was used to monitor cell cycle progression.

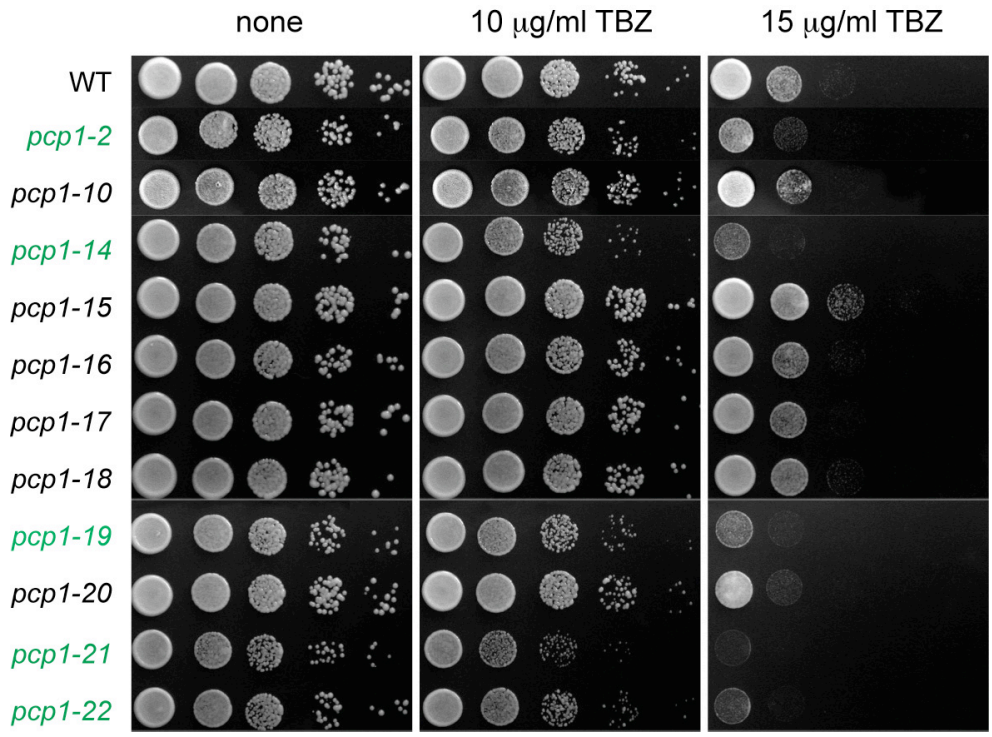

Figure 2.7 Thiabendazole sensitivity of the *pcp1* mutants.

Ten-fold serial dilution assays on rich YE5S media. $5x10^4$ cells were applied in the first spot and the plates were incubated at 27°C or 36°C for 3 to 4 d. Highlighted in green are the *pcp1* mutants that showed reduced growth compared to wild-type cells in the presence of thiabendazole (TBZ).

From hereon, I analysed mainly *pcp1-15* and *pcp1-18*, the two mutants that showed the strongest ts phenotype as judged by growth defects in serial dilution assays, and exhibited normal Pcp1 protein levels and SPB localisation (Figure 2.6). In wild type cells, viability remained high throughout the cell cycle (Figure 2.8a). In contrast, both the *pcp1-15* and *pcp1-18* mutants exhibited a sharp decline in viability after 100 min at 36^{o}C, which coincided with mitotic entry (light red columns in Figure 2.8a). Furthermore, as noted in the *pcp1-18* cells, viability loss occurred in a step-wise manner that corresponded to the two mitotic divisions that occurred during the course of the experiment (at 100 and 220 min). This showed that the loss of viability in the *pcp1* mutants was specific to the mitotic stage.

The viability drop also paralleled the emergence of chromosome missegregation (blue lines in Figure 2.8a), monitored by 4',6-diamidine-2'-phenylindole (DAPI) staining (Figure 2.8b). These data again supported my observation that the *pcp1* mutants lost viability during mitosis. Taken together, these results demonstrate that Pcp1 plays an essential role during mitosis, but not interphase.

2.7 *pcp1* mutants are defective in spindle microtubule nucleation

Overexpression of Pcp1 was shown to cause spindle abnormalities (Flory et al., 2002), suggesting a role for Pcp1 in spindle assembly like its orthologues in other species. I next examined the spindle morphology of the *pcp1* mutants by immunofluorescence microscopy. Cells progressing through the cell cycle synchronously at 36^{o}C were harvested at 100 min, and were stained for α-tubulin (microtubule component) and Sad1 (SPB component) with TAT-1 and anti-Sad1 antibodies, respectively. In wild-type cells, bipolar spindles formed and SPB separation took place as cells entered mitosis (Figure 2.9a). However, in the *pcp1-15* and *pcp1-18* mutants, the cells formed monopolar spindles, i.e. spindles without SPBs flanking their two ends (Figure 2.9a).

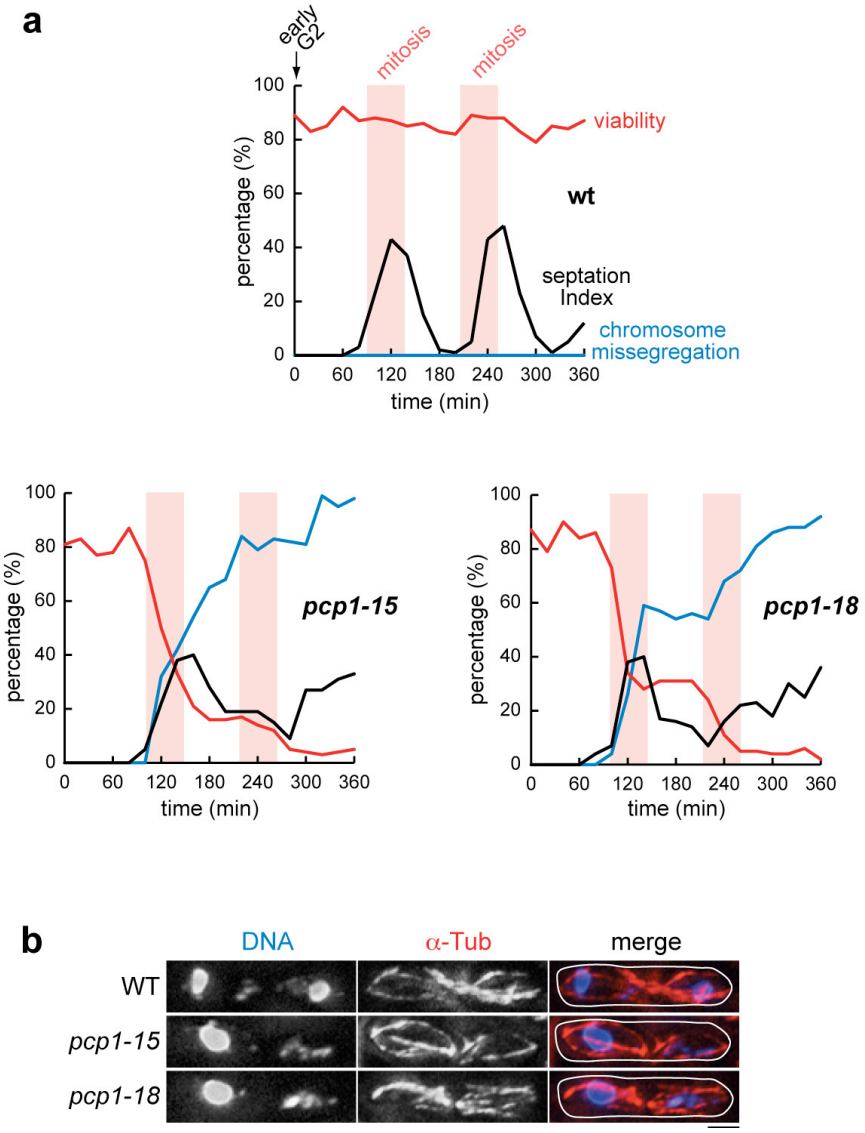

Figure 2.8 Pcp1's function is essential for mitosis.

(a) Viability of cells in synchronous culture analyses. Small G2 cells grown at 27°C were collected by centrifugal elutriation and shifted to 36°C at time 0. The percentage of septated cells was used to monitor cell cycle progression. Light red columns mark periods in mitosis. (b) Chromosome segregation defects. Immunofluorescence microscopy was performed with anti-α-tubulin antibody (TAT-1, red) and DAPI (blue) at 120 min time-point in synchronous culture experiments at 36°C as in a. Cells completed the first mitosis, as indicated by the presence of post-anaphase arrays with unequally segregated chromosomes. Scale bar, 2 μm.

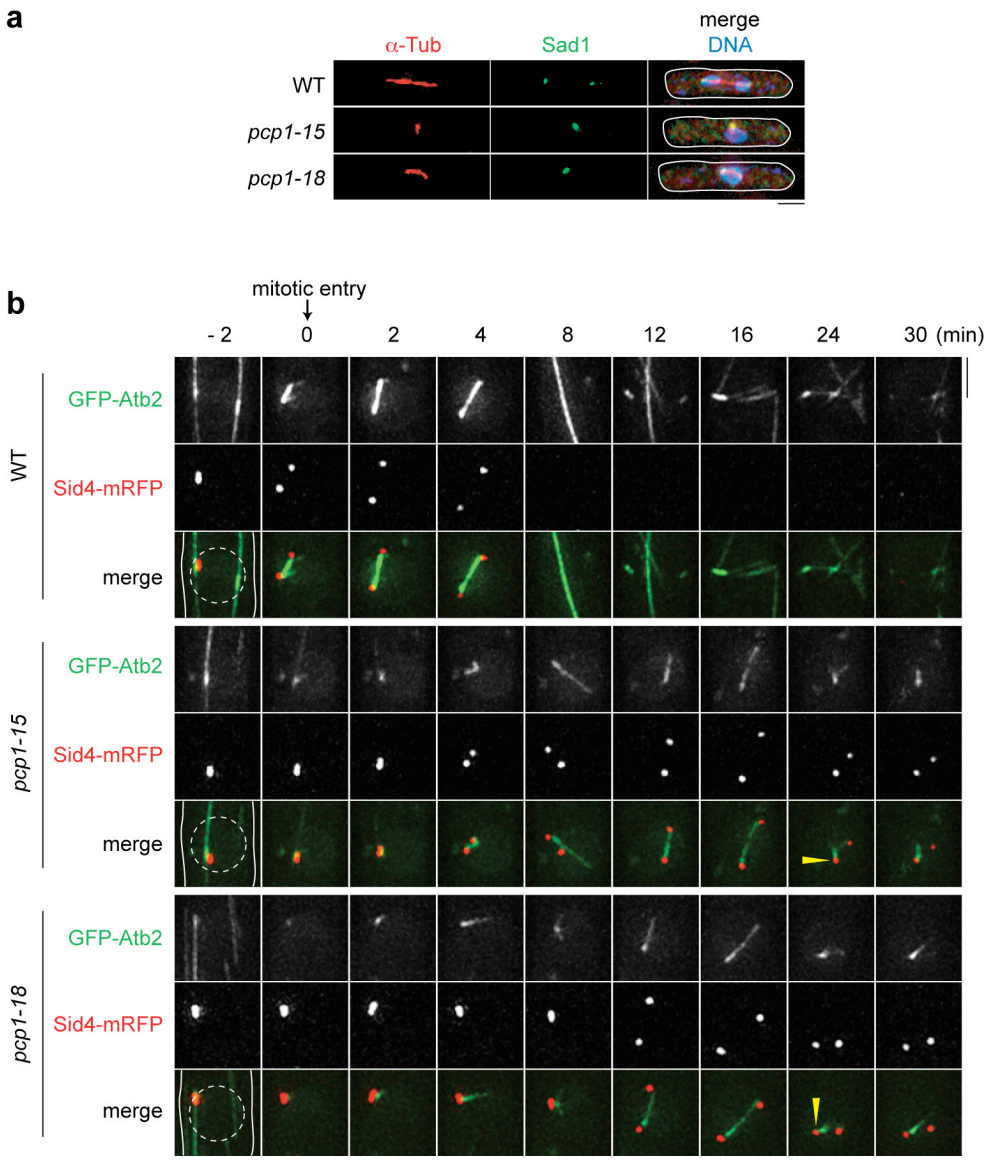

Figure 2.9 The *pcp1* mutants exhibit defects in spindle formation.

(a) Monopolar spindle defects in the *pcp1* mutants. Immunofluorescence microscopy was performed with anti-α-tubulin antibody (TAT-1, red), anti-Sad1 antibody (green) and DAPI (blue) at 100 min time-point in synchronous culture experiments at 36°C (n > 100). (b) Time-lapse fluorescence montages of spindle microtubules (GFP-Atb2, green) and SPB (Sid4-mRFP, red) structures during the first mitosis. A representative cell of each strain is shown. Note that during wild-type anaphase B (the second row, 8 min and thereafter) SPBs became out of frame due to spindle elongation. Dashed circles outline the nuclei. Arrowheads (24 min): SPBs nucleating spindle microtubules. n > 20. Scale bars, 2 μm.

To explore further the spindle defects, I monitored spindle behaviour in the *pcp1* mutants by observing GFP-Atb2 (α2-tubulin) and Sid4-mRFP (SPB component) in live cells. 200 μl of cells were transferred onto a lectin-coated glass dish and were incubated at 36^{o}C for 30 min on a temperature-controlled microscope before image acquisition was started. Wild-type cells formed bipolar spindles with two SPBs flanking the ends of the spindles as they progressed though mitosis (top 3 rows in Figure 2.9b). By contrast, in about 80% of the *pcp1-15* and *pcp1-18* cells, monopolar spindles that emanate from only one of the two SPBs were formed (bottom 6 rows, emphasised by arrowheads at 24 min). These monopolar spindles were unstable, as they always collapsed at some point during the course of the mitosis, bringing the two SPBs back towards each other. Furthermore, compared to wild-type spindles, the monopolar spindles displayed significantly lower GFP-Atb2 signal intensities (Figure 2.9b, Figure 2.10). This indicates that Pcp1 is required for efficient nucleation/assembly of spindle microtubules from the SPB.

The formation of monopolar spindles could be the result of a SPB duplication defect. However, I was able to detect two separate Sid4-mRFP signals of similar intensities during mitosis in both the *pcp1-15* and *pcp1-18* cells (e.g. time-point 12 min, Figure 2.9b), indicating that the duplication of the SPB was unaffected in the *pcp1* mutants.

Another anomaly that I observed during the live-cell analysis was that the *pcp1* mutants were exhibiting mitotic delay. Whilst wild-type cells took about 16 min to complete mitosis, as indicated by the formation of the post-anaphase array (Figure 2.9b), the *pcp1-15* and *pcp1-18* mutants were still attempting to assemble spindles even after 30 minutes into mitosis (Figure 2.9b).

In summary, the *pcp1-15* and *pcp1-18* mutants exhibited spindle assembly defects. As a consequence, a safety mechanism, most likely the spindle assembly checkpoint, was activated in an attempt to rectify the defect. I also demonstrated that the spindle assembly defect was not due to an SPB duplication defect.

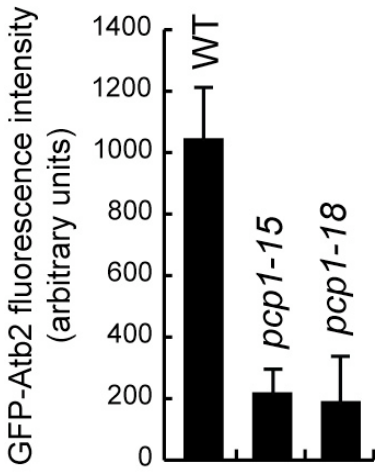

Figure 2.10 Spindle microtubule nucleation is reduced in the *pcp1* mutants.

Quantification of GFP-Atb2 fluorescence. Images were merged into a single projection using a maximum intensity algorithm. Fluorescence signals were then quantified using maximum intensity, after subtracting background signals. *n* > 50; error bars, standard deviation.

2.8 *pcp1* mutants are capable of nucleating spindle microtubules from the mother SPB

As shown earlier, the majority of the *pcp1-15* and *pcp1-18* cells managed to nucleate spindles from one of the two SPBs, instead of exhibiting a complete lack of spindle formation (Figure 2.9b). The fission yeast SPB duplicates in a conservative manner (Bridge et al., 1998; Grallert et al., 2004). I posited that mutant Pcp1 proteins would be less heat-sensitive once they are incorporated into the mother SPB prior to its duplication and separation, thereby retaining the capacity of spindle formation in an asymmetrical fashion. To evaluate this possibility, I exploited the asymmetric SPB localisation of the septation initiation network kinase Cdc7 (Sohrmann et al., 1998).

To analyse localisation of Cdc7 in the *pcp1* mutants, I introduced Cdc7-GFP, Sfi1-mRFP (SPB half-bridge component)(Kilmartin, 2003) and mCherry-Atb2 into the strains. In wild-type cells, as reported, Cdc7-GFP localises to both SPBs in early mitosis, but remains on only one of the SPBs in late anaphase (Figure 2.11) (Sohrmann et al., 1998). In both the *pcp1-15* and *pcp1-18* mutants, Cdc7-GFP localised to the SPBs devoid of spindles (Figure 2.11), indicating that the mother SPB is the origin of the monopolar spindles in these cells.

2.9 Generation of the anti-Pcp1 antibody

An antibody against Pcp1 is a valuable tool for the analysis of Pcp1's function. I therefore set out to create polyclonal antibodies against Pcp1. To this end, I cloned the N-terminus (1-1812 bp), C-terminus (1813-3624 bp), and the complete open reading frame of *pcp1*$^{+}$ gene (1-3624 bp) into the pET14b expression vector (Figure 2.12a). The plasmids were transformed into FB810 *E. coli* expression host, and a pilot experiment was done to assess the protein expression level. After 2 h induction with 1 mM isopropyl β-D-1-thiogalactopyranoside (IPTG) at 37^{o}C, I observed an increase in the amount of

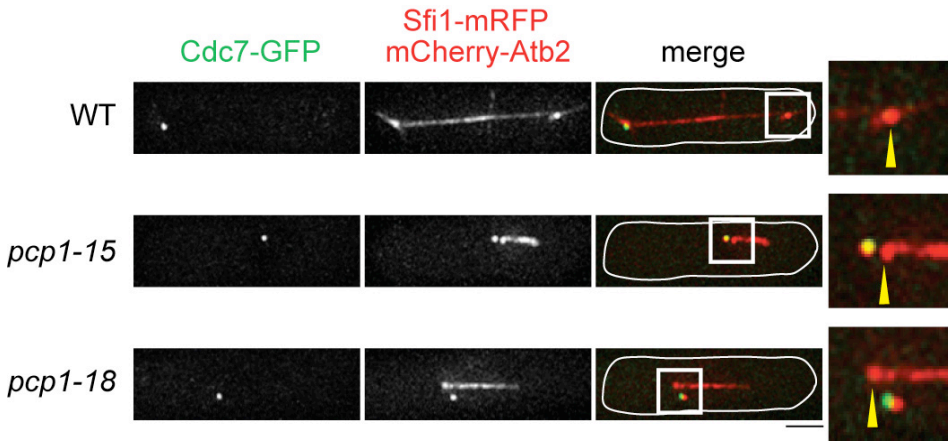

Figure 2.11 Only the mother SPB nucleates spindle microtubules in the *pcp1* mutants.

Monopolar spindles emanating from the mother SPB. Cdc7-GFP (green) is a marker for the daughter SPB. Arrowheads: mother SPBs (negative for Cdc7-GFP). Sfi1-mRFP and mCherry-Atb2 (red) mark the SPB and the spindle, respectively. Merged images of emanating spindles from the mother SPB to which Cdc7-GFP does not localise (white squares) are enlarged on the right. ~75% of monopolar spindles emanate from the mother SPB, $n > 10$. Scale bar, 2 μm.

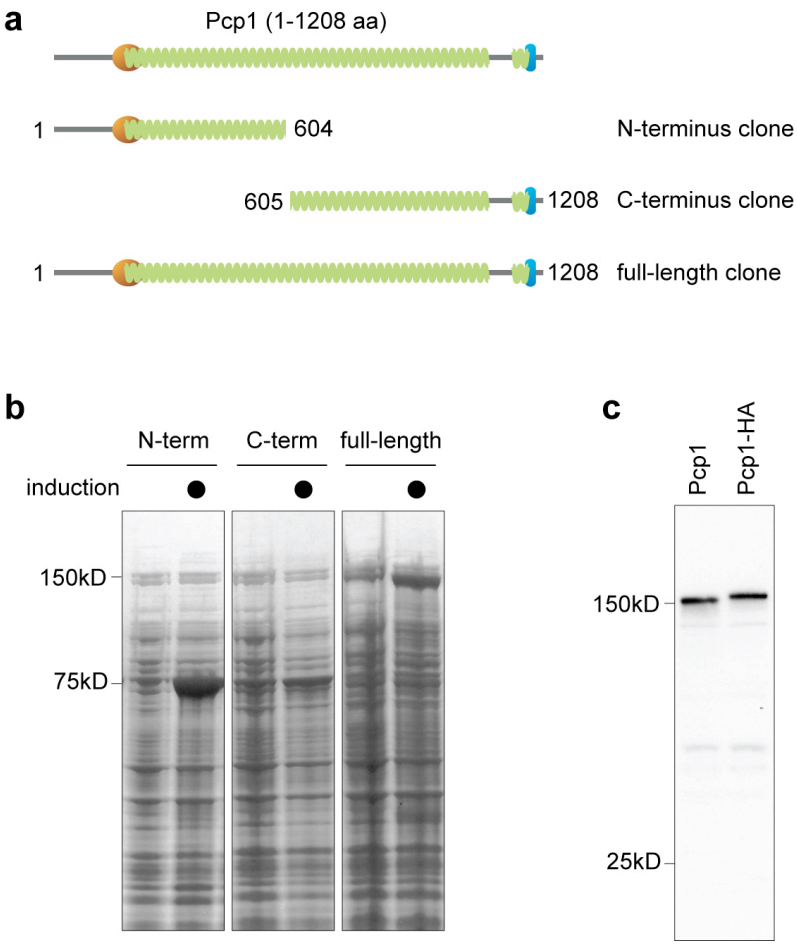

Figure 2.12 The generation of anti-Pcp1 antibody.

(a) A schematic of the expression clones generated for Pcp1 antibody production. Orange, green and blue regions represent centrosomin motif 1, coiled-coil domain and calmodulin binding site, respectively. (b) Coomassie blue staining of whole-cell protein extracts. Protein expression was induced by incubation with 1 mM IPTG at 37^{o}C for 2 h. (c) Immunoblotting of Pcp1 with anti-Pcp1. Antibody was affinity-purified from serum with Pcp1 antigen, and used at 1:5000 dilution. Note that due to HA-tagging (3 copies), the size of recognised band is increased. The antibody was also successfully used for immunofluorescence microscopy analysis (see Figure 2.6).

N-terminus, C-terminus (modestly) and full-length Pcp1 in the protein extracts (Figure 2.12b).

The plasmids were then sent to the Protein Isolation Laboratory at Cancer Research UK London Research Institute for large-scale protein expression and purification. However, as the large-scale production of the C-terminus and full-length Pcp1 was not successful, the purification of these proteins was not pursued further. On the other hand, expression of the N-terminus Pcp1 yielded sufficient material for protein purification. As the protein was tagged with a 6xHis at its N-terminus, purification was achieved using a nickel-column. The purified protein was then used to immunise 2 rabbits.

About 140 ml of serum was collected from two immunised rabbits. I affinity purified 60 ml of the serum against Pcp1 antigen. The purified antibody (700 μg/ml, 6 ml) was stored in phosphate buffered saline (PBS) at -20^{o}C. Specificity test showed that the anti-Pcp1 antibody recognised a single band of ~150 kDa in a wildtype fission yeast protein extract (Figure 2.12c). When probed against a HA-tagged version of Pcp1, a corresponding increase in size of the recognised band was observed (Figure 2.12c). These data hence confirm the specificity of the anti-Pcp1 antibody. I have also successfully used the antibody for immunofluorescence microscopy analysis (see Figure 2.6).

2.10 Summary

This chapter presented the isolation of 11 temperature-sensitive mutants of *pcp1*, of which *pcp1-15* and *pcp1-18* were the focus of this thesis. The protein levels and SPB localisation of Pcp1-15 and Pcp1-18 were shown to be unaffected. I found that both *pcp1-15* and *pcp1-18* lost viability when the cells entered mitosis, indicating that Pcp1's function is essential for mitosis. The viability loss is likely due to the massive chromosome missegregation observed. Examination of the spindle morphology revealed that both *pcp1-15* and *pcp1-18* experienced a defect in spindle assembly, leading to the formation monopolar

spindles and a mitotic delay. The spindle assembly defect was not due to a failure in SPB duplication as two SPBs were detected in all the mutant cells. I have also generated a polyclonal antibody against the N-terminal half of Pcp1, and have successfully used the antibody for immunoblot analysis and immunofluorescence microscopy.

3 Pcp1 recruits γ-TuC to the mitotic SPB

3.1 Overview

This chapter describes the further characterisation of the *pcp1* mutants, focusing mainly on the molecular defects of the *pcp1-15* mutant. Localisation of the γ-TuC components in the mutants was examined. I found that γ-TuC delocalised from the SPB in the *pcp1-15* mutant, but not in *pcp1-18*. The role of Pcp1 in γ-TuC recruitment was confirmed by the suppression of the *pcp1-15* mutant, through restoring γ-TuC localisation to the SPB. The temporal involvement of Pcp1 in γ-TuC recruitment was also determined in synchronous culture analyses. Together, these findings demonstrate that one of the essential functions of Pcp1 lies in γ-TuC recruitment to the mitotic SPB.

3.2 Pcp1 is required for γ-TuC recruitment to the SPB

Human pericentrin and *Drosophila* centrosomin were shown to be required for γ-TuC recruitment to the mitotic centrosome (Zhang and Megraw, 2007; Zimmerman et al., 2004). I therefore asked whether the *pcp1* mutants exhibit γ-TuC delocalisation from the SPB at the restrictive temperature. To address this, I introduced an endogenous, GFP-tagged version of one of the γ-TuC components, Alp4 (orthologue of GCP2/Spc97), into the *pcp1* mutants (Vardy and Toda, 2000). This allowed me to monitor the localisation of γ-TuC using fluorescence microscopy. I also introduced Sfi1-mRFP, a core SPB component, into the cells to mark the SPB.

Exponentially growing cultures grown at 27^{o}C were shifted up to 36^{o}C, and samples were harvested at 0, 2 and 4 h for fluorescence miscroscopy. In wild-type cells, Alp4-GFP localised to the SPB at all times in all cells (Figure 3.1a, b). On the contrary, about 80% of the *pcp1-15* cells lost Alp4-GFP from the SPB

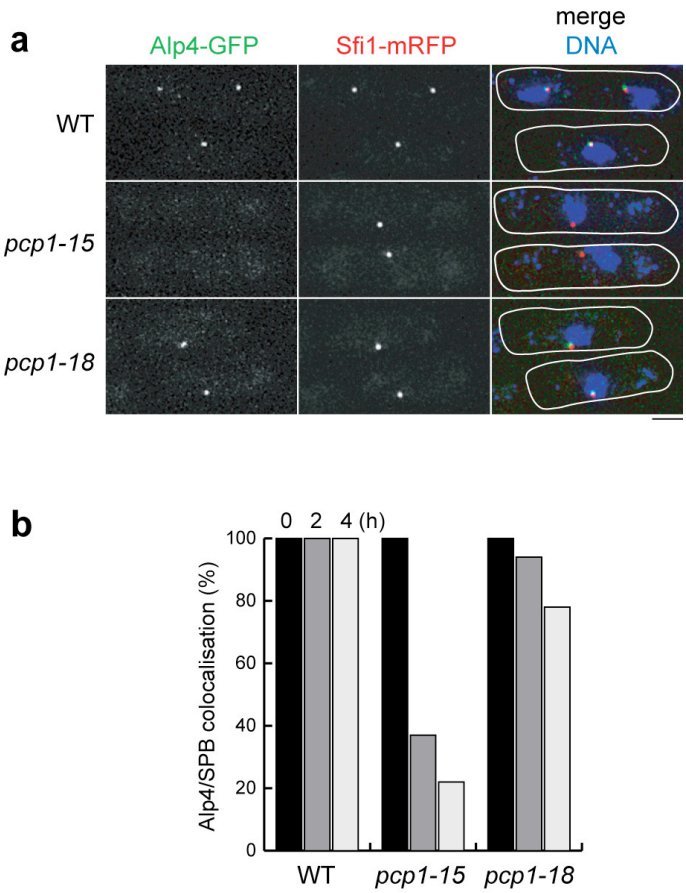

Figure 3.1 Pcp1 plays an essential role in Alp4 recruitment to the SPB.

(a) Alp4-GFP localisation after 2 h incubation at 36°C. Sfi1-mRFP is an SPB marker. Cells were fixed in 1.6% para-formaldehyde. (b) Percentage of cells with Alp4-GFP at the SPB in the experiment described in (a). *n* > 100. Scale bar, 2 μm.

after 4 h incubation at 36°C (Figure 3.1a, b). The loss of Alp4-GFP is not a consequence of the general disruption to the SPB structure, as I could still observe Sfi1-mRFP fluorescence signals in the cells (Figure 3.1a). Consistent with an overall integrity of the SPB, I have shown in Figure 2.6b that Cut12-GFP and Pcp1 could be detected, and colocalised with each other in the *pcp1* mutants.

Because it was possible that the loss of Alp4-GFP from the SPB in the *pcp1-15* mutant was specific to Alp4, and that the localisation of other γ-TuC components in this mutant were unaffected, I could not conclude in confidence that Pcp1 is required for the recruitment of the whole γ-TuC to the SPB. To rule out the possibility that my observation was an Alp4-specific phenotype, I examined the localisation of another γ-TuC component, Alp6 (orthologue of GCP3/Spc98), in *pcp1-15* cells (Vardy and Toda, 2000). Consistent with my previous observation, Alp6-GFP also delocalised from the SPB at the restrictive temperature in *pcp1-15* cells (Figure 3.2). Hence, these data show that Pcp1 is required for γ-TuC recruitment to the SPB.

One very interesting observation I made during the γ-TuC localisation analysis was that although the *pcp1-15* mutant exhibits delocalisation of Alp4-GFP and Alp6-GFP from the SPB, localisation of these γ-TuC components in the *pcp1-18* cells was largely unaffected (Figure 3.1a, b, Figure 3.2). The seemingly normal localisation of γ-TuC in the *pcp1-18* mutant could not be explained by a weak temperature-sensitive phenotype, as both the *pcp1-15* and *pcp1-18* mutants exhibited similar degree of cell death and mitotic defects upon exposure to 36°C (Figure 2.8a, b, Figure 2.9a, b). In fact, the difference in the γ-TuC localisation pattern between the *pcp1-15* and *pcp1-18* mutants suggested that Pcp1 has distinct functions during cell division, and that these functions are genetically separable. The investigation into the molecular defects of the *pcp1-18* mutant is presented in Chapter 4.

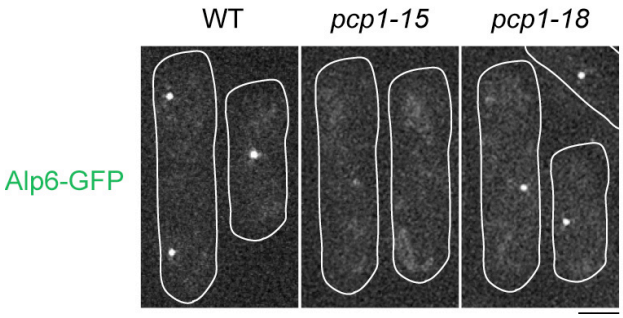

Figure 3.2 γ-TuC component Alp6 delocalises from the SPB in the *pcp-15* mutant.

Fluorescence images of cells fixed in para-formaldehyde, showing Alp6-GFP localisation after 2 h incubation at 36°C. *n* > 100. Scale bar, 2 μm.

3.3 Restoring γ-TuC localisation to the SPB suppresses the *pcp1-15* mutant

Although I have shown that Pcp1 is required for γ-TuC recruitment to the SPB (Figure 3.1a, b, Figure 3.2), that was not sufficient to infer that Pcp1's function is to recruit γ-TuC. One could argue that the γ-TuC delocalisation from the SPB in the *pcp1-15* cells was a secondary defect of the mitotic failure of the mutant. To look into this, I devised a way to restore γ-TuC localisation to the SPB, and asked whether this could suppress the temperature sensitivity of the *pcp1-15* cells. If the γ-TuC delocalisation in the *pcp1-15* cells was a primary defect of the mutant, or in other words, Pcp1's function is indeed to recruit γ-TuC to the SPB, reversing the γ-TuC delocalisation defect should rescue the temperature sensitivity of the *pcp1-15* cells.

My first attempt to restore γ-TuC localisation to the SPB was to introduce an SPB-targeting sequence into Alp4. However, I couldn't identify an SPB-targeting sequence that would localise Alp4 to the inner plaque of the SPB, which is the face of the SPB where Alp4 is recruited during mitosis for spindle microtubule nucleation. Although there were instances where proteins were artificially targeted to the SPB through fusing the proteins with the SPB-targeting motifs of Sid2, Sid4 or Cdc11 (Morrell et al., 2004; Tomlin et al., 2002), these fusion proteins were likely to be recruited to the outer plaque of the SPB, i.e. the cytoplasmic side of the SPB and, hence, unsuitable for the purpose of my experiment.

Changing the strategy, I used a plasmid where Alp4 expression is controlled under the thiamine repressible promoter *nmt1*. Expression of genes under *nmt1* is repressed or induced in the presence or absence of thiamine, respectively. The rationale behind this approach is that supplying an increased amount of a protein might facilitate an otherwise weak interaction between the overexpressed protein and other components. In my case, I attempted to increase the interaction between Alp4 and Pcp1 to restore γ-TuC localisation to the SPB.

Highly overexpressing any of the γ-TuC components is lethal to cells (Vardy and Toda, 2000). To achieve mild overexpression of Alp4, I grew the *pcp1-15* cells carrying *nmt1-alp4*$^{+}$ plasmid in rich medium (YE5S), which naturally contains thiamine. Although I have mentioned that *nmt1* is repressed in the presence of thiamine, this promoter is so robust that even under its repressed condition, there is a significant level of basal expression. In addition, it is important to note that the plasmid exists in multiple copies in the cell, further boosting expression. This basal level of expression, which at times is considered as an undesirable feature of *nmt1*, was utilised to my advantage in this experiment.

The mild overexpression of Alp4 indeed restored γ-TuC localisation to the SPB, as indicated by a small increase in the proportion of cells displaying Alp6-GFP at the SPB (Figure 3.3a, b). This ameliorated growth of the *pcp1-15* cells at the semi-restrictive temperature of 34^{o}C (Figure 3.4). The same condition did not confer significant advantage to the *pcp1-18* cells (Figure 3.4), consistent with the fact that γ-TuC localisation to the SPB is unaffected in this mutant (Figure 3.1a, b, Figure 3.2). Collectively, these data demonstrate that one of the essential functions of Pcp1 lies in γ-TuC recruitment to the SPB.

3.4 Pcp1 recruits γ-TuC only to the mitotic SPB

Previous work showed that although Pcp1 and γ-TuC appear to colocalise at the SPB throughout the cell cycle (Flory et al., 2002), there is a profound difference in their geometry between interphase and mitosis. Whilst γ-TuC localises predominantly inside the nucleus throughout the cell cycle, Pcp1 stays in the cytoplasm during interphase and is separated from the γ-TuC by the nuclear envelope. Pcp1 enters the nucleus only upon mitotic entry when it becomes spatially closer to γ-TuC (see Figure 1.7)(Flory et al., 2002). It is, therefore, plausible that Pcp1 is only required for γ-TuC recruitment during mitosis.

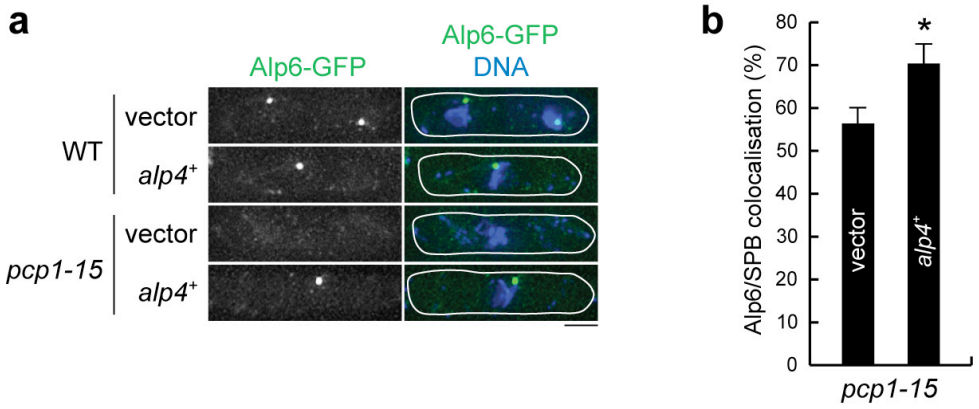

Figure 3.3 Mild overexpression of Alp4 restores γ-TuC to the SPB in the *pcp1-15* mutant.

(a) Alp6-GFP localisation at the SPB with or without mild overexpression of Alp4. Alp4 was mildly overexpressed through repression of the *nmt1* promoter (pREP1-Alp4) on rich liquid YE5S media incubated for 4 h at 34°C. (b) Percentage of cells with Alp6-GFP at the SPB in the experiment described in (a). Asterisk indicates that the difference is statistically significant (Student's *t*-test, $p < 0.05$). $n > 100$; error bars, standard deviation from three independent experiments. Scale bar, 2 μm.

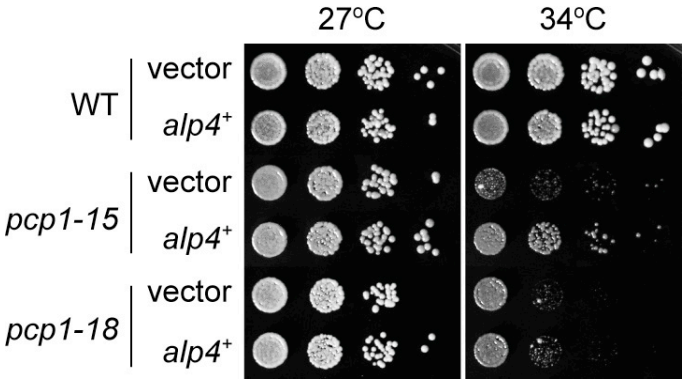

Figure 3.4 Restoring γ-TuC to the SPB suppresses the temperature-sensitivity of the *pcp1-15* mutant.

Ten-fold serial dilution assays on YE5S media.

To clarify the temporal involvement of Pcp1 in γ-TuC recruitment to the SPB, centrifugal elutriation was performed again and Alp4-GFP signals were followed over time at 36°C (Figure 3.5a, red line, culture 1). I found that Alp4-GFP is retained at the SPB during interphase, but delocalised from the SPB coincidentally as the *pcp1-15* cells entered mitosis from 60 min onwards (red line in Figure 3.5b).

To exclude the possibility that the timing of Alp4-GFP delocalisation reflects the minimum duration required for the heat-inactivation of the Pcp1-15 mutant protein, half of the initial culture was incubated at 27°C for a further 40 min during G2 phase, followed by a shift up to 36°C (Figure 3.5a, blue line, culture 2). If the delocalisation of Alp4-GFP in the previous experiment was in fact due to mitotic entry, I would observe in this experiment that Alp4-GFP also delocalise when cells entered mitosis, but after significantly shorter period of time at 36°C. Indeed, similar to the previous observation, Alp4-GFP in this parallel experiment delocalised from the SPB after 60 min, as soon as cells entered mitosis (blue line in Figure 3.5b).

It was possible that the loss of γ-TuC in the nucleoplasm was masked by the γ-TuC from the cytoplasm that was recruited by Mto1, an SPB component structurally related to Pcp1 but which plays a role in the organisation of cytoplasmic microtubules (Sawin et al., 2004; Sawin and Tran, 2006; Venkatram et al., 2004; Zimmerman and Chang, 2005). I asked if γ-TuC localisation remained unaffected during interphase in the *mto1Δ* mutant background, which abolished γ-TuC recruitment from the outer plaque of the SPB. The same result was obtained in the *mto1Δ* mutant, where Alp4-GFP also delocalised only when cells entered mitosis (Figure 3.5c). Taken together, these findings not only establish that Pcp1 is required for γ-TuC recruitment to the mitotic SPB, but also suggest that γ-TuC recruitment during interphase is mediated by a Pcp1- and Mto1-independent mechanism.

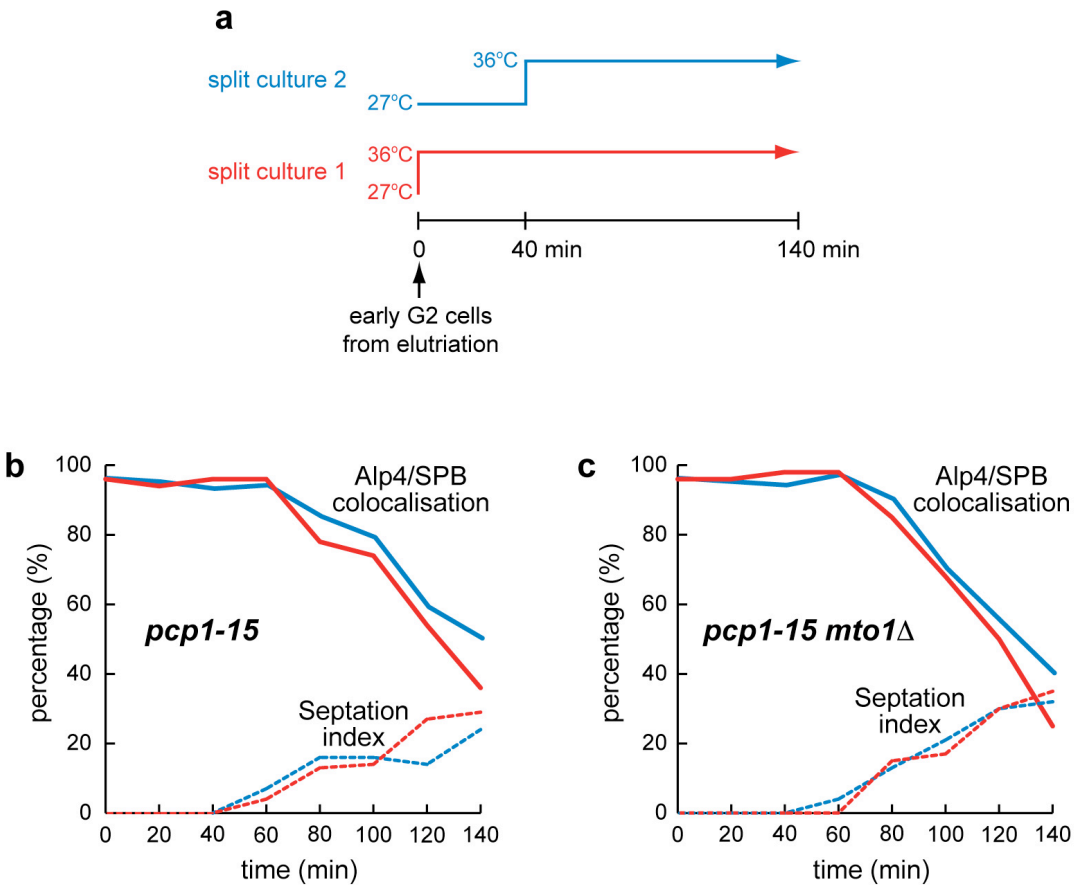

Figure 3.5 Pcp1 is required for γ-TuC recruitment to the SPB specifically during mitosis.

(a) Diagram depicting the experimental procedures. Synchronous cultures of early G2 cells (grown at 27°C) were divided into two at time 0. One culture was immediately shifted to 36°C (culture 1, red), whilst the other was kept at 27°C for another 40 min, followed by a shift to 36°C (culture 2, blue). (b) Alp4-GFP localisation at the SPB in synchronous culture experiments. Alp4-GFP signals were monitored at each time point. (c) Alp4-GFP localisation at the SPB in the double mutant *pcp1-15 mto1Δ*, in synchronous culture experiments.

3.5 Summary

I have presented in this chapter that γ-TuC delocalised from the SPB in *pcp1-15*, but not in *pcp1-18*. I also demonstrated that restoring γ-TuC localisation to the SPB in *pcp1-15* by mildly overexpressing Alp4 suppressed the growth defects of the mutant at the semi-permissive temperature. Further analysis showed that the γ-TuC delocalisation occurred only when cells entered mitosis at the restrictive temperature, indicating that Pcp1 is important for γ-TuC recruitment to the SPB only during mitosis. These findings verified the postulated role of Pcp1 in γ-TuC recruitment during mitosis.

4 Pcp1 recruits Plo1 to the mitotic SPB

4.1 Overview

In Chapter 3, I showed that the two *pcp1* mutants exhibited different molecular defects. Unlike the *pcp1-15* mutant, *pcp1-18* did not display γ-TuC delocalisation from the SPB at the restrictive temperature. In this chapter, I present the analysis of *pcp1-18* mutant. A multicopy suppressor screen was performed to search for clues about the underlying defect in the mutant. Nuclear pore complex (NPC) components and an essential SPB component Cut12 were isolated as multicopy suppressors of *pcp1-18* mutant. I consequently examined Pcp1's role in nuclear envelope reorganisation and SPB insertion. The link between Pcp1, Cut12 (the regulator of Plo1) and Plo1 was also investigated. Furthermore, I provided evidence for the physical interaction between Pcp1 and Plo1. Finally, the role of Pcp1 in mitotic entry regulation was established. Taken together, these data unveiled a novel role for Pcp1 in the recruitment of Plo1 to the SPB to drive mitotic entry, nuclear envelope reorganisation and SPB insertion.

4.2 Multicopy suppressor screen of the *pcp1-18* mutant

As I have described in Chapter 3, whilst both the *pcp1-15* and *pcp1-18* cells display similar mitotic defects, unlike *pcp1-15*, γ-TuC localisation to the SPB is not significantly impaired in the *pcp1-18* mutant (Figure 3.1a, b, Figure 3.2). This implies that Pcp1 plays an essential role in mitosis that is independent of γ-TuC recruitment to the mitotic SPB. To uncover this postulated additional role of Pcp1, I performed a multicopy suppressor screen.

A multicopy suppressor screen is a genetic screen where one transforms a complementary DNA (cDNA) or a genomic DNA library into mutant cells with an unknown molecular defect. When a mutant cell acquires a plasmid that

overexpresses a protein that is related to the function of the mutated protein, the overexpressed protein could sometimes compensate for the defective function, and consequently revert or suppress the mutant phenotype. The identity of the overexpressed proteins in these reverted mutants could be subsequently defined. These multicopy suppressors could be interacting proteins or proteins acting downstream of the mutant protein, and will usually provide clues to the function of the protein originally in question.

Considering that many multicopy suppresors do not fully suppress the mutant phenotype, it is desirable to perform the screen under a condition where the function of the mutant protein is only partially disrupted. In my case, the extent to which the function of the mutant Pcp1 is disrupted depends on the temperature the mutants are incubated at.

I therefore assessed the growth profile of the *pcp1-18* mutant at temperatures ranging from 27^{o}C to 36^{o}C. I found that 34^{o}C is the temperature where the *pcp1-18* cells started to exhibit a partial growth defect, indicating that Pcp1's function was only partially disrupted at this semi-restrictive temperature (Figure 4.1). Based on this observation, I decided to screen for multicopy suppressors of the *pcp1-18* mutant at both 36^{o}C and 34^{o}C.

For the screen, I transformed a genomic DNA library (cloned into pAL-SK vector) into the *pcp1-18* mutant. Transformants were selected on –LEU plates (the vector contained a budding yeast Sc*LEU2* marker that complement the fission yeast *leu1* mutation), and colonies were allowed to form in the permissive temperature of 27^{o}C (incubating the plates for 6-7 days). Approximately 15,000 transformants were then replica plated onto multiple YE5S plates containing phloxin B, and the plates were incubated at 36^{o}C or 34^{o}C for 2 days. Transformants that were capable of forming colonies at either 36^{o}C or 34^{o}C were identified as suppressor candidates and were selected for plasmid dependency analysis.

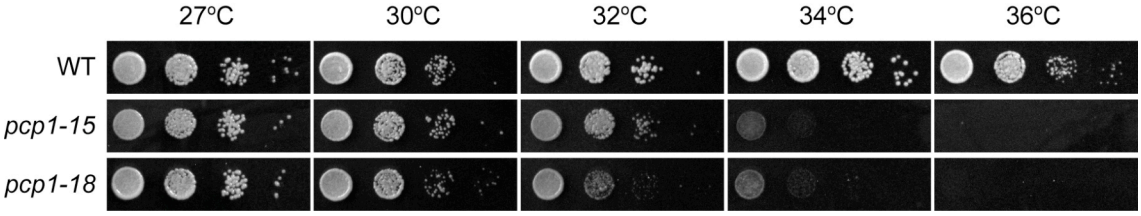

Figure 4.1 Temperature-sensitivity of the *pcp1* mutants at a range of temperatures.

Ten-fold serial dilutions of the *pcp1* mutants were spotted onto YE5S media and incubated for 2 to 3 d at the temperatures indicated.

Plasmid dependency analysis is used to check if the suppression in the mutant cells was due to the genes carried on the plasmids or to a random extragenic mutation. Bona fide multicopy suppressors are mutant cells that show co-segregation of their suppression and the presence of a plasmid. First, suppressor candidates were grown in YE5S medium (non-selective medium) overnight, during which some cells failed to maintain their plasmids. About 300 cells were then plated onto YE5S plates. Colonies were replica plated onto –LEU plates and YE5S plates containing phloxin B. The –LEU plates were incubated at 27^{o}C, while the YE5S plates were incubated at 34^{o}C and 36^{o}C for 2 days. For all selected suppressor candidates only the colonies harbouring plasmids exhibited improved growth at 34^{o}C or 36^{o}C (data not shown), thus confirming the suppression property of the proteins expressed by the plasmids.

Following that, plasmids were recovered from the suppressors and were transformed into *E. coli* for amplification. Amplified plasmids were then extracted from the *E. coli* and were sequenced to identify the inserts. Apart from identifying *pcp1*$^{+}$ as one of the suppressor genes, which validated my screen, I also pulled out a few other suppressor genes that are presented and discussed in the following sections (see Table 4.1 for a complete list of suppressors). A final confirmation of the suppression was done by re-transforming the plasmids into the *pcp1-18* mutant, which provided suppression in all the cases. I believed that my screen has covered the whole genome, as I managed to identify the same suppressor genes more than once. Also, although I did not subclone a single gene to verify suppression in many cases, I inferred the relevant suppressor gene from its function.

4.3 Nuclear pore complex components specifically suppresses the *pcp1-18* mutant

Two of the suppressor genes that specifically rescued *pcp1-18* were those encoding the nuclear pore complex (NPC) components – Cut11 (orthologue of NDC1) and Pom152 (orthologue of GP210) (Figure 4.2) (Tran and Wente, 2006; West et al., 1998). Both of these proteins are transmembrane

	suppression	
genes	*pcp1-15*	*pcp1-18*
pcp1$^+$	yes (2x)	yes (1x)
cut11$^+$	no	yes (4x)
pom152$^+$	no	yes (1x)
cut12$^+$	no	yes (3x)
kms2$^+$	no	yes (2x)
tcg1$^+$	no	yes (2x)
alp4$^+$*	yes	no

Table 4.1 List of multicopy suppressor genes of the *pcp1* mutants.

pcp1$^+$ validated the screen (number in brackets indicates the frequency of hits). The role of *cut11*$^+$, *pom152*$^+$ and *cut12*$^+$ in suppressing the *pcp1-18* mutant is presented in later sections in this thesis. *kms2*$^+$ encodes an SPB component (Ding et al., 2000; Miki et al., 2004), whilst *tcg1*$^+$ encodes a potential homologue of budding yeast ribonucleoprotein Rnp1 (Cusick, 1994). Functions of *kms2*$^+$ and *tcg1*$^+$ and how increased expression of these genes suppresses the *pcp1-18* mutant are unknown at the moment.

* *alp4*$^+$ suppresses the *pcp1-15* mutant under the control of *nmt1* promoter (see section 3.3).

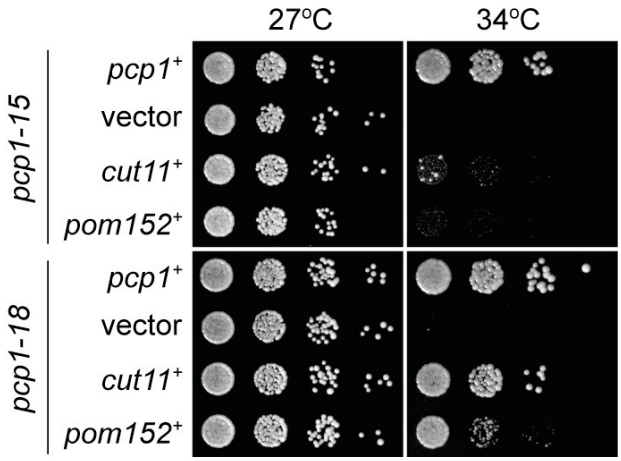

Figure 4.2 Increased expression of nuclear pore complex components specifically suppresses *pcp1-18*.

Ten-fold serial dilutions of the *pcp1* mutants harbouring the indicated multicopy suppressor plasmids. Cells were grown overnight in selective medium at 27°C prior to spotting onto YE5S medium and incubated for 3 d at 27°C or 34°C.

nucleoporins that constitute the inner membrane ring of the NPC (Alber et al., 2007). In fission yeast that undergoes a closed mitosis, Cut11 is not only an essential NPC component but also accumulates specifically at the SPB upon mitotic onset (West et al., 1998). Furthermore, this protein is required for SPB insertion into the nuclear envelope (NE) during mitosis (West et al., 1998).

Pom152 is not an essential protein. Its localisation was examined by tagging the gene with GFP at its C-terminus, and at the endogenous locus of the gene. Furthermore, expression of the fusion protein was under the control of the endogenous promoter. Under this condition, I observed that Pom152 localised to the NE (Figure 4.3). However, unlike Cut11, Pom152 did not localise to the SPB during mitosis (Figure 4.3).

Because of the close proximity between Pom152 and Cut11, I postulate that suppression of the *pcp1-18* mutant by increased expression of Pom152 is mediated indirectly through the function of Cut11, for instance through increased recruitment of Cut11 to the mitotic SPB.

4.4 The *pcp1-18* mutant is defective in nuclear envelope reorganisation and SPB insertion

Given the role of Cut11/Ndc1 in SPB insertion, I investigated whether *pcp1-18* cells are able to reorganise the NE for SPB insertion in mitosis. To this end, the ultrastructure of the NE and SPB were examined by electron microscopy (EM).

In order to increase the percentage of mitotic cells, I performed a synchronous culture analysis by elutriating early G2 cells and shifting the culture up to 36^{o}C for 100 min before samples were harvested for EM processing. This procedure enriched the culture for mitotic cells to about 40% (as opposed to about 10% in an asynchronous culture), and was especially important for EM analysis as the chances of detecting a small structure such as an SPB in the samples were increased. In addition, the synchronous culture analysis also allowed me to infer

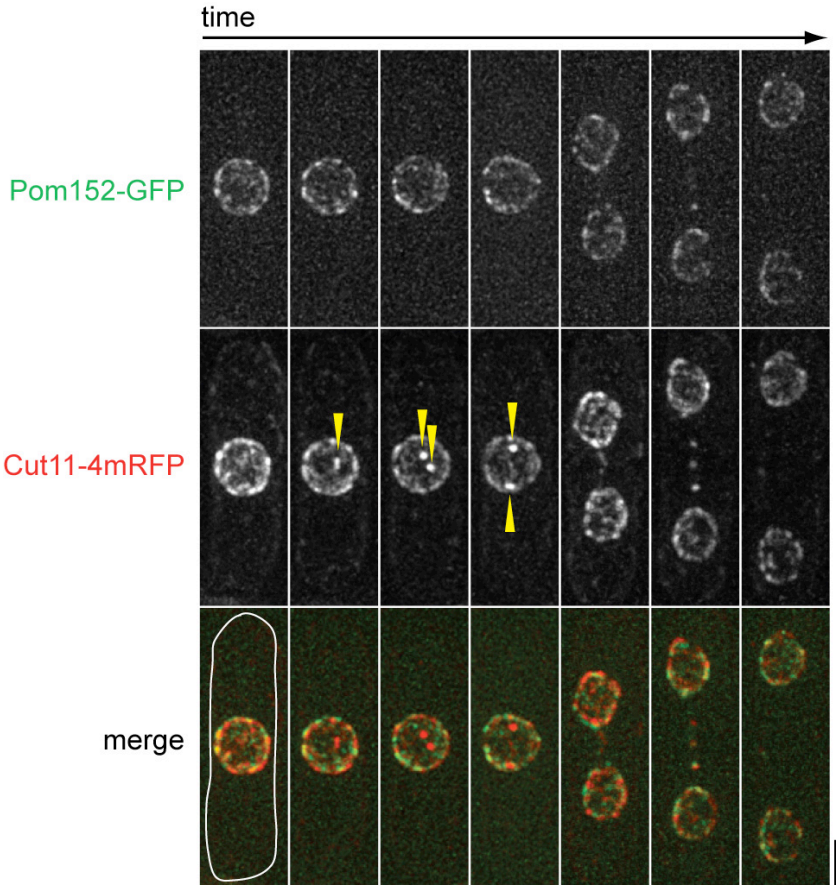

Figure 4.3 Pom152 does not exhibit SPB-specific localisation in mitosis.

Live analysis of Pom152-GFP localisation, observed concurrently with another nuclear pore complex component Cut11-4mRFP. In contrast to Cut11-4mRFP that localises to both the SPBs (arrowheads) in early mitosis and the NE throughout the cell cycle, Pom152-GFP only localises to the NE discontinuously. $n > 15$. Scale bar, 2 μm.

that any defect I observe is indeed the primary defect that appears in the *pcp1-18* mutant, and not a subsequent/secondary defect.

Cells were harvested by filtration and were cryofixed by high-pressure freezing. Freeze-substitution of cells was carried out in anhydrous acetone containing 0.01% osmium tetraoxide, 0.1% glutaraldehyde and 0.25% uranyl acetate for 3 days at -90^{o}C. The samples were gradually warmed to -20^{o}C and were finally infiltrated with Epon. Serial thin sections of about 60 nm of the hardened Epon were cut and placed on pioloform-coated slot grids. The serial thin sections were post-stained with 2% uranyl acetate in 70% methanol for 4 min, followed by lead citrate staining for 1 min. The sample processing steps from freeze-substitution to serial thin sectioning were done by Ken Blight from the Electron Microscopy Unit at the Cancer Research UK London Research Institute.

In wild-type mitotic cells, as reported previously, the electron-sparse NE discontinued underneath the electron-dense SPB, indicating that the NE opened up to form a fenestra for SPB insertion (Figure 4.4a)(Ding et al., 1997). In striking contrast, in the *pcp1-18* cells, the NE underneath one of the SPBs remained intact (Figure 4.4b, and the SPB on the left hand side in Figure 4.4c). The examined cells are indeed in mitosis, as indicated either by the NE herniation (the result of monopolar spindles prodding on the NE, Figure 4.4b and see also Figure 4.5) or the presence of spindles emanating from the second, abnormally inserted SPB (Figure 4.4c). These results indicate that Pcp1 is required for NE reorganisation and SPB insertion during mitosis.

I also observed NE and SPB structures in the *pcp1-15* mitotic cells. In clear contrast to *pcp1-18*, the NE formed a fenestra normally in this mutant (Figure 4.4d), consistent with my suppression data showing that an increased dosage of Cut11 does not restore growth defect of the *pcp1-15* mutant at the semi-permissive temperature. However I noticed that the SPB was placed obliquely, rather than in parallel, above the NE, indicating that despite the apparent NE fenestra, SPB insertion into the NE may be somewhat compromised in this mutant.

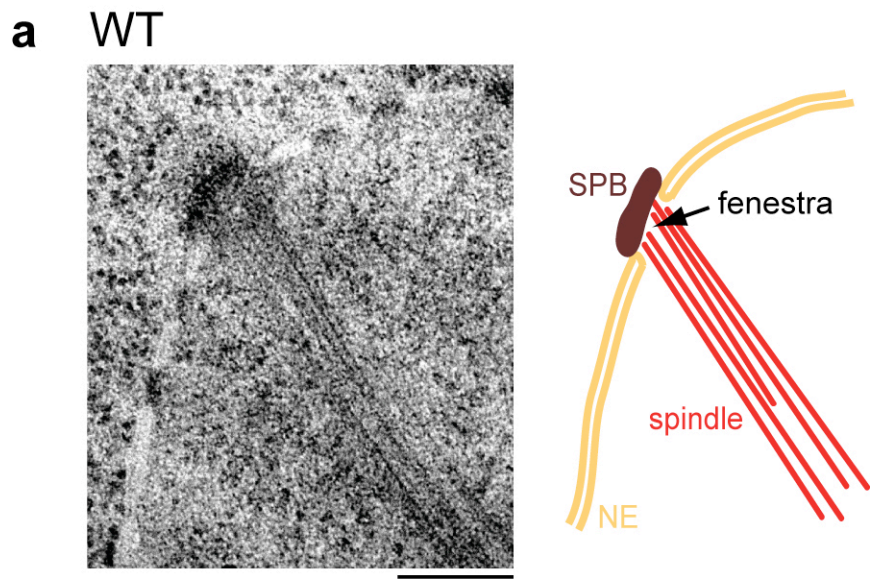

(Figure 4.4b, c and d are on the following pages)

Figure 4.4 The formation of a fenestra in the NE and SPB insertion are impaired in the *pcp1-18* mutant.

(a, b, c, d) Electron micrograph showing the ultrastructure of the SPB, the NE and spindle microtubules. Synchronised cultures (incubated at 36°C for 100 min to enrich for mitotic cells) were processed for EM. Schematic diagrams are included next to or below each electron micrograph. Monopolar spindles in c originate from the SPB on the right (overlaid from adjacent section, presumably the mother SPB) that is abnormally inserted into the NE. *n* = 5. Scale bars, 200 nm.

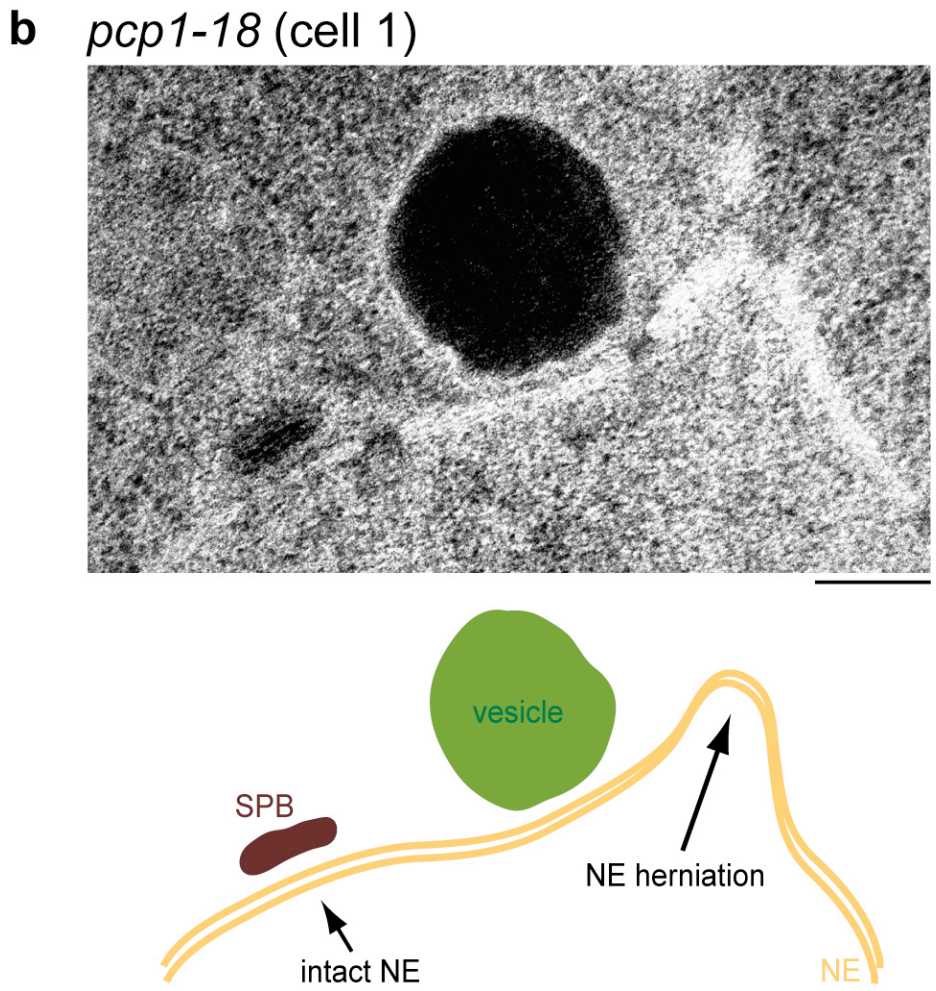

(Figure 4.4a is on the previous page, c and d are on the following pages)

c *pcp1-18* (cell 2)

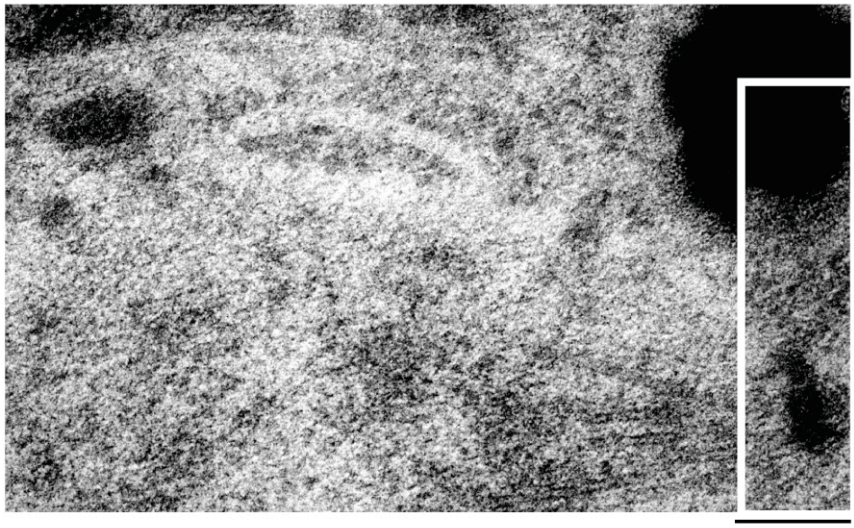

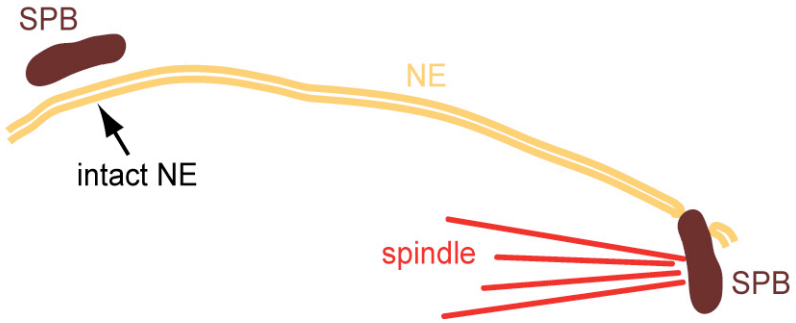

(Figure 4.4a and b are on the previous pages, d is on the following page)

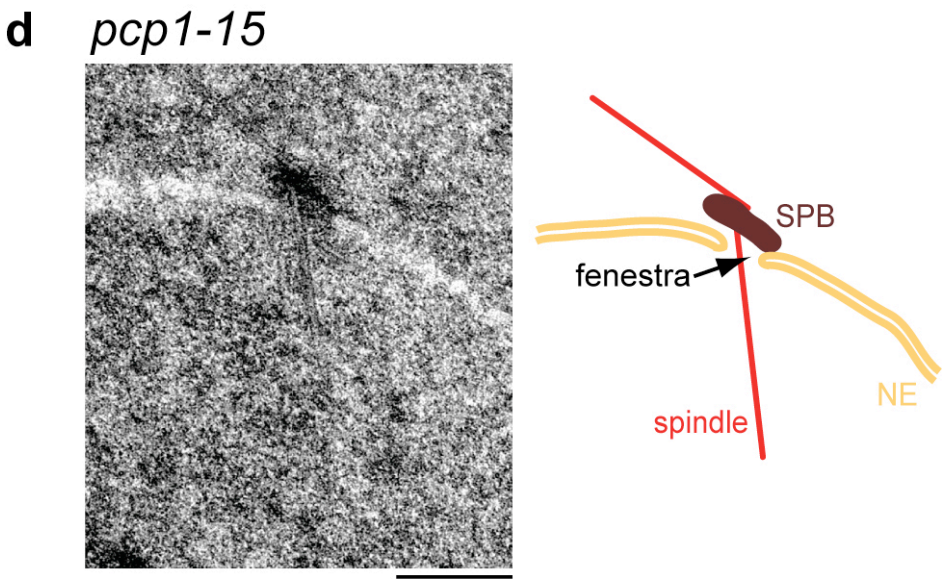

(Figure 4.4a, b and c are on the previous pages)

4.5 Cut11 localises to the nuclear envelope and the mitotic SPB normally in the *pcp1* mutants

The fact that increased expression of Cut11 suppresses the *pcp1-18* mutant, and that the *pcp1-18* cells showed defects in NE reorganisation and SPB insertion led me to wonder whether Pcp1 is involved in the recruitment of Cut11 to the SPB in mitosis. To address this, I introduced an endogenous, C-terminally tagged Cut11-GFP into the *pcp1-18* mutant and observed its localisation at 36^{o}C. mCherry-Atb2 was used to mark the microtubules but, most importantly, to identify mitotic cells through the detection of spindle microtubules.

In wild-type cells, Cut11-GFP localised to the nuclear membrane as well as the SPB during mitosis (Figure 4.5) (West et al., 1998). Interestingly, I observed a similar Cut11-GFP localisation pattern in the *pcp1-18* mutant (Figure 4.5), suggesting that Cut11 localisation is normal in the mutant.

4.6 Overexpression of Cut12 suppresses the *pcp1-18* mutant

Probing further into the underlying molecular defect in the *pcp1-18* mutant, I revisited the list of allele-specific multicopy suppressors and noticed that overproduction of the essential SPB component Cut12 also suppressed the temperature sensitivity of the *pcp1-18* mutant (Figure 4.6a) (Bridge et al., 1998). I accordingly examined whether Pcp1 is involved in Cut12 recruitment to the SPB, but again Cut12-GFP localised normally to the SPB in the *pcp1-18* cells at 36^{o}C (Figure 4.6b). These data imply that functional activities, rather than localisation, of Cut11 and Cut12 are impaired in the *pcp1-18* mutant.

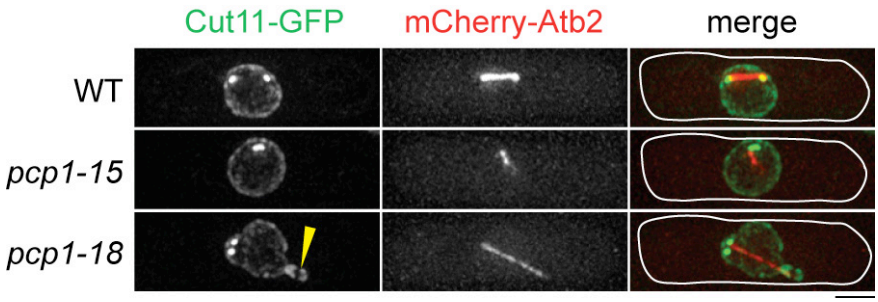

Figure 4.5 Cut11 localises to the mitotic SPB and nuclear envelope in the *pcp1* mutants.

Localisation of Cut11-GFP in live mitotic cells at 36°C. Arrowhead: NE herniation (probably corresponding to the NE deformation shown in EM picture in Figure 4.4b for *pcp1-18*). *n* > 50. Scale bar, 2 μm.

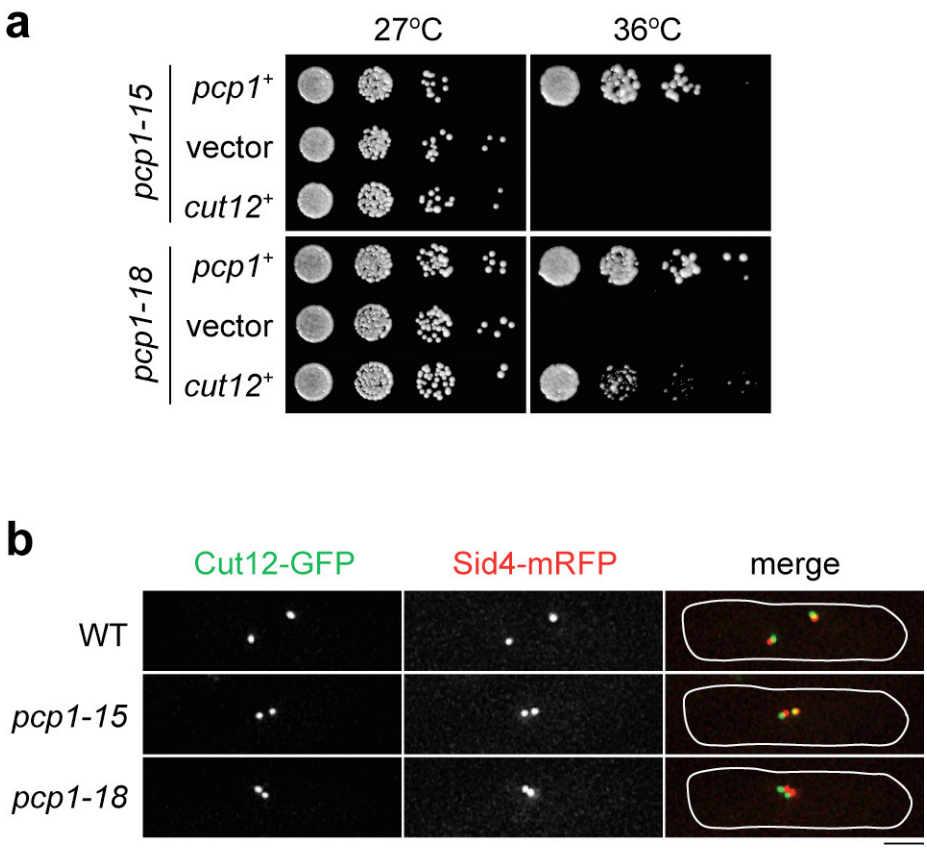

Figure 4.6 Cut12 overexpression specifically suppresses the *pcp1-18* mutant.

(a) Ten-fold serial dilutions of the *pcp1* mutants harbouring the indicated multicopy suppressors. (b) Live fluorescence imaging showing the normal localisation of Cut12-GFP to the SPB during mitotis at 36°C. *n* > 100. Scale bar, 2 μm.

4.7 Plo1 recruitment to the SPB is compromised in the *pcp1-18* mutant

Previous work showed that Cut12 plays a role in promoting G2 to M transition by activating polo kinase Plo1 upon mitotic entry (MacIver et al., 2003; Petersen and Hagan, 2005). Therefore, it is conceivable that Pcp1 is involved in regulating the function of Plo1. Suppression of *pcp1-18* by overexpression of Cut12 was perhaps brought about through Cut12's influence on the activity of Plo1. Given this notion, I examined Plo1-GFP localisation in the *pcp1-18* mutant at 36^{o}C. Sfi1-mRFP and mCherry-Atb2 were used to mark the SPB and microtubules, respectively.

In wild-type cells, Plo1-GFP localised to the SPB during mitosis (Figure 4.7a, b). Interestingly, I observed a significant reduction in Plo1-GFP signal at the SPB in the *pcp1-18* mutant, indicating partial delocalisation of Plo1 from the SPB at 36^{o}C (Figure 4.7a, b). This result was confirmed by an additional experiment, in which a *pcp1-15* or *pcp1-18* strain (each carrying Pol1-GFP, Sfi1-mRFP and mCherry-Atb2) was mixed with wild type cells (carrying only Plo1-GFP) in the same culture and shifted to the restrictive temperature. Under this condition, *pcp1-18* cells specifically lost GFP (Plo1) signals from the SPB (the top right panel in Figure 4.7c), whilst either wild type or *pcp1-15* cells retained GFP-Plo1 signals (top two panels). These data hence demonstrate a role for Pcp1 in Plo1 recruitment to the mitotic SPB.

It is worth noting that Plo1-GFP localisation in the *pcp1-15* mutant at 36^{o}C was less affected (Figure 4.7a, b), consistent with my previous data that Cut12 overexpression did not suppress the mutant.

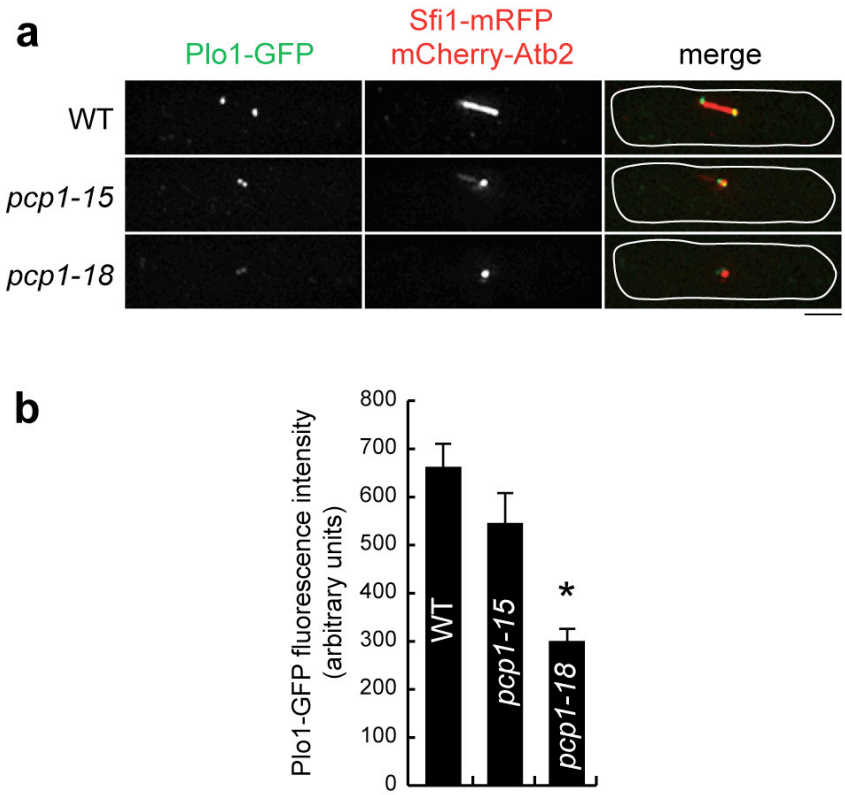

(Figure 4.7c is on the following page)

Figure 4.7 Pcp1 is required for recruitment of Plo1 to the SPB.

(a) Live fluorescence imaging showing delocalisation of Plo1-GFP from the mitotic SPB specifically in the *pcp1-18* mutant. (b) Quantification of Plo1-GFP signal intensity at the SPB in (a). Images were merged into a single projection using maximum intensity algorithm. Fluorescence signals were then quantified using maximum intensity, after subtracting background signals. Asterisk indicates that the difference is statistically significant (Student's *t*-test, $p < 0.01$). $n > 50$; error bars, standard error. (c) Cells of wild type (carrying Pcp1-GFP) and *pcp1-15* (left, carrying Plo1-GFP, Sfi1-mRFP and mCherry-Atb2) or *pcp1-18* (right, carrying Plo1-GFP, Sfi1-mRFP and mCherry-Atb2) were mixed in the same culture, shifted from 27°C to 36°C and incubated for 4 h. Live images of these mixed cell populations were shown. Note that Plo1-GFP signals disappeared from SPBs only in the *pcp1-18* cells (arrowheads). $n > 25$. Scale bar, 2 μm.

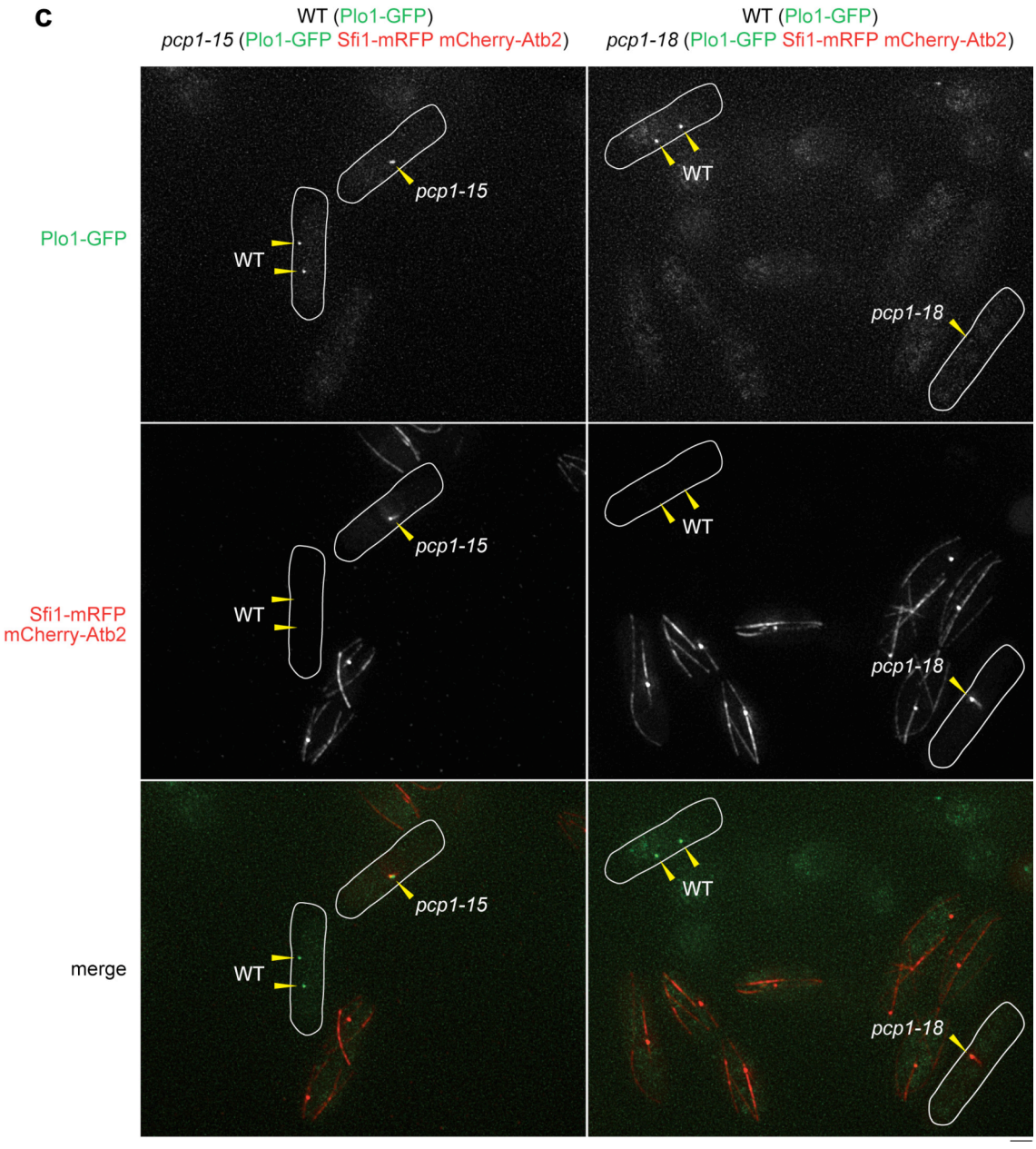

(Figure 4.7a and b are on the previous page)

4.8 Enhancing Plo1 recruitment to the SPB suppresses the *pcp1-18* mutant

To find out if the delocalisation of Plo1 was a primary defect of the *pcp1-18* mutant, I asked whether potentiating Plo1 recruitment to the SPB in the *pcp1-18* cells could suppress the mutant. For this purpose, I utilised a hypermorphic allele of *cut12, cut12.s11,* that enhances Plo1 recruitment to the mitotic SPB, through hyperactivating Plo1 activity (Hudson et al., 1990; MacIver et al., 2003; Petersen and Hagan, 2005). Indeed, *pcp1-18 cut12.s11* double mutants were capable of forming colonies at 34^{o}C, the semi-restrictive temperature for *pcp1-18* (Figure 4.8a). Furthermore it was found that Plo1 is recruited to the SPB in *pcp1-18cut12.s11* cells (Figure 4.8b and c). It is of note that not only *cut12.s11* but also multicopy *cut11*$^{+}$ restored Plo1 recruitment to the SPB in *pcp1-18* cells (Figure 4.9a and b).

Consistent with my previous observation that Plo1 localisation in the *pcp1-15* mutant was largely unaffected, no improvement in growth was seen in the double mutant *pcp1-15 cut12.s11* under the same condition (Figure 4.8a). Therefore, together with the Plo1 delocalisation data, these findings demonstrate that another function of Pcp1 in mitosis is to recruit Plo1 to the SPB.

4.9 Promoting mitotic entry also suppresses the *pcp1-18* mutant

Polo kinase plays pivotal roles in a variety of processes in cell division (Archambault and Glover, 2009; Nigg, 2007; Takaki et al., 2008). One of the established functions of Plo1 at the SPB is the advancement of mitotic entry (MacIver et al., 2003; Petersen and Hagan, 2005). If Pcp1's role in Plo1 recruitment lies in promoting mitotic entry, forced advancement in the onset of mitosis independently of Plo1 would suppress the *pcp1-18* mutant. To test this scenario, I constructed a double mutant between *pcp1-18* and *wee1-50*, a

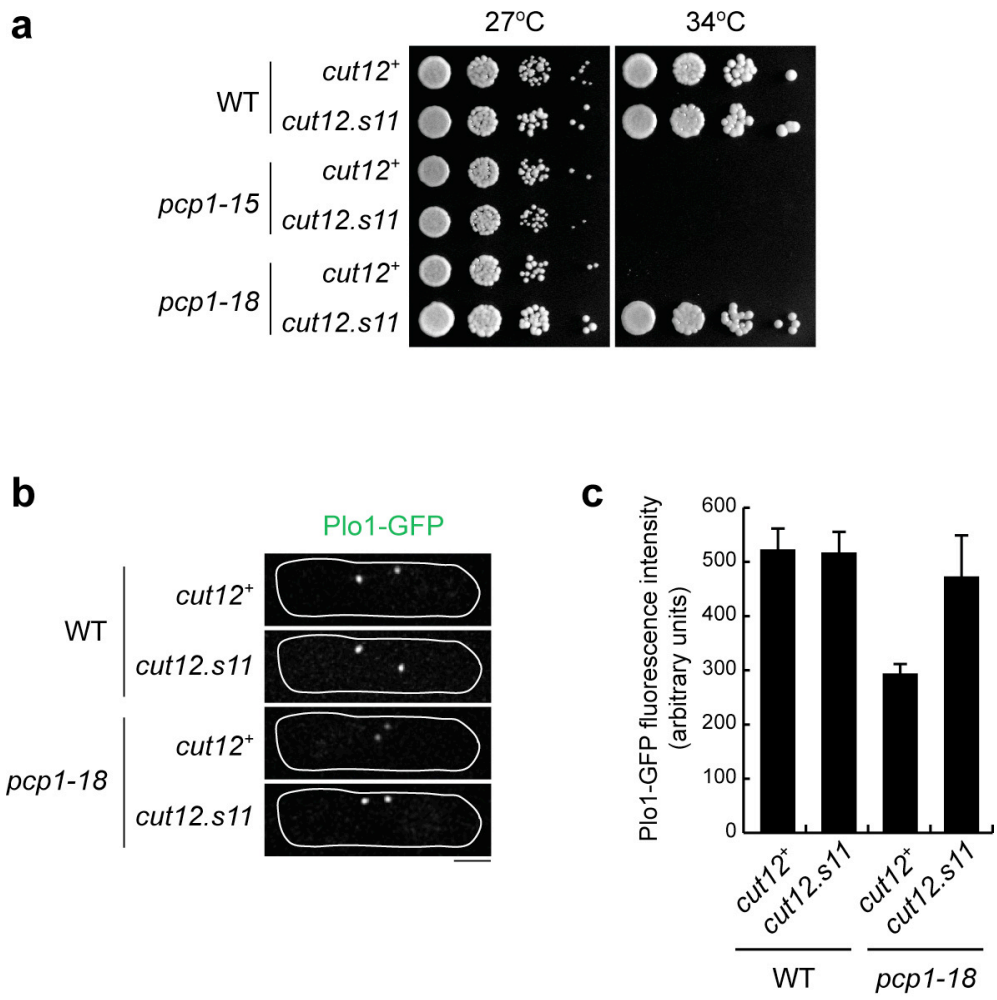

Figure 4.8 *pcp1-18* is suppressed by enhancing Plo1 recruitment to the SPB.

(a) Ten-fold serial dilution assays on YE5S media. (b) Increased recruitment of Plo1-GFP at the SPB in the *pcp1-18cut12.s11* double mutant at the semi-permissive temperature of 34°C. (c) Quantification of Plo1-GFP signal intensity at the SPB in G. $n > 50$; error bars indicate standard error. Scale bars, 2 μm.

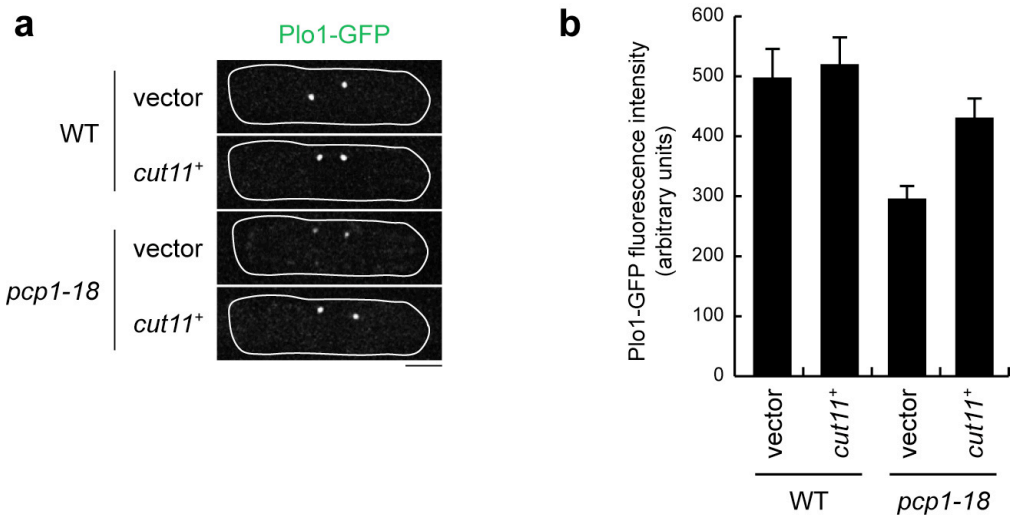

Figure 4.9 Plo1-GFP localisation to the SPB is restored in *pcp1-18* by introducing multicopy suppressor *cut11*$^{+}$.

(a) Plo1-GFP localisation to the SPB with or without the multicopy suppressor *cut11*$^{+}$ when incubated at 34^{o}C. (b) Quantification of Plo1-GFP signal intensity at the SPB in (a). $n > 50$; error bars represent standard error. Scale bar, 2 μm.

mutation that causes premature entry into mitosis due to untimely activation of Cdc2 (CDK1) (Nurse, 1990), and thus results in shorter cells compared to the wild-type. Remarkably, *pcp1-18wee1-50*, but not *pcp1-15wee1-50*, exhibited improved growth at the semi-permissive temperature of 32^{o}C (Figure 4.10a). Consistently, promoting mitotic entry with *cdc2-1w* (Nurse and Thuriaux, 1980) or *cdc2-3w* (Fantes, 1981) also specifically rescued the growth defects of *pcp1-18* (Figure 4.10b and c). These results, therefore, have uncovered a novel role for Pcp1 in the recruitment of Plo1 to the SPB to promote mitotic entry, and at the same time established a link between Plo1 recruitment, mitotic entry and SPB insertion into the NE (see more in General Discussion).

4.10 Synthetic genetic interactions between *pcp1* and its interacting genes

Synthetic genetic interaction is another way to establish functional interaction between two genes. We therefore examined synthetic genetic interaction between *pcp1-15* or *pcp1-18* and various temperature-sensitive mutations in genes that were identified in this study. These include *alp4*, *alp6*, *plo1*, *cut11* and *cut12*. Intriguingly temperature-sensitive *cut11.1* (West et al., 1998) or *cut12.1* mutants (Bridge et al., 1998) are synthetically lethal with either of *pcp1-15* or *pcp1-18* (Figure 4.11a). Furthermore although double mutants between *pcp1-15* or *pcp1-18* and *alp4-1891*, *alp6-719* (Vardy and Toda, 2000) or *plo1.ts19* (MacIver et al., 2003) were viable, their restriction temperatures were all lowered (Figure 4.11b). We posit that these results substantiate our findings on roles of Pcp1 in recruitment of the γ-TuC and Plo1 to the mitotic SPB. As both γ-TuC and Plo1 are essential for cell viability, simultaneous mutants either in the same or different pathways would lead to synthetic lethality.

As *pcp1-15* and *pcp1-18* show distinct defects, namely the failure in recruitment of the γ-TuC and Plo1, respectively, to the mitotic SPB, one might expect these two alleles to display intragenic complementation. To address this, we constructed various types of diploid strains containing heterozygous

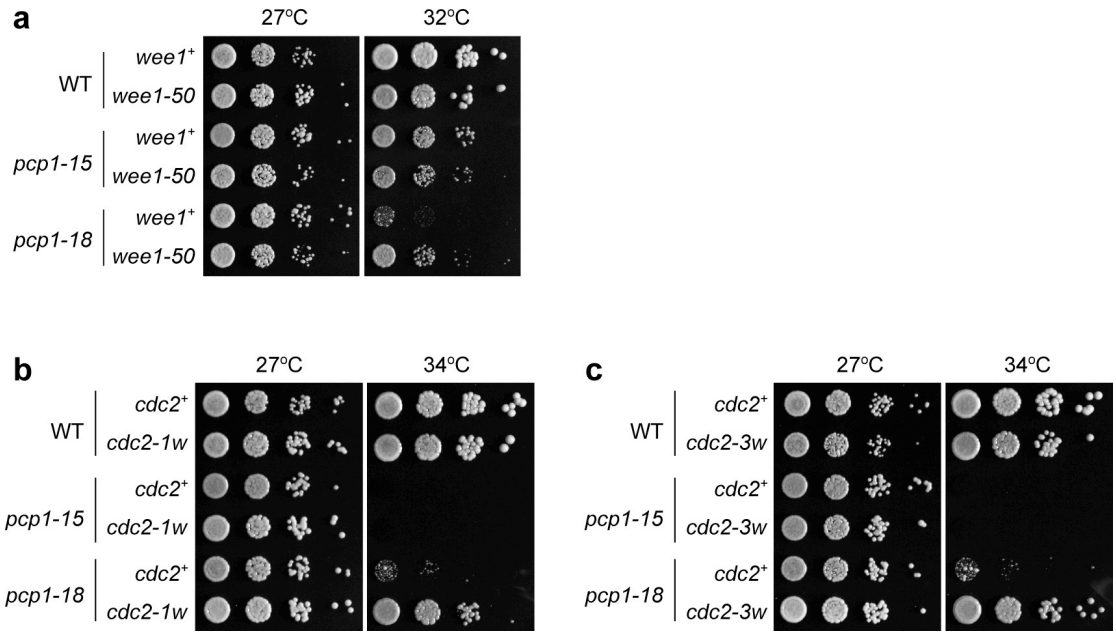

Figure 4.10 Premature mitotic entry suppresses the *pcp1-18* mutant specifically.

(a, b, c) Ten-fold serial dilution assays on YE5S media. *pcp1-18*, but not *pcp1-15*, is suppressed by promoting mitotic entry using the *wee1-50* (a), *cdc2-1w* (b) or *cdc2-3w* (c).

a

	synthetic lethal				
	cut11-1	*cut12.1*	*alp4-1891*	*alp6-719*	*plo1.ts19*
pcp1-15	yes	yes	*	*	*
pcp1-18	yes	yes	*	*	*

* restrictive temperature lowered (see caption)

b

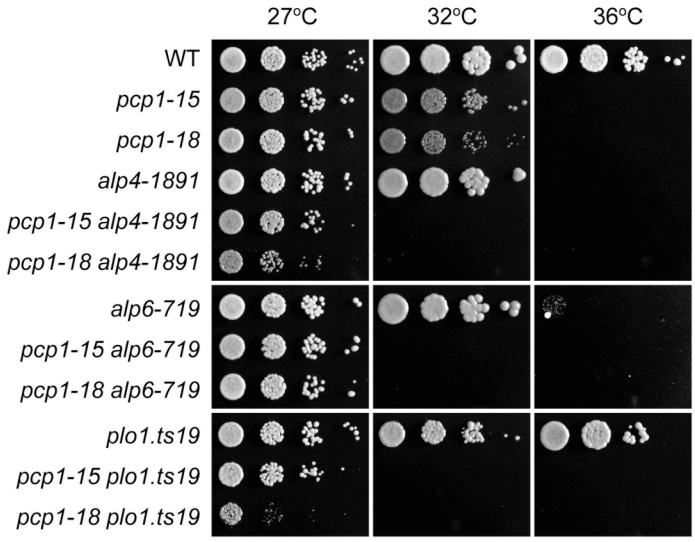

c

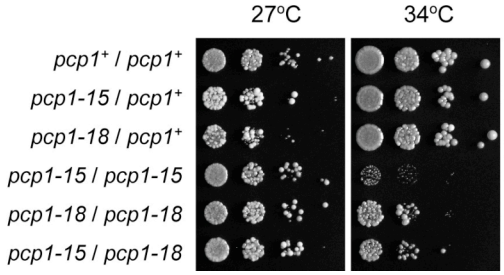

Figure 4.11 Synthetic genetic interactions between *pcp1* mutants and the mutants in genes that functionally and/or physically interact with Pcp1.

(a, b) Genetic interaction between *pcp1* mutants and individual mutants. *cut11.1* or *cut12.1* shows synthetic lethal interaction with both *pcp1-15* and *pcp1-18* (a). In contrast, double mutants between *alp4-1891*, *alp6-719* or *plo1.ts19* and *pcp1-15* or *-18* are viable, but their restriction temperature was lowered substantially (a, b). (b) Ten-fold serial dilution assays on rich YE5S media. (c) *pcp1-15* and *pcp1-18* do not show intragenic complementation. Temperature-sensitivity of diploid containing indicated genotypes were examined. Haploid strains were also spotted as controls. Note that both *pcp1-15* and *pcp1-18 are recessive, as pcp1-15/pcp1*$^+$ and *pcp1-18/pcp1*$^+$ heterozygous diploid strains could grow at the restrictive temperature.

(*pcp1-15/pcp1-18*) or homozygous *pcp1* alleles (*pcp1-15/pcp1-15, pcp1-15/pcp1*$^+$, *pcp1-18/pcp1-18* or *pcp1-18/pcp1*$^+$) and examined temperature sensitivity of each diploid. It was found that *pcp1-15* and *pcp1-18* mutations are recessive but no intragenic complementation was observed (Figure 4.11c).

4.11 Pcp1 physically interacts with Plo1 (and γ-TuC)

My data show that Pcp1 recruits γ-TuC and Plo1 to the SPB. Hence, this suggests the existence of physical interactions between Pcp1 and both γ-TuC and Plo1. To address this point, immunoprecipitation experiments were performed using an affinity purified anti-Pcp1 antibody with cell extracts prepared from wild type and the *pcp1* mutants.

I observed co-immunoprecipitation of both γ-TuC and Plo1 with Pcp1 (Figure 4.12, lane 13), indicating that Pcp1 physically interacted with both γ-TuC and Plo1. The interaction appeared to be fairly tight, as binding was sustainable against washing with high salt buffers (lanes 14 and 15, with buffers containing 0.3 and 0.5 M NaCl, respectively). Co-immunoprecipitation was specific as I did not pull down γ-TuC or Plo1 when pre-immune sera were used (lanes 4 to 6).

Next I performed immunoprecipitation with mutant extracts prepared from cultures under restrictive conditions (4 h at 36^{o}C). Contrary to a simple scenario predicting an impaired interaction between Pcp1 and γ-TuC/Plo1 in the mutants, the amounts of co-immunoprecipitated γ-TuC or Plo1 were not noticeably different between wild type and *pcp1-15* or *pcp1-18* even under the stringent, high salt wash conditions (Figure 4.12, lanes 16 to 21).

I envision that Pcp1 at the SPB constitutes only a small proportion of all Pcp1 in a cell. Consequently, changes in Pcp1's capacity to interact with γ-TuC and Plo1 at the SPB are masked by the pool of soluble Pcp1 in the cell. Indeed, in support of this speculation, I also did not detect a difference in the amount of co-immunoprecipitated γ-TuC and Plo1 with Pcp1, between interphase and

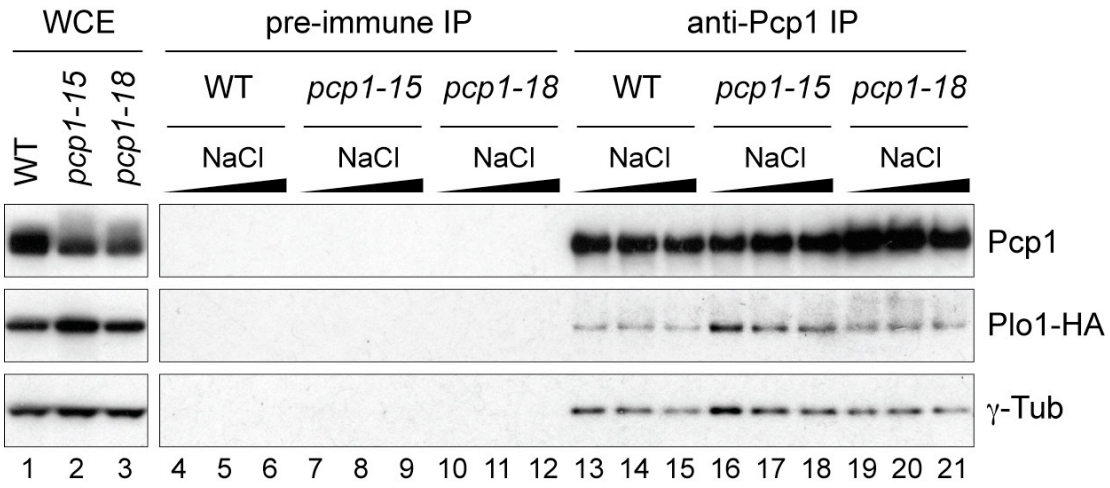

Figure 4.12 Pcp1 physically interacts with both γ-TuC and Plo1.

Wild type, *pcp1-15* or *pcp1-18* cells containing Plo1-GFP-HA were grown at 27°C and shifted up to 36°C for 4 h. Extracts were prepared and immunoprecipitation was performed with affinity-purified anti-Pcp1 antibodies. Immunoprecipitates were run on SDS-PAGE and immunoblotting was performed with anti-Pcp1 (1:5000), anti-HA (1:200) and anti-γ-tubulin (1:500) antibodies (lanes 13, 16 and 18). As a negative control, preimmune sera were used (lanes 4, 7 and 10). Immunoprecipitates on beads were further washed with high salt buffers containing 0.3 or 0 5 M NaCl (lanes 5, 8, 11, 14, 17 and 20 or lanes 6, 9, 12, 15, 18 and 21 respectively). Note that the salt concentration of original buffers is 0.15 M NaCl. 0.5 mg equivalent of immunoprecipitates and 30 μg of whole cell extract (WCE, lanes 1 to 3) were loaded.

mitosis even in wild-type cells (Figure 4.13), while cell biological data suggest an increased interaction between γ-TuC and Plo1 with Pcp1 during mitosis. Nonetheless, these results point towards the possibility that Pcp1 directly interacts with γ-TuC and Plo1, thereby playing a structural role as a mitotic platform for these factors to be recruited the SPB.

4.12 Summary

This chapter presented the analysis of the *pcp1-18* mutant. A multicopy suppressor screen identified the nuclear pore complex components, Cut11 and Pom152, and an essential SPB component Cut12 as specific suppressors of *pcp1-18* mutant, but not *pcp1-15*. Electron microscopy analysis showed that the *pcp1-18* mutant was defective in nuclear envelope reorganisation and SPB insertion. In addition to SPB insertion defects, *pcp1-18* also displayed reduced recruitment of polo kinase Plo1 to the SPB during mitosis. Furthermore, enhancing Plo1 recruitment to the SPB using the *cut12.s11* mutant, which restored Plo1 recruitment to the SPB in *pcp1-18*, suppressed the temperature sensitivity of the mutant. These data demonstrate that Pcp1 is required for Plo1 recruitment to the SPB during mitosis. Interestingly, promoting mitotic entry using the *wee1-50*, *cdc2-1w* or *cdc2-3w* also suppressed the growth defects of *pcp1-18*, hence establishing a role for Pcp1 in mitotic entry regulation. These findings unveiled a novel role for Pcp1 in the recruitment of Plo1 to the SPB to drive mitotic entry, nuclear envelope reorganisation and SPB insertion.

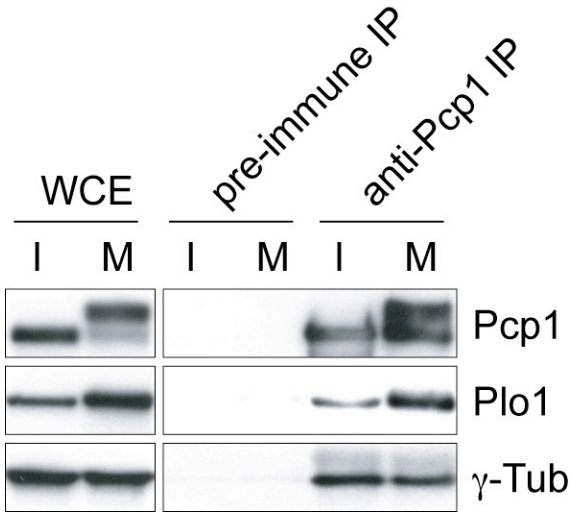

Figure 4.13 No increase in co-immunoprecipitated Plo1 and γ-TuC with Pcp1 was detected in a mitotic extract.

The strain used in this experiment carries the *nda3-311*, which arrests cells in mitosis at low temperatures (Hiraoka et al., 1984; Toda et al., 1983) (see section 5.3 for more information about the mutation). Interphase cells were prepared by incubating an exponentially growing culture with 12.5 mM hydroxyurea (HU) for 4 h at 30°C. Mitotic cells were prepared by incubating a culture at 20°C for 6 h. Immunoblotting was performed with anti-Pcp1 (1:5000), anti-HA (1:200, for detection of Plo1-GFP-HA) and anti-γ-tubulin (1:500) antibodies. I: interphase extract, M: mitotic extract, WCE: whole-cell extract. Note that the increase in co-immunoprecipitated Plo1 in the mitotic extract is probably due to an increased expression of Plo1 in mitotically-arrested cells. It is also of note that Pcp1 shows a mobility shift during mitosis (see Chapter 5).

5 Pcp1 is phosphorylated by polo kinase during mitosis

5.1 Overview

This chapter describes my attempt to understand the potential biological significance of Pcp1 phosphorylation. I present evidence for post-translational modification of Pcp1 during mitosis. Further analysis established that Pcp1 is phosphorylated by polo kinase Plo1. I also describe the strategy that I used to generate an integrated phospho-residue mutant of Pcp1, and the subsequent analysis done on the mutant. Finally, I report my attempt to map *in vivo* phosphorylation sites of Pcp1 using mass spectrometry. These data show that Pcp1 is phosphorylated by Plo1 during mitosis, although I was so far unable to define the function of the phosphorylation.

5.2 Pcp1 carries putative mitotic kinases phosphorylation sites

I have shown that Pcp1 recruits Plo1 to the SPB to drive mitotic entry and SPB insertion during mitosis. This raised the possibility that Pcp1 is subject to regulation by Plo1 phosphorylation. Indeed, Spc110 was shown to be phosphorylated during mitosis, although by different protein kinases (Friedman et al., 1996; Stirling and Stark, 1996) (see section 1.10.1).

First, I made a visual inspection of Pcp1 sequence and found one putative polo-box-domain (PBD) recognition motif, $SSP^{905-907}$ (consensus sequence S-[ST]-P), and >30 potential polo kinase phosphorylation sites (consensus sequence [ED]-X-[ST]) (Figure 5.1a, polo kinase phosphorylation sites not shown). It has been shown that the binding of polo kinase to its substrates requires a priming kinase, hence it was not surprising that I also detected two putative cyclin-dependent kinase (CDK) phosphorylation sites on Pcp1, $TPLR^{55-58}$ and

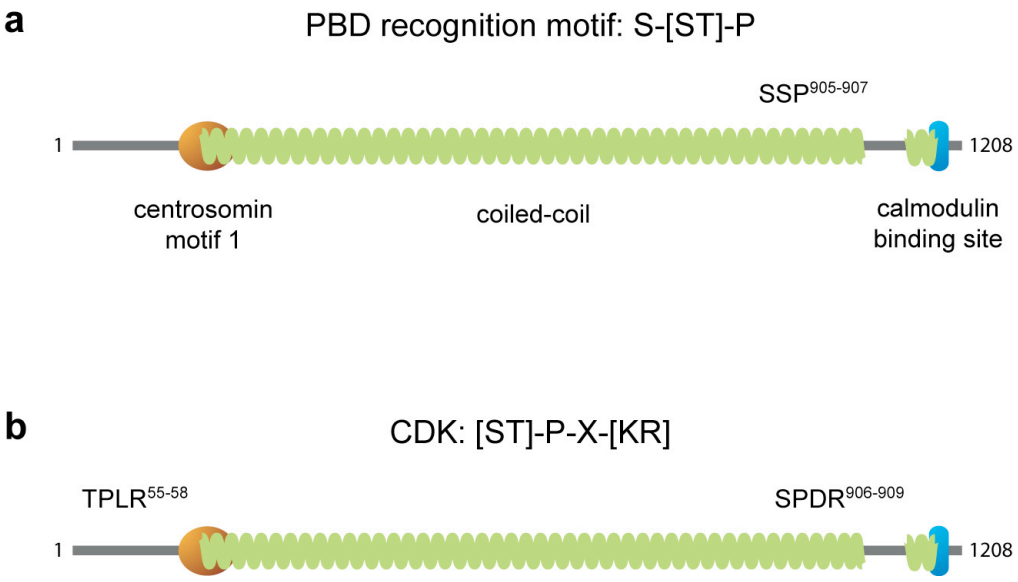

Figure 5.1 Putative mitotic kinase phosphorylation sites in Pcp1.

Pcp1 carries one putative polo-box-domain (PBD) recognition motif ($SSP^{905-907}$) and two putative cyclin-dependent kinase (CDK) phosphorylation sequences ($TPLR^{55-58}$, $SPDR^{906-909}$). The CDK site found at the C-terminus overlaps with the PBD recognition motif in Pcp1.

SPDR$^{906-909}$ (consensus sequence [ST]-P-X-[KR]), with the latter located right within the PBD recognition motif (Figure 5.1b). While this work was being carried out, it was reported that serine 905 and 906 of Pcp1 were indeed phosphorylated *in vivo* (Wilson-Grady et al., 2008). These observations raised the possibility that CDK and polo kinase regulate the function of Pcp1 through phosphorylation.

5.3 Pcp1 is post-translationally modified during mitosis

Before I examined if the putative mitotic kinase phosphorylation sites have a role in regulating Pcp1's function, I asked whether Pcp1 is indeed a cell-cycle dependent phosphoprotein. I first examined whether there is a mobility shift in Pcp1 in cells progressing through the cell cycle synchronously.

For this experiment, I utilised the temperature-sensitive *cdc25-22*, a mutant that is arrested in late G2 and is unable to enter mitosis at the restrictive temperature of 36^{o}C (Fantes, 1979). Firstly, an exponentially growing culture of *cdc25-22* was shifted up to 36^{o}C for 4 h 15 min, to arrest the cells in late G2. The arrested cells were then shifted down to 26^{o}C to allow the cells to synchronously enter mitosis. Samples were harvested every 15 min for 2 h for immunoblot analysis, scoring of septation index and DNA staining. Anti-Pcp1 antibody was used to detect Pcp1.

When the protein extracts were run on a 3-8% tris-acetate polyacrylamide gel, which provided a better resolution for proteins with high molecular weight (Pcp1 is about 150 kDa in size), I observed a mobility shift in Pcp1 peaking at around 45 min after the temperature shift-down (Figure 5.2a). This corresponded to the period the cells were in mitosis, as observed by DNA staining. Furthermore, the mobility shift disappeared at around 75 min, close to the time the septation index peaked, or S phase occured (Figure 5.2a).

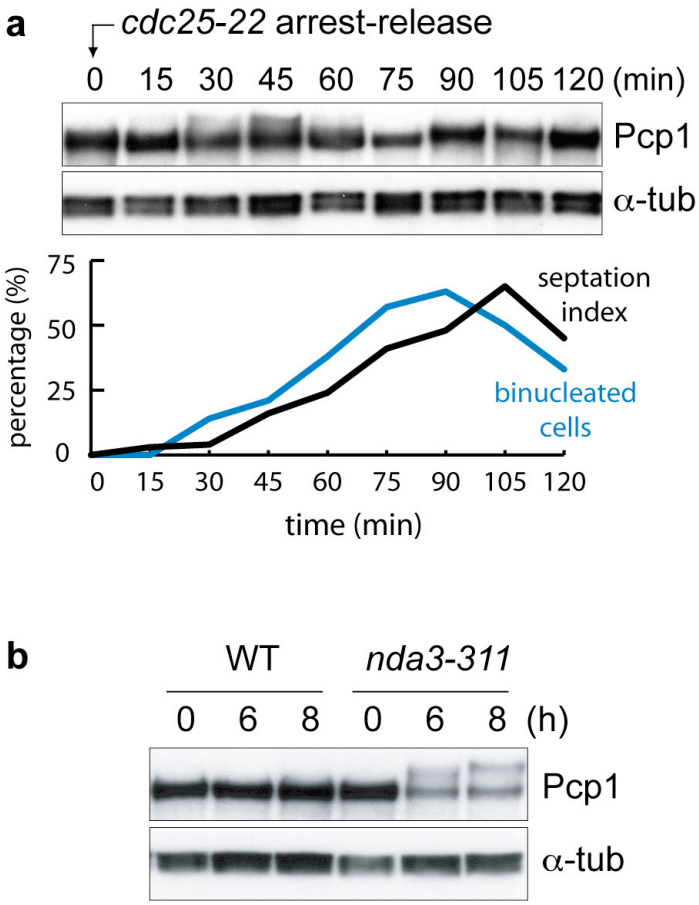

Figure 5.2 Post-translational modification of Pcp1 during mitosis.

Immunoblots of Pcp1 following electrophoresis on 3-8% tris-acetate polyacrylamide gels. α-tubulin was used as a loading control. (a) Cells progressed through the cell cycle synchronously following a *cdc25-22* arrest-release. Cell cycle progression was monitored through septation index and DNA staining. (b) Cells were arrested in mitosis using the *nda3-311* mutant.

To confirm this mitosis-specific mobility shift, I examined Pcp1's mobility in mitotically-arrested cells using the cold-sensitive *nda3-311*, a β-tubulin mutant that disrupts spindle assembly and arrests cells in mitosis (Hiraoka et al., 1984; Toda et al., 1983). In this experiment, an exponentially growing culture of the *nda3-311* mutant was incubated at 20°C for 8 h, to arrest cells in mitosis. Samples were harvested at 0, 6 and 8 h for immunoblot analysis. Indeed, I observed a mobility shift in Pcp1 at 6 and 8 h into the mitotic arrest (Figure 5.2b). Taken together, these data show that Pcp1 is likely to be posttranslationally modified during mitosis.

5.4 Pcp1 is phosphorylated during mitosis

Many forms of posttranslational modification can cause a mobility shift in a protein gel, including phosphorylation and acetylation. To find out if the mobility shift observed in Pcp1 is indeed due to phosphorylation, I tested whether phosphatase treatment reversed the mobility shift.

I immunoprecipitated Pcp1 from mitotic-arrested cells using anti-Pcp1 coupled protein A dynabeads. Then, 100 U of λ-phosphatase was added to the beads, with or without the presence of phosphatase inhibitors (10 mM NaV, 50 mM NaF). The reactions were incubated at 30°C for 30 min. Pcp1 was finally eluted from the beads and subjected to immunoblot analysis. I observed that when λ-phosphatase was added to the beads, the mobility shift in Pcp1 was abolished (Figure 5.3). Consistently, inhibiting the λ-phosphatase activity by adding the phosphatase inhibitors preserved the mobility shift of Pcp1 (Figure 5.3). Taken together, these findings show that Pcp1 is phophorylated in mitosis.

5.5 Pcp1 is phosphorylated by polo kinase Plo1

The fact that Pcp1 recruits Plo1 and the presence of a putative PBD recognition motif as well as multiple polo kinase phosphorylation sites on Pcp1 suggest that Plo1 might be responsible for the phosphorylation observed in Pcp1. To

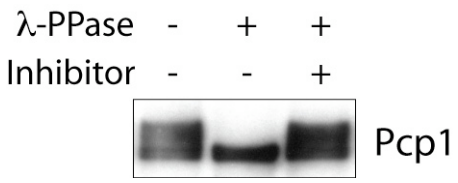

Figure 5.3 Pcp1 is post-translationally modified by phosphorylation.

Immunno-precipitated Pcp1 prepared from mitotically-arrested cells (using *nda3-311*) was treated with λ-phosphatase, with or without phosphatase inhibitors. Immunoblot was done with anti-Pcp1 antibody.

address this, I examined whether phosphorylation of Pcp1 in mitosis is abolished in the temperature-sensitive *plo1* mutant, *plo1-ts19* (MacIver et al., 2003).

I compared mitotic-arrested cells in the presence or absence of functional Plo1, using the temperature-sensitive *nda3-1828* and *plo1-ts19* mutants, respectively. The *plo1-ts19* mutant arrests cells in mitosis and has severely reduced Plo1 activity (MacIver et al., 2003). The *nda3-1828* mutant also arrests cells in mitosis (Radcliffe et al., 1998), but presumably in the presence of normal level of Plo1 activity, and hence served as a control in this experiment.

Cells were harvested after 3 h incubation at 36^{o}C. Microtubules were stained with TAT-1 to detect spindle microtubules for mitotic index scoring. I observed that the phosphorylated form of Pcp1 was notably reduced in the *plo1-ts19* mutant (Figure 5.4a). The reduction in Pcp1 phosphorylation in the *plo1-ts19* mutant was not due to the cell's inability to enter mitosis, as I detected comparable percentage of mitotic cells in both the control and the *plo1-ts19* mutant (Figure 5.4a).

To provide further evidence that Pcp1 is phosphorylated by Plo1, I overexpressed a constitutively active variant of Plo1, Plo1.SDTD (MacIver et al., 2003), under the thiamine-repressible attenuated promoter *nmt41* (Basi et al., 1993). I then assessed if Pcp1 phosphorylation is induced even in interphase cells. Interestingly, I could observe a mobility shift in Pcp1 when Plo1.SDTD was overexpressed, but not in the control experiment where a wild-type Plo1 was overexpressed (Figure 5.4b). As confirmed by microtubule staining, the cells indeed remained in interphase, demonstrating that the mobility shift was not due to accumulation of mitotic cells. Taken together, these data demonstrate that Pcp1 is phosphorylated by Plo1 in mitosis.

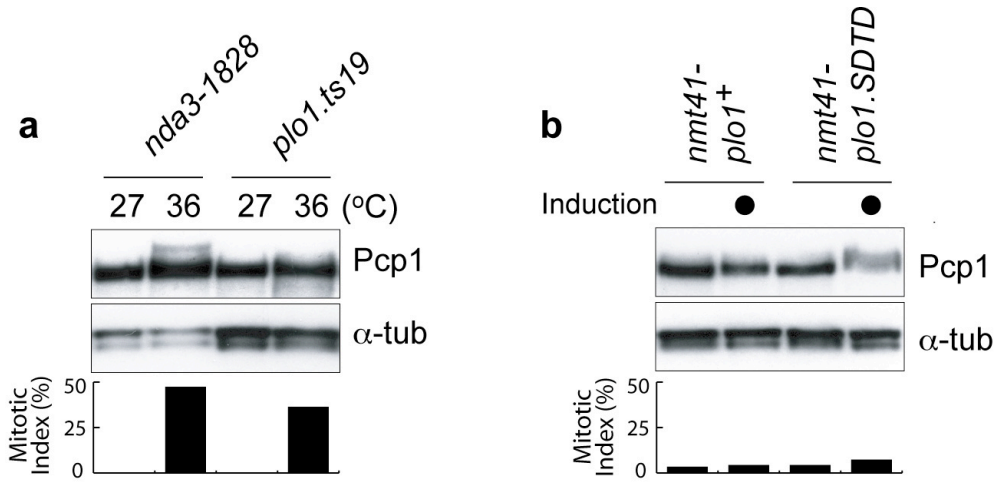

Figure 5.4 Pcp1 is phosphorylated by polo kinase Plo1.

(a) Pcp1 phosphorylation is significantly reduced in the polo kinase mutant *plo1.ts19*. (b) Pcp1 phosphorylation is induced in interphase cells when the constitutively active variant of polo kinase, *plo1.SDTD*, is overexpressed under the control of the thiamine repressible *nmt41* promoter. Thiamine removal induces expression of the proteins, after 22 h at 27°C. In both a and b, mitotic index was monitored with microtubule staining using the TAT-1 antibody. α-tubulin was used as a loading control.

5.6 Generation of an integrated phospho-residue mutant of Pcp1

To understand the biological significance of Pcp1 phosphorylation, I attempted to create a phospho-deficient mutant of Pcp1. To this end, I mutated the phospho-residues (threonine 55 and serine 906) of the two CDK phosphorylation sites (threonine 55 is putative) on Pcp1 (Figure 5.5a). I also mutated serine 905 of the putative PBD recognition motif (Figure 5.5a), aiming to disrupt the binding of Plo1 to Pcp1 and consequently prevent the phosphorylation of Pcp1. Postulating that phosphorylation is essential for Pcp1 function, I then assessed whether this mutant exhibits any defective phenotype.

To do this, I devised a system where I could introduce a mutated version of *pcp1* into the genome, while the viability of the strain is maintained by a wild-type copy of *pcp1*$^+$ on a plasmid. First, I deleted one copy of *pcp1*$^+$ in a stable diploid background using an *ura4*$^+$ cassette. Tetrad analysis was then performed to confirm that URA+ spores were non-viable (Figure 5.5b). I found that the non-viable spores were able to germinate but were not able to go through cell division and died at the one-cell stage (Figure 5.5b).

A plasmid with *pcp1*$^+$ (containing a Sc*LEU2* marker) was transformed into the hemizygous diploid. The diploid was sporulated and a haploid strain that was URA+ and LEU+ was selected. This haploid strain, *pcp1::ura4*$^+$ *pAL-SK-pcp1*$^+$, was viable because of the extragenic copy of *pcp1*$^+$ carried on the plasmid.

At the same time as I was isolating the haploid strain, I performed site-directed mutagenesis to mutate the two phopho-residues of CDK and the serine residue of PBD recognition motif in *pcp1*$^+$. The mutagenised *pcp1* was PCR amplified and the DNA fragments were transformed into the haploid strain. This allowed integration of the mutated *pcp1* into the genome to replace the *ura4*$^+$ cassette. The integrants which were now URA- were selected on 5-fluoroorotic acid (5-FOA) plates. Positive integrant was confirmed by the presence of restriction sites introduced during the site-directed mutagenesis (see Materials

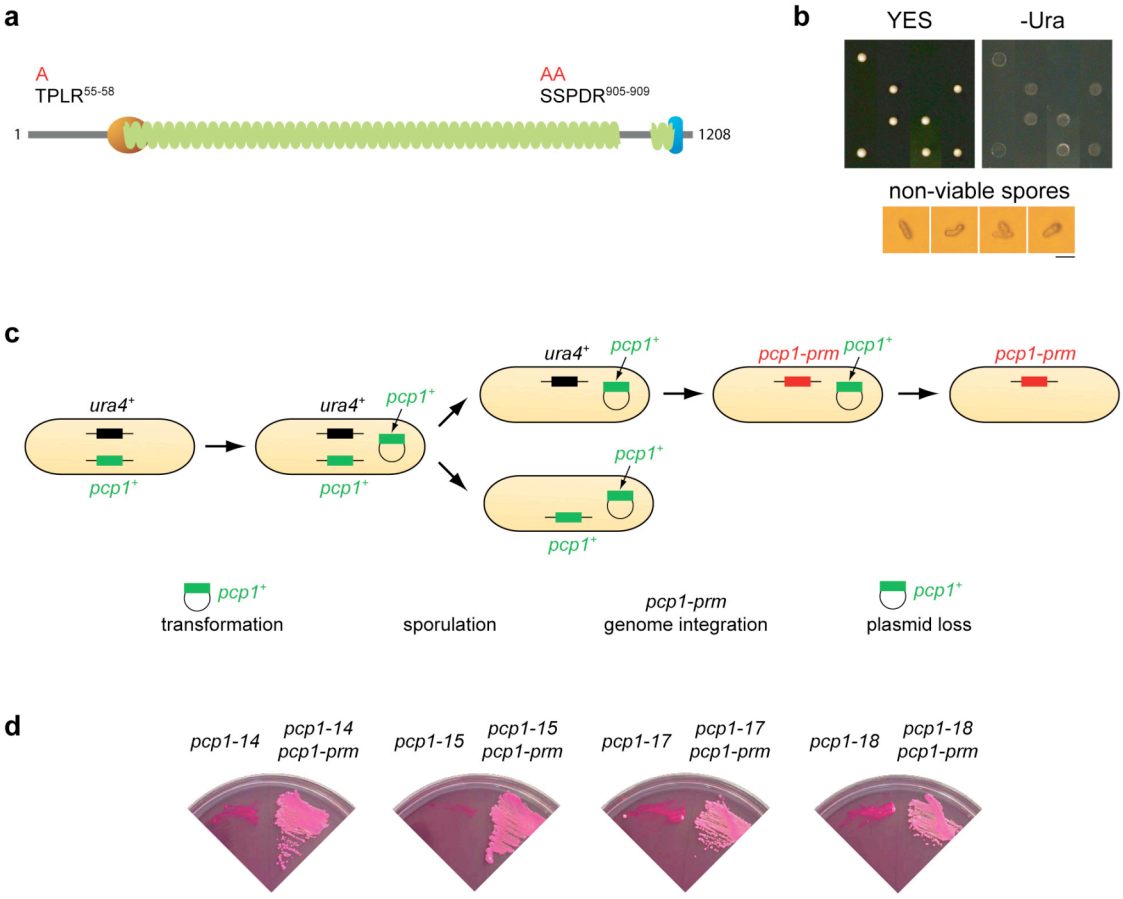

Figure 5.5 Generation of *pcp1-prm* mutant.

(a) Threonine 55, serine 905 and serine 906 were mutated to alanine in Pcp1. (b) Tetrad analysis of *pcp1* hemizygous diploid. Two out of four spores were inviable, and none of the viable spores were URA+, confirming the essentiality of *pcp1*. Most non-viable spores germinated but did not manage to divide. (c) A schematic diagram of *pcp1-prm* mutant generation. A plasmid carrying $pcp1^+$ was transformed into *pcp1* hemizygous diploid. The diploid strain was sporulated. The haploid strain with $ura4^+$ cassette and $pcp1^+$ plasmid was transformed with *pcp1-prm* PCR fragments for genome integration. The $pcp1^+$ plasmid was then removed from the integrant by growing in the non-selective medium YE5S. (d) Suppression of growth defects at 36°C when the plasmid containing *pcp1-prm* was transformed into the *pcp1* mutants. Scale bar, 10 μm.

and Methods). One positive integrant was obtained from this procedure, and was named *pcp1-prm* (*prm* for phospho-residue mutant) (see Figure 5.5c for a schematic diagram of *pcp1-prm* mutant generation).

The plasmid carrying *pcp1*$^{+}$ was removed from the integrant by growing the cells in a non-selective medium. I was able to obtain a high number of LEU- colonies. This indicates that *pcp1-prm* is not essential for viability. Consistently, transforming the plasmid carrying *pcp1-prm* into the *pcp1* mutants suppressed temperature-sensitivity at 36^{o}C (Figure 5.5d).

5.7 Mutating the Pcp1 phospho-residues did not abolish Pcp1 phosphorylation

Upon the successful isolation of the *pcp1-prm* mutant, I examined whether Pcp1 phosphorylation in mitosis is abolished in the mutant. Unfortunately, I did not see a significant reduction of Pcp1 phosphorylation in the mutant when the cells were arrested in mitosis using the cold-sensitive *nda3-311* (Figure 5.6a)(see more in General Discussion).

I also investigated if the phospho-residue mutant displays any temperature-sensitive, cold-sensitive or TBZ sensitive phenotype. However, I did not observe any difference in growth compared to wild-type cells under the conditions tested (Figure 5.6b). Taken together, I conclude that the phospho-residue mutant I created did not affect Pcp1 phosphorylation, nor its function.

5.8 An attempt to map Pcp1 phosphorylation sites by mass spectrometry

I was unable to disrupt phosphorylation of Pcp1 by mutating the phospho-residues of the two CDK phosphorylation sites (one is putative) and the putative PBD recognition motif. I therefore sought to determine *in vivo* phosphorylation

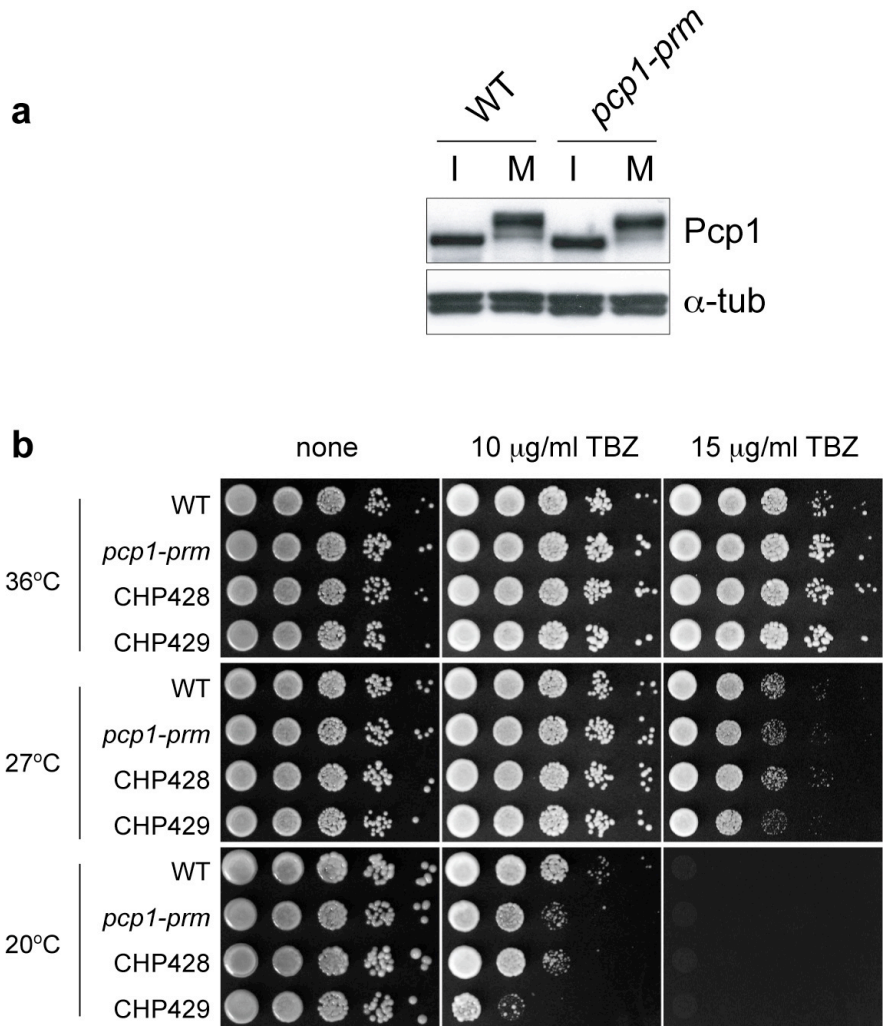

Figure 5.6 Pcp1's phosphorylation is not abolished in the *pcp1-prm* mutant.

(a) Immunoblot of Pcp1. Interphase and mitotic cells were prepared by hydroxyurea (HU) and *nda3-311* arrest, respectively. I: interphase extract, M: mitotic extract. (b) Ten-fold serial dilution assays on YE5S media. CHP428 and CHP429 were the two parental haploid strains used to create the diploid strain, from which *pcp1-prm* was isolated.

sites of Pcp1 by mass spectrometry. To do this, I performed large-scale purification of phosphorylated Pcp1 from cells arrested in mitosis by immunoprecipitation. I grew 40 L of the *nda3-311* mutant at 32^{o}C overnight until it reached a cell density of 5x10^{6} cells/ml. The culture was then shifted down to 20^{o}C for 6 h to arrest the cells in mitosis. Cells were harvested and washed in 800 ml STOP buffer. Cells were spun down again and were resuspended in 80 ml IP buffer. Cell 'popcorn' was prepared and stored at -80^{o}C until it was ready for cell breakage. Cell 'popcorn' was ground with a freezer mill, with the following settings – 2 min grind, 2 min cool, 14 impact rate, 6 cycles. About 65 g of ground cells were collected at the end of the grinding. 80 ml of IP buffer was added to the cells.

For the immunoprecipitation, I added 200 μl of anti-Pcp1 coupled protein A dynabeads to 25 ml of protein extract. The reaction was incubated at 4^{o}C for 1 h before extensive wash was applied. 60 μl of SDS loading buffer was added to the beads. After elution, 30 μl of the extract was loaded onto a 3-8% tris-acetate polyacrylamide gel. The gel was stained with Coomassie Blue (Figure 5.7). Pcp1 band was excised from the gel dried in a tube with a speed vac for 30 min. The dried gel was then sent to Duncan Smith at the Paterson Institute for Cancer Research (Manchester) for QTRAP mass spectrometry analysis.

Although I was able to detect Pcp1 peptide in the gel after trypsin digestion, with a peptide coverage of about 75%, I was unable to detect any phosphorylation sites on Pcp1. I was not sure of the reason for the inability to detect phosphorylation sites in the peptides, although it was suggested that an alternative digestion method that would achieve 95% peptide coverage could improve phosphorylation site detection. I have not pursued this aspect of the project since.

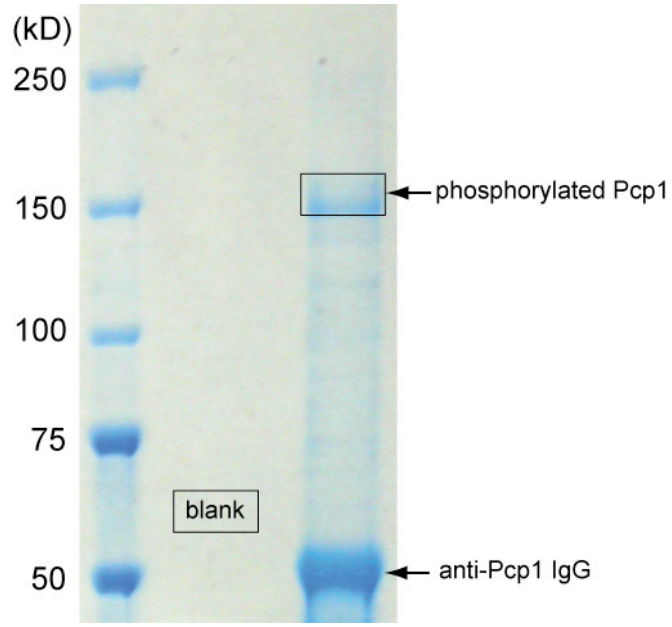

Figure 5.7 Large-scale immunoprecipitation of phosphorylated Pcp1 for mass spectrometry analysis.

Immunoprecipitated Pcp1 was subjected to SDS-PAGE, and the gel was stained with Coomassie blue. A blank gel was excised for background control.

5.9 Summary

This chapter presented the characterisation of Pcp1 phosphorylation in mitosis. Pcp1 was found to carry >30 potential polo kinase phosphorylation sites (consensus sequence [ED]-X-[ST]), and I showed that Pcp1 was indeed phosphorylated by polo kinase Plo1 during mitosis. Pcp1 phosphorylation is reduced in the *plo1* mutant, and conversely overexpression of a constitutively active variant of *plo1* induced phosphorylation of Pcp1 during interphase. Although I have created an integrated phospho-residue mutant of Pcp1, the mutant still exhibited phosphorylation during mitosis. Furthermore, I did not observe any growth defects that might suggest a compromise in Pcp1 function. In conclusion, the phospho-residue mutant of Pcp1 I created was not affecting Pcp1 phosphorylation nor its function. Lastly, my first attempt to map the *in vivo* phosphorylation sites of Pcp1 by mass spectrometry was not successful, which could be due to technical reasons.

6 General Discussion

The spindle pole body component Pcp1 was identified as the fission yeast orthologue of the pericentrin family of proteins (Flory et al., 2002). It is a large coiled-coil protein with a calmodulin binding domain and a centrosomin motif 1 at the C- and N-terminus, respectively. Its overexpression was shown to cause the assembly of ectopic SPB-like structures that were capable of nucleating spindle microtubules, which resulted in the formation of monopolar spindles and ultimately, chromosome missegregation (Flory et al., 2002). Consistent with a role in spindle assembly, deletion of *pcp1*$^{+}$ was shown to be lethal to the cell (Flory et al., 2002).

Pcp1 was postulated, but was never shown, to be the γ-TuC recruitment factor to the SPB based on its sequence homology to the pericentrin-like proteins, many of which are associated with a role in γ-TuC recruitment (Fong et al., 2008; Kawaguchi and Zheng, 2004; Knop and Schiebel, 1997; Samejima et al., 2008; Sawin et al., 2004; Takahashi et al., 2002; Zhang and Megraw, 2007; Zimmerman et al., 2004). However, Pcp1's location at the SPB periphery and its large size suggests that it could be more than just a γ-TuC recruitment factor, but a recruitment platform for multiple regulatory or structural proteins that regulate multiple functions of the SPB.

6.1 Role of Pcp1 in spindle assembly

Our approach in studying the functions of Pcp1 through the generation of temperature-sensitive *pcp1* mutants enabled the isolation of separation-of-function mutants. This overcame the limitation of analysis of gene deletion or shut-off mutants, where all of the functions of a protein were removed, leading to compounded defects that are difficult to delineate. Among the 11 temperature-sensitive *pcp1* mutants isolated (from a screen of about 5000

transformants), *pcp1-15* and *pcp1-18* were two of the mutants that exhibited no defect in Pcp1 stability and localisation to the SPB.

We showed that both *pcp1-15* and *pcp1-18* mutants exhibited a monopolar spindle phenotype, which led to chromosome segregation defects, mitotic delay and loss of viability in mitosis. We also demonstrated that the monopolar spindles originated from the mother SPB, presumably because once the mutant Pcp1 proteins were incorporated into the mother SPB, they were less sensitive to heat denaturation at 36^{o}C and thereby retained some spindle assembly capacity in an asymmetrical fashion. The possibility that the spindle assembly defect was due to an SPB duplication defect was ruled out as we observed two SPBs in the mutant cells at 36^{o}C.

Spindle microtubule fluorescence intensity in the *pcp1* mutant was significantly reduced compared to wild-type cells. This is, however, not a general feature of mutants that are defective in bipolar spindle formation. For instance, the kinesin-5 mutant *cut7-24*, which fails to interdigitate microtubules emanating from the two SPBs during mitosis, is also defective in bipolar spindle formation (Hagan and Yanagida, 1990, 1992). Yet, the *cut7-24* mutant does not show a reduction in spindle microtubule fluorescence intensity when compared to wild type cells (personal communication, Dr. Hirohisa Masuda). These results therefore suggest that spindle microtubule nucleation is impaired in the *pcp1* mutants.

The fact that the two SPBs in the *pcp1* mutants were separated at some point during mitosis, as indicated in our live-cell analysis, was intriguing to us. One of the essential steps of SPB or centrosome separation is the interdigitation of the two half spindles from the duplicated SPBs (de Gramont et al., 2007; Hagan and Yanagida, 1992; Mayer et al., 1999; Roof et al., 1992; Saunders and Hoyt, 1992). In the *pcp1* mutants, although spindle microtubules were emanated from only one of the SPBs (the mother SPB), the duplicated SPBs could be separated. One possible explanation is that the daughter SPB is still nucleating some spindle microtubules (albeit below detection with our microscopy system),

which interdigitate with the spindle microtubules nucleated from the mother SPB to allow SPB separation. Alternatively, even when the daughter SPB is completely incapable of nucleating spindle microtubules, it is linked to currently unidentified components that have affinity to the plus-end of spindle microtubules from the mother SPB. These abnormal 'pole-to-pole' spindle microtubules then push the two SPBs apart as the microtubules elongate, without the need to interdigitate microtubules from two SPBs.

A third possibility is that the SPB separation in the *pcp1* mutants is microtubule-independent, but relies on the motion force of other factors such as actin filaments, as shown for centrosome separation in metazoans during prophase (Rosenblatt et al., 2004; Wang et al., 2008; Whitehead et al., 1996). Whether SPB separation is dependent on the action of microtubules or actin filaments could be tested by the addition of carbendazim (CBZ/MBC) or latrunculin to the *pcp1* mutants, which would disrupt the microtubules and actin filaments respectively. The effect of these drugs on SPB separation in the mutants is then observed. If indeed the SPB separation were dependent on microtubule function, treatment with CBZ/MBC, but not latrunculin, would prevent the separation of the SPBs in the *pcp1* mutants.

6.2 Pcp1 and γ-TuC recruitment

We showed that Pcp1 was required for γ-TuC recruitment to the SPB, which confirmed its postulated role, and is in line with the function of the characterised pericentrin-like proteins (Fong et al., 2008; Kawaguchi and Zheng, 2004; Knop and Schiebel, 1997; Samejima et al., 2008; Sawin et al., 2004; Takahashi et al., 2002; Zhang and Megraw, 2007; Zimmerman et al., 2004). Delocalisation of γ-TuC from the SPB was observed only in the *pcp1-15* mutant, but not in *pcp1-18*. Consistent with this observation, restoring γ-TuC localisation to the SPB by mild overexpression of a γ-TuC component, Alp4/Spc97/GCP2, specifically suppressed the temperature sensitivity of the *pcp1-15* mutant, while conferred no growth advantage to *pcp1-18* at the same semi-restrictive temperature.

Crucially, the suppression of *pcp1-15* by restoring γ-TuC localisation to the SPB indicates that γ-TuC delocalisation is a primary defect, but not a secondary consequence of the mitotic failure of the mutant.

A conserved γ-TuC binding domain has recently been identified in pericentrin-related proteins including centrosomin, Mto1 and Pcp1 (Samejima et al., 2008; Zhang and Megraw, 2007). Deletion or mutations in centrosomin motif 1 in centrosomin and Mto1 were shown to disrupt γ-TuC recruitment to the centrosome and SPB, leading to defects in microtubule assembly (Samejima et al., 2008; Zhang and Megraw, 2007). Interestingly, *pcp1-15* harbours a mutation within the conserved centrosomin motif 1 (Figure 2.3), consistent with the defect in γ-TuC localisation to the SPB observed in the mutant.

Further characterisation shows that delocalisation of γ-TuC in the *pcp1-15* mutant occurs only when the cells entered mitosis. This suggests that Pcp1 is only required for γ-TuC recruitment to the SPB during mitosis. It is important to note that we cannot rule out the possibility that Pcp1 also has a role in γ-TuC recruitment during interphase, which could be distinct from the mitotic γ-TuC recruitment role, and is left intact in the *pcp1-15* mutant due to the nature of the allele. Assuming that Pcp1 is not required for the recruitment of nucleoplasmic γ-TuC to the nuclear envelope underneath the SPB during interphase, this then raises a new interesting question. What is the mechanism that recruits the nucleoplasmic γ-TuC during interphase?

Such a mechanism is likely to involve proteins that span across the double lipid bilayers. The candidate proteins are the SUN- and KASH-domain proteins, which localise to the inner nuclear membrane and outer nuclear membrane, respectively (Tzur et al., 2006). In fission yeast, telomeres are attached to the nuclear envelope and clustered at the SPB during meiosis, forming a polarised chromosomal structure known as the ‘bouquet’ (Chikashige et al., 1994). The bouquet formation requires the interaction between the Taz1-bound telomeres and the SUN-domain protein Sad1, via Bqt1 and Bqt2 (Chikashige et al., 2006; Tomita and Cooper, 2007), as well as the interaction between Sad1 and the

KASH-domain protein Kms1 (Niwa et al., 2000). The association of Kms1 with the SPB then brings the telomeres to the SPB during meiosis. It is possible that a similar mechanism is exploited during the vegetative cell cycle to recruit γ-TuC (and possibly also for centromore clustering) to the nuclear envelope underneath the SPB.

6.3 SPB insertion defect in *pcp1-18*

The *pcp1-15* and *pcp1-18* mutants exhibited similar mitotic defects. However, γ-TuC localisation was only affected in the *pcp1-15* cells, but not in *pcp1-18*. This prompted the possibility that Pcp1 has an additional essential role in mitosis that is independent of γ-TuC recruitment to the SPB. Interestingly, a multicopy suppressor screen identified two transmembrane nucleoporins that constitute the inner membrane ring of the nuclear pore complex (NPC) components, Cut11/NDC1 and Pom152/GP210, as specific suppressors of the *pcp1-18* mutant.

Cut11 localises to the nuclear pores throughout the cell cycle, and to the SPB during mitosis (West et al., 1998). In fission yeast that undergoes closed mitosis, Cut11 is essential for insertion of the SPB into the nuclear envelope (NE) during mitosis (West et al., 1998), allowing spindle microtubules to capture the chromosomes in the nucleoplasm. Pom152 is not an essential protein. We showed that unlike Cut11, Pom152 localised to the NE, but not to the SPB during mitosis. However, due to the presumed close association with Cut11 (based on Pom152 and Ndc1 data in budding yeast) (Alber et al., 2007), we propose that overexpression of Pom152 enhances the recruitment of Cut11 to the mitotic SPB, which then suppresses the *pcp1-18* mutant indirectly through the function of Cut11. However, further work would be needed to substantiate this claim.

Ultrastructural analysis by electron microscopy (EM) revealed that SPB insertion was impaired in the *pcp1-18* mutant. Interestingly, the non-equal

spindle assembly defects between the mother and the daughter SPB, as observed in the live-cell fluorescence microscopy analysis, was extended to the abnormality in SPB insertion in the *pcp1-18* mutant; whilst the mother SPB was inserted into the NE (although appeared loosely attached to the NE), the daughter SPB was in its interphase configuration with the NE underneath the SPB remained intact. Examination of the *pcp1-15* mutant showed that the SPB was inserted into the NE obliquely, but nonetheless an NE fenestra was clearly formed and spindle microtubules were seen to have gained access to the nucleoplasm.

The SPB insertion defects in the *pcp1-18* mutant are highly reminiscent of those reported for *cut11.1* (West et al., 1998), and for *cut12.1* as was published while this work was carried out (Tallada et al., 2009). In both mutants, the mother SPB nucleates spindle microtubules, whilst the daughter SPB remains inactive and is not inserted into the NE. The mother SPB is inserted into the NE, but fails to be attached to the NE properly. This results in the mother SPB becoming loosely attached to the NE fenestra at one of its end, or in some extreme cases, the complete falling of the mother SPB into the heart of the nucleoplasm (West et al., 1998). Our findings therefore demonstrate that Pcp1 is required for NE reorganisation and SPB insertion during mitosis.

One of the most straightforward explanations for the SPB insertion defects observed in the *pcp1-18* mutant was that Cut11 recruitment to the mitotic SPB was disrupted. However, we found that it was not the case, as Cut11 clearly formed foci at the SPBs, similar to the wild-type cells. When probed further into the underlying molecular defect in the *pcp1-18* mutant, we found that *cut12*$^{+}$ was another multicopy suppressor that specifically suppressed the temperature-sensitivity of the mutant. An ensuing examination into the localisation of Cut12 in the *pcp1-18* mutant at 36^{o}C found that Cut12 also localised properly to the SPB. These observations indicate that it is the functions of Cut11 and Cut12, rather than their localisation that are compromised in the *pcp1-18* mutant.

6.4 Pcp1 and Plo1 recruitment

Cut12 is an essential SPB component. Similar to Pcp1, it localises to the inner plaque of the SPB (Bridge et al., 1998). Also, as mentioned previously, the *pcp1-18* and *cut12.1* mutants share multiple mitotic defects. In both mutants, monopolar spindes are formed and the daughter SPBs are not inserted into the nuclear envelope during mitosis (Bridge et al., 1998).

It has been shown that Cut12 is a cell-cycle regulator, promoting G2 to M transition through the activation of polo kinase Plo1 at mitotic entry (MacIver et al., 2003; Petersen and Hagan, 2005). The *cut12.s11* mutant, a gain-of-function mutant of *cut12*, enhances localisation of Plo1 to the SPB (MacIver et al., 2003). This increases Plo1 activity at the SPB and thus drives mitotic entry. Postulating that Pcp1 may also influence Plo1 activity, we examined localisation of Plo1 in the *pcp1-18* mutant. Interestingly, we observed a significant reduction in Plo1 recruitment to the SPB, indicating that Pcp1 is required for Plo1 recruitment. We also demonstrated that Plo1 delocalisation was a primary defect of the *pcp1-18* mutant, as enhancing Plo1 recruitment to the SPB with the *cut12.s11* allele suppressed the mutant. The incomplete delocalisation of Plo1 from the SPB in the *pcp1-18* mutant could be due to the following reasons: firstly, there could be other SPB components that serve as recruitment factors for Plo1, which act in parallel with Pcp1. Alternatively, the hypomorphic nature of the *pcp1-18* allele did not abolish completely the Plo1 recruitment function of Pcp1.

Polo-like kinases regulate multiple functions during cell division, including centrosome maturation, mitotic entry, chromosome segregation and cytokinesis (Archambault and Glover, 2009; Nigg, 2007; Takaki et al., 2008). In fission yeasts, one of the established functions of Plo1 at the SPB is the advancement of mitotic entry (MacIver et al., 2003; Petersen and Hagan, 2005). In line with this, we showed that promoting mitotic entry with a Wee1 kinase mutant, *wee1-50*, which advances mitotic entry due to untimely activation of Cdc2/CDK1 (Nurse, 1990), bypassed the requirement for Plo1 at the SPB and suppressed

the *pcp1-18* mutant. Therefore, apart from γ-TuC recruitment, Pcp1 is also required for Plo1 recruitment to the SPB at G2 to M transition to promote mitotic entry.

6.5 Physical interaction between Pcp1 and γ-TuC/Plo1

The roles of Pcp1 in γ-TuC and Plo1 recruitment were supported by the physical interactions detected between these components by co-immunoprecipiation experiments. Intriguingly, we were unable to recapitulate a reduced recruitment of γ-TuC and Plo1 by immunoprecipitation at the restrictive temperature in the *pcp1-15* and *pcp1-18* mutants, respectively. Two possible reasons could account for this observation. Firstly, there could be two pools of Pcp1 in a cell, an SPB-associated pool and a cytoplasmic pool. The SPB-associated pool of Pcp1 could constitute only a small fraction of Pcp1 molecules compared to those found in the cytoplasm. Therefore, any changes affecting the SPB-associated Pcp1 could be masked by the predominant cytoplasmic pool of Pcp1 in the cell. Secondly, the SPB could remain insoluble in the protein extracts, and would be removed from the soluble fraction after centrifugation. In support of these two possibilities, in wild-type cells, we were unable to detect a difference in the level of physical interaction between Pcp1 and γ-TuC or Plo1, between interphase and mitosis (although our cell biological data clearly demonstrate that γ-TuC and Plo1 are specifically recruited to the SPB during mitosis).

6.6 Potential role of Pcp1 phosphorylation

Since Pcp1 recruits Plo1 to the SPB during mitosis, it is perhaps not surprising to find that Pcp1 is phosphorylated by Plo1 in a cell-cycle dependent manner. Pcp1 harbours a putative polo-box-domain (PBD) recognition motif, $SSP^{905-907}$, and more than 30 putative polo kinase phosphorylation sites. It also has two cyclin-dependent kinase (CDK) phosphorylation sites, $TPLR^{55-58}$ (putative) and

SPDR$^{906-909}$, with the latter reside right in the PBD recognition motif and therefore CDK could potentially act as the priming kinase for Plo1 binding to Pcp1 (Cheng et al., 2003; Elia et al., 2003a; Elia et al., 2003b). We show that Pcp1 phosphorylation is significantly reduced when Plo1 activity is compromised. Furthermore, when Plo1 activity is increased in cells, Pcp1 phosphorylation is detected even in interphase cells. Altogether our data suggest that Plo1 might be directly phosphorylating Pcp1, and raise the intriguing possibility that Pcp1 function is regulated by Plo1 phosphorylation.

Unfortunately, however, our attempt to isolate a phospho-mutant of Pcp1 was not successful. We mutated the putative PBD recognition motif SSP$^{905-907}$ to AAP$^{905-907}$, and the CDK phosphorylation site TPLR$^{55-58}$ to APLR$^{55-58}$, by site-directed mutagenesis, and the mutant allele was introduced into the genome to replace the wild-type *pcp1*$^{+}$. However, rather disappointing to us, this Pcp1 mutant did not show obvious reduction in mitotic-specific phosphorylation, or any growth defect under a range of experimental conditions. One of the possible reasons for this is that phosphoresidues located nearby the mutated sites could act as secondary binding sites for Plo1 on Pcp1. Our second approach to isolate a phosphomutant of Pcp1 by first mapping out the *in vivo* phosphorylation sites by QTRAP mass spectrometry was again unsuccessful. Although it was proposed that a different peptide digestion method could improve the phosphorylation site detection method, it was not pursued further (see Future Directions for more details). Therefore, we currently do not understand the biological significance of Pcp1 phosphorylation by Plo1.

6.7 Multiple essential mitotic processes converge at Pcp1

To our knowledge, this is the first study in any organism to identify a spindle pole component that is required for polo kinase recruitment to the SPB/centrosome. It is known that CDK1 and cyclin B localise to the mitotic centrosome in animal cells (Jackman et al., 2003) and to the SPB in fission yeast (Alfa et al., 1990; Decottignies et al., 2001), implying a universal role for the centrosome/SPB in the temporal regulation of mitotic onset. Precedent work

in fission yeast indicated that Cut12 potentiates Plo1 activity upon mitotic onset (MacIver et al., 2003). However, Cut12 is not required for Plo1 recruitment to the SPB per se, in other words, Plo1 is still recruited to the SPB during mitosis even in the *cut12*-null mutant (Mulvihill et al., 1999). This indicates that Cut12, albeit physically interacting with Plo1 (MacIver et al., 2003), is not a receptor that is directly responsible for recruitment of Plo1 to the mitotic SPB, but instead it is Pcp1 that performs this task. It remains to be determined how Pcp1 and Cut12 functionally and physically interact. It is possible that Pcp1 is involved in mitosis-specific activation of Cut12 through a hitherto unknown mechanism. Alternatively, as Cut12 is capable of localising to the SPB in *pcp1-18* mutants, Cut12 may act either upstream or independently of Pcp1.

Our data also demonstrate that Pcp1 controls SPB insertion and NE invagination during mitosis through Plo1 recruitment. This is because both defects in SPB insertion and Plo1 recruitment are only observed in *pcp1-18*, but not *pcp1-15* cells. Furthermore, enhancement of Plo1 localisation to the mitotic SPB using the gain-of-function *cut12.s11* mutant specifically suppressed the *pcp1-18* mutant. Importantly, the loss-of-function *cut12.1* mutant, which is defective in Plo1 activation, also displays SPB insertion defects (Tallada et al., 2009). This indicates that Pcp1, Cut12 and Plo1 form a functional network via their physical binding in SPB-mediated mitotic entry and NE reorganisation for SPB insertion.

Although NE-mediated processes such as NE invagination and SPB insertion may be regarded as a closed mitosis-specific event, it is known that in metazoans the NE undergoes dynamic structural alterations upon mitotic entry, in which the small restricted regions of the NE below the centrosome invaginate prior to NE breakdown (NEBD) (Beaudouin et al., 2002; D'Angelo and Hetzer, 2008; Hetzer et al., 2005; Salina et al., 2002; Tran and Wente, 2006). This suggests that SPB insertion in fission yeast and NEBD in metazoans could be mechanistically analogous. It would be of great interest to see whether NE invagination and NEBD in animal cells is also regulated by polo kinase.

In conclusion, we show that a single SPB component Pcp1 plays multiple roles in mitosis by independently recruiting two essential components, γ-TuC and Plo1. The *pcp1-15* mutant is defective in γ-TuC recruitment to the mitotic SPB, whilst *pcp1-18* fails to target Plo1 to this site. We have shown that these defects are allele-specific. This work therefore verify Pcp1's postulated role in γ-TuC-mediated spindle assembly and unveils its unanticipated function in Plo1-dependent mitotic entry and structural reorganisation of the NE (see Figure 6.1 for a model). Crucially, our work demonstrates that mitotic entry, NE reorganisation for SPB insertion, and spindle formation converge at Pcp1. Therefore, our study provides insight into the molecular mechanisms by which the centrosome orchestrates multiple cellular pathways. As centrosomal aberrations are common in cancer cells, the central role of Pcp1 in orchestrating multiple SPB functions may be relevant to cancer development.

6.8 Future directions

It is still unclear what is the biological significance of the Plo1-dependent Pcp1 phosphorylation in mitosis. Our first attempt to map out the *in vivo* phosphorylation sites on Pcp1 using mass spectrometry was unsuccessful. Two troubleshooting steps could be applied. First, the peptide sequence coverage with a trypsin digest was only about 75%, which could potentially cause loss of phoshopeptides in the analysis. Thus, alternative protein cleavage enzymes could be used to increase the sequence coverage to at least 95%. Second, Pcp1 might be a phosphoprotein with a low stoichiometry of phosphorylation, i.e. only a small fraction of Pcp1 molecules is phosphorylated. Enrichment of phosphopeptides in the sample with titanium dioxide immobilised metal affinity chromatography (IMAC) could increase the success rate of phosphopeptide identification.

We are puzzled by the finding that although γ-TuC and Plo1 co-immunoprecipitated with Pcp1, no reduction in the amount of co-immunoprecipitated γ-TuC and Plo1 was seen in either of the *pcp1* mutants, or

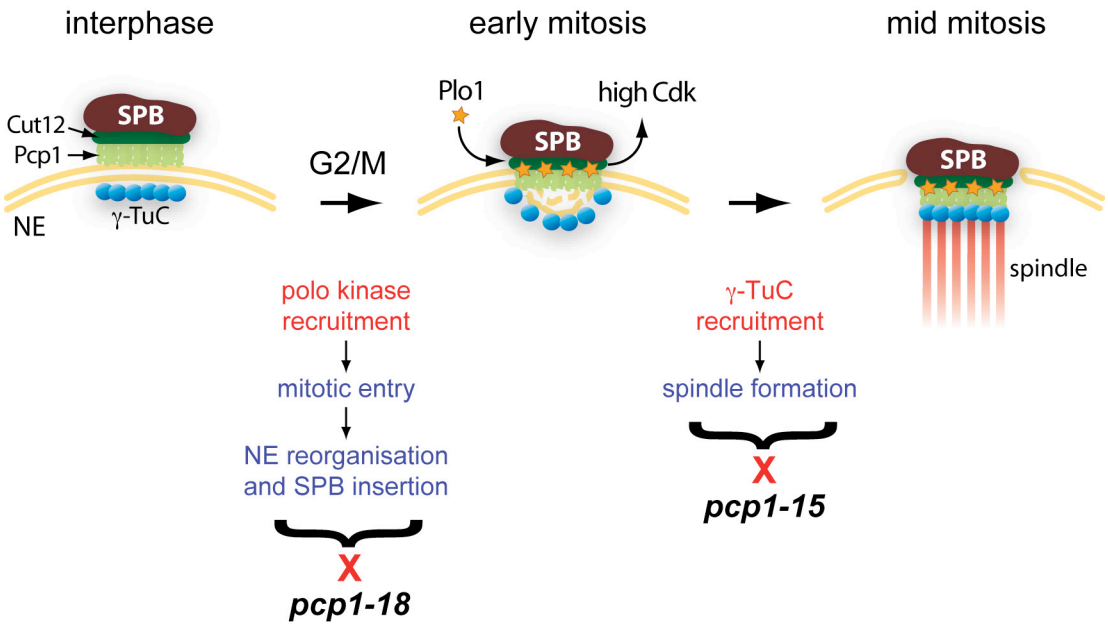

Figure 6.1 A model of Pcp1's function during cell division.

Pcp1 recruits Plo1 to the SPB at the G2 to M transition, leading to full activation of Cdk (Cdc2) and mitotic entry. Note that activated Cdc2 in turn activates Plo1 via a positive feedback loop. This drives NE reorganisation and SPB insertion. At the same time Pcp1 recruits γ-TuC to the mitotic SPB to initiate spindle formation. The nature of interactions between Pcp1 and Cut11 (not depicted) or Cut12 remains unclear at this moment. SPB (brown), Cut12 (dark green), Pcp1 (light green), γ-TuC (blue circles), NE (yellow), Plo1 (orange star), spindle (red lines).

throughout the cell cycle in wild-type cells. The potential complications with the insolubility of the SPB or the ratio of cytoplasmic to SPB pool of Pcp1, as explained in section 6.5, could be overcome by GST pull-down assays, where Pcp1 could be purified from bacteria and bound to beads. In this case, the interaction (or the lack of interaction) between γ-TuC/Plo1 and Pcp1 will be experienced by all the Pcp1 molecules (GST-tagged), instead of being confined to the SPB in the *in vivo* situation.

We have shown that *pcp1-18*, a loss-of-function mutant of *pcp1*$^+$, was unable to recruit sufficient amount of Plo1 to the SPB, resulting in the impairment of mitotic entry. It would be of great interest to investigate if a gain-of function mutation of *pcp1*$^+$ - one that would enhance the recruitment of Plo1 to the SPB, could bypass the requirement for *cdc25*$^+$ for mitotic entry (analogous to *cut12.s11*). The isolation of such a mutant would not only be a nice complement to our current model for Pcp1's role in Plo1 recruitment, but would also generate an additional tool for the study of cell cycle regulation at the SPB.

The G2 to M arrest observed in some animal cell lines in the absence of pericentrin function was proposed to be due to the activation of a centrosome maturation checkpoint, as a consequent of the defect in γ-TuC recruitment (Zimmerman et al., 2004). Our finding now provides a plausible alternative explanation that the cell-cycle arrest is a consequence of impaired recruitment of the important cell cycle regulator, i.e. polo kinase. This hypothesis could be tested by examining whether polo kinase recruitment to the centrosome is indeed reduced when pericentrin is knockdown by siRNA. The analysis could also be extended to asking whether the G2 to M arrest could be liberated by restoring polo kinase recruitment, or enhancing polo kinase activity at the centrosome.

Although we have gained insight into how multicopy suppressors such as *cut11*$^+$, *pom152*$^+$ and *cut12*$^+$ restore the growth defect of the *pcp1-18* mutant, it remains unclear whether all these genes directly influence Plo1 recruitment/activity at the SPB. We hypothesise that overexpression of *cut12*$^+$

probably achieves the same effect as *cut12.s11*, where the latter has been shown to increase recruitment of Plo1 to the SPB. However, we are yet to understand whether or how overexpression of *cut11*$^{+}$ and *pom152*$^{+}$ increases Plo1 recruitment to the SPB in *pcp1-18*. We would like to address this by investigating whether Plo1 localisation at the SPB is restored in the *pcp1-18* mutant in the presence of the multicopy suppressor genes. The analysis will shed light on the complex communication between SPB insertion and Plo1-mediated mitotic entry regulation.

The role of the other two multicopy suppressors *kms2*$^{+}$ and *tcg1*$^{+}$ remains to be elucidated. Kms2 is a KASH-domain protein that localises to the SPB (Ding et al., 2000), and is likely to function together with Kms1 to tether SPB to the outer nuclear membrane (Miki et al., 2004; Niwa et al., 2000; Shimanuki et al., 1997). It will be interesting to examine whether the SPB in the *pcp1-18* mutant is detached from the nuclear envelope. Alternatively, Kms2 could be involved in SPB insertion, which would then add another component and potentially a window into the understanding of this poorly characterised process.

Tcg1 has been shown to be a single-stranded telomeric DNA binding protein *in vitro* (Pang et al., 2003), but intriguingly it has been reported to localise to the cytoplasm in a genome-wide protein localisation study (Matsuyama et al., 2006). A similar observation was made in our hands when Tcg1 was tagged with GFP at its endogenous locus and expressed under its endogenous promoter (data not shown). One of the ways to unlock the mystery on the mechanism by which Tcg1 suppresses *pcp1-18* is to perform a yeast two-hybrid screen on Tcg1 to identify its interacting proteins, which hopefully would provide the missing links to Tcg1's role at the SPB and its interaction with Pcp1.

In this study, we have closely examined two alleles of *pcp1*, *pcp1-15* and *pcp1-18*, and characterised two distinct roles of Pcp1 in mitosis. Analysis of the remaining uncharacterised alleles of *pcp1* could potentially uncover additional roles of Pcp1 in cell division. There are two ways one could avoid characterising mutants with identical molecular defects as those found in the *pcp1-15* and

pcp1-18 mutants. First, we could transform the remaining *pcp1* alleles with the suppressor plasmids *cut11*$^{+}$, *pom152*$^{+}$, *cut12*$^{+}$ and *alp4*$^{+}$, or introducing into them the *cut12.s11* mutation. Any *pcp1* alleles that are suppressed under these conditions are likely to have the same molecular defects as the *pcp1-15* or *pcp1-18* mutants, and could be ruled out from further characterisation. Alternatively, we could perform an intragenic complementation analysis where the *pcp1* alleles are crossed with the *pcp1-15* and *pcp1-18* mutants to create diploid strains. The diploid strains that are no longer temperature-sensitive probably harbour different molecular defects that are complemented by the presence of a wild-type copy of the gene in the diploid. The corresponding *pcp1* alleles can then be subject to further detailed molecular characterisation, including multicopy suppressor screens.

7 Materials and Methods

7.1 Laboratory stocks and solutions

7.1.1 Media

Name	Components
EMM	14.7 mM potassium hydrogen phthalate, 15 mM Na_2HPO_4, 93.5 mM NH_4Cl, 2% w/v glucose, salt stock, vitamin stock, mineral stock
EMM- NH_4Cl	Same as EMM but without NH_4Cl
L Broth	170 mM NaCl, 0.5% (w/v) yeast extract, 1% (w/v) bactotryptone, pH 7.0
YE5S	0.5% Difco yeast extract, 3% dextrose, 250 mg/ml uracil, adenine, histidine, lysine, leucine.
YFM	YE5S with 15% glycerol

7.1.2 Buffers

Name	Components
TE	10 mM Tris-HCl, pH 7.5, 1 mM EDTA
TBE	0.02 M Tris borate, 0.4 mM Na_2EDTA
TAE	0.08 M Tris acetate, 2 mM Na_2EDTA

Name	Components
6x loading dye	30% glycerol, 0.1% bromophenol blue
Breaking buffer	2% Triton X-100, 1% SDS, 100 mM NaCl, 10 mM Tris-HCl pH 8.0, 1 mM Na_2EDTA pH8.0
LiAc/TE	100 mM lithium acetate pH 7.4, 10 mM Tris.HCl pH 7.4, 1 mM EDTA pH 8.0
40% PEG4000/LiAc/TE	40% polyethylene glycol 4000 (or 3640), 100 mM lithium acetate pH 7.4, 10 mM Tris.HCl pH 7.4, 1 mM EDTA pH 8.0
Transfer Buffer	39 mM glycine, 48 mM Tris base, 20% methanol.
PBS	170 mM sodium chloride, 3 mM KCl, 10 mM Na_2HPO_4, 2 mM KH_2PO_4
PBST	Same as above, plus 0.1% Tween-20
PEM	100 mM PIPES, 1 mM EGTA, 1 mM $MgSO_4$, pH 6.9
PEMS	PEM, 1.2 M sorbitol
PEMBAL	PEM, 1% BSA, 0.1% NaN_3, 100 mM lysine hydrochloride
STOP	150 mM NaCl, 50 mM NaF, 10 mM EDTA, 0.007% (v/v) NaN_3
Lysis buffer	50 mM Tris.HCl pH 7.4, 1 mM EDTA pH 8.0, 150 mM NaCl, 0.05% NP-40, 10% glycerol, add just before use the following, 1 mM DTT, 15 mM *p*-nitrophenyl phosphate (pNPP), 1x protease cocktail inhibitor (Sigma), 1 mM phenylmethylsulphonyl fluoride (PMSF)
Wash buffer (IP)	50 mM Tris.HCl pH 7.4, 1 mM EDTA pH 8.0, 150 mM NaCl, 0.05% NP-40, 10% glycerol, add just before use the

Name	Components
	following, 1 mM DTT, 1.5 mM *p*-nitrophenyl phosphate (pNPP), 1x protease cocktail inhibitor (Sigma), 0.1 mM phenylmethylsulphonyl fluoride (PMSF)
2x sample buffer	125 mM Tris.HCl pH 6.8, 50% glycerol, 4% SDS, 0.02% bromophenol blue, 100 mM DTT
phosphatase inhibitors	10 mM NaV, 50 mM NaF
SZB	1 M sorbitol, 0.1 M sodium citrate pH 7.0, 60 mM EDTA pH 8.0, 0.8% (v/v) β-mercaptoethanol, 600 μg/ml zymolyase
SDS-TE	2% SDS, 100 mM Tris.HCl pH 7.4, 10 mM EDTA pH 8.0

7.1.3 Commercial kits

TaKaRa LA Taq™ – polymerase chain reaction (PCR) system
TaKaRa Z Taq™ – polymerase chain reaction (PCR) system
Promega Wizard® DNA Clean-up – DNA purification system
Stratagene QuikChange® II – site-directed mutagenesis kit
Criterion XT™ Precast Gel – protein resolution system
Amersham ECL Plus ™ – immunoblotting detection reagents

7.2 Strain growth and maintenance

Fission yeast strains were frozen, stored, revived, grown and maintained according to well-described methods (Moreno et al., 1991). Cells were grown either in liquid culture media or on agar plates containing 1.6% agar. The recipes for different media are listed in section 7.1.1. Stocks of yeast strains were stored in YFM media at -70°C. Selective media plates were made by

adding various drugs to bottles of cooled molten agar medium, as detailed in the table below.

Name	Components
Hygromycin B	YE5S, 300 μg/ml hygromycin B (Roche)
G418	YE5S, 100 μg/ml Geneticin (Sigma)
clonNAT	YE5S, 100 μg/ml nourseothricin (Werner Bio-agents)
Aureobasidin A	YE5S, 0.5 μg/ml aureobasidin A (Takara Bio)
Phloxin B	YE5S, 7.5 μg/ml Phloxin B (Sigma)
5-FOA	YE5S, 1 mg/ml 5-fluoroorotic acid

7.3 Fission yeast transformation

20 ml YE5S was inoculated and incubated at 27°C so that the culture would be about $5x10^6$ cells/ml the next morning. 20 ml cells was adequate for most transformations. To increase transformation efficiency, 50 ml of cells were used. Cells were harvested by spinning at 2000 rpm, 1 min. Cells were washed in 1 ml LiAc/TE, twice. Cells were then resuspended in 100 μl LiAc/TE. 7.5 μl of 10 mg/ml salmon sperm carrier DNA and 10 μl PCR fragment (or 2 μl plasmid DNA) were added and were mixed gently (salmon sperm carrier DNA was denatured by incubation at 95°C for 5 min, immediately followed by incubation on ice for 5 min. This was done for the first time any new tube of carrier DNA was used). Cells were incubated at room temperature for 10 min, on a rotating mixer. 260 μl 40% PEG4000/LiAc/TE was added and the mixture was vortexed. The tube was then incubated at 27°C for 30 min to 3 h on a rotating mixer. 43 μl DMSO was added and mixed gently by flicking the tube. Cells were heat-shocked at 42°C for 1 to 5 min. They were washed with YE5S (5000 rpm, 10 s), resuspended in 500 μl YE5S and incubated at 27°C for 90 min. Cells were

plated and incubated at 27^{o}C until colonies appeared. For plasmid transformation, the cells were plated directly onto selective plates. For DNA integration transformation, cells were first plated onto a YE5S plate and incubated at 27^{o}C for 24 h until a lawn of cells had grown. They were then replica plated onto a selective plate.

7.4 Gene tagging and deletion

Gene tagging at endogenous loci and deletion was performed using a one-step PCR-based method (Bahler et al., 1998). Oligonucleotides used carried 80 bp of homology to flanking sequences of the insertion site at the endogenous locus, and 20 bp of homology to the cassette to be amplified from template plasmids. All templates for PCR were based on the pFA6a plasmid, and contained one of the following selective markers: *kanR, ura4+, nat, hph* (Sato et al., 2005). Integrants were selected on selective plates. Correct tagging and disruption of genes of interest were verified by colony PCR.

7.5 Long oligo polymerase chain reaction

In gene amplification for genomic integration, each of the primers carried 80 bp 5'-overhangs that match the sites of integration, and 20 bp of homology to the tagging or deletion cassettes to be amplified. The reaction mixture and the PCR cycling program for 100-mer oligo amplification were as follows.

Reaction mixture

Components	Vol (μl)
10x LA Taq buffer (plus $MgCl_2$)	5
$MgCl_2$ (25 mM)	5
dNTP mix (2.5 mM of each)	16

Components	Vol (μl)
Template DNA (~100 ng/μl)	1
Fwd primer (10 μM)	5
Rev primer (10 μM)	5
H_2O	12
LA Taq	1
Total	**50**

PCR program

Temp (°C)	Time (min)	
95	3	
95	1	5 cycles
48	2	
74	4	
95	1	35 cycles
52	2	
74	2	
74	5	
4	∞	

7.6 Fission yeast genomic DNA preparation

A cell pellet of 50 μl was collected from a freshly streaked plate. Cells were washed in 0.5 ml of H_2O, and were resuspended in 200 μl of breaking buffer. 0.3 g of acid-washed 425-600 μm glass beads (one PCR tube-full) was added, along with 200 μl of phenol:chloroform:isoamyl alcohol. The mixture was vortexed using the Fastprep FP120 cell disruptor (Savant Co.), with a setting of 5, 5 s. 200 μl of TE was then added and the mixture were centrifuged for 5 min at room temperature. The top aqueous layer was transferred to a fresh tube. 1 ml of ethanol was added and the mixture was incubated at room temperature for 5 min. The genomic DNA was pelleted by centrifuging for 3 min, rinsed once with 500 μl of 70% ethanol, and then air-dried at room temperature. The pellet was resuspended in 50 μl TE.

7.7 Fission yeast plasmid DNA isolation

5 ml culture was grown overnight to saturation. Cells were harvested, washed with 1 ml of H_2O, and were resuspended in 150 μl of SZB buffer. The cells were incubated at 37°C for 30 min with mixing. 150 μl of SDS-TE was then added and the mixture was incubated at 65°C for 30 min. Then, 150 μl of 5 M potassium acetate was added, vortexed briefly, and the mixture was kept on ice for 30 min. The supernatant was cleared by centrifugation at 13,000 rpm at 4°C for 15 min. 400 μl of cleared supernatant was transferred to a new tube. Plasmid DNA was purified from the supernatant using the Wizard DNA clean-up kit (Promega), according to the manufacturer's instructions.

7.8 Isolation of temperature-sensitive mutants

For isolation of temperature-sensitive *pcp1* mutants, *pcp1*$^+$ was first C-terminally tagged with HA epitope and *hph*^{r} gene (method described in section 7.4). After the successful tagging of *pcp1*$^+$ to create *pcp1*$^+$*-HA-hph*^{r}, genomic DNA was

purified and *pcp1*$^{+}$*-HA-hph*^{r} was PCR amplified with a primer set that annealed to 406 bp upstream and 168 bp downstream of *pcp1*$^{+}$. The PCR-amplified *pcp1*$^{+}$*-HA-hph*^{r} fragments were randomly mutagenised during an error-prone PCR amplification using Vent DNA polymerase (New England Biolabs Ltd.) supplemented with 2.5 mM (10X) deoxyguanosine triphosphate (dGTP), while the rest of the deoxynucleoside triphosphates (dNTPs) were kept at the normal level of 0.25 mM. The mutagenised *pcp1* fragments were ethanol precipitated and transformed into a wild-type strain (513). Transformants were selected YE5S plates containing hygromycin at 27^{o}C. Colonies were then replicated onto plates containing phloxin B. Replicated plates were then incubated at 27^{o}C and 36^{o}C for 1 to 2 days. Temperature-sensitive (ts) mutants were identified on the basis of the ability to form a colony at 27^{o}C, but not at 36^{o}C. Dead cells were confirmed by the phloxin B staining. Approximately 5,000 transformants were screened for temperature sensitivity at 36^{o}C. Temperature-sensitive mutants isolated were backcrossed to *pcp1*$^{+}$*-mRFP-kan*^{r} to ensure proper integration and to remove potential off-site mutations. The right temperature-sensitive mutants should not show co-resistance to hygromycin and kanamycin. Also, they should show co-segregation of temperature sensitivity and hygromycin resistance. The procedures for the isolation of cold-sensitive mutants were essentially the same as those performed for temperature-sensitive mutants. The only difference was that the selection for dead colonies was done at the low temperature of 22^{o}C.

7.9 Dilution assay

An exponentially growing culture was prepared. Cell density was determined by KX-21N cell counter (Sysmex Corp.). 500 μl of 2x10^{7} cells/ml was prepared and 10-fold serial dilutions of the culture were made. Cells were spotted onto plates with a 48-pin replicator. Plates were incubated at appropriate temperatures for 2 to 3 days before being photographed.

7.10 Cell viability assay

Cell density was measured using the KX-21N cell counter (Sysmex Corp.). 250 cells at 20 min intervals were plated out on YE5S, and were incubated at the permissive temperature of 26^{o}C for 2 to 3 days. Colonies that could grow were counted. Viability was determined as a percentage of 250 cells that formed colonies.

7.11 Random spore analysis

Strains used in our study were constructed by random spore analysis. Cells of opposite mating type, *h*$^{-}$ and *h*$^{+}$, carrying different genotypes and markers were mixed on EMM plates lacking nitrogen to induce conjugation and sporulation. Once asci were observed, usually after 2 to 3 days at 27^{o}C, they were treated with 0.5% helicase (Biosepra) for 2 to 3 h at 27^{o}C, to break down the ascus wall. 43 μl ethanol was added to the tube and was left to incubate at room temperature for 30 min, to kill any non-sporulating cells. The spores were pelleted, resuspended in 1 ml of H_2O, and were plated onto YE5S plates. Colonies formed were replica plated onto appropriate selection plates to select for the desired genotypes.

7.12 Centrifugal elutriation

200 ml of overnight YE5S culture grown at 27^{o}C was prepared. 3 L of YE5S was inoculated so that it reached 1x10^{7} cells/ml the next morning. Usually this involved inoculation of the 3 L culture at 3x10^{5} cells/ml at 7 p.m.. After 15 h incubation at 27^{o}C, the culture reached 1x10^{7} cells/ml at 10 a.m. the next day. Before using the elutriator (Avanti J-20 XP equipped with JE-5.0 rotor, Beckman Coulter Inc.), the chamber temperature was set to 27^{o}C, and the system was washed with 2 L of H_2O, at a pump flow rate of 150 ml/min (or setting 2.5 using the Masterflex 7016-20 pump, Cole Parmer Co.). Washing was repeated with YE5S, ensuring that no bubbles were trapped in the system. Bubbles could be

removed by stopping and restarting the rotor several times. Also ensured that the bubble trap was completely filled with YE5S. Rotor speed was increased to 3500 rpm, flow rate was decreased to 85 ml/min (setting 1.8). Cells were loaded, and an obvious front developed quickly in the elutriation chamber. Pump flow rate was increased to 120 ml/min (setting 2.3), with the cell front maintained at 10 mm from the elutriation boundary. While loading the final litre of cells, the rotor speed and flow rate was gradually decreased (50 rpm and 5 ml/min or setting 0.05) to 3000 rpm and 60 ml/min (setting 1.5), while maintaining the cell front at the same level. Once all the cells were loaded into the elutriator, fresh YE5S was pump into the system. The pump flow rate was increased gradually at 5 ml/min (setting 0.05) until the cell front was at the elutriation boundary. Once there was only a 'chink of light', cells were flowing out from the elutriator. The first 200 ml of cells were mainly dead and stationary cells, and were discarded. The subsequent 1 L of cells was collected, which were the small early G2 cells and were typically at a cell density of $1x10^6$ cells/ml. The culture was concentrated to $5x10^6$ cells/ml by filtration. Synchronous culture analysis was started. The elutriator was cleaned by passing 3 L of H_2O, making sure that there were no cells remaining in the system. Lastly, 500 ml of 70% ethanol was passed through the system and the elutriation chamber was left in 70% ethanol.

7.13 Cell-cycle arrest

Cell-cycle arrest was achieved through hydroxyurea (HU) treatment or the use of the cell cycle mutants, *cdc25-22* and *nda3-311*. For S phase arrest, 12.5 mM HU was added, and the culture was left to incubate for 4 h at 30^{o}C. For late G2 arrest, the temperature-sensitive *cdc25-22* mutant that was unable to enter mitosis and arrested in late G2 was used (Fantes, 1979). Exponentially growing *cdc25-22* cells, grown at 27^{o}C, were shifted up to 36^{o}C for 4 h 15 min to induce late G2 arrest. The arrested cells were then shifted down to 26^{o}C to allow the cells to synchronously enter mitosis. Septation index and DNA staining with 4',6-diamidine-2'-phenylindole (DAPI) were used to monitor cell cycle progression. For mid mitosis arrest, the cold-sensitive *nda3-311* mutant was

used (Hiraoka et al., 1984; Toda et al., 1983). *nda3-311* cells were grown at 27^{o}C overnight. The culture was then shifted to 20^{o}C for 6 or 8 h, to arrest cells in mid mitosis.

7.14 Multicopy suppressor screen

A genomic DNA library (cloned into pAL-SK vector) obtained from Dr. Taro Nakamura and Dr. Chikashi Shimoda was transformed into the *pcp1* mutants. Transformants were selected on –LEU plates (the vector contained a Sc*LEU2 marker*), and colonies were allowed to form at the permissive temperature of 27^{o}C (incubating the plates for 6-7 days). Approximately 15,000 transformants growing on the selection plates were replica plated onto YE5S plates containing phloxin B, and the plates were incubated at 36^{o}C or 34^{o}C for 2 days. Transformants that grew at either 36^{o}C or 34^{o}C were identified as suppressor candidates and were selected for plasmid dependency analysis. Suppressor candidates were grown in YE5S broth (non-selective medium) overnight at 27^{o}C. About 300 cells were then plated onto YE5S plates. Colonies were replica plated onto –LEU plates and YE5S plates containing phloxin B. The –LEU plates were incubated at 27^{o}C, while the YE5S plates were incubated at 34^{o}C and 36^{o}C for 2 days. True multicopy suppressors are mutant cells that show co-segregation of their suppression and the presence of a plasmid. Plasmids were then extracted from the suppressors (method described in section 7.7) and were sequenced to identify the suppressor genes. Plasmids were retransformed into the *pcp1* mutants to confirm suppression.

7.15 Fluorescence microscopy

For fluorescence microscopy, an AxioplanII microscope (Zeiss Lts.) with Volocity software (Improvision Co.) and the DeltaVision-SoftWoRx system (Olympus and Applied Precision Co.) were used. For time-lapse microscopy, a 35 mm glass bottom culture dish (MatTek Corporation) was coated with 200 mg/ml soybean lectin (Sigma). 200 μl of cells were deposited in the well. The

culture dish was sealed with parafilm and allowed to sit for 30 min at 36°C before image acquisition began. Images were acquired using an Olympus IX70 wide-field inverted epifluorescence microscope equipped with an Olympus PlanApo 100x, NA 1.4, oil immersion objective, and the DeltaVision-SoftWoRx 3.3.0 software. Images were taken at 15 sections along the *z* axis at 0.2- to 0.4-mm intervals. They were then deconvolved and merged into a single projection using the maximum intensity algorithm. Images were processed with Adobe Photoshop CS2 (version 9.0).

For fixed-cell image acquisition, cells were fixed either with para-formaldehyde or methanol (methanol fixation is described in section 7.17). For para-formaldehyde fixation, 900 μl of cells were added to 100 μl of 16% para-formaldehyde, and were incubated at room temperature for 10 min. The cells were washed in PBS once, resuspended in 10 μl of PBS, and were kept at 4°C until ready for analysis. For GFP-containing strains, images were acquired the same day to avoid signal fading. To visualise DNA, 0.5 μl of 4',6-diamidine-2'-phenylindole (DAPI, Vectashield, Vector Laboratories) was added to the same volume of cell suspension. To visualise cell wall and septa, 0.5 μl of 50 μg/ml Calcofluor (Sigma) was used instead. A coverslip was placed on top of the cells before examination by fluorescence microscopy.

7.16 Fluorescence signal intensity quantification

z sections of images were merged into a single projection using the maximum intensity algorithm in Deltavision-SoftWoRx (Olympus and Applied Precision Ltd.). Fluorescence signals were quantified using maximum intensity. Background signals were quantified from the region within the cytoplasm and were subtracted from the fluorescence signals of the object of interest.

7.17 Indirect immunofluorescence microscopy

Cells were harvested by filtration from 10 ml of $5x10^6$ cells/ml culture. The filter was submerged in 20 ml of -80°C methanol, and was left in -80°C freezer for 10 min. After removing the filter from the tube, cells were spun down at 3000 rpm for 3 min. Supernatant was discarded and cells were resuspended in 1 ml PEM buffer. The cells were washed 3x with PEM buffer. Pelleting of cells were achieved by spinning at 11,000 rpm for 10 s, switching the orientation of the tube by 180°, and followed another spin at 11,000 rpm for 10s. The cell wall was digested by addition of 1 ml of 0.6 mg/ml 20T Zymolase (MP Biomedicals)/PEMS, incubated at 37°C for 70 min with gentle shaking. Cells were pelleted, resuspended in 1 ml of 1% TritonX100/PEMS, and incubated at room temperature for 5 min. This was followed by washing with PEM buffer, 3x. Cells were then resuspended in 1 ml of PEMBAL, incubated at room temperature for 30 min. Cells were pelleted and 40 μl of primary antibody, diluted in PEMBAL, was added. The tube was rotated at room temperature overnight. Cells were then washed with PEMBAL, 3x, 200 μl of secondary antibody was added, and the tube was rotated at room temperature for 2 h. Cells were washed with PEMBAL, 3x, and were resuspended in 50 μl 0.1% NaN_3/PBS. Images were acquired with fluorescence microscopy. The following antibody dilution was used for the indirect immunofluorescence microscopy, diluted in PEMBAL: anti-Pcp1 (1:5000 or 140 ng/ml), polyclonal anti-Sad1 (provided by Iain Hagan)(1:200), TAT-1 (α-tubulin monoclonal antibody provided by K. Gull, Oxford University, United Kingdom)(1:200), Cy3-conjugated anti-mouse antibody (1:1000), Cy3-conjugated anti-rabbit antibody (1:200) and fluorescein-conjugated anti-rabbit antibody (1:40).

7.18 Electron microscopy

To enrich for mitotic cells, elutriation was performed as described in section 7.12. Immediately after the harvest of small early G2 cells, the culture was incubated at 36°C. At time 100 and 120 min, when cells were entering mitosis,

10 ml of samples were harvested for indirect immunofluorescence microscopy (to confirm enrichment of mitotic cells by TAT-1 staining, method described in section 7.17) and electron microscopy. For electron microscopy, cells were collected by filtration, and the cell paste was transferred onto a sample carrier. The sample was then cryofixed by high-pressure freezing using EM PACT2 (Leica Microsystems). Freeze-substitution was carried out in anhydrous acetone containing 0.01% osmium tetraoxide, 0.1% glutaraldehyde and 0.25% uranyl acetate for 3 days at -90^{o}C using a EM AFS (Leica Microsystems). Freeze-substituted cells were gradually warmed to -20^{o}C and were finally infiltrated with Epon. Serial thin sections of ~60 nm were cut using Ultracut UCT microtome (Leica Microsystems) and placed on pioloform-coated slot grids. Sections were poststained with 2% uranyl acetate in 70% methanol for 4 min and with lead citrate for 1 min. Electron micrographs were acquired with a Tecnai Biotwin electron microscope (FEI Company) and DigitalMicrograph (Gatan Inc.). Captured images were processed with Adobe Photoshop CS2 (version 9.0).

7.19 Protein extraction

7.19.1 Quick alkaline method

Cells were harvested from 20 ml of 2x10^{6} cells/ml culture. They were washed in 1 ml of H_2O and resuspended in 0.5 ml of H_2O. 0.5 ml of 0.6N NaOH was added and the mixture was incubated at room temperature for 10 min. Cells were spun down at 4000 rpm for 2 min, and the supernatant was removed. 100 μl of 1x sample buffer was added and the sample was boiled for 5 min. The tube was spun at 13,000 rpm for 1 min and the sample was kept at 4^{o}C until ready for gel loading.

7.19.2 Glass bead method

Cells were harvested from 50 ml of 1x10^7 cells/ml culture. They were washed in 1 ml of STOP buffer, and were resuspended in 0.1 ml of lysis buffer (all buffers were pre-chilled at 4^{o}C hereon). 0.5 g of acid-washed 425-600 μm glass beads (one and a half PCR tube-full) was added. Cells were broken using a Fastprep FP120 cell disruptor (Savant Co.), with a setting of 5.5, 25 s, twice, in a cold room. Samples were chilled on ice between each disruption. Cell lysis was confirmed visually under a microscope, by the presence of 'ghost' cells. The base of each tube was pierced with a needle, and the extract was spun into a clean tube at 5000 rpm, 1 min, 4^{o}C. The protein extract was cleared by spinning at 13000 rpm, 15 min, 4^{o}C. 140 μl was cleared extract was transferred into a new tube. 200 μl of lysis buffer was added to the extract and protein concentration was determined by Bradford assay (BioRad). Extract was used for subsequent analysis.

7.20 Immunoprecipitation

Protein extract was prepared as described in section 7.19.2. 20 μl of extract was set aside as whole-cell extract control. The remaining extract, usually about 5 mg of total protein, was used for immunoprecipitation. 10 μl of protein A Dynabeads (Invitrogen) bound with affinity-purified anti-Pcp1 antibody or pre-immune serum was added to the protein extract. The mixture was rotated at 4^{o}C for 1 h. Beads were then washed 5x with wash buffer, and 80 μl of 1x sample buffer was added. The beads were boiled for 5 min, spun at 13,000 rpm for 1 min and the sample was kept at 4^{o}C until ready for gel loading.

7.21 Immunoblot analysis

Protein extracts were loaded onto 3-8% tris-acetate Criterion XT gels (BioRad). The resolved proteins were transferred onto Immobilon-P membrane (Millipore).

Membrane was blocked with 5% skimmed milk/PBST at room temperature for 1 h, or at 4°C for overnight. Primary antibody was added to the membrane, and was incubated at room temperature for 1 h. Membrane was washed in PBST, 3x, 5 min. Secondary antibody was then added, and was incubated at room temperature for 1 h. The membrane was washed with PBST 3x, 5 min, followed by PBS, 3x, 5 min. Bound proteins were visualised using chemiluminescence ECL Kit (GE Healthcare Co.). The following antibody dilution was used in the immunoblotting, diluted in 3% milk/PBST: anti-Pcp1 (1:5000 or 140 ng/ml), anti-HA 16B12 (BabCo)(1:200), anti-γ-tubulin (Sigma)(1:500), anti-α-tubulin (Sigma)(1:20,000), horseradish peroxidase-conjugated anti-rabbit antibody (1:2000) and horseradish peroxidase-conjugated anti-mouse antibody (1:2000).

7.22 λ-phosphatase treatment

Pcp1 was immunoprecipitated from mitotic-arrested cells using anti-Pcp1 coupled protein A dynabeads (method described in section 7.20). 100 U of λ-phosphatase (New England Biolabs Ltd.) was added to the beads. The reactions were incubated at 30°C for 30 min. As a control, phosphatase inhibitors (10 mM NaV, 50 mM NaF) were added to one of the reactions. Pcp1 was finally eluted from the beads by addition of sample buffer and boiled at 95°C for 5 min. 15 μl of the extract was loaded onto 3-8% tris-acetate Criterion XT gels (BioRad). Immunoblot was carried out as described in section 7.21.

7.23 Pcp1 antibody generation

The N-terminus (1-1812 bp), C-terminus (1813-3624 bp), and the complete open reading frame of *pcp1*$^+$ gene (1-3624 bp) were cloned into the pET14b expression vector, at the Nde1/BamHI sites. The plasmids were transformed into FB810 *E. coli* expression host, and transformants were selected on ampicillin-containing Luria-Bertani (LB) plates. Colonies were picked and inoculated into 3 ml of ampicillin-containing LB broth, and were incubated at 37°C, 300 rpm, for 5 h until the density of the culture reached OD_{600} 0.5.

Isopropyl β-D-1-thiogalactopyranoside (IPTG) was added to a final concentration of 1 mM, and the culture was further incubated at 37°C for 2 h. After the confirmation of protein expression, the plasmids were sent to the Protein Isolation Laboratory at Cancer Research UK London Research Institute for large-scale protein expression and purification. Only N-terminus Pcp1 was produced in large-scale. Since the protein was tagged with a 6xHis at its N-terminus, it was purified using the HisTrap Kit according to the manufacturer's instruction (GE Healthcare Co.). The purified protein was sent to Harlan Sera Lab for rabbit immunisation. The serum collected was affinity purified against Pcp1 antigen, and the purified antibody (700 μg/ml, 6 ml) was stored in PBS at -20°C. Specificity of the antibody was verified by immunoblot analysis using wild-type and 3HA-tagged Pcp1.

7.24 Fission yeast nomenclature

cis-elements such as gene names are italicised, e.g. *pcp1*. The wild-type allele is represented by a superscript plus, e.g. *pcp1*$^{+}$. If a mutant allele of the gene is being referred to, its allele number will follow the gene name, e.g. *pcp1-15*. A gene that has been tagged is denoted by the gene name followed by the name of the tag with its specific marker, e.g. *pcp1*$^{+}$*-GFP-hph*^{r}. If a gene is tagged at its 5'-end, the tag will precede the gene name, e.g. *hph*^{r}*-GFP-pcp1*$^{+}$. Gene products are presented in Roman type (i.e. non-italicized), with the first letter capitalised e.g. Pcp1. Tagged gene products are written with the protein name followed by the name of the tag, e.g. Pcp1-GFP. When a gene has been deleted with a specific marker gene, it is presented as the gene name followed by the name of the gene that is replacing it, separated by a '::', e.g. *pcp1::hph*^{r}. A gene deletion is also commonly denoted by a '*Δ*' after the gene name, e.g. *pcp1Δ*.

7.25 Strain list

Strains	Genotypes*	source
513	*h- leu1 ura4*	Lab stock
TP108-3D	*h+ leu1 ura4 his2*	Lab stock
CHP428	*h+ leu1 ura4 his7 ade6-M210*	Lab stock
CHP429	*h- leu1 ura4 his7 ade6-M216*	Lab stock
MS1030	*h- pcp1^{+}-HA-hph^{r} leu1 ura4*	Lab stock
CSF0040	*h- pcp1-2-HA-hph^{r} leu1 ura4*	This study
CSF0056	*h- pcp1-10-HA-hph^{r} leu1 ura4*	This study
CSF0074	*h- pcp1-14-HA-hph^{r} leu1 ura4*	This study
CSF0076	*h- pcp1-15-HA-hph^{r} leu1 ura4*	This study
CSF0078	*h- pcp1-16-HA-hph^{r} leu1 ura4*	This study
CSF0080	*h- pcp1-17-HA-hph^{r} leu1 ura4*	This study
CSF0082	*h- pcp1-18-HA-hph^{r} leu1 ura4*	This study
CSF0084	*h- pcp1-19-HA-hph^{r} leu1 ura4*	This study
CSF0086	*h- pcp1-20-HA-hph^{r} leu1 ura4*	This study
CSF0088	*h- pcp1-21-HA-hph^{r} leu1 ura4*	This study
CSF0090	*h- pcp1-22-HA-hph^{r} leu1 ura4*	This study
MS235	*h+ cut12^{+}-GFP-ura4^{+} leu1 ura4 his2*	Lab stock
CSF0148	*h- pcp1^{+}-HA-hph^{r} cut12^{+}-GFP-ura4^{+} leu1 ura4*	This study
CSF0150	*h- pcp1-15-HA-hph^{r} cut12^{+}-GFP-ura4^{+} leu1 ura4*	This study
CSF0405	*h+ pcp1-18-HA-hph^{r} cut12^{+}-GFP-ura4^{+} leu1 ura4 ade6-?*	This study
HRT173	*h- plo1^{+}-GFP-HA-kan^{r} sid4^{+}-mRFP-kan^{r} leu1 ura4 lys1*	Lab stock
CSF0355	*h- sid4^{+}-mRFP-nat^{r} leu1 ura4*	This study
HR1676	*h+ aur^{r}-pnda3-GFP-atb2^{+} leu1 ura4 his2*	Lab stock
CSF0363	*h- pcp1^{+}-HA-hph^{r} sid4^{+}-mRFP-nat^{r}*	This study

Strains	Genotypes*	source
	aur^r-pnda3-GFP-atb2$^+$ leu1 ura4	
CSF0364	*h- pcp1-15-HA-hph^r sid4$^+$-mRFP-nat^r aur^r-pnda3-GFP-atb2 leu1 ura4*	This study
CSF0365	*h- pcp1-18-HA-hph^r sid4$^+$-mRFP-nat^r aur^r-pnda3-GFP-atb2$^+$ leu1 ura4*	This study
CSF0380	*h+ sfi1$^+$-mRFP-nat^r leu1 ura4 his2*	This study
MS247	*h- cdc7$^+$-GFP-kan^r leu1 ura4 ade6-M210*	Lab stock
HR1649	*h+ aur^r-pnda3-mCh-atb2$^+$ leu1 ura4 his2*	Lab stock
CSF0511	*h- pcp1$^+$-HA-hph^r cdc7$^+$-GFP-kan^r sfi1$^+$-mRFP-nat^r aur^r-pnda3-mCh-atb2$^+$ leu1 ura4 ade6-M210*	This study
CSF0513	*h- pcp1-15-HA-hph^r cdc7$^+$-GFP-kan^r sfi1$^+$-mRFP-nat^r aur^r-pnda3-mCh-atb2$^+$ leu1 ura4*	This study
CSF0515	*h- pcp1-18-HA-hph^r cdc7$^+$-GFP-kan^r sfi1$^+$-mRFP-nat^r aur^r-pnda3-mCh-atb2$^+$ leu1 ura4*	This study
CSF0093	*h+ alp4$^+$-GFP-kan^r leu1 ura4 his2*	This study
CSF0395	*h- pcp1$^+$-HA-hph^r alp4$^+$-GFP-kan^r sfi1$^+$-mRFP-nat^r leu1 ura4*	This study
CSF0397	*h- pcp1-15-HA-hph^r alp4$^+$-GFP-kan^r sfi1$^+$-mRFP-nat^r leu1 ura4*	This study
CSF0399	*h- pcp1-18-HA-hph^r alp4$^+$-GFP-kan^r sfi1$^+$-mRFP-nat^r leu1 ura4*	This study
MT417	*h+ alp6$^+$-GFP-kan^r leu1 ura4 his2*	Lab stock
CSF0346	*h- pcp1$^+$-HA-hph^r alp6$^+$-GFP-kan^r leu1 ura4*	This study
CSF0348	*h- pcp1-15-HA-hph^r alp6$^+$-GFP-kan^r leu1 ura4*	This study
CSF0350	*h- pcp1-18-HA-hph^r alp6$^+$-GFP-kan^r leu1 ura4*	This study
CSF0466	*h- pcp1$^+$-HA-hph^r alp6$^+$-GFP-kan^r leu1 ura4 +pREP1*	This study
CSF0468	*h- pcp1$^+$-HA-hph^r alp6$^+$-GFP-kan^r leu1 ura4*	This study

Strains	Genotypes*	source
	+pREP1-alp4^{+}	
CSF0470	*h- pcp1-15-HA-hph*^{r} *alp6*$^{+}$*-GFP-kan*^{r} *leu1 ura4 +pREP1*	This study
CSF0472	*h- pcp1-15-HA-hph*^{r} *alp6*$^{+}$*-GFP-kan*^{r} *leu1 ura4 +pREP1-alp4*$^{+}$	This study
CSF0338	*h- pcp1*$^{+}$*-HA-hph*^{r} *leu1 ura4 +pREP1*	This study
CSF0339	*h- pcp1*$^{+}$*-HA-hph*^{r} *leu1 ura4 +pREP1-alp4*$^{+}$	This study
CSF0340	*h- pcp1-15-HA-hph*^{r} *leu1 ura4 +pREP1*	This study
CSF0341	*h- pcp1-15-HA-hph*^{r} *leu1 ura4 +pREP1-alp4*$^{+}$	This study
CSF0342	*h- pcp1-18-HA-hph*^{r} *leu1 ura4 +pREP1*	This study
CSF0343	*h- pcp1-18-HA-hph*^{r} *leu1 ura4 +pREP1-alp4*$^{+}$	This study
CSF0257	*h- pcp1-15-HA-hph*^{r} *leu1 ura4 +pSK-pcp1*$^{+}$	This study
CSF0276	*h- pcp1-15-HA-hph*^{r} *leu1 ura4 +pSK*	This study
CSF0555	*h- pcp1-15-HA-hph*^{r} *leu1 ura4 +pSK-cut11*$^{+}$	This study
CSF0556	*h- pcp1-15-HA-hph*^{r} *leu1 ura4 +pSK-pom152*$^{+}$	This study
CSF0269	*h- pcp1-18-HA-hph*^{r} *leu1 ura4 +pSK-pcp1*$^{+}$	This study
CSF0282	*h- pcp1-18-HA-hph*^{r} *leu1 ura4 +pSK*	This study
CSF0284	*h- pcp1-18-HA-hph*^{r} *leu1 ura4 +pSK-cut11*$^{+}$	This study
CSF0285	*h- pcp1-18-HA-hph*^{r} *leu1 ura4 +pSK-pom152*$^{+}$	This study
CSF0486	*h+ pom152*$^{+}$*-GFP-kan*^{r} *leu1 ura4 his2*	This study
CSF0490	*h- pom152*$^{+}$*-GFP-kan*^{r} *cut11*$^{+}$*-4mRFP-nat*^{r} *leu1 ura4*	This study
MT197	*h+ cut11*$^{+}$*-GFP-ura4*$^{+}$ *leu1 ura4*	Lab stock
CSF0474	*h- pcp1*$^{+}$*-HA-hph*^{r} *aur*^{r}*-pnda3-mCh-atb2*$^{+}$ *cut11*$^{+}$*-GFP-ura4*$^{+}$ *leu1 ura4*	This study
CSF0476	*h- pcp1-15-HA-hph*^{r} *aur*^{r}*-pnda3-mCh-atb2*$^{+}$ *cut11*$^{+}$*-GFP-ura4*$^{+}$ *leu1 ura4*	This study
CSF0478	*h- pcp1-18-HA-hph*^{r} *aur*^{r}*-pnda3-mCh-atb2*$^{+}$ *cut11*$^{+}$*-GFP-ura4*$^{+}$ *leu1 ura4*	This study
CSF0277	*h- pcp1-15-HA-hph*^{r} *leu1 ura4 +pSK-cut12*$^{+}$	This study
CSF0283	*h- pcp1-18-HA-hph*^{r} *leu1 ura4 +pSK-cut12*$^{+}$	This study

Strains	Genotypes*	source
MS235	*h+ cut12^{+}-GFP-ura4^{+} leu1 ura4 his2*	Lab stock
CSF0448	*h- pcp1^{+}-HA-hph^{r} cut12^{+}-GFP-ura4^{+} sid4^{+}-mRFP-nat^{r} leu1 ura4*	This study
CSF0450	*h- pcp1-15-HA-hph^{r} cut12^{+}-GFP-ura4^{+} sid4^{+}-mRFP-nat^{r} leu1 ura4*	This study
CSF0452	*h- pcp1-18-HA-hph^{r} cut12^{+}-GFP-ura4^{+} sid4^{+}-mRFP-nat^{r} leu1 ura4*	This study
HRT71	*h+ plo1^{+}-GFP-HA-kan^{r} leu1 ura4 lys1*	Lab stock
CSF0517	*h? pcp1^{+}-HA-hph^{r} plo1^{+}-GFP-HA-kan^{r} sfi1^{+}-mRFP-nat^{r} aur^{r}-pnda3-mCh-atb2^{+} leu1 ura4*	This study
CSF0519	*h? pcp1-15-HA-hph^{r} plo1^{+}-GFP-HA-kan^{r} sfi1^{+}-mRFP-nat^{r} aur^{r}-pnda3-mCh-atb2^{+} leu1 ura4*	This study
CSF0521	*h? pcp1-18-HA-hph^{r} plo1^{+}-GFP-HA-kan^{r} sfi1^{+}-mRFP-nat^{r} aur^{r}-pnda3-mCh-atb2^{+} leu1 ura4*	This study
MS466	*h+ cut12.s11 alp7^{+}-YFP-kan^{r} leu1 ura4 his2*	Lab stock
CSF0523	*h- pcp1^{+}-HA-hph^{r} cut12.s11 leu1 ura4*	This study
CSF0525	*h- pcp1-15-HA-hph^{r} cut12.s11 leu1 ura4*	This study
CSF0527	*h- pcp1-18-HA-hph^{r} cut12.s11 leu1 ura4*	This study
Wee1-50	*h- wee1-50 leu1*	Lab stock
CSF0549	*h- pcp1^{+}-HA-hph^{r} wee1-50 leu1*	This study
CSF0551	*h- pcp1-15-HA-hph^{r} wee1-50 leu1*	This study
CSF0553	*h- pcp1-18-HA-hph^{r} wee1-50 leu1*	This study
CSF0200	*h- pcp1^{+}-HA-hph^{r} plo1^{+}-GFP-HA-kan^{r} leu1 ura4*	This study
CSF0204	*h- pcp1-15-HA-hph^{r} plo1^{+}-GFP-HA-kan^{r} leu1 ura4*	This study
CSF0208	*h- pcp1-18-HA-hph^{r} plo1^{+}-GFP-HA-kan^{r} leu1 ura4*	This study
KM311-	*h+ nda3-311 leu1 his2*	Lab stock

Strains	Genotypes*	source
210		
CSF0198	*h- plo1^{+}-GFP-HA-kan^{r} nda3-311 leu1 ura4*	This study
Cdc25-22	*h+ cdc25-22*	Lab stock
KZ34	*h+ nda3-1828 leu1 ura4 his2*	Lab stock
IH1636	*h- plo1.ts19:ura4^{+} leu1 ura4 ade6-210*	Dr. Iain Hagan
NR172	*h- leu1::nmt41-GFP-plo1:ura4^{+} leu1 ura4 ade6-704*	Lab stock
IH2893	*h- leu1::nmt41-plo1.SDTD:ura4^{+} leu1 ura4*	Dr. Iain Hagan
CSF0275	*h-/h+ pcp1::ura4^{+}/pcp1^{+} leu1/leu1 ura4/ura4 his7/his7 ade6-M210/ade6-M216*	This study
CSF0302	*h+ pcp1-prm nda3-311 leu1 ura4 his7*	This study

* *leu1* is *leu1-32* and *ura4* is *ura4-D18*

7.26 Oligonucleotides

For C-terminal tagging of *pcp1^{+}*:

Pcp1HA-F: (5' to 3')
TGAAGAATGAGTGGCTAAAACAAGCTCAATTGAAACAATCATTGCAAAGAG
CTGCCGCAAAGGCAAAGACCGCAAACTACCGGATCCCCGGGTTAATTAA

Pcp1HA-R: (5' to 3')
ATAAATTAAAATAATTATAGTAGTAGAATTAATTGAATGTTGTTAAAAAAAAA
GAGAGTAAAAAACGTAAGTATCCCAGAGAATTCGAGCTCGTTTAAAC

For mutagenesis of *pcp1^{+}* for temperature-sensitive mutant isolation:

P7.Pcp1-U406-(F): 5'-ATTCATGTTTACGTTTTGGACCCTA-3'

P9.Pcp1-D168-(R): 5'-TTTTACGCTTTAATACCATTACTAC-3'

For cloning of *pcp1* for antibody generation:

P3.Pcp1half-F: 5'-TATACATATGATGTCTGAACGAGATTTTAA-3’

P4.Pcp1half-R: 5'-TATAGGATCCTTAATTAATGGATTCATGAAACC-3'

P5.Pcp2half-F: 5'-TATACATATGAAATTACAAGATCGAGAGAA-3'

P6.Pcp2half-R: 5'-TATAGGATCCTTAGTAGTTTGCGGTCTTTG-3'

For sequencing of *pcp1* mutant alleles:

Pcp1-U105-(F): 5’-TTGCTTTTTAATGATTCTGCC-3’

Pcp1-196-(F): 5’-GGTAGTTTGGAATTTACTCCATTAT-3’

Pcp1-501-(F): 5’-ACTTCGAATCAAAATTGTATG-3’

Pcp1-1001-(F): 5’-ATGAGGAGAATTCAAGCTACG-3’

Pcp1-1501-(F): 5’-TTGCAAGAAGTCACTAAAGAAC-3’

Pcp1-1996-(F): 5’-TCAGTACTTCAGCGGCAGCTTACC-3’

Pcp1-2441-(F): 5’-TGATGGGATGTGATTATTCTTC-3’

Pcp1-2899-(F): 5’-TGGTTAGAAAGAGAACGTTCGATAC-3’

Pcp1-3153-(F): 5’-CGATCATCTGTCTACTATTTTGG-3’

For site-directed mutagenesis to create *pcp1-prm* mutant:

P47.NTermMut1-F
5'-GATAAATCATCTTTCCAGGCGCCTTTGCGCAACGGCTC-3'

P48.NTermMut1-R
5'-GAGCCGTTGCGCAAAGGCGCCTGGAAAGATGATTTATC-3'

P53.CTermMut2&3-F
5'-CTGCCCAAAAGTTTTTTGCCGCTCCTGATCGGAAGAATG-3'

P54.CTermMut2&3-R
5'-CATTCTTCCGATCAGGAGCGGCAAAAAACTTTTGGGCAG-3'

P43.NTerm-F
5'-ATGTCTGAACGAGATTTTAATACGC-3'

P44.NTerm-R
5'-CCAAAGTTTTCTCTGCTAACTTTCTC-3'

P45.CTerm-F
5'-TTTGAAAAATTTGGATTGGGAACTG-3'

P46.CTerm-R
5'-CTTTCGTCGGTAACATTGGAAGTC-3'

For deletion of *pcp1*$^{+}$:

P57.pcp1::ura4-F: (5' to 3')
TAAGTAGTTTCTATATAATTTTATGCACTTGCGCTAGTTGGTGGATAATTTTA
ATAAATACATGCATCCGCAGTTACGTTCGCCAGGGTTTTCCCAGTCACGAC

P58.pcp1::ura4-R: (5’ to 3’)
ATAAATTAAAATAATTATAGTAGTAGAATTAATTGAATGTTGTTAAAAAAAAA
GAGAGTAAAAAACGTAAGTATCCCAGAAGCGGATAACAATTTCACACAGGA

For C-terminal tagging of *pom152*$^{+}$:

P69.FYpom152GFP-F: (5’ to 3’)
TTGAAGGTGTCTATACTGTATTGAGTGTTCAAGACAAGTACTGTCGCTACC
CTCAGGATTCGACATCATCTTCTAACATTCGGATCCCCGGGTTAATTAA

P69.FYpom152GFP-R: (5’ to 3’)
AAAAGCAACTAAATTATTTTTATTCTACCAACAAACTCTAAAAGAAAAAGAAA
GATAGATTCGTTCTTAATAAACGCGCAGAATTCGAGCTCGTTTAAAC

8 References

Abrieu, A., Brassac, T., Galas, S., Fisher, D., Labbe, J.C., and Doree, M. (1998). The Polo-like kinase Plx1 is a component of the MPF amplification loop at the G2/M-phase transition of the cell cycle in Xenopus eggs. J Cell Sci *111 (Pt 12)*, 1751-1757.

Adams, I.R., and Kilmartin, J.V. (1999). Localization of core spindle pole body (SPB) components during SPB duplication in Saccharomyces cerevisiae. J Cell Biol *145*, 809-823.

Aebi, U., Cohn, J., Buhle, L., and Gerace, L. (1986). The nuclear lamina is a meshwork of intermediate-type filaments. Nature *323*, 560-564.

Alber, F., Dokudovskaya, S., Veenhoff, L.M., Zhang, W., Kipper, J., Devos, D., Suprapto, A., Karni-Schmidt, O., Williams, R., Chait, B.T.*, et al.* (2007). The molecular architecture of the nuclear pore complex. Nature *450*, 695-701.

Alderton, G.K., Joenje, H., Varon, R., Borglum, A.D., Jeggo, P.A., and O'Driscoll, M. (2004). Seckel syndrome exhibits cellular features demonstrating defects in the ATR-signalling pathway. Hum Mol Genet *13*, 3127-3138.

Alfa, C.E., Ducommun, B., Beach, D., and Hyams, J.S. (1990). Distinct nuclear and spindle pole body population of cyclin-cdc2 in fission yeast. Nature *347*, 680-682.

Alvarez, B., Martinez, A.C., Burgering, B.M., and Carrera, A.C. (2001). Forkhead transcription factors contribute to execution of the mitotic programme in mammals. Nature *413*, 744-747.

Anders, A., Lourenco, P.C., and Sawin, K.E. (2006). Noncore components of the fission yeast gamma-tubulin complex. Mol Biol Cell *17*, 5075-5093.

Araki, Y., Lau, C.K., Maekawa, H., Jaspersen, S.L., Giddings, T.H., Jr., Schiebel, E., and Winey, M. (2006). The Saccharomyces cerevisiae spindle pole body (SPB) component Nbp1p is required for SPB membrane insertion

and interacts with the integral membrane proteins Ndc1p and Mps2p. Mol Biol Cell *17*, 1959-1970.

Archambault, V., and Glover, D.M. (2009). Polo-like kinases: conservation and divergence in their functions and regulation. Nat Rev Mol Cell Biol *10*, 265-275.

Badano, J.L., Teslovich, T.M., and Katsanis, N. (2005). The centrosome in human genetic disease. Nat Rev Genet *6*, 194-205.

Bahler, J., Wu, J.Q., Longtine, M.S., Shah, N.G., McKenzie, A., 3rd, Steever, A.B., Wach, A., Philippsen, P., and Pringle, J.R. (1998). Heterologous modules for efficient and versatile PCR-based gene targeting in Schizosaccharomyces pombe. Yeast *14*, 943-951.

Bailly, E., Doree, M., Nurse, P., and Bornens, M. (1989). p34cdc2 is located in both nucleus and cytoplasm; part is centrosomally associated at G2/M and enters vesicles at anaphase. EMBO J *8*, 3985-3995.

Balczon, R., Simerly, C., Takahashi, D., and Schatten, G. (2002). Arrest of cell cycle progression during first interphase in murine zygotes microinjected with anti-PCM-1 antibodies. Cell Motil Cytoskeleton *52*, 183-192.

Barr, F.A., Sillje, H.H., and Nigg, E.A. (2004). Polo-like kinases and the orchestration of cell division. Nat Rev Mol Cell Biol *5*, 429-440.

Basi, G., Schmid, E., and Maundrell, K. (1993). TATA box mutations in the Schizosaccharomyces pombe nmt1 promoter affect transcription efficiency but not the transcription start point or thiamine repressibility. Gene *123*, 131-136.

Bassermann, F., Frescas, D., Guardavaccaro, D., Busino, L., Peschiaroli, A., and Pagano, M. (2008). The Cdc14B-Cdh1-Plk1 axis controls the G2 DNA-damage-response checkpoint. Cell *134*, 256-267.

Basto, R., Lau, J., Vinogradova, T., Gardiol, A., Woods, C.G., Khodjakov, A., and Raff, J.W. (2006). Flies without centrioles. Cell *125*, 1375-1386.

Beaudouin, J., Gerlich, D., Daigle, N., Eils, R., and Ellenberg, J. (2002). Nuclear envelope breakdown proceeds by microtubule-induced tearing of the lamina. Cell *108*, 83-96.

Bettencourt-Dias, M., and Glover, D.M. (2007). Centrosome biogenesis and function: centrosomics brings new understanding. Nat Rev Mol Cell Biol *8*, 451-463.

Bettencourt-Dias, M., Rodrigues-Martins, A., Carpenter, L., Riparbelli, M., Lehmann, L., Gatt, M.K., Carmo, N., Balloux, F., Callaini, G., and Glover, D.M. (2005). SAK/PLK4 is required for centriole duplication and flagella development. Curr Biol *15*, 2199-2207.

Bobinnec, Y., Khodjakov, A., Mir, L.M., Rieder, C.L., Edde, B., and Bornens, M. (1998). Centriole disassembly in vivo and its effect on centrosome structure and function in vertebrate cells. J Cell Biol *143*, 1575-1589.

Bornens, M. (2002). Centrosome composition and microtubule anchoring mechanisms. Curr Opin Cell Biol *14*, 25-34.

Bourett, T.M., Sweigard, J.A., Czymmek, K.J., Carroll, A., and Howard, R.J. (2002). Reef coral fluorescent proteins for visualizing fungal pathogens. Fungal Genet Biol *37*, 211-220.

Boveri, T. (1901). Uber die Natur der Centrosomen, Vol 28.

Bridge, A.J., Morphew, M., Bartlett, R., and Hagan, I.M. (1998). The fission yeast SPB component Cut12 links bipolar spindle formation to mitotic control. Genes Dev *12*, 927-942.

Buck, V., Ng, S.S., Ruiz-Garcia, A.B., Papadopoulou, K., Bhatti, S., Samuel, J.M., Anderson, M., Millar, J.B., and McInerny, C.J. (2004). Fkh2p and Sep1p regulate mitotic gene transcription in fission yeast. J Cell Sci *117*, 5623-5632.

Budde, P.P., Kumagai, A., Dunphy, W.G., and Heald, R. (2001). Regulation of Op18 during spindle assembly in Xenopus egg extracts. J Cell Biol *153*, 149-158.

Bullitt, E., Rout, M.P., Kilmartin, J.V., and Akey, C.W. (1997). The yeast spindle pole body is assembled around a central crystal of Spc42p. Cell *89*, 1077-1086.

Byers, B., and Goetsch, L. (1974). Duplication of spindle plaques and integration of the yeast cell cycle. Cold Spring Harb Symp Quant Biol *38*, 123-131.

Byers, B., and Goetsch, L. (1975a). Behavior of spindles and spindle plaques in the cell cycle and conjugation of Saccharomyces cerevisiae. J Bacteriol *124*, 511-523.

Byers, B., and Goetsch, L. (1975b). Electron microscopic observations on the meiotic karyotype of diploid and tetraploid Saccharomyces cerevisiae. Proc Natl Acad Sci U S A *72*, 5056-5060.

Casenghi, M., Barr, F.A., and Nigg, E.A. (2005). Phosphorylation of Nlp by Plk1 negatively regulates its dynein-dynactin-dependent targeting to the centrosome. J Cell Sci *118*, 5101-5108.

Casenghi, M., Meraldi, P., Weinhart, U., Duncan, P.I., Korner, R., and Nigg, E.A. (2003). Polo-like kinase 1 regulates Nlp, a centrosome protein involved in microtubule nucleation. Dev Cell *5*, 113-125.

Cheng, J., Turkel, N., Hemati, N., Fuller, M.T., Hunt, A.J., and Yamashita, Y.M. (2008). Centrosome misorientation reduces stem cell division during ageing. Nature *456*, 599-604.

Cheng, K.Y., Lowe, E.D., Sinclair, J., Nigg, E.A., and Johnson, L.N. (2003). The crystal structure of the human polo-like kinase-1 polo box domain and its phospho-peptide complex. EMBO J *22*, 5757-5768.

Chial, H.J., Rout, M.P., Giddings, T.H., and Winey, M. (1998). Saccharomyces cerevisiae Ndc1p is a shared component of nuclear pore complexes and spindle pole bodies. J Cell Biol *143*, 1789-1800.

Chikashige, Y., Ding, D.Q., Funabiki, H., Haraguchi, T., Mashiko, S., Yanagida, M., and Hiraoka, Y. (1994). Telomere-led premeiotic chromosome movement in fission yeast. Science *264*, 270-273.

Chikashige, Y., Tsutsumi, C., Yamane, M., Okamasa, K., Haraguchi, T., and Hiraoka, Y. (2006). Meiotic proteins bqt1 and bqt2 tether telomeres to form the bouquet arrangement of chromosomes. Cell *125*, 59-69.

Collas, P. (1999). Sequential PKC- and Cdc2-mediated phosphorylation events elicit zebrafish nuclear envelope disassembly. J Cell Sci *112 (Pt 6)*, 977-987.

Cusick, M.E. (1994). RNP1, a new ribonucleoprotein gene of the yeast Saccharomyces cerevisiae. Nucleic Acids Res *22*, 869-877.

D'Angelo, M.A., and Hetzer, M.W. (2008). Structure, dynamics and function of nuclear pore complexes. Trends Cell Biol *18*, 456-466.

de Gramont, A., Barbour, L., Ross, K.E., and Cohen-Fix, O. (2007). The spindle midzone microtubule-associated proteins Ase1p and Cin8p affect the number and orientation of astral microtubules in Saccharomyces cerevisiae. Cell Cycle *6*, 1231-1241.

De Luca, M., Lavia, P., and Guarguaglini, G. (2006). A functional interplay between Aurora-A, Plk1 and TPX2 at spindle poles: Plk1 controls centrosomal localization of Aurora-A and TPX2 spindle association. Cell Cycle *5*, 296-303.

De Souza, C.P., Ellem, K.A., and Gabrielli, B.G. (2000). Centrosomal and cytoplasmic Cdc2/cyclin B1 activation precedes nuclear mitotic events. Exp Cell Res *257*, 11-21.

Decottignies, A., Zarzov, P., and Nurse, P. (2001). In vivo localisation of fission yeast cyclin-dependent kinase cdc2p and cyclin B cdc13p during mitosis and meiosis. J Cell Sci *114*, 2627-2640.

Dictenberg, J.B., Zimmerman, W., Sparks, C.A., Young, A., Vidair, C., Zheng, Y., Carrington, W., Fay, F.S., and Doxsey, S.J. (1998). Pericentrin and gamma-

tubulin form a protein complex and are organized into a novel lattice at the centrosome. J Cell Biol *141*, 163-174.

Ding, D.Q., Tomita, Y., Yamamoto, A., Chikashige, Y., Haraguchi, T., and Hiraoka, Y. (2000). Large-scale screening of intracellular protein localization in living fission yeast cells by the use of a GFP-fusion genomic DNA library. Genes Cells *5*, 169-190.

Ding, R., West, R.R., Morphew, D.M., Oakley, B.R., and McIntosh, J.R. (1997). The spindle pole body of Schizosaccharomyces pombe enters and leaves the nuclear envelope as the cell cycle proceeds. Mol Biol Cell *8*, 1461-1479.

do Carmo Avides, M., and Glover, D.M. (1999). Abnormal spindle protein, Asp, and the integrity of mitotic centrosomal microtubule organizing centers. Science *283*, 1733-1735.

do Carmo Avides, M., Tavares, A., and Glover, D.M. (2001). Polo kinase and Asp are needed to promote the mitotic organizing activity of centrosomes. Nat Cell Biol *3*, 421-424.

Donaldson, M.M., Tavares, A.A., Ohkura, H., Deak, P., and Glover, D.M. (2001). Metaphase arrest with centromere separation in polo mutants of Drosophila. J Cell Biol *153*, 663-676.

Doxsey, S.J., Stein, P., Evans, L., Calarco, P.D., and Kirschner, M. (1994). Pericentrin, a highly conserved centrosome protein involved in microtubule organization. Cell *76*, 639-650.

Drechsel, D.N., and Kirschner, M.W. (1994). The minimum GTP cap required to stabilize microtubules. Curr Biol *4*, 1053-1061.

Drummond, D.R., and Cross, R.A. (2000). Dynamics of interphase microtubules in Schizosaccharomyces pombe. Curr Biol *10*, 766-775.

Dutertre, S., Cazales, M., Quaranta, M., Froment, C., Trabut, V., Dozier, C., Mirey, G., Bouche, J.P., Theis-Febvre, N., Schmitt, E.*, et al.* (2004).

Phosphorylation of CDC25B by Aurora-A at the centrosome contributes to the G2-M transition. J Cell Sci *117*, 2523-2531.

Elia, A.E., Cantley, L.C., and Yaffe, M.B. (2003a). Proteomic screen finds pSer/pThr-binding domain localizing Plk1 to mitotic substrates. Science *299*, 1228-1231.

Elia, A.E., Rellos, P., Haire, L.F., Chao, J.W., Ivins, F.J., Hoepker, K., Mohammad, D., Cantley, L.C., Smerdon, S.J., and Yaffe, M.B. (2003b). The molecular basis for phosphodependent substrate targeting and regulation of Plks by the Polo-box domain. Cell *115*, 83-95.

Erickson, H.P., and Stoffler, D. (1996). Protofilaments and rings, two conformations of the tubulin family conserved from bacterial FtsZ to alpha/beta and gamma tubulin. J Cell Biol *135*, 5-8.

Fantes, P. (1979). Epistatic gene interactions in the control of division in fission yeast. Nature *279*, 428-430.

Fantes, P.A. (1981). Isolation of cell size mutants of a fission yeast by a new selective method: characterization of mutants and implications for division control mechanisms. J Bacteriol *146*, 746-754.

Fava, F., Raynaud-Messina, B., Leung-Tack, J., Mazzolini, L., Li, M., Guillemot, J.C., Cachot, D., Tollon, Y., Ferrara, P., and Wright, M. (1999). Human 76p: A new member of the gamma-tubulin-associated protein family. J Cell Biol *147*, 857-868.

Favreau, C., Worman, H.J., Wozniak, R.W., Frappier, T., and Courvalin, J.C. (1996). Cell cycle-dependent phosphorylation of nucleoporins and nuclear pore membrane protein Gp210. Biochemistry *35*, 8035-8044.

Ferris, D.K., Maloid, S.C., and Li, C.C. (1998). Ubiquitination and proteasome mediated degradation of polo-like kinase. Biochem Biophys Res Commun *252*, 340-344.

Flory, M.R., Morphew, M., Joseph, J.D., Means, A.R., and Davis, T.N. (2002). Pcp1p, an Spc110p-related calmodulin target at the centrosome of the fission yeast Schizosaccharomyces pombe. Cell Growth Differ *13*, 47-58.

Fode, C., Motro, B., Yousefi, S., Heffernan, M., and Dennis, J.W. (1994). Sak, a murine protein-serine/threonine kinase that is related to the Drosophila polo kinase and involved in cell proliferation. Proc Natl Acad Sci U S A *91*, 6388-6392.

Fong, K.W., Choi, Y.K., Rattner, J.B., and Qi, R.Z. (2008). CDK5RAP2 is a pericentriolar protein that functions in centrosomal attachment of the gamma-tubulin ring complex. Mol Biol Cell *19*, 115-125.

Friedman, D.B., Kern, J.W., Huneycutt, B.J., Vinh, D.B., Crawford, D.K., Steiner, E., Scheiltz, D., Yates, J., 3rd, Resing, K.A., Ahn, N.G.*, et al.* (2001). Yeast Mps1p phosphorylates the spindle pole component Spc110p in the N-terminal domain. J Biol Chem *276*, 17958-17967.

Friedman, D.B., Sundberg, H.A., Huang, E.Y., and Davis, T.N. (1996). The 110-kD spindle pole body component of Saccharomyces cerevisiae is a phosphoprotein that is modified in a cell cycle-dependent manner. J Cell Biol *132*, 903-914.

Fujita, A., Vardy, L., Garcia, M.A., and Toda, T. (2002). A fourth component of the fission yeast gamma-tubulin complex, Alp16, is required for cytoplasmic microtubule integrity and becomes indispensable when gamma-tubulin function is compromised. Mol Biol Cell *13*, 2360-2373.

Furge, K.A., Wong, K., Armstrong, J., Balasubramanian, M., and Albright, C.F. (1998). Byr4 and Cdc16 form a two-component GTPase-activating protein for the Spg1 GTPase that controls septation in fission yeast. Curr Biol *8*, 947-954.

Geiser, J.R., Sundberg, H.A., Chang, B.H., Muller, E.G., and Davis, T.N. (1993). The essential mitotic target of calmodulin is the 110-kilodalton component of the spindle pole body in Saccharomyces cerevisiae. Mol Cell Biol *13*, 7913-7924.

Geissler, S., Pereira, G., Spang, A., Knop, M., Soues, S., Kilmartin, J., and Schiebel, E. (1996). The spindle pole body component Spc98p interacts with the gamma-tubulin-like Tub4p of Saccharomyces cerevisiae at the sites of microtubule attachment. EMBO J *15*, 3899-3911.

Gerace, L., and Blobel, G. (1980). The nuclear envelope lamina is reversibly depolymerized during mitosis. Cell *19*, 277-287.

Golsteyn, R.M., Mundt, K.E., Fry, A.M., and Nigg, E.A. (1995). Cell cycle regulation of the activity and subcellular localization of Plk1, a human protein kinase implicated in mitotic spindle function. J Cell Biol *129*, 1617-1628.

Golsteyn, R.M., Schultz, S.J., Bartek, J., Ziemiecki, A., Ried, T., and Nigg, E.A. (1994). Cell cycle analysis and chromosomal localization of human Plk1, a putative homologue of the mitotic kinases Drosophila polo and Saccharomyces cerevisiae Cdc5. J Cell Sci *107 (Pt 6)*, 1509-1517.

Gould, R.R., and Borisy, G.G. (1977). The pericentriolar material in Chinese hamster ovary cells nucleates microtubule formation. J Cell Biol *73*, 601-615.

Grallert, A., Krapp, A., Bagley, S., Simanis, V., and Hagan, I.M. (2004). Recruitment of NIMA kinase shows that maturation of the S. pombe spindle-pole body occurs over consecutive cell cycles and reveals a role for NIMA in modulating SIN activity. Genes Dev *18*, 1007-1021.

Griffith, E., Walker, S., Martin, C.A., Vagnarelli, P., Stiff, T., Vernay, B., Al Sanna, N., Saggar, A., Hamel, B., Earnshaw, W.C*., et al.* (2008). Mutations in pericentrin cause Seckel syndrome with defective ATR-dependent DNA damage signaling. Nat Genet *40*, 232-236.

Gromley, A., Jurczyk, A., Sillibourne, J., Halilovic, E., Mogensen, M., Groisman, I., Blomberg, M., and Doxsey, S. (2003). A novel human protein of the maternal centriole is required for the final stages of cytokinesis and entry into S phase. J Cell Biol *161*, 535-545.

Gruenbaum, Y., Wilson, K.L., Harel, A., Goldberg, M., and Cohen, M. (2000). Review: nuclear lamins--structural proteins with fundamental functions. J Struct Biol *129*, 313-323.

Hachet, V., Canard, C., and Gonczy, P. (2007). Centrosomes promote timely mitotic entry in C. elegans embryos. Dev Cell *12*, 531-541.

Hagan, I., and Yanagida, M. (1990). Novel potential mitotic motor protein encoded by the fission yeast cut7+ gene. Nature *347*, 563-566.

Hagan, I., and Yanagida, M. (1992). Kinesin-related cut7 protein associates with mitotic and meiotic spindles in fission yeast. Nature *356*, 74-76.

Hanks, S.K., Quinn, A.M., and Hunter, T. (1988). The protein kinase family: conserved features and deduced phylogeny of the catalytic domains. Science *241*, 42-52.

Hartwell, L.H. (1974). Saccharomyces cerevisiae cell cycle. Bacteriol Rev *38*, 164-198.

Hase, M.E., and Cordes, V.C. (2003). Direct interaction with nup153 mediates binding of Tpr to the periphery of the nuclear pore complex. Mol Biol Cell *14*, 1923-1940.

Hayden, J.H., Bowser, S.S., and Rieder, C.L. (1990). Kinetochores capture astral microtubules during chromosome attachment to the mitotic spindle: direct visualization in live newt lung cells. J Cell Biol *111*, 1039-1045.

Heitz, M.J., Petersen, J., Valovin, S., and Hagan, I.M. (2001). MTOC formation during mitotic exit in fission yeast. J Cell Sci *114*, 4521-4532.

Hetzer, M.W., Walther, T.C., and Mattaj, I.W. (2005). Pushing the envelope: structure, function, and dynamics of the nuclear periphery. Annu Rev Cell Dev Biol *21*, 347-380.

Hinchcliffe, E.H., Miller, F.J., Cham, M., Khodjakov, A., and Sluder, G. (2001). Requirement of a centrosomal activity for cell cycle progression through G1 into S phase. Science *291*, 1547-1550.

Hiraoka, Y., Toda, T., and Yanagida, M. (1984). The NDA3 gene of fission yeast encodes beta-tubulin: a cold-sensitive nda3 mutation reversibly blocks spindle formation and chromosome movement in mitosis. Cell *39*, 349-358.

Hirota, T., Kunitoku, N., Sasayama, T., Marumoto, T., Zhang, D., Nitta, M., Hatakeyama, K., and Saya, H. (2003). Aurora-A and an interacting activator, the LIM protein Ajuba, are required for mitotic commitment in human cells. Cell *114*, 585-598.

Horio, T., Uzawa, S., Jung, M.K., Oakley, B.R., Tanaka, K., and Yanagida, M. (1991). The fission yeast gamma-tubulin is essential for mitosis and is localized at microtubule organizing centers. J Cell Sci *99 (Pt 4)*, 693-700.

Huang, J., and Raff, J.W. (1999). The disappearance of cyclin B at the end of mitosis is regulated spatially in Drosophila cells. EMBO J *18*, 2184-2195.

Hudson, J.D., Feilotter, H., and Young, P.G. (1990). stf1: non-wee mutations epistatic to cdc25 in the fission yeast Schizosaccharomyces pombe. Genetics *126*, 309-315.

Huisman, S.M., Smeets, M.F., and Segal, M. (2007). Phosphorylation of Spc110p by Cdc28p-Clb5p kinase contributes to correct spindle morphogenesis in S. cerevisiae. J Cell Sci *120*, 435-446.

Inoue, D., and Sagata, N. (2005). The Polo-like kinase Plx1 interacts with and inhibits Myt1 after fertilization of Xenopus eggs. EMBO J *24*, 1057-1067.

Jackman, M., Lindon, C., Nigg, E.A., and Pines, J. (2003). Active cyclin B1-Cdk1 first appears on centrosomes in prophase. Nat Cell Biol *5*, 143-148.

Jang, Y.J., Lin, C.Y., Ma, S., and Erikson, R.L. (2002a). Functional studies on the role of the C-terminal domain of mammalian polo-like kinase. Proc Natl Acad Sci U S A *99*, 1984-1989.

Jang, Y.J., Ma, S., Terada, Y., and Erikson, R.L. (2002b). Phosphorylation of threonine 210 and the role of serine 137 in the regulation of mammalian polo-like kinase. J Biol Chem *277*, 44115-44120.

Janson, M.E., Setty, T.G., Paoletti, A., and Tran, P.T. (2005). Efficient formation of bipolar microtubule bundles requires microtubule-bound gamma-tubulin complexes. J Cell Biol *169*, 297-308.

Jin, Y., Mancuso, J.J., Uzawa, S., Cronembold, D., and Cande, W.Z. (2005). The fission yeast homolog of the human transcription factor EAP30 blocks meiotic spindle pole body amplification. Dev Cell *9*, 63-73.

Kalt, A., and Schliwa, M. (1993). Molecular components of the centrosome. Trends Cell Biol *3*, 118-128.

Kawaguchi, S., and Zheng, Y. (2004). Characterization of a Drosophila centrosome protein CP309 that shares homology with Kendrin and CG-NAP. Mol Biol Cell *15*, 37-45.

Keating, T.J., and Borisy, G.G. (1999). Centrosomal and non-centrosomal microtubules. Biol Cell *91*, 321-329.

Keating, T.J., and Borisy, G.G. (2000). Immunostructural evidence for the template mechanism of microtubule nucleation. Nat Cell Biol *2*, 352-357.

Kehlenbach, R.H., and Gerace, L. (2000). Phosphorylation of the nuclear transport machinery down-regulates nuclear protein import in vitro. J Biol Chem *275*, 17848-17856.

Kelm, O., Wind, M., Lehmann, W.D., and Nigg, E.A. (2002). Cell cycle-regulated phosphorylation of the Xenopus polo-like kinase Plx1. J Biol Chem *277*, 25247-25256.

Keryer, G., Witczak, O., Delouvee, A., Kemmner, W.A., Rouillard, D., Tasken, K., and Bornens, M. (2003). Dissociating the centrosomal matrix protein AKAP450 from centrioles impairs centriole duplication and cell cycle progression. Mol Biol Cell *14*, 2436-2446.

Khodjakov, A., Cole, R.W., Oakley, B.R., and Rieder, C.L. (2000). Centrosome-independent mitotic spindle formation in vertebrates. Curr Biol *10*, 59-67.

Kilmartin, J.V. (2003). Sfi1p has conserved centrin-binding sites and an essential function in budding yeast spindle pole body duplication. J Cell Biol *162*, 1211-1221.

Kilmartin, J.V., Dyos, S.L., Kershaw, D., and Finch, J.T. (1993). A spacer protein in the Saccharomyces cerevisiae spindle poly body whose transcript is cell cycle-regulated. J Cell Biol *123*, 1175-1184.

Kilmartin, J.V., and Goh, P.Y. (1996). Spc110p: assembly properties and role in the connection of nuclear microtubules to the yeast spindle pole body. EMBO J *15*, 4592-4602.

Kimble, M., and Kuriyama, R. (1992). Functional components of microtubule-organizing centers. Int Rev Cytol *136*, 1-50.

Kirschner, M., and Mitchison, T. (1986). Beyond self-assembly: from microtubules to morphogenesis. Cell *45*, 329-342.

Kiseleva, E., Rutherford, S., Cotter, L.M., Allen, T.D., and Goldberg, M.W. (2001). Steps of nuclear pore complex disassembly and reassembly during mitosis in early Drosophila embryos. J Cell Sci *114*, 3607-3618.

Kitada, K., Johnson, A.L., Johnston, L.H., and Sugino, A. (1993). A multicopy suppressor gene of the Saccharomyces cerevisiae G1 cell cycle mutant gene dbf4 encodes a protein kinase and is identified as CDC5. Mol Cell Biol *13*, 4445-4457.

Knecht, R., Elez, R., Oechler, M., Solbach, C., von Ilberg, C., and Strebhardt, K. (1999). Prognostic significance of polo-like kinase (PLK) expression in squamous cell carcinomas of the head and neck. Cancer Res *59*, 2794-2797.

Knop, M., Pereira, G., Geissler, S., Grein, K., and Schiebel, E. (1997). The spindle pole body component Spc97p interacts with the gamma-tubulin of

Saccharomyces cerevisiae and functions in microtubule organization and spindle pole body duplication. EMBO J *16*, 1550-1564.

Knop, M., and Schiebel, E. (1997). Spc98p and Spc97p of the yeast gamma-tubulin complex mediate binding to the spindle pole body via their interaction with Spc110p. EMBO J *16*, 6985-6995.

Kramer, A., Mailand, N., Lukas, C., Syljuasen, R.G., Wilkinson, C.J., Nigg, E.A., Bartek, J., and Lukas, J. (2004). Centrosome-associated Chk1 prevents premature activation of cyclin-B-Cdk1 kinase. Nat Cell Biol *6*, 884-891.

Kumagai, A., and Dunphy, W.G. (1996). Purification and molecular cloning of Plx1, a Cdc25-regulatory kinase from Xenopus egg extracts. Science *273*, 1377-1380.

Lane, H.A., and Nigg, E.A. (1996). Antibody microinjection reveals an essential role for human polo-like kinase 1 (Plk1) in the functional maturation of mitotic centrosomes. J Cell Biol *135*, 1701-1713.

Laoukili, J., Kooistra, M.R., Bras, A., Kauw, J., Kerkhoven, R.M., Morrison, A., Clevers, H., and Medema, R.H. (2005). FoxM1 is required for execution of the mitotic programme and chromosome stability. Nat Cell Biol *7*, 126-136.

Lau, C.K., Giddings, T.H., Jr., and Winey, M. (2004). A novel allele of Saccharomyces cerevisiae NDC1 reveals a potential role for the spindle pole body component Ndc1p in nuclear pore assembly. Eukaryot Cell *3*, 447-458.

Lee, K.S., Grenfell, T.Z., Yarm, F.R., and Erikson, R.L. (1998). Mutation of the polo-box disrupts localization and mitotic functions of the mammalian polo kinase Plk. Proc Natl Acad Sci U S A *95*, 9301-9306.

Lee, M.G., and Nurse, P. (1987). Complementation used to clone a human homologue of the fission yeast cell cycle control gene cdc2. Nature *327*, 31-35.

Lenart, P., Rabut, G., Daigle, N., Hand, A.R., Terasaki, M., and Ellenberg, J. (2003). Nuclear envelope breakdown in starfish oocytes proceeds by partial

NPC disassembly followed by a rapidly spreading fenestration of nuclear membranes. J Cell Biol *160*, 1055-1068.

Llamazares, S., Moreira, A., Tavares, A., Girdham, C., Spruce, B.A., Gonzalez, C., Karess, R.E., Glover, D.M., and Sunkel, C.E. (1991). polo encodes a protein kinase homolog required for mitosis in Drosophila. Genes Dev *5*, 2153-2165.

Loffler, H., Bochtler, T., Fritz, B., Tews, B., Ho, A.D., Lukas, J., Bartek, J., and Kramer, A. (2007). DNA damage-induced accumulation of centrosomal Chk1 contributes to its checkpoint function. Cell Cycle *6*, 2541-2548.

Lowery, D.M., Lim, D., and Yaffe, M.B. (2005). Structure and function of Polo-like kinases. Oncogene *24*, 248-259.

Ma, S., Charron, J., and Erikson, R.L. (2003). Role of Plk2 (Snk) in mouse development and cell proliferation. Mol Cell Biol *23*, 6936-6943.

Macaulay, C., Meier, E., and Forbes, D.J. (1995). Differential mitotic phosphorylation of proteins of the nuclear pore complex. J Biol Chem *270*, 254-262.

MacIver, F.H., Tanaka, K., Robertson, A.M., and Hagan, I.M. (2003). Physical and functional interactions between polo kinase and the spindle pole component Cut12 regulate mitotic commitment in S. pombe. Genes Dev *17*, 1507-1523.

Macurek, L., Lindqvist, A., Lim, D., Lampson, M.A., Klompmaker, R., Freire, R., Clouin, C., Taylor, S.S., Yaffe, M.B., and Medema, R.H. (2008). Polo-like kinase-1 is activated by aurora A to promote checkpoint recovery. Nature *455*, 119-123.

Marschall, L.G., Jeng, R.L., Mulholland, J., and Stearns, T. (1996). Analysis of Tub4p, a yeast gamma-tubulin-like protein: implications for microtubule-organizing center function. J Cell Biol *134*, 443-454.

Matsuyama, A., Arai, R., Yashiroda, Y., Shirai, A., Kamata, A., Sekido, S., Kobayashi, Y., Hashimoto, A., Hamamoto, M., Hiraoka, Y.*, et al.* (2006).

ORFeome cloning and global analysis of protein localization in the fission yeast Schizosaccharomyces pombe. Nat Biotechnol *24*, 841-847.

Mayer, T.U., Kapoor, T.M., Haggarty, S.J., King, R.W., Schreiber, S.L., and Mitchison, T.J. (1999). Small molecule inhibitor of mitotic spindle bipolarity identified in a phenotype-based screen. Science *286*, 971-974.

McNally, F.J., and Vale, R.D. (1993). Identification of katanin, an ATPase that severs and disassembles stable microtubules. Cell *75*, 419-429.

Miki, F., Kurabayashi, A., Tange, Y., Okazaki, K., Shimanuki, M., and Niwa, O. (2004). Two-hybrid search for proteins that interact with Sad1 and Kms1, two membrane-bound components of the spindle pole body in fission yeast. Mol Genet Genomics *270*, 449-461.

Miller, M.W., Caracciolo, M.R., Berlin, W.K., and Hanover, J.A. (1999). Phosphorylation and glycosylation of nucleoporins. Arch Biochem Biophys *367*, 51-60.

Mirzayan, C., Copeland, C.S., and Snyder, M. (1992). The NUF1 gene encodes an essential coiled-coil related protein that is a potential component of the yeast nucleoskeleton. J Cell Biol *116*, 1319-1332.

Mitchison, T., and Kirschner, M. (1984). Dynamic instability of microtubule growth. Nature *312*, 237-242.

Mitchison, T.J. (1993). Localization of an exchangeable GTP binding site at the plus end of microtubules. Science *261*, 1044-1047.

Moens, P.B., and Rapport, E. (1971). Spindles, spindle plaques, and meiosis in the yeast Saccharomyces cerevisiae (Hansen). J Cell Biol *50*, 344-361.

Moreno, S., Klar, A., and Nurse, P. (1991). Molecular genetic analysis of fission yeast Schizosaccharomyces pombe. Methods Enzymol *194*, 795-823.

Moritz, M., Braunfeld, M.B., Guenebaut, V., Heuser, J., and Agard, D.A. (2000). Structure of the gamma-tubulin ring complex: a template for microtubule nucleation. Nat Cell Biol *2*, 365-370.

Moritz, M., Braunfeld, M.B., Sedat, J.W., Alberts, B., and Agard, D.A. (1995). Microtubule nucleation by gamma-tubulin-containing rings in the centrosome. Nature *378*, 638-640.

Morrell, J.L., Tomlin, G.C., Rajagopalan, S., Venkatram, S., Feoktistova, A.S., Tasto, J.J., Mehta, S., Jennings, J.L., Link, A., Balasubramanian, M.K.*, et al.* (2004). Sid4p-Cdc11p assembles the septation initiation network and its regulators at the S. pombe SPB. Curr Biol *14*, 579-584.

Mulvihill, D.P., Petersen, J., Ohkura, H., Glover, D.M., and Hagan, I.M. (1999). Plo1 kinase recruitment to the spindle pole body and its role in cell division in Schizosaccharomyces pombe. Mol Biol Cell *10*, 2771-2785.

Murphy, S.M., Preble, A.M., Patel, U.K., O'Connell, K.L., Dias, D.P., Moritz, M., Agard, D., Stults, J.T., and Stearns, T. (2001). GCP5 and GCP6: two new members of the human gamma-tubulin complex. Mol Biol Cell *12*, 3340-3352.

Murphy, S.M., Urbani, L., and Stearns, T. (1998). The mammalian gamma-tubulin complex contains homologues of the yeast spindle pole body components spc97p and spc98p. J Cell Biol *141*, 663-674.

Nakajima, H., Toyoshima-Morimoto, F., Taniguchi, E., and Nishida, E. (2003). Identification of a consensus motif for Plk (Polo-like kinase) phosphorylation reveals Myt1 as a Plk1 substrate. J Biol Chem *278*, 25277-25280.

Neef, R., Preisinger, C., Sutcliffe, J., Kopajtich, R., Nigg, E.A., Mayer, T.U., and Barr, F.A. (2003). Phosphorylation of mitotic kinesin-like protein 2 by polo-like kinase 1 is required for cytokinesis. J Cell Biol *162*, 863-875.

Nigg, E.A. (2007). Centrosome duplication: of rules and licenses. Trends Cell Biol *17*, 215-221.

Niwa, O., Shimanuki, M., and Miki, F. (2000). Telomere-led bouquet formation facilitates homologous chromosome pairing and restricts ectopic interaction in fission yeast meiosis. EMBO J *19*, 3831-3840.

Nogales, E., Whittaker, M., Milligan, R.A., and Downing, K.H. (1999). High-resolution model of the microtubule. Cell *96*, 79-88.

Nogales, E., Wolf, S.G., and Downing, K.H. (1998). Structure of the alpha beta tubulin dimer by electron crystallography. Nature *391*, 199-203.

Nurse, P. (1990). Universal control mechanism regulating onset of M-phase. Nature *344*, 503-508.

Nurse, P., and Thuriaux, P. (1980). Regulatory genes controlling mitosis in the fission yeast Schizosaccharomyces pombe. Genetics *96*, 627-637.

O'Driscoll, M., Ruiz-Perez, V.L., Woods, C.G., Jeggo, P.A., and Goodship, J.A. (2003). A splicing mutation affecting expression of ataxia-telangiectasia and Rad3-related protein (ATR) results in Seckel syndrome. Nat Genet *33*, 497-501.

O'Toole, E.T., Winey, M., and McIntosh, J.R. (1999). High-voltage electron tomography of spindle pole bodies and early mitotic spindles in the yeast Saccharomyces cerevisiae. Mol Biol Cell *10*, 2017-2031.

Oakley, C.E., and Oakley, B.R. (1989). Identification of gamma-tubulin, a new member of the tubulin superfamily encoded by mipA gene of Aspergillus nidulans. Nature *338*, 662-664.

Oegema, K., Wiese, C., Martin, O.C., Milligan, R.A., Iwamatsu, A., Mitchison, T.J., and Zheng, Y. (1999). Characterization of two related Drosophila gamma-tubulin complexes that differ in their ability to nucleate microtubules. J Cell Biol *144*, 721-733.

Ohkura, H., Hagan, I.M., and Glover, D.M. (1995). The conserved Schizosaccharomyces pombe kinase plo1, required to form a bipolar spindle, the actin ring, and septum, can drive septum formation in G1 and G2 cells. Genes Dev *9*, 1059-1073.

Okano-Uchida, T., Okumura, E., Iwashita, M., Yoshida, H., Tachibana, K., and Kishimoto, T. (2003). Distinct regulators for Plk1 activation in starfish meiotic and early embryonic cycles. EMBO J *22*, 5633-5642.

Oshimori, N., Ohsugi, M., and Yamamoto, T. (2006). The Plk1 target Kizuna stabilizes mitotic centrosomes to ensure spindle bipolarity. Nat Cell Biol *8*, 1095-1101.

Ovechkina, Y., Maddox, P., Oakley, C.E., Xiang, X., Osmani, S.A., Salmon, E.D., and Oakley, B.R. (2003). Spindle formation in Aspergillus is coupled to tubulin movement into the nucleus. Mol Biol Cell *14*, 2192-2200.

Paintrand, M., Moudjou, M., Delacroix, H., and Bornens, M. (1992). Centrosome organization and centriole architecture: their sensitivity to divalent cations. J Struct Biol *108*, 107-128.

Pang, T.L., Wang, C.Y., Hsu, C.L., Chen, M.Y., and Lin, J.J. (2003). Exposure of single-stranded telomeric DNA causes G2/M cell cycle arrest in Saccharomyces cerevisiae. J Biol Chem *278*, 9318-9321.

Pardee, A.B. (1974). A restriction point for control of normal animal cell proliferation. Proc Natl Acad Sci U S A *71*, 1286-1290.

Perez-Mongiovi, D., Beckhelling, C., Chang, P., Ford, C.C., and Houliston, E. (2000). Nuclei and microtubule asters stimulate maturation/M phase promoting factor (MPF) activation in Xenopus eggs and egg cytoplasmic extracts. J Cell Biol *150*, 963-974.

Petersen, J., and Hagan, I.M. (2005). Polo kinase links the stress pathway to cell cycle control and tip growth in fission yeast. Nature *435*, 507-512.

Petretti, C., and Prigent, C. (2005). The Protein Kinase Resource: everything you always wanted to know about protein kinases but were afraid to ask. Biol Cell *97*, 113-118.

Picard, A., Karsenti, E., Dabauvalle, M.C., and Doree, M. (1987). Release of mature starfish oocytes from interphase arrest by microinjection of human centrosomes. Nature *327*, 170-172.

Pickett-Heaps, J.D. (1969). The evolution of the mitotic apparatus: An attempt at comparative ultrastructural cytology in dividing plant cells. Cytobios *3*, 257-280.

Pockwinse, S.M., Krockmalnic, G., Doxsey, S.J., Nickerson, J., Lian, J.B., van Wijnen, A.J., Stein, J.L., Stein, G.S., and Penman, S. (1997). Cell cycle independent interaction of CDC2 with the centrosome, which is associated with the nuclear matrix-intermediate filament scaffold. Proc Natl Acad Sci U S A *94*, 3022-3027.

Portier, N., Audhya, A., Maddox, P.S., Green, R.A., Dammermann, A., Desai, A., and Oegema, K. (2007). A microtubule-independent role for centrosomes and aurora a in nuclear envelope breakdown. Dev Cell *12*, 515-529.

Preuss, U., Bierbaum, H., Buchenau, P., and Scheidtmann, K.H. (2003). DAP-like kinase, a member of the death-associated protein kinase family, associates with centrosomes, centromers, and the contractile ring during mitosis. Eur J Cell Biol *82*, 447-459.

Prigozhina, N.L., Oakley, C.E., Lewis, A.M., Nayak, T., Osmani, S.A., and Oakley, B.R. (2004). gamma-tubulin plays an essential role in the coordination of mitotic events. Mol Biol Cell *15*, 1374-1386.

Qian, Y.W., Erikson, E., and Maller, J.L. (1998). Purification and cloning of a protein kinase that phosphorylates and activates the polo-like kinase Plx1. Science *282*, 1701-1704.

Qian, Y.W., Erikson, E., and Maller, J.L. (1999). Mitotic effects of a constitutively active mutant of the Xenopus polo-like kinase Plx1. Mol Cell Biol *19*, 8625-8632.

Radcliffe, P., Hirata, D., Childs, D., Vardy, L., and Toda, T. (1998). Identification of novel temperature-sensitive lethal alleles in essential beta-tubulin and nonessential alpha 2-tubulin genes as fission yeast polarity mutants. Mol Biol Cell *9*, 1757-1771.

Rajagopalan, S., Bimbo, A., Balasubramanian, M.K., and Oliferenko, S. (2004). A potential tension-sensing mechanism that ensures timely anaphase onset upon metaphase spindle orientation. Curr Biol *14*, 69-74.

Rauch, A., Thiel, C.T., Schindler, D., Wick, U., Crow, Y.J., Ekici, A.B., van Essen, A.J., Goecke, T.O., Al-Gazali, L., Chrzanowska, K.H.*, et al.* (2008). Mutations in the pericentrin (PCNT) gene cause primordial dwarfism. Science *319*, 816-819.

Reynolds, N., and Ohkura, H. (2003). Polo boxes form a single functional domain that mediates interactions with multiple proteins in fission yeast polo kinase. J Cell Sci *116*, 1377-1387.

Robinow, C.F., and Marak, J. (1966). A fiber apparatus in the nucleus of the yeast cell. J Cell Biol *29*, 129-151.

Roof, D.M., Meluh, P.B., and Rose, M.D. (1992). Kinesin-related proteins required for assembly of the mitotic spindle. J Cell Biol *118*, 95-108.

Rosenblatt, J., Cramer, L.P., Baum, B., and McGee, K.M. (2004). Myosin II-dependent cortical movement is required for centrosome separation and positioning during mitotic spindle assembly. Cell *117*, 361-372.

Rost, B., Casadio, R., Fariselli, P., and Sander, C. (1995). Transmembrane helices predicted at 95% accuracy. Protein Sci *4*, 521-533.

Salina, D., Bodoor, K., Eckley, D.M., Schroer, T.A., Rattner, J.B., and Burke, B. (2002). Cytoplasmic dynein as a facilitator of nuclear envelope breakdown. Cell *108*, 97-107.

Samejima, I., Miller, V.J., Groocock, L.M., and Sawin, K.E. (2008). Two distinct regions of Mto1 are required for normal microtubule nucleation and efficient association with the gamma-tubulin complex in vivo. J Cell Sci *121*, 3971-3980.

Sandal, T., Aumo, L., Hedin, L., Gjertsen, B.T., and Doskeland, S.O. (2003). Irod/Ian5: an inhibitor of gamma-radiation- and okadaic acid-induced apoptosis. Mol Biol Cell *14*, 3292-3304.

Sato, M., Dhut, S., and Toda, T. (2005). New drug-resistant cassettes for gene disruption and epitope tagging in Schizosaccharomyces pombe. Yeast *22*, 583-591.

Saunders, W.S., and Hoyt, M.A. (1992). Kinesin-related proteins required for structural integrity of the mitotic spindle. Cell *70*, 451-458.

Sawin, K.E., Lourenco, P.C., and Snaith, H.A. (2004). Microtubule nucleation at non-spindle pole body microtubule-organizing centers requires fission yeast centrosomin-related protein mod20p. Curr Biol *14*, 763-775.

Sawin, K.E., and Tran, P.T. (2006). Cytoplasmic microtubule organization in fission yeast. Yeast *23*, 1001-1014.

Schnorrer, F., Luschnig, S., Koch, I., and Nusslein-Volhard, C. (2002). Gamma-tubulin37C and gamma-tubulin ring complex protein 75 are essential for bicoid RNA localization during drosophila oogenesis. Dev Cell *3*, 685-696.

Schramm, C., Elliott, S., Shevchenko, A., and Schiebel, E. (2000). The Bbp1p-Mps2p complex connects the SPB to the nuclear envelope and is essential for SPB duplication. EMBO J *19*, 421-433.

Schulman, H., Hanson, P.I., and Meyer, T. (1992). Decoding calcium signals by multifunctional CaM kinase. Cell Calcium *13*, 401-411.

Seki, A., Coppinger, J.A., Jang, C.Y., Yates, J.R., and Fang, G. (2008). Bora and the kinase Aurora a cooperatively activate the kinase Plk1 and control mitotic entry. Science *320*, 1655-1658.

Shimanuki, M., Miki, F., Ding, D.Q., Chikashige, Y., Hiraoka, Y., Horio, T., and Niwa, O. (1997). A novel fission yeast gene, kms1+, is required for the formation of meiotic prophase-specific nuclear architecture. Mol Gen Genet *254*, 238-249.

Shirayama, M., Zachariae, W., Ciosk, R., and Nasmyth, K. (1998). The Polo-like kinase Cdc5p and the WD-repeat protein Cdc20p/fizzy are regulators and substrates of the anaphase promoting complex in Saccharomyces cerevisiae. EMBO J *17*, 1336-1349.

Sibon, O.C., Kelkar, A., Lemstra, W., and Theurkauf, W.E. (2000). DNA-replication/DNA-damage-dependent centrosome inactivation in Drosophila embryos. Nat Cell Biol *2*, 90-95.

Simizu, S., and Osada, H. (2000). Mutations in the Plk gene lead to instability of Plk protein in human tumour cell lines. Nat Cell Biol *2*, 852-854.

Smith, C.M. (1999). The protein kinase resource and other bioinformation resources. Prog Biophys Mol Biol *71*, 525-533.

Smith, C.M., Shindyalov, I.N., Veretnik, S., Gribskov, M., Taylor, S.S., Ten Eyck, L.F., and Bourne, P.E. (1997). The protein kinase resource. Trends Biochem Sci *22*, 444-446.

Sohrmann, M., Schmidt, S., Hagan, I., and Simanis, V. (1998). Asymmetric segregation on spindle poles of the Schizosaccharomyces pombe septum-inducing protein kinase Cdc7p. Genes Dev *12*, 84-94.

Spang, A., Geissler, S., Grein, K., and Schiebel, E. (1996). gamma-Tubulin-like Tub4p of Saccharomyces cerevisiae is associated with the spindle pole body substructures that organize microtubules and is required for mitotic spindle formation. J Cell Biol *134*, 429-441.

Stavru, F., Hulsmann, B.B., Spang, A., Hartmann, E., Cordes, V.C., and Gorlich, D. (2006). NDC1: a crucial membrane-integral nucleoporin of metazoan nuclear pore complexes. J Cell Biol *173*, 509-519.

Stearns, T., Evans, L., and Kirschner, M. (1991). Gamma-tubulin is a highly conserved component of the centrosome. Cell *65*, 825-836.

Stevenson, V.A., Kramer, J., Kuhn, J., and Theurkauf, W.E. (2001). Centrosomes and the Scrambled protein coordinate microtubule-independent actin reorganization. Nat Cell Biol *3*, 68-75.

Stirling, D.A., Rayner, T.F., Prescott, A.R., and Stark, M.J. (1996). Mutations which block the binding of calmodulin to Spc110p cause multiple mitotic defects. J Cell Sci *109 (Pt 6)*, 1297-1310.

Stirling, D.A., and Stark, M.J. (1996). The phosphorylation state of the 110 kDa component of the yeast spindle pole body shows cell cycle dependent regulation. Biochem Biophys Res Commun *222*, 236-242.

Stirling, D.A., Welch, K.A., and Stark, M.J. (1994). Interaction with calmodulin is required for the function of Spc110p, an essential component of the yeast spindle pole body. EMBO J *13*, 4329-4342.

Sundberg, H.A., and Davis, T.N. (1997). A mutational analysis identifies three functional regions of the spindle pole component Spc110p in Saccharomyces cerevisiae. Mol Biol Cell *8*, 2575-2590.

Sundberg, H.A., Goetsch, L., Byers, B., and Davis, T.N. (1996). Role of calmodulin and Spc110p interaction in the proper assembly of spindle pole body compenents. J Cell Biol *133*, 111-124.

Sunkel, C.E., and Glover, D.M. (1988). polo, a mitotic mutant of Drosophila displaying abnormal spindle poles. J Cell Sci *89 (Pt 1)*, 25-38.

Takahashi, M., Yamagiwa, A., Nishimura, T., Mukai, H., and Ono, Y. (2002). Centrosomal proteins CG-NAP and kendrin provide microtubule nucleation sites by anchoring gamma-tubulin ring complex. Mol Biol Cell *13*, 3235-3245.

Takaki, T., Trenz, K., Costanzo, V., and Petronczki, M. (2008). Polo-like kinase 1 reaches beyond mitosis--cytokinesis, DNA damage response, and development. Curr Opin Cell Biol *20*, 650-660.

Tallada, V.A., Tanaka, K., Yanagida, M., and Hagan, I.M. (2009). The S. pombe mitotic regulator Cut12 promotes spindle pole body activation and integration into the nuclear envelope. J Cell Biol *185*, 875-888.

Tanaka, K., Petersen, J., MacIver, F., Mulvihill, D.P., Glover, D.M., and Hagan, I.M. (2001). The role of Plo1 kinase in mitotic commitment and septation in Schizosaccharomyces pombe. EMBO J *20*, 1259-1270.

Terasaki, M., Campagnola, P., Rolls, M.M., Stein, P.A., Ellenberg, J., Hinkle, B., and Slepchenko, B. (2001). A new model for nuclear envelope breakdown. Mol Biol Cell *12*, 503-510.

Terasaki, M., Okumura, E., Hinkle, B., and Kishimoto, T. (2003). Localization and dynamics of Cdc2-cyclin B during meiotic reinitiation in starfish oocytes. Mol Biol Cell *14*, 4685-4694.

Thomas, J.H., and Botstein, D. (1986). A gene required for the separation of chromosomes on the spindle apparatus in yeast. Cell *44*, 65-76.

Tibelius, A., Marhold, J., Zentgraf, H., Heilig, C.E., Neitzel, H., Ducommun, B., Rauch, A., Ho, A.D., Bartek, J., and Kramer, A. (2009). Microcephalin and pericentrin regulate mitotic entry via centrosome-associated Chk1. J Cell Biol *185*, 1149-1157.

Toda, T., Umesono, K., Hirata, A., and Yanagida, M. (1983). Cold-sensitive nuclear division arrest mutants of the fission yeast Schizosaccharomyces pombe. J Mol Biol *168*, 251-270.

Tomita, K., and Cooper, J.P. (2007). The telomere bouquet controls the meiotic spindle. Cell *130*, 113-126.

Tomlin, G.C., Morrell, J.L., and Gould, K.L. (2002). The spindle pole body protein Cdc11p links Sid4p to the fission yeast septation initiation network. Mol Biol Cell *13*, 1203-1214.

Toyoshima-Morimoto, F., Taniguchi, E., Shinya, N., Iwamatsu, A., and Nishida, E. (2001). Polo-like kinase 1 phosphorylates cyclin B1 and targets it to the nucleus during prophase. Nature *410*, 215-220.

Tran, E.J., and Wente, S.R. (2006). Dynamic nuclear pore complexes: life on the edge. Cell *125*, 1041-1053.

Tran, P.T., Marsh, L., Doye, V., Inoue, S., and Chang, F. (2001). A mechanism for nuclear positioning in fission yeast based on microtubule pushing. J Cell Biol *153*, 397-411.

Tsvetkov, L., Xu, X., Li, J., and Stern, D.F. (2003). Polo-like kinase 1 and Chk2 interact and co-localize to centrosomes and the midbody. J Biol Chem *278*, 8468-8475.

Tzur, Y.B., Wilson, K.L., and Gruenbaum, Y. (2006). SUN-domain proteins: 'Velcro' that links the nucleoskeleton to the cytoskeleton. Nat Rev Mol Cell Biol *7*, 782-788.

Vardy, L., and Toda, T. (2000). The fission yeast gamma-tubulin complex is required in G(1) phase and is a component of the spindle assembly checkpoint. EMBO J *19*, 6098-6111.

Venkatram, S., Tasto, J.J., Feoktistova, A., Jennings, J.L., Link, A.J., and Gould, K.L. (2004). Identification and characterization of two novel proteins affecting fission yeast gamma-tubulin complex function. Mol Biol Cell *15*, 2287-2301.

Verollet, C., Colombie, N., Daubon, T., Bourbon, H.M., Wright, M., and Raynaud-Messina, B. (2006). Drosophila melanogaster gamma-TuRC is dispensable for targeting gamma-tubulin to the centrosome and microtubule nucleation. J Cell Biol *172*, 517-528.

Vogt, N., Koch, I., Schwarz, H., Schnorrer, F., and Nusslein-Volhard, C. (2006). The gammaTuRC components Grip75 and Grip128 have an essential microtubule-anchoring function in the Drosophila germline. Development *133*, 3963-3972.

Vorobjev, I.A., and Nadezhdina, E.S. (1987). The centrosome and its role in the organization of microtubules. Int Rev Cytol *106*, 227-293.

Wakefield, J.G., Huang, J.Y., and Raff, J.W. (2000). Centrosomes have a role in regulating the destruction of cyclin B in early Drosophila embryos. Curr Biol *10*, 1367-1370.

Wang, Q., Xie, S., Chen, J., Fukasawa, K., Naik, U., Traganos, F., Darzynkiewicz, Z., Jhanwar-Uniyal, M., and Dai, W. (2002). Cell cycle arrest and apoptosis induced by human Polo-like kinase 3 is mediated through perturbation of microtubule integrity. Mol Cell Biol *22*, 3450-3459.

Wang, W., Chen, L., Ding, Y., Jin, J., and Liao, K. (2008). Centrosome separation driven by actin-microfilaments during mitosis is mediated by centrosome-associated tyrosine-phosphorylated cortactin. J Cell Sci *121*, 1334-1343.

Watanabe, N., Arai, H., Nishihara, Y., Taniguchi, M., Hunter, T., and Osada, H. (2004). M-phase kinases induce phospho-dependent ubiquitination of somatic Wee1 by SCFbeta-TrCP. Proc Natl Acad Sci U S A *101*, 4419-4424.

Weiss, E., and Winey, M. (1996). The Saccharomyces cerevisiae spindle pole body duplication gene MPS1 is part of a mitotic checkpoint. J Cell Biol *132*, 111-123.

West, R.R., Vaisberg, E.V., Ding, R., Nurse, P., and McIntosh, J.R. (1998). cut11(+): A gene required for cell cycle-dependent spindle pole body anchoring in the nuclear envelope and bipolar spindle formation in Schizosaccharomyces pombe. Mol Biol Cell *9*, 2839-2855.

Whitby, F.G., Kent, H., Stewart, F., Stewart, M., Xie, X., Hatch, V., Cohen, C., and Phillips, G.N., Jr. (1992). Structure of tropomyosin at 9 angstroms resolution. J Mol Biol *227*, 441-452.

Whitehead, C.M., Winkfein, R.J., and Rattner, J.B. (1996). The relationship of HsEg5 and the actin cytoskeleton to centrosome separation. Cell Motil Cytoskeleton *35*, 298-308.

Wiese, C., and Zheng, Y. (2000). A new function for the gamma-tubulin ring complex as a microtubule minus-end cap. Nat Cell Biol *2*, 358-364.

Wiese, C., and Zheng, Y. (2006). Microtubule nucleation: gamma-tubulin and beyond. J Cell Sci *119*, 4143-4153.

Wilson-Grady, J.T., Villen, J., and Gygi, S.P. (2008). Phosphoproteome analysis of fission yeast. J Proteome Res *7*, 1088-1097.

Winey, M., Goetsch, L., Baum, P., and Byers, B. (1991). MPS1 and MPS2: novel yeast genes defining distinct steps of spindle pole body duplication. J Cell Biol *114*, 745-754.

Winey, M., Hoyt, M.A., Chan, C., Goetsch, L., Botstein, D., and Byers, B. (1993). NDC1: a nuclear periphery component required for yeast spindle pole body duplication. J Cell Biol *122*, 743-751.

Wood, V., Gwilliam, R., Rajandream, M.A., Lyne, M., Lyne, R., Stewart, A., Sgouros, J., Peat, N., Hayles, J., Baker, S.*, et al.* (2002). The genome sequence of Schizosaccharomyces pombe. Nature *415*, 871-880.

Wu, L., Osmani, S.A., and Mirabito, P.M. (1998). A role for NIMA in the nuclear localization of cyclin B in Aspergillus nidulans. J Cell Biol *141*, 1575-1587.

Yano, K., Araki, Y., Hales, S.J., Tanaka, M., and Ikebe, M. (1993). Boundary of the autoinhibitory region of smooth muscle myosin light-chain kinase. Biochemistry *32*, 12054-12061.

Yarm, F.R. (2002). Plk phosphorylation regulates the microtubule-stabilizing protein TCTP. Mol Cell Biol *22*, 6209-6221.

Zhang, J., and Megraw, T.L. (2007). Proper recruitment of gamma-tubulin and D-TACC/Msps to embryonic Drosophila centrosomes requires Centrosomin Motif 1. Mol Biol Cell *18*, 4037-4049.

Zheng, Y., Jung, M.K., and Oakley, B.R. (1991). Gamma-tubulin is present in Drosophila melanogaster and Homo sapiens and is associated with the centrosome. Cell *65*, 817-823.

Zheng, Y., Wong, M.L., Alberts, B., and Mitchison, T. (1995). Nucleation of microtubule assembly by a gamma-tubulin-containing ring complex. Nature *378*, 578-583.

Zimmerman, S., and Chang, F. (2005). Effects of {gamma}-tubulin complex proteins on microtubule nucleation and catastrophe in fission yeast. Mol Biol Cell *16*, 2719-2733.

Zimmerman, W.C., Sillibourne, J., Rosa, J., and Doxsey, S.J. (2004). Mitosis-specific anchoring of gamma tubulin complexes by pericentrin controls spindle organization and mitotic entry. Mol Biol Cell *15*, 3642-3657.

The EMBO Journal (2009), 1–11 | © 2009 European Molecular Biology Organization | Some Rights Reserved 0261-4189/09
www.embojournal.org

THE EMBO JOURNAL

EMBO open

Fission yeast Pcp1 links polo kinase-mediated mitotic entry to γ-tubulin-dependent spindle formation

Chii Shyang Fong, Masamitsu Sato[1] and Takashi Toda*

Laboratory of Cell Regulation, Cancer Research UK, London Research Institute, Lincoln's Inn Fields Laboratories, London, UK

The centrosomal pericentrin-related proteins play pivotal roles in various aspects of cell division; however their underlying mechanisms remain largely elusive. Here we show that fission-yeast pericentrin-like Pcp1 regulates multiple functions of the spindle pole body (SPB) through recruiting two critical factors, the γ-tubulin complex (γ-TuC) and polo kinase (Plo1). We isolated two *pcp1* mutants (*pcp1-15* and *pcp1-18*) that display similar abnormal spindles, but with remarkably different molecular defects. Both mutants exhibit defective monopolar spindle microtubules that emanate from the mother SPB. However, while *pcp1-15* fails to localise the γ-TuC to the mitotic SPB, *pcp1-18* is specifically defective in recruiting Plo1. Consistently Pcp1 forms a complex with both γ-TuC and Plo1 in the cell. *pcp1-18* is further defective in the mitotic-specific reorganisation of the nuclear envelope (NE), leading to impairment of SPB insertion into the NE. Moreover *pcp1-18*, but not *pcp1-15*, is rescued by overproducing nuclear pore components or advancing mitotic onset. The central role for Pcp1 in orchestrating these processes provides mechanistic insight into how the centrosome regulates multiple cellular pathways.

The EMBO Journal advance online publication, 26 November 2009; doi:10.1038/emboj.2009.331
Subject Categories: cell cycle
Keywords: γ-tubulin complex; centrosome; nuclear envelope; Polo kinase; SPB

Introduction

The centrosome was classically defined as the primary microtubule-organising centre (MTOC) of the cell. However, recent advances of our understanding about this organelle have further linked it to many other processes, including cell-cycle transition, DNA-damage checkpoint, asymmetric cell division, and ageing (Cowan and Hyman, 2004; Hachet *et al*, 2007; Cheng *et al*, 2008). Despite the recognition of its ever-growing importance, the molecular mechanisms by which the centrosome executes its diverse roles have remained unsolved. In yeast, the centrosome equivalent spindle pole body (SPB) is also known to regulate multiple pathways. For example, in fission yeast this structure is important for spindle microtubule formation (Hagan and Yanagida, 1995; Vardy and Toda, 2000), mitotic entry (Bridge *et al*, 1998; Petersen and Hagan, 2005), SIN (Septation Initiation Network) signalling (Krapp and Simanis, 2008), and cell morphogenesis and polarity (Kanai *et al*, 2005). Despite this, we are still largely ignorant at the molecular levels as to how the SPB is involved in each distinct pathway.

Fission-yeast Pcp1 is an evolutionarily conserved pericentrin-related protein that localises to the inner plaque of the SPB throughout the cell cycle (Flory *et al*, 2002). Its orthologues, pericentrin (human beings), Spc110 (budding yeast), and centrosomin (*Drosophila*), are all linked to a role of spindle microtubule nucleation and assembly via the γ-tubulin complex (γ-TuC) during mitosis (Knop and Schiebel, 1997, 1998; Zimmerman *et al*, 2004; Muller *et al*, 2005; Zhang and Megraw, 2007). Spc110 was shown to interact with the γ-TuC (Knop and Schiebel, 1997, 1998) and its mutation leads to dissociation of the Spc110-containing complex from the main SPB structure towards the nucleoplasm (Yoder *et al*, 2005). In human and fly cells, it is shown that disrupting the function of pericentrin and centrosomin, respectively, caused γ-TuC delocalisation from the centrosome (Zimmerman *et al*, 2004; Zhang and Megraw, 2007). Mto1 is another fission-yeast SPB protein structurally similar to Pcp1. Unlike Pcp1, however, Mto1 localises to distinct cytoplasmic foci, including the outer side of the SPB, the nuclear periphery (interphase MTOC), and the medial region (equatorial MTOC), whereby it is responsible for the assembly of cytoplasmic microtubules nucleating from these sites during interphase (Sawin and Tran, 2006). In contrast to these precise analyses of Mto1, the roles for Pcp1 in cell division and microtubule formation have not been pursued except to identify that it is essential for cell viability (Flory *et al*, 2002), and it is proposed that this protein is involved in sensing proper spindle alignment (Rajagopalan *et al*, 2004).

Polo kinase plays vital roles during mitotic progression, DNA-damage checkpoint, and cytokinesis, and acts both upstream and downstream of CDKs (Nigg, 2007; Takaki *et al*, 2008; Archambault and Glover, 2009). Unlike other mitotic kinases such as CDK1 and aurora kinases, polo kinase does not have regulatory subunits that act as molecules

*Corresponding author. Laboratory of Cell Regulation, Cancer Research UK, London Research Institute, Lincoln's Inn Fields Laboratories, 44 Lincoln's Inn Fields, London WC2A 3PX, UK. Tel.: +44 20 7269 3535; Fax: +44 20 7269 3258; E-mail: toda@cancer.org.uk
[1]Present address: Department of Biophysics and Biochemistry, Graduate School of Science, University of Tokyo, Tokyo 113-0033, Japan

Received: 9 July 2009; accepted: 16 October 2009

responsible for targeting kinase catalytic subunits to specific cellular locations. Instead this kinase has been shown to localise by associating with proteins already recruited to a distinct cellular position (Elia *et al*, 2003). In fission yeast, as in other organisms, polo kinase (Plo1) executes myriad functions, including cell-cycle control, SIN signalling, and stress-responsive MAP kinase pathways (Ohkura *et al*, 1995; Bähler *et al*, 1998a; Cullen *et al*, 2000; Tanaka *et al*, 2001; Anderson *et al*, 2002; Petersen and Hagan, 2005). Plo1 localises to multiple sites in the cell in a cell cycle-dependent manner. For instance, Plo1 localises to the SPB, spindle microtubules, and the medial ring specifically during the M phase (Bähler *et al*, 1998a; Mulvihill *et al*, 1999). Despite this distinct cell-cycle-dependent Plo1 localisation, its spatial regulation remains largely elusive except that the involvement of the SPB component Cut12 and NIMA-related kinase Fin1 has been reported (Grallert and Hagan, 2002; MacIver *et al*, 2003).

In this study we characterise the molecular roles of Pcp1 during the cell cycle. We have found that like other members of pericentrin-related molecules, Pcp1 is required for γ-TuC recruitment to the SPB. In addition our analysis unveils unexpected roles of Pcp1 in mitotic entry and structural reorganisation of the nuclear envelope (NE) during mitosis. We further uncover that Pcp1 executes these roles by recruiting polo kinase to the mitotic SPB. We discuss the significance of our findings in view of conserved mechanisms underlying centrosome/SPB-mediated mitotic control.

Results

pcp1 mutants are defective in bipolar spindle assembly and chromosome segregation

To analyse the essential functions of Pcp1 in cell division, we isolated temperature-sensitive (ts) mutants of *pcp1*$^+$ using an error-prone PCR method (Figure 1A; see Supplementary data and Supplementary Figure S1). As Pcp1 was expected to perform multiple roles at the SPB, we wanted to isolate mutant alleles that were specifically defective in distinct aspects of Pcp1 functions, rather than a complete loss-of-function mutant. To this end, ts mutants that exhibited Pcp1 delocalisation from the SPB at the restrictive temperature were first excluded, as these mutants were expected to mimic Pcp1 deletions. Among six mutants screened in this manner, we focused our analysis on two representative alleles, *pcp1-15* and *pcp1-18* (Supplementary Figure S2).

In order to define the cell-cycle stage for which Pcp1 function is essential, we performed synchronous culture analyses with centrifugal elutriation. Cultures with early-G_2 cells were harvested by elutriation at 27°C, shifted up to 36°C, and cell viability was monitored as cells proceeded through the cell cycle. Both *pcp1-15* and *pcp1-18* mutants exhibited a sharp decline in viability after 100 min at 36°C, which coincided with mitotic entry (light red columns in Figure 1B). This viability drop paralleled the emergence of massive chromosomal mis-segregation (blue lines in Figure 1B and post-mitotic cells with mis-segregated chromosomes are shown in Figure 1C). This result demonstrates that Pcp1 plays an essential role in cell proliferation during mitosis.

Overexpression of Pcp1 results in spindle abnormalities (Flory *et al*, 2002). These precedent results suggest a role for Pcp1 in spindle assembly like its orthologues in other species. We then examined spindle behaviour in the *pcp1* mutants by observing GFP–Atb2 (α2-tubulin) and Sid4–mRFP (an SPB component) in live cells incubated at 36°C. Wild-type cells formed bipolar spindles with two SPBs flanking the ends of the spindle as they progressed through mitosis (top 3 rows in Figure 1D and Supplementary Movie S1). By contrast, in ~80% of *pcp1-15* and *pcp1-18* cells spindle microtubules that emanated from only one SPB (we refer to monopolar spindles hereafter) were formed (bottom 6 rows, emphasised by arrowheads at 8 and 24 min; Supplementary Movies S2 and S3). Duplication of the SPB is unlikely to be affected in these *pcp1* mutants, as we detected two separate Sid4–mRFP signals (e.g., time point 12 min; Figure 1D). Thus the results indicate that Pcp1 is required for efficient nucleation/assembly of spindle microtubules from the SPB. In addition, live-image analysis showed that mitotic progression was delayed in both *pcp1* mutants (~15 min in the wild type versus >30 min in *pcp1* mutants; Figure 1D).

Monopolar spindles in pcp1 mutants emanate from the mother SPB

As noted earlier, the majority of *pcp1-15* and *pcp1-18* cells managed to nucleate spindles from one of the two SPBs, instead of displaying a complete lack of spindle formation (see Figure 1D). Fission-yeast SPB duplicates in a conservative manner (Grallert *et al*, 2004). We posited that mutant Pcp1 proteins would be less heat-sensitive once they are incorporated into the mother SPB prior to its duplication and separation, thereby retaining the capacity of spindle formation in an asymmetrical manner. To evaluate this possibility, we exploited asymmetric SPB localisation of Cdc7, one of the SIN kinases (Sohrmann *et al*, 1998). Cdc7 localises to both SPBs in early mitosis, but remains only on the daughter SPB in late anaphase (Figure 2A, top, wild type). Indeed, in the *pcp1* mutants, Cdc7–GFP localised to the SPBs devoid of spindles (the second and third rows), confirming that the mother SPB is the origin of monopolar spindles in these cells. In addition, compared with wild-type spindles, these mutant spindles exhibited significantly lower GFP–Atb2 signal intensities (Figure 2B). This result shows that both *pcp1* mutants exhibited compromised nucleating activities of spindle microtubules, in which only the mother SPB manages to retain nucleation capability to some extent.

γ-TuC is not recruited to the SPB in the absence of Pcp1 function

Human pericentrin and *Drosophila* centrosomin were shown to be required for γ-TuC recruitment to the mitotic centrosome (Zimmerman *et al*, 2004; Zhang and Megraw, 2007). We therefore asked whether the *pcp1* mutants exhibit γ-TuC delocalisation from the SPB at the restrictive temperature. In wild-type cells, Alp4–GFP (orthologue of the γ-TuC component GCP2/Spc97) (Vardy and Toda, 2000) localised normally to the SPB in almost all the cells (Figure 3A and B). On the contrary, ~80% of *pcp1-15* cells lost Alp4–GFP from the SPB after 4-h incubation at 36°C (Figure 3A and B). Similar results were obtained when localisation of another γ-TuC component, Alp6 (orthologue of GCP3/Spc98) (Vardy and Toda, 2000), was analysed (Supplementary Figure S3). This shows that Pcp1 is required for γ-TuC recruitment to the SPB.

Intriguingly γ-TuC localisation was largely unaffected in *pcp1-18* cells, suggesting that *pcp1-15* and *pcp1-18* mutants are defective in distinct functions, which are genetically

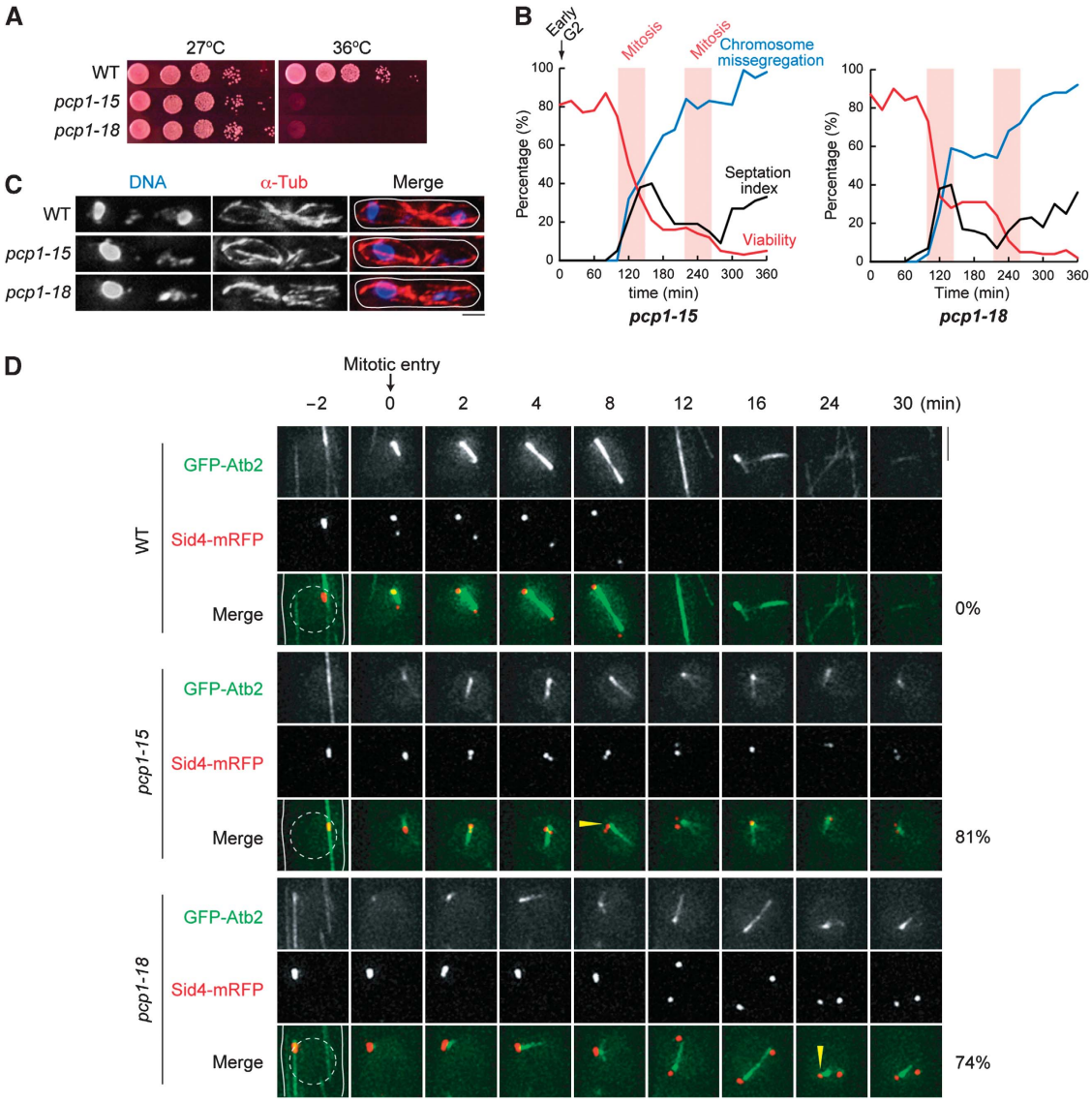

Figure 1 Two *pcp1* mutants exhibit similar mitotic defects in spindle formation and chromosome segregation. (**A**) Ten-fold serial dilution assays on rich YES media. A total of 5×10^4 cells were applied in the first spot and incubated at 27 or 36°C for 3 days. (**B**) Viability of cells in synchronous culture analyses. Small G_2 cells grown at 27°C were collected with centrifugal elutriation and shifted to 36°C at time 0. The percentage of septated cells was used to monitor cell-cycle progression. Light red columns mark periods in mitosis ($n > 100$). (**C**) Chromosome segregation defects. Immunofluorescence microscopy was performed with anti-α-tubulin antibody (TAT-1, red) and DAPI (blue) at the 120-min time point in synchronous culture experiments at 36°C as described in panel **B**. Cells completed the first mitosis, as indicated by the presence of post-anaphase arrays with two unequally segregated chromosomes. (**D**) Time-lapse fluorescence montages of spindle microtubules (GFP–Atb2, green) and SPB (Sid4–mRFP, red) structures during the first mitosis. A representative cell of each strain is shown. Note that during wild-type anaphase-B (the second row, 8 min and thereafter) SPBs became out of frame due to spindle elongation. Dashed circles outline the nuclei. Arrowheads (8 and 24 min): SPBs nucleating spindle microtubules ($n > 20$). The percentage indicates the proportion of cells displaying monopolar spindle phenotype. Live images are shown in Supplementary Movies S1–3. Scale bars, 2 μm.

separable (see below). It is of interest to point out that as shown earlier (see Figures 1D and 2A), mitotic spindles nucleate from the mother SPB despite an apparent loss of γ-TuC from the SPB. We envisage that under this condition a residual low amount of the γ-TuC at the mother SPB would manage to support the nucleation of spindle microtubules. Similar phenotypes were observed previously in temperature-sensitive *alp4* and *alp6* mutants (Vardy and Toda, 2000).

To substantiate our finding that Pcp1 is required for γ-TuC recruitment, we tested whether restoring γ-TuC localisation to the SPB could suppress the temperature sensitivity of *pcp1-15* cells. Mild overexpression of Alp4 (note that strong over-expression of Alp4 is lethal) (Vardy and Toda, 2000) restored Alp6–GFP localisation to the SPB (Figure 3C and D) and moreover indeed ameliorated the growth of *pcp1-15* cells at the semi-restrictive temperature (34°C; Figure 3E). The same condition did not confer growth advantage to *pcp1-18* cells (Figure 3E), consistent with the fact that γ-TuC localisation is not the underlying defect in this mutant. Collectively, our data demonstrate that one of the essential functions of Pcp1 lies in γ-TuC recruitment to the SPB.

Pcp1 is required for γ-TuC recruitment to the SPB during mitosis but not interphase

Previous work showed that although Pcp1 and the γ-TuC appear to colocalise to the SPB, there is a profound difference

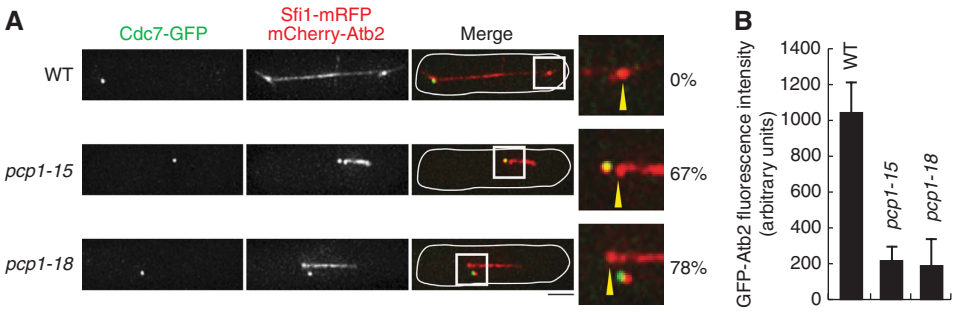

Figure 2 Only the mother SPB nucleates spindle microtubules in *pcp1* mutants. (**A**) Monopolar spindles emanating from the mother SPB. Cdc7–GFP (green) is a marker for the daughter SPB (Sohrmann *et al*, 1998). Arrowheads: Mother SPBs (negative for Cdc7–GFP). Sfi1–mRFP and mCherry–Atb2 (red) mark the SPB and the spindle, respectively. Merged images of emanating spindles from the mother SPB to which Cdc7–GFP does not localise (white squares) are enlarged on the right ($n>15$). The percentage indicates the proportion of cells displaying monopolar spindles emanating from the mother SPB. (**B**) Quantification of GFP–Atb2 fluorescence signals ($n>50$); the error bars represent standard error. Scale bars, 2 μm.

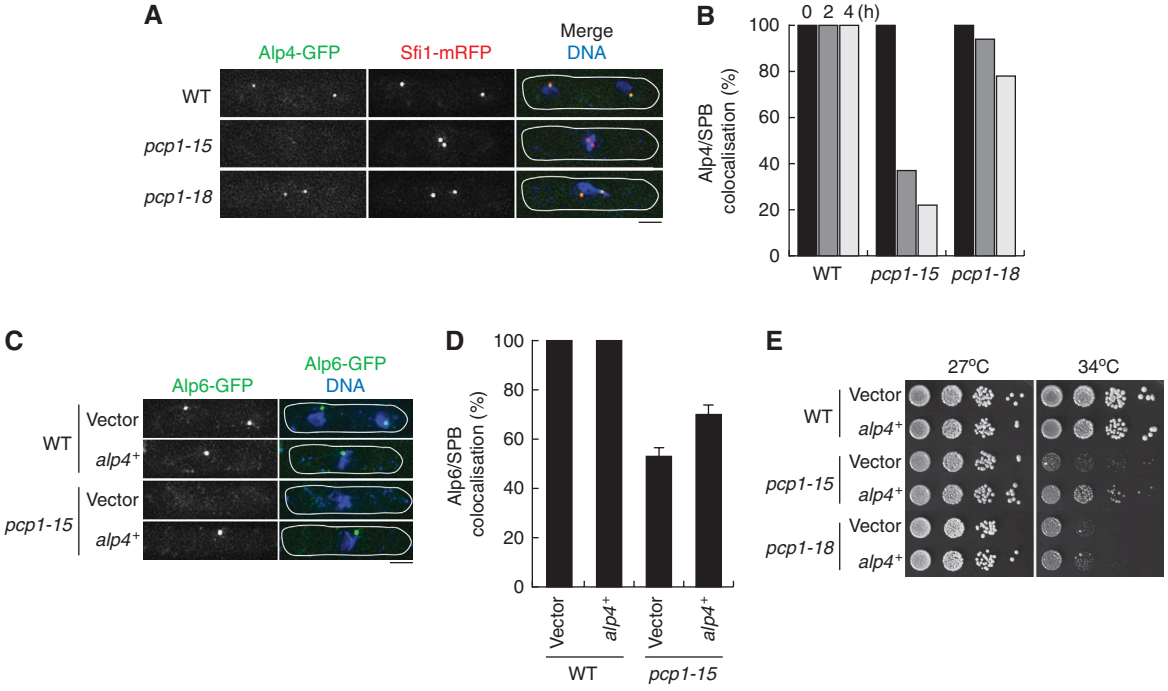

Figure 3 Pcp1 plays an essential role in γ-TuC recruitment to the SPB. (**A**) Alp4–GFP localisation after 2-h incubation at 36°C. Sfi1–mRFP is an SPB marker. (**B**) Percentage of cells with Alp4–GFP at the SPB in the experiment described in panel A ($n>100$). (**C**) Alp6–GFP localisation at the SPB with or without mild overexpression of Alp4. Alp4 was mildly overexpressed through repression of the *nmt1* promoter (pREP1–Alp4) on rich liquid YES media incubated for 4 h at 34°C. (**D**) Percentage of cells with Alp6–GFP at the SPB in the experiment described in panel **C** ($n>100$); the error bars represent standard deviation from three independent experiments. (**E**) Ten-fold serial dilution assays on YES media. Scale bars, 2 μm.

in their geometry between interphase and mitosis (Flory *et al*, 2002). While the γ-TuC localises predominantly inside the nucleus throughout the cell cycle (Ding *et al*., 1997), Pcp1 stays in the cytoplasm during interphase and enters the nucleus only upon mitotic entry. It is, therefore, conceivable that Pcp1 is only required for γ-TuC recruitment during mitosis. To clarify the temporal involvement of Pcp1 in γ-TuC recruitment to the SPB, centrifugal elutriation was performed again in the *pcp1-15* mutant and Alp4–GFP signals were followed over time at 36°C (Figure 4A, culture 1). We found that Alp4–GFP is retained at the SPB during interphase, but started to delocalise from the SPB coincidentally as *pcp1-15* cells entered mitosis (Figure 4B, 60–80 min).

To exclude the possibility that the timing of Alp4–GFP delocalisation reflects the minimum duration required for heat inactivation of the Pcp1-15 mutant protein, half of the initial culture was incubated at 27°C for a further 40 min during G_2 phase, followed by a shift up to 36°C (Figure 4A, culture 2). Similar to the previous observation, Alp4–GFP in this parallel experiment delocalised from the SPB as cells entered mitosis (Figure 4B, 60–80 min). Note that the same result was obtained in the deletion background of another pericentrin-related Mto1, which plays a critical role in the organisation of cytoplasmic microtubules (Sawin and Tran, 2006, data not shown). Taken together, our findings not only establish that Pcp1 is required for γ-TuC recruitment to the

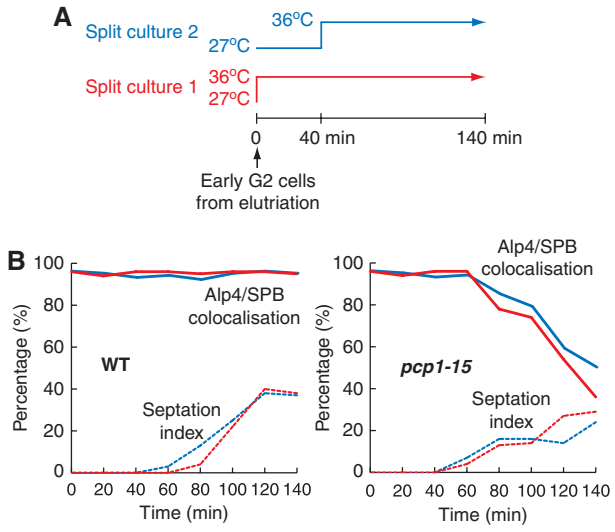

Figure 4 Pcp1 is required for γ-TuC recruitment to the SPB specifically during mitosis. (**A**) Experimental diagram. Synchronous cultures of early G_2 cells (grown at 27°C) were divided into two at time 0. One culture was immediately shifted to 36°C (culture 1, red), while the other was kept at 27°C for another 40 min, followed by shift to 36°C (culture 2, blue). (**B**) Alp4–GFP localisation at the SPB in synchronous culture experiments. Alp4–GFP signals were monitored in wild-type (left) or pcp1-15 cells (right) at each time point ($n > 100$).

mitotic SPB, but also suggest that γ-TuC recruitment during interphase is mediated by a Pcp1- and Mto1-independent mechanism. Given that centromeres are clustered in close proximity to the SPB during interphase (Funabiki *et al*, 1993), γ-TuC might be tethered to this location via interaction with some kinetochore components (Appelgren *et al*, 2003).

pcp1-18 is defective in NE reorganisation and SPB insertion during mitosis

As noted earlier, while both *pcp1-15* and *pcp1-18* cells display similar mitotic defects, unlike *pcp1-15*, γ-TuC localisation is not significantly impaired in the *pcp1-18* mutant (Figure 3A). This implies that Pcp1 plays an essential role independent of γ-TuC recruitment to the mitotic SPB. To uncover this additional role of Pcp1, we performed a multi-copy suppressor screen. Among the suppressor genes that specifically rescued *pcp1-18* were those encoding the nuclear pore complex (NPC) components—Cut11 (orthologue of Ndc1; West *et al*, 1998) and Pom152 (potential orthologue of GP210; Tran and Wente, 2006) (Figure 5A; see Table I for a complete list of suppressors). Both these proteins are transmembrane nucleoporins that constitute the inner membrane rings of the NPC (Alber *et al*, 2007b). In fission yeast that undergoes closed mitosis, Cut11 is not only an essential NPC component, but also accumulates specifically to the SPB upon mitotic onset (West *et al*, 1998). Furthermore, this protein is required for SPB insertion into the NE during mitosis (West *et al*, 1998; see Supplementary Figure S4 for Pom152 localisation).

Given the role of Cut11 in SPB insertion, we investigated whether *pcp1-18* cells fail to reorganise the NE and the SPB in mitosis. To this end, the ultrastructures were examined by electron microscopy (EM) in high-pressure-frozen cells. In wild-type mitotic cells, as reported previously (Ding *et al*, 1997), the electron-sparse NE discontinued underneath the electron-dense SPB, indicating that the NE opened up to form a fenestra for SPB insertion (Figure 5B). By striking contrast, in *pcp1-18* cells the NE underneath one of the SPBs remained intact (the SPB on the left hand side in Figure 5D and E). The examined cells are indeed in mitosis, as indicated either by NE herniation (the result of monopolar spindles prodding on the NE; Figure 5D, and see also Figure 6A) or the presence of spindle microtubules (Figure 5E).

We also observed NE and SPB structures in *pcp1-15* mitotic cells. In clear contrast to *pcp1-18*, the NE formed a fenestra normally in this mutant (Figure 5C), consistent with our suppression data showing that an increased dosage of Cut11 does not restore growth of *pcp1-15* mutants (Figure 5A). However, we noticed that the SPB was placed obliquely, rather than in parallel, above the NE, indicating that despite the apparent NE invagination, SPB insertion into the NE is somewhat compromised in this mutant. These results indicate that Pcp1 is required for NE invagination and SPB insertion during mitosis.

Plo1 recruitment to the mitotic SPB is impaired in pcp1-18

We next sought to examine whether Cut11 localisation is disrupted in *pcp1-18* cells. However, we observed no abnormalities in Cut11–GFP localisation (Figure 6A). Probing further into the underlying defect in the *pcp1-18* mutant, we inspected the list of allele-specific multi-copy suppressors again and noticed that overproduction of the essential SPB component Cut12 (Bridge *et al*, 1998) also suppressed the temperature sensitivity of the *pcp1-18* mutant (Figure 6B). We accordingly examined whether Pcp1 is involved in Cut12 recruitment to the SPB, but again Cut12–GFP localised normally to the SPB in *pcp1-18* cells at 36°C (Figure 6C). These data imply that functional activities, rather than localisation, of Cut11 and Cut12 are impaired in the *pcp1-18* mutant.

Previous work showed that Cut12 plays a role in promoting G_2/M transition by activating polo kinase Plo1 upon mitotic entry (Bridge *et al*, 1998; MacIver *et al*, 2003; Petersen and Hagan, 2005). Given this notion, we examined Plo1–GFP localisation in *pcp1-18* cells. Notably we found a significant reduction in its signal at the SPB in this mutant (Figure 6D and E). This result was confirmed by an additional experiment in which a *pcp1-15* or *pcp1-18* strain (each carrying Plo1–GFP, Sfi1–mRFP, and mCherry–Atb2) was mixed with wild-type cells (carrying only Plo1–GFP) in the same culture and shifted to the restrictive temperature. Under this condition, *pcp1-18* cells specifically lost the GFP (Plo1) signals from the SPB (the top right panel in Supplementary Figure S5), while either wild-type or *pcp1-15* cells retained the GFP–Plo1 signals (top two panels). These results demonstrate an essential role for Pcp1 in Plo1 recruitment to the mitotic SPB.

We consequently asked if potentiation of Plo1 recruitment to the SPB could suppress the *pcp1-18* mutant. For this purpose, we used a hypermorphic allele of *cut12*, *cut12.s11*, that enhances Plo1 recruitment to the mitotic SPB (Hudson *et al*, 1990; MacIver *et al*, 2003; Petersen and Hagan, 2005). Indeed, *pcp1-18cut12.s11* double mutants were capable of forming colonies at 34°C, the semi-restrictive temperature for *pcp1-18* (Figure 6F). Furthermore it was found that Plo1 is recruited to the SPB in *pcp1-18cut12.s11* cells (Figure 6H

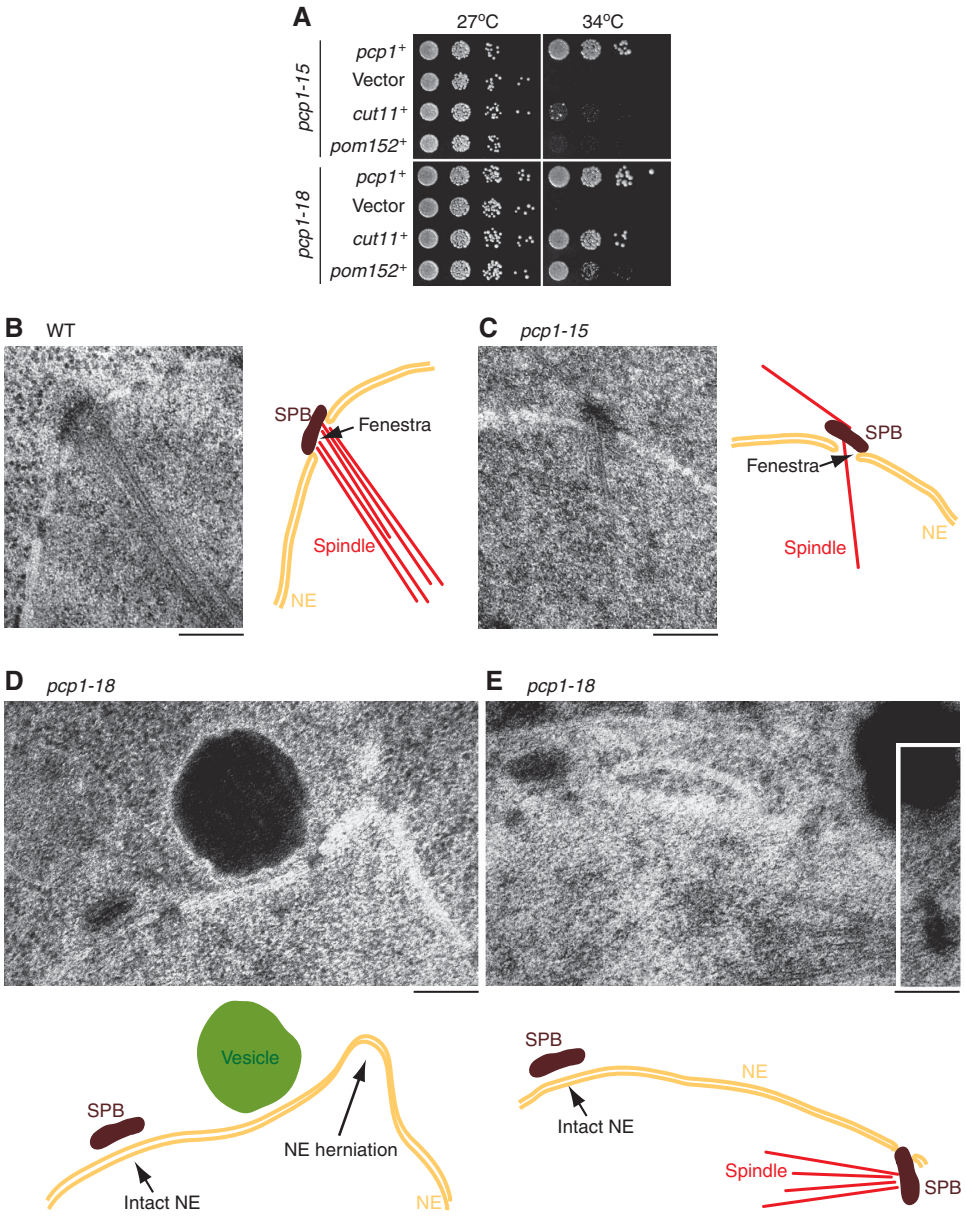

Figure 5 In the *pcp1-18* mutant, formation of a fenestra in the NE and SPB insertion are impaired. (**A**) Ten-fold serial dilutions of the *pcp1* mutants harbouring the indicated multi-copy suppressor plasmids. Cells were grown overnight in selective media at 27°C prior to spotting onto YES media and incubated for 3 days at 27 or 34°C. (**B–E**) Electron micrographs showing ultrastructures of the SPB, the NE, and spindle microtubules. Synchronised cultures (incubated at 36°C for 100 min, enriched mitotic cells) were processed for EM. Schematic diagrams are included next to or below each electron micrograph. Monopolar spindles in panel **E** originate from the SPB on the right (overlaid from adjacent section, presumably the mother SPB) that is abnormally inserted into the NE ($n = 5$) (four out of five *pcp1-18* cells showed SPB insertion defects). Scale bars, 200 nm.

Table I List of multi-copy suppressor genes of the *pcp1* mutants

Genes	Suppression	
	pcp1-15	*pcp1-18*
pcp1$^+$	Yes	Yes
cut11$^+$	No	Yes
pom152$^+$	No	Yes
cut12$^+$	No	Yes
kms2$^+$	No	Yes
tcg1$^+$	No	Yes

kms2$^+$ encodes an SPB component (Miki *et al*, 2004), while *tcg1*$^+$ encodes a potential homologue of budding-yeast ribonucleoprotein Rnp1 (Cusick, 1994). Functions of either protein are unknown at the moment.

and G). It is of note that not only *cut12.s11* but also multi-copy *cut11*$^+$ restored Plo1 recruitment to the SPB in *pcp1-18* cells (Supplementary Figure S6A and B). Together, these findings demonstrate that Pcp1 is required for Plo1 recruitment to the SPB during mitosis.

Promotion of mitotic entry rescues defects in growth and SPB recruitment of Plo1 in the pcp1-18 mutant

Polo kinase plays pivotal roles in a variety of processes in cell-cycle control (Nigg, 2007; Takaki *et al*, 2008; Archambault and Glover, 2009). Among them, one of its established functions at the centrosome and SPB is the advancement of mitotic entry (MacIver *et al*, 2003; Petersen

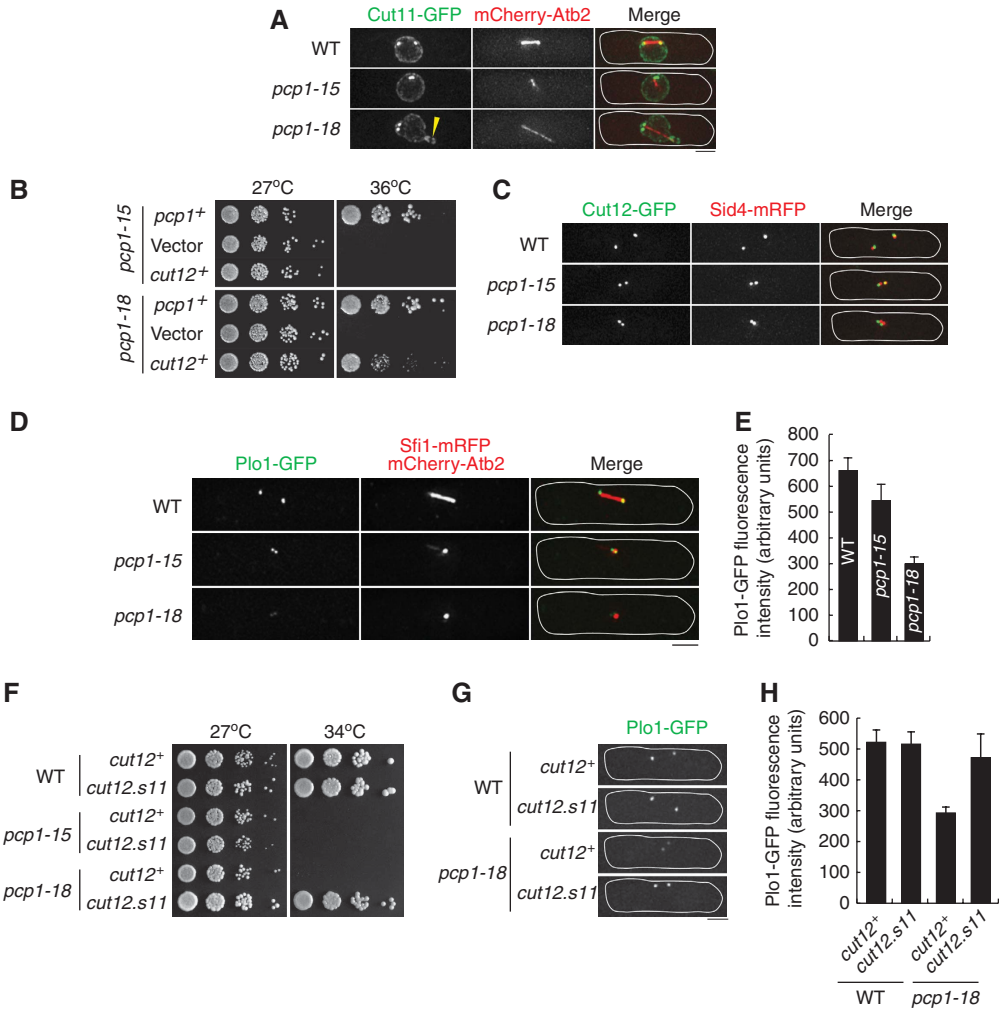

Figure 6 Pcp1 is required for recruitment of Plo1 to the SPB. (**A**) Localisation of Cut11–GFP in mitotic cells at 36°C. NE herniation (arrowhead), probably corresponding to the EM picture shown in Figure 3D for *pcp1-18*, was observed in which Cut11 appears to somewhat accumulate ($n>50$). (**B**) Ten-fold serial dilutions of the *pcp1* mutants harbouring the indicated multi-copy suppressors. (**C**) Normal localisation of Cut12–GFP to the SPB during mitotic at 36°C ($n>100$). (**D**) Plo1–GFP delocalises from the mitotic SPB specifically in *pcp1-18* mutants. Fluorescence images (**A**, **C**, and **D**) were taken from live cells. (**E**) Quantification of Plo1–GFP signal intensity at the SPB in panel D ($n>50$); the error bars indicate standard error. (**F**) Ten-fold serial dilution assays on YES media. (**G**) Increased recruitment of Plo1–GFP at the SPB in the *pcp1-18cut12.s11* double mutant at the semi-permissive temperature of 34°C. (**H**) Quantification of Plo1–GFP signal intensity at the SPB in panel G ($n>50$); the error bars indicate standard error. Fluorescence images (**A**, **C**, **D**, and **F**) were taken from live cells. Scale bars, 2 μm.

and Hagan, 2005; Takaki *et al*, 2008). If Pcp1's role in Plo1 recruitment lies in promoting mitotic entry, forced advancement in the onset of mitosis independently of Plo1 would suppress this mutant. To test this idea, we constructed a double mutant between *pcp1-18* and *wee1-50*, a mutation that causes premature entry into mitosis due to untimely activation of Cdc2 (CDK1) (Nurse, 1990). Remarkably, *pcp1-18wee1-50*, but not *pcp1-15wee1-50*, exhibited improved growth at the semi-permissive temperature of 32°C (Figure 7A). These results, therefore, have uncovered a novel role for Pcp1 in the recruitment of Plo1 to the SPB to promote mitotic entry, and at the same time established a link between Plo1 recruitment and mitotic NE reorganisation for SPB insertion.

Pcp1 interacts with the γ-TuC and Plo1

Results presented above suggest that Pcp1 physically interacts with the γ-TuC and Plo1, thereby recruiting these two factors directly to the SPB. To address this point, cell extracts were prepared from wild type and *pcp1* mutants, and co-immunoprecipitation experiments were performed. As shown in Figure 7B, we did detect an interaction between Pcp1 and either the γ-TuC or Plo1 (lane 13). This interaction appeared fairly tight, as binding was sustainable against washing with high-salt buffers (lanes 14 and 15, 0.3 and 0.5 M NaCl, respectively). Co-immunoprecipitation was specific as no Plo1 or γ-TuC was pulled down when preimmune sera were used for precipitation (lanes 4–6). Interestingly, budding-yeast Spc110 is also reported to interact with both γ-TuC and Cdc5 (budding-yeast polo kinase; Knop and Schiebel, 1997, 1998; Snead *et al*, 2007).

Next we performed immunoprecipitation using mutant extracts prepared from cultures incubated under restrictive conditions (4 h, at 36°C). Contrary to a simple scenario predicting impaired interaction in mutants, the amount of precipitated γ-TuC or Plo1 did not appear noticeably different between the wild type and *pcp1-15* or *pcp1-18* even under stringent high-salt conditions (Figures 7B, lanes 16–21). We

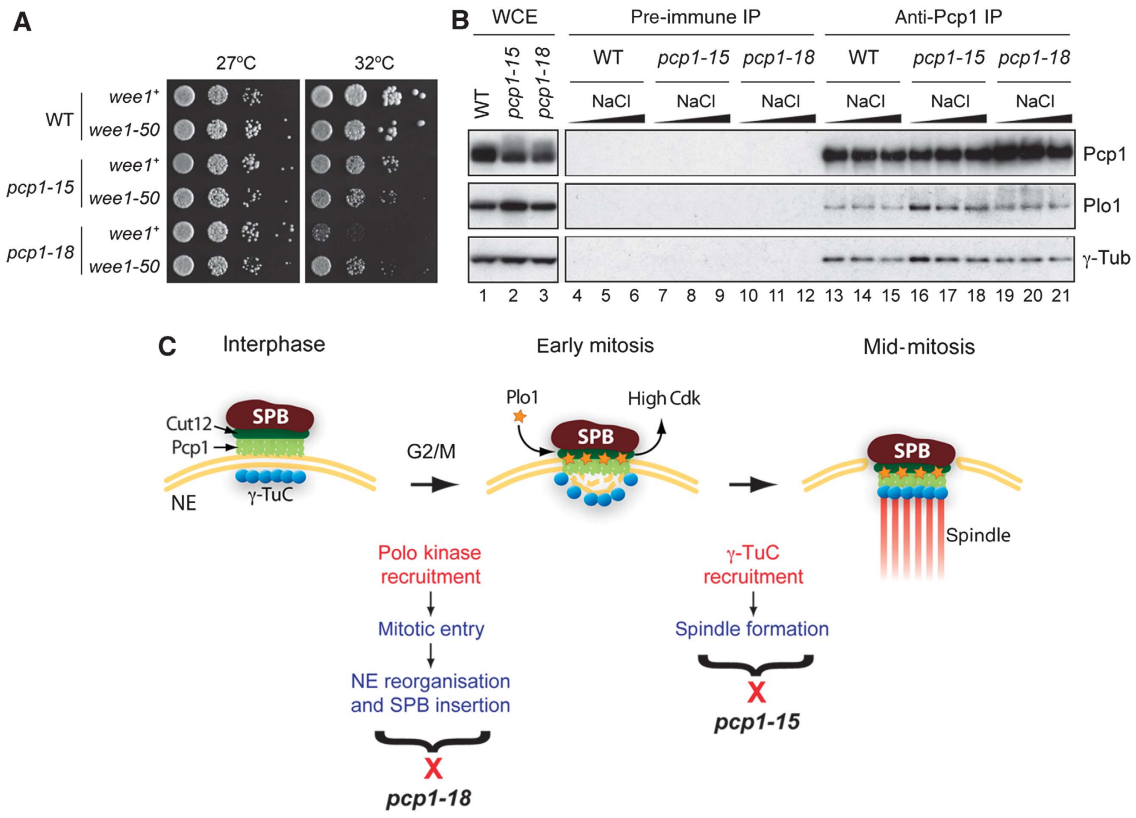

Figure 7 Rescue of *pcp1-18* by premature mitotic entry, physical interaction between Pcp1 and Plo1 or γ-tubulin, and a working model. (**A**) *pcp1-18*, but not *pcp1-15*, is suppressed by premature mitotic entry. Ten-fold serial dilution assays on YES media. (**B**) Pcp1 physically interacts with both γ-TuC and Plo1. Wild-type, *pcp1-15*, or *pcp1-18* cells containing Plo1–GFP–HA were grown at 27°C and shifted up to 36°C for 4 h. Extracts were prepared and immunoprecipitation was performed with affinity-purified anti-Pcp1 antibodies. Precipitates were subjected to SDS–PAGE and immunoblotting was performed with anti-Pcp1, anti-HA, and anti-γ-tubulin antibodies (lanes 13, 16, and 18). As negative control, preimmune sera were used (lanes 4, 7, and 10). Immunoprecipitates on beads were further washed with high-salt buffers containing 0.3 or 0.5 M NaCl (lanes 5, 8, 11, 14, 17, and 20, or lanes 6, 9, 12, 15, 18, and 21, respectively). Note that the salt concentration of original buffers is 0.15 M NaCl; 0.5-mg equivalents of immunoprecipitates and 30 μg of whole-cell extracts (WCE, lanes 1–3) were loaded. (**C**) A model of Pcp1's function during cell division. Pcp1 recruits Plo1 to the SPB at G_2/M transition, leading to full activation of Cdk (Cdc2) and mitotic entry. Note that activated Cdc2 in turn activates Plo1 via a positive-feedback loop. This drives directly or indirectly NE reorganisation and SPB insertion. At the same time Pcp1 recruits γ-TuC to the mitotic SPB to initiate spindle formation. The nature of interactions between Pcp1 and Cut11 (not depicted) or Cut12 remains unclear at this moment. SPB: brown; Cut12: dark green; Pcp1: light green; γ-TuC: blue circles; NE: yellow; Plo1: orange star; and spindle: red lines.

envision that only a small proportion of γ-TuC or Plo1 forms a complex with Pcp1 at the SPB during mitosis (see Discussion). Nonetheless, this result points towards a possibility that Pcp1 directly interacts with γ-TuC and Plo1, thereby playing a structural role as a platform for these factors loading to the mitotic SPB. In sum, our work verifies Pcp1's plausible role in γ-TuC-mediated spindle assembly and unveils its unanticipated function in Plo1-dependent mitotic entry and structural reorganisation of the NE.

Discussion

Our work presented here shows that a single SPB component Pcp1 plays multiple roles in mitosis by independently recruiting two essential components, γ-TuC and Plo1. The *pcp1-15* mutant is defective in γ-TuC recruitment to the mitotic SPB, while *pcp1-18* fails to target Plo1 to this site. We have shown that these defects are allele-specific. Despite these differences, both mutants display similar monopolar spindles, in which only the mother SPB could nucleate spindle microtubules, albeit with reduced intensity. Importantly EM analysis has revealed that *pcp1-18* is further impaired in mitosis-specific NE invagination beneath the daughter SPB, accompanied by failure in SPB insertion into the NE. We believe that this asymmetrical SPB defect is the main reason for monopolar spindle phenotypes observed in this mutant allele. Our study, therefore, illuminates that SPB-mediated mitotic processes, including spindle formation, NE reorganisation, and SPB insertion converge via Pcp1 (see Figure 7C for a model); on one hand, Pcp1 recruits γ-TuC, thereby promoting nucleation and assembly of spindle microtubules; on the other Pcp1 interacts with Plo1 and is responsible for NE invagination and subsequent SPB insertion. Another SPB component, Cut12, plays a corroborative role with Pcp1 in Plo1 regulation at the SPB (Figure 7C). Importantly the core cell-cycle machinery that activates CDK1/Cdc2, thereby determining the timing of mitotic commitment, cooperates at the SPB with the Pcp1–Plo1 pathway by forming a positive-feedback loop (Hagan, 2008).

A conserved γ-TuC-binding domain has recently been identified in a family of pericentrin-related proteins, including centrosomin, Spc110, Mto1, and Pcp1 (Zhang and Megraw,

2007; Samejima *et al*, 2008). It is, therefore, conceivable that Pcp1 directly recruits γ-TuC to the SPB during mitosis. Physical binding between Pcp1 and γ-tubulin supports this notion. Interestingly, *pcp-15*, which fails to recruit the γ-TuC to the mitotic SPB, harbours a mutation within this γ-TuC-binding domain (Supplementary Figure S1). In budding yeast, the temperature-sensitive *spc110-221* allele that carries multiple mutations in the N-terminal region was rescued by overproduction of Spc98 (Alp6 homologue; Nguyen *et al*, 1998), which might be in parallel with our finding described in this study.

Although we are so far unable to recapitulate a reduced recruitment of the γ-TuC to the mitotic SPB by co-immunoprecipitation in the *pcp1-15* mutant, a population of Pcp1 that colocalises with the γ-TuC to the mitotic SPB could be too small to detect by pull-down methods. It is of note that even in wild-type cells, we have not succeeded in showing enhanced interaction between Pcp1 and the γ-TuC or Plo1 during mitosis as compared with the interphase (data not shown). Alternatively, as SPB components expectedly remain insoluble upon protein extractions, we might not be able to show impaired recruitment to the SPB in the mutants under conditions currently used. Further biochemical analyses would determine the underlying mechanism in more detail.

With regard to Plo1 localisation to the mitotic SPB, to our knowledge, this is the first study in any organisms to identify genetically a spindle pole component that plays a critical role in polo kinase recruitment to the SPB/centrosome. It is known that CDK1 and cyclin-B localise to the mitotic centrosome in animal cells (Jackman *et al*, 2003) and to the SPB in fission yeast (Alfa *et al*, 1990; Decottignies *et al*, 2001), implying a universal role for the centrosome/SPB in the temporal regulation of mitotic onset. Precedent work using fission yeast indicated that Cut12 potentiates Plo1 activity upon mitotic onset; however, it should be noted that Cut12 is not required for Plo1 recruitment to the SPB *per se*; in other words Plo1 is still recruited apparently normally to the SPB during mitosis even in the *cut12*-null mutant (Mulvihill *et al*, 1999). This indicates that Cut12, albeit physically interacting with Plo1 (MacIver *et al*, 2003), is not a receptor that is directly responsible for recruitment of this kinase to the mitotic SPB, but instead it is Pcp1 that performs this task. Although at the moment it remains to be determined how Pcp1 and Cut12 functionally and physically interact, it might be stated that Pcp1 is involved in mitosis-specific activation of Cut12 through a hitherto unknown mechanism. Alternatively, as Cut12 is capable of localising to the SPB in *pcp1-18* mutants, Cut12 acts either upstream or independently of Pcp1 (see below).

We also demonstrate that Pcp1 controls SPB insertion and NE invagination during mitosis. Importantly, these processes could be under the control of SPB-localising Plo1, as the defect is only observed in *pcp1-18*, but not *pcp1-15*, cells. Furthermore, the enhancement of Plo1 localisation to the mitotic SPB using gain-of-function *cut12.s11* is sufficient to suppress the *pcp1-18* mutant. Very recently it was shown that the temperature-sensitive, loss-of-function *cut12.1* mutant also displays SPB insertion defects (Tallada *et al*, 2009) as that we observed in *pcp1-18*. This indicates that Pcp1, Cut12, and Plo1 form a functional network via physical binding in SPB-mediated mitotic entry and progression. It would be of interest to examine whether *plo1* mutants display similar SPB insertion defects.

We isolated Cut11 and Pom152, as well as Cut12, as dosage-dependent, allele-specific suppressors of *pcp1-18*. The first two proteins are conserved membrane-integral nucleoporins (Cut11/Ndc1 and Pom152/GP210) and form a stoichiometric subcomplex in both human and budding yeast, thereby constituting an internal membrane ring (Madrid *et al*, 2006; Mansfeld *et al*, 2006; Stavru *et al*, 2006; Alber *et al*, 2007a, b; Galy *et al*, 2008). As Cut11 is enriched at the SPB during fission-yeast mitosis (West *et al*, 1998), it would be tempting to speculate that this integral membrane protein is directly involved in mitotic NE invagination and SPB insertion. Indeed it is shown that the temperature-sensitive *cut11.1* mutant has monopolar spindles with asymmetric SPB defects, as in the *cut12.1* or *pcp1* mutants analysed here (West *et al*, 1998; Tallada *et al*, 2009). An intriguing possibility is that Cut11 and/or Pom152 are downstream effectors of Plo1, including phospho-substrates, although suppression of Plo1 recruitment to the SPB by *cdc12.s11* or multi-copy *cut11*$^+$ implies a more complicated scenario such as a positive-feedback loop rather than a simple linear pathway. We have addressed whether or not it would be possible to genetically differentiate distinct functions of Pcp1 using *pcp1-15* and *pcp1-18* mutants, but so far these two mutant alleles behave similarly in terms of non-complementation and synthetic lethal interactions with mutations in other related genes (see Supplementary Notes 1 and 2, and Supplementary Figure S7).

Although NE-mediated processes such as NE invagination and SPB insertion may be regarded as a close mitosis-specific event, it is known that in animal cells the NE undergoes dynamic structural alterations upon mitotic entry, in which the small restricted regions of the NE below the centrosome indeed invaginate prior to mitotic NE breakdown (Beaudouin *et al*, 2002; Salina *et al*, 2002; Hetzer *et al*, 2005; Tran and Wente, 2006; D'Angelo and Hetzer, 2008), which might well be analogous to the formation of NE fenestra observed in fission yeast (Ding *et al*, 1997). It would be of instant interest to see whether NE invagination in animal cells is regulated by polo kinase. In conclusion, our work has unearthed that Pcp1 and possibly the analogous pericentrin-like proteins play a more central and integral role in the orchestration of cell-cycle events than previously anticipated, and may provide insight into tumorigenesis and other types of human diseases attributed to centrosomal dysfunction.

Materials and methods

Yeast genetics and strains

Strains used in this study are listed in Supplementary Table S1. Standard methods for yeast genetics and gene tagging were used (Moreno *et al*, 1991; Bähler *et al*, 1998b; Sato *et al*, 2005, 2009). For isolation of temperature-sensitive *pcp1* mutant, *pcp1*$^+$ fragments containing C-terminally tagged HA epitope and *hph*^{r} gene (*pcp1*$^+$-*HA-hph*^{r}) were randomly mutagenised during error-prone PCR amplification using Vent DNA polymerase (New England Biolabs Ltd.) supplemented with 10× deoxyguanosine triphosphate (dGTP). PCR fragments were ethanol-precipitated and transformed into a wild-type strain (513; Supplementary Table S1). Approximately 5000 transformants were screened for temperature sensitivity at 36°C. The isolated temperature-sensitive mutants were backcrossed to *pcp1*$^+$-*mRFP-kan*^{r} to ensure proper integration and to remove potential off-site mutations.

Multi-copy suppressor screening

The *pcp1* mutants were transformed with a genomic DNA library. Approximately 15 000 transformants growing on selection plates at 27°C were replica-plated onto YES containing phloxin-B and the plates were incubated at 36 or 34°C. Plasmids were isolated from the growing colonies and sequenced to identify the suppressor genes. Plasmids were retransformed into the *pcp1* mutants to reconfirm suppression.

Microscopy

For fluorescence microscopy an AxioplanII microscope (Zeiss Ltd.) with Volocity software (Improvision Co.) and the Deltavision-SoftWoRx system (Olympus and Applied Precision Co.) were used. Images were taken at 15 sections along the *z*-axis at 0.2- to 0.4-mm intervals; they were then deconvolved and merged into a single projection. For immunofluorescence microscopy, TAT-1 (α-tubulin monoclonal antibody provided by K Gull, Oxford University, UK) was used. The captured images were processed with Adobe Photoshop CS2 (version 9.0).

Electron microscopy

Samples were cryofixed by high-pressure freezing using a Leica EM PACT2. Freeze substitution was performed in anhydrous acetone containing 0.01% osmium tetraoxide, 0.1% glutaraldehyde, and 0.25% uranyl acetate for 3 days at −90°C using a Leica EM AFS. Freeze-substituted cells were gradually warmed to −20°C and were finally infiltrated with Epon. Serial thin sections of ∼60 nm were cut using a Leica Ultracut UCT microtome and placed on pioloform-coated slot grids. Sections were post-stained with 2% uranyl acetate in 70% methanol for 4 min and with lead citrate for 1 min. Images were acquired with a FEI Tecnai Biotwin electron microscope and Gatan DigitalMicrograph. The captured images were processed with Adobe Photoshop CS2 (version 9.0).

Immunochemistry

Immunofluorescence microscopy was performed with methanol-fixed samples. Cells were processed in PEM-based buffers (200 mM Pipes, 2 mM EGTA, 2 mM $MgSO_4$, adjusted to pH 6.9). TAT-1 (anti-α-tubulin antibody) and anti-Pcp1 antibodies were used at 1:200 and 1:5000, respectively.

Immunoprecipitation was performed using standard procedures as briefly described below. Proteins were extracted in lysis buffer (50 mM Tris–HCl (pH 7.4); 1 mM EDTA (pH 8.0); 150, 300, and 150 mM NaCl; 0.05% NP-40; 10% glycerol) by breaking the cells at 4°C with glass beads (setting 5.5, 25 s, 2 ×) in a FastPrep FP120 apparatus (Savant. Co., MN, USA). The protein extracts were collected after 15 min of centrifugation at 13 000 *g* at 4°C. The co-immunoprecipitations were performed by adding 4 mg of protein extract to protein-A dynabeads (Invitrogen Ltd., CA, USA) bound with anti-Pcp1 antibody or preimmune serum. For immunoblotting anti-Pcp1, anti-HA (16B12, Covance Inc., CA, USA), and anti-γ-tubulin (Sigma) antibodies were used at 1:5000, 1:200, and 1:500, respectively.

Supplementary data

Supplementary data are available at *The EMBO Journal* Online (http://www.embojournal.org).

Acknowledgements

We thank Iain Hagan, Keith Gull, and Paul Young for the reagents and strains used in this study. We are grateful to Frank Uhlmann for critical reading and Iain Hagan, Janni Petersen, and Ken Sawin for inspiring discussions. Special thanks to C Antony, Johanna L Höög, L Collinson, and K Blight for instruction and help with EM studies, and Muneyoshi Kanai and Dai Hirata for technical advice on centrifugal elutriation. MS was supported by abroad fellowship from Japan Society for the Promotion of Science and Grant-in-Aid for Young Scientists A of MEXT, Japan. This work was supported by Cancer Research UK (TT).

Conflict of interest

The authors declare that they have no conflict of interest.

References

Alber F, Dokudovskaya S, Veenhoff LM, Zhang W, Kipper J, Devos D, Suprapto A, Karni-Schmidt O, Williams R, Chait BT, Rout MP, Sali A (2007a) Determining the architectures of macromolecular assemblies. *Nature* **450:** 683–694

Alber F, Dokudovskaya S, Veenhoff LM, Zhang W, Kipper J, Devos D, Suprapto A, Karni-Schmidt O, Williams R, Chait BT, Sali A, Rout MP (2007b) The molecular architecture of the nuclear pore complex. *Nature* **450:** 695–701

Alfa CE, Ducommun B, Beach D, Hyams JS (1990) Distinct nuclear and spindle pole body populations of cyclin–cdc2 in fission yeast. *Nature (Lond)* **347:** 680–682

Anderson M, Ng SS, Marchesi V, MacIver FH, Stevens FE, Riddell T, Glover DM, Hagan IM, McInerny CJ (2002) *plo1*$^+$ regulates gene transcription at the M–G1 interval during the fission yeast mitotic cell cycle. *EMBO J* **21:** 5745–5755

Appelgren H, Kniola B, Ekwall K (2003) Distinct centromere domain structures with separate functions demonstrated in live fission yeast cells. *J Cell Sci* **116**(Part 19)**:** 4035–4042

Archambault V, Glover DM (2009) Polo-like kinases: conservation and divergence in their functions and regulation. *Nat Rev Mol Cell Biol* **10:** 265–275

Bähler J, Steever AB, Wheatley S, Wang Y-I, Pringle JR, Gould KL, McCollum D (1998a) Role of polo kinase and Mid1p in determining the site of cell division in fission yeast. *J Cell Biol* **143:** 1603–1616

Bähler J, Wu J, Longtine MS, Shah NG, McKenzie III A, Steever AB, Wach A, Philippsen P, Pringle JR (1998b) Heterologous modules for efficient and versatile PCR-based gene targeting in *Schizosaccharomyces pombe*. *Yeast* **14:** 943–951

Beaudouin J, Gerlich D, Daigle N, Eils R, Ellenberg J (2002) Nuclear envelope breakdown proceeds by microtubule-induced tearing of the lamina. *Cell* **108:** 83–96

Bridge AJ, Morphew M, Bartlett R, Hagan IM (1998) The fission yeast SPB component Cut12 links bipolar spindle formation to mitotic control. *Genes Dev* **12:** 927–942

Cheng J, Turkel N, Hemati N, Fuller MT, Hunt AJ, Yamashita YM (2008) Centrosome misorientation reduces stem cell division during ageing. *Nature* **456:** 599–604

Cowan CR, Hyman AA (2004) Centrosomes direct cell polarity independently of microtubule assembly in *C. elegans* embryos. *Nature* **431:** 92–96

Cullen CF, May KM, Hagan IM, Glover DM, Ohkura H (2000) A new genetic method for isolating functionally Interacting genes: high *plo1*$^+$-dependent mutants and their suppressors define genes in mitotic and septation pathways in fission yeast. *Genetics* **155:** 1521–1534

Cusick ME (1994) RNP1, a new ribonucleoprotein gene of the yeast *Saccharomyces cerevisiae*. *Nucleic Acids Res* **22:** 869–877

D'Angelo MA, Hetzer MW (2008) Structure, dynamics and function of nuclear pore complexes. *Trends Cell Biol* **18:** 456–466

Decottignies A, Zarzov P, Nurse P (2001) *In vivo* localisation of fission yeast cyclin-dependent protein kinase cdc2p and cyclin B during mitosis and meiosis. *J Cell Sci* **114:** 2627–2649

Ding R, West RR, Morphew M, Oakley BR, McIntosh JR (1997) The spindle pole body of *Schizosaccharomyces pombe* enters and leaves the nuclear envelope as the cell cycle proceeds. *Mol Biol Cell* **8:** 1461–1479

Elia AE, Cantley LC, Yaffe MB (2003) Proteomic screen finds pSer/pThr-binding domain localizing Plk1 to mitotic substrates. *Science* **299:** 1228–1231

Flory MR, Morphew M, Joseph JD, Means AR, Davis TN (2002) Pcp1p, an Spc110p-related calmodulin target at the centrosome of the fission yeast *Schizosaccharomyces pombe*. *Cell Growth Differ* **13:** 47–58

Funabiki H, Hagan IM, Uzawa S, Yanagida M (1993) Cell cycle-dependent specific positioning and clustering of centromeres and telomeres in fission yeast. *J Cell Biol* **121:** 961–976

Galy V, Antonin W, Jaedicke A, Sachse M, Santarella R, Haselmann U, Mattaj I (2008) A role for gp210 in mitotic nuclear-envelope breakdown. *J Cell Sci* **121**(Part 3)**:** 317–328

Grallert A, Hagan IM (2002) *Schizosaccharomyces pombe* NIMA-related kinase, Fin1, regulates spindle formation and an affinity of Polo for the SPB. *EMBO J* **21:** 3096–3107

Grallert A, Krapp A, Bagley S, Simanis V, Hagan IM (2004) Recruitment of NIMA kinase shows that maturation of the *S. pombe* spindle-pole body occurs over consecutive cell cycles and reveals a role for NIMA in modulating SIN activity. *Genes Dev* **18:** 1007–1021

Hachet V, Canard C, Gonczy P (2007) Centrosomes promote timely mitotic entry in *C.elegans* embryos. *Dev Cell* **12:** 531–541

Hagan I, Yanagida M (1995) The product of the spindle formation gene *sad1*$^+$ associates with the fission yeast spindle pole body and is essential for viability. *J Cell Biol* **129:** 1033–1047

Hagan IM (2008) The spindle pole body plays a key role in controlling mitotic commitment in the fission yeast *Schizosaccharomyces pombe*. *Biochem Soc Trans* **36**(Part 5)**:** 1097–1101

Hetzer MW, Walther TC, Mattaj IW (2005) Pushing the envelope: structure, function, and dynamics of the nuclear periphery. *Annu Rev Cell Dev Biol* **21:** 347–380

Hudson JD, Feilotter H, Young PG (1990) *stf1*: non-wee mutations epistatic to *cdc25* in the fission yeast *Schizosaccharomyces pombe*. *Genetics* **126:** 309–315

Jackman M, Lindon C, Nigg EA, Pines J (2003) Active cyclin B1–Cdk1 first appears on centrosomes in prophase. *Nat Cell Biol* **5:** 143–148

Kanai M, Kume K, Miyahara K, Sakai K, Nakamura K, Leonhard K, Wiley DJ, Verde F, Toda T, Hirata D (2005) Fission yeast MO25 protein is localized at SPB and septum and is essential for cell morphogenesis. *EMBO J* **24:** 3012–3025

Knop M, Schiebel E (1997) Spc98p and Spc97p of the yeast γ-tubulin complex mediate binding to the spindle pole body via their interaction with Spc110p. *EMBO J* **16:** 6985–6995

Knop M, Schiebel E (1998) Receptors determine the cellular localization of a γ-tubulin complex and thereby the site of microtubule formation. *EMBO J* **17:** 3952–3967

Krapp A, Simanis V (2008) An overview of the fission yeast septation initiation network (SIN). *Biochem Soc Trans* **36**(Part 3)**:** 411–415

MacIver FH, Tanaka K, Robertson AM, Hagan IM (2003) Physical and functional interactions between polo kinase and the spindle pole component Cut12 regulate mitotic commitment in *S. pombe*. *Genes Dev* **17:** 1507–1523

Madrid AS, Mancuso J, Cande WZ, Weis K (2006) The role of the integral membrane nucleoporins Ndc1p and Pom152p in nuclear pore complex assembly and function. *J Cell Biol* **173:** 361–371

Mansfeld J, Guttinger S, Hawryluk-Gara LA, Pante N, Mall M, Galy V, Haselmann U, Muhlhausser P, Wozniak RW, Mattaj IW, Kutay U, Antonin W (2006) The conserved transmembrane nucleoporin NDC1 is required for nuclear pore complex assembly in vertebrate cells. *Mol Cell* **22:** 93–103

Miki F, Kurabayashi A, Tange Y, Okazaki K, Shimanuki M, Niwa O (2004) Two-hybrid search for proteins that interact with Sad1 and Kms1, two membrane-bound components of the spindle pole body in fission yeast. *Mol Genet Genomics* **270:** 449–461

Moreno S, Klar A, Nurse P (1991) Molecular genetic analyses of fission yeast *Schizosaccharomyces pombe*. *Methods Enzymol* **194:** 773–782

Muller EG, Snydsman BE, Novik I, Hailey DW, Gestaut DR, Niemann CA, O'Toole ET, Giddings Jr TH, Sundin BA, Davis TN (2005) The organization of the core proteins of the yeast spindle pole body. *Mol Biol Cell* **16:** 3341–3352

Mulvihill DP, Petersen J, Ohkura H, Glover DM, Hagan IM (1999) Plo1 kinase recruitment to the spindle pole body and its role in cell division in *Schizosaccharomyces pombe*. *Mol Biol Cell* **10:** 2771–2785

Nguyen T, Vinh DBN, Crawford DK, Davis TN (1998) A genetic analysis of interactions with Spc110p reveals distinct functions of Spc97p and Spc98p, components of the yeast γ-tubulin complex. *Mol Biol Cell* **9:** 2201–2216

Nigg EA (2007) Centrosome duplication: of rules and licenses. *Trends Cell Biol* **17:** 215–221

Nurse P (1990) Universal control mechanism regulating onset of M-phase. *Nature (Lond)* **344:** 503–508

Ohkura H, Hagan IM, Glover DM (1995) The conserved *Schizosaccharomyces pombe* kinase plo1, required to form a bipolar spindle, the actin ring, and septum, can drive septum formation in G_1 and G_2. *Genes Dev* **9:** 1059–1073

Petersen J, Hagan IM (2005) Polo kinase links the stress pathway to cell cycle control and tip growth in fission yeast. *Nature* **435:** 507–512

Rajagopalan S, Bimbo A, Balasubramanian MK, Oliferenko S (2004) A potential tension-sensing mechanism that ensures timely anaphase onset upon metaphase spindle orientation. *Curr Biol* **14:** 69–74

Salina D, Bodoor K, Eckley DM, Schroer TA, Rattner JB, Burke B (2002) Cytoplasmic dynein as a facilitator of nuclear envelope breakdown. *Cell* **108:** 97–107

Samejima I, Miller VJ, Groocock LM, Sawin KE (2008) Two distinct regions of Mto1 are required for normal microtubule nucleation and efficient association with the γ-tubulin complex *in vivo*. *J Cell Sci* **121:** 3971–3980

Sato M, Dhut S, Toda T (2005) New drug-resistant cassettes for gene disruption and epitope tagging in *Schizosaccharomyces pombe*. *Yeast* **22:** 583–591

Sato M, Toya M, Toda T (2009) Visualization of fluorescence-tagged proteins in fission yeast and the analysis of mitotic spindle dynamics using GFP–tubulin under the native promoter. In *Methods in Molecular Biology—Mitosis, Methods and Protocols*, McAinsh AD (ed). pp 185–203. Humana Press: Springer, NJ, USA

Sawin KE, Tran PT (2006) Cytoplasmic microtubule organization in fission yeast. *Yeast* **23:** 1001–1014

Snead JL, Sullivan M, Lowery DM, Cohen MS, Zhang C, Randle DH, Taunton J, Yaffe MB, Morgan DO, Shokat KM (2007) A coupled chemical-genetic and bioinformatic approach to Polo-like kinase pathway exploration. *Chem Biol* **14:** 1261–1272

Sohrmann M, Schmidt S, Hagan I, Simanis V (1998) Asymmetric segregation on spindle poles of the *Schizosaccharomyces pombe* septum-inducing protein kinase Cdc7p. *Genes Dev* **12:** 84–94

Stavru F, Hulsmann BB, Spang A, Hartmann E, Cordes VC, Gorlich D (2006) NDC1: a crucial membrane-integral nucleoporin of metazoan nuclear pore complexes. *J Cell Biol* **172:** 509–519

Takaki T, Trenz K, Costanzo V, Petronczki M (2008) Polo-like kinase 1 reaches beyond mitosis—cytokinesis, DNA damage response, and development. *Curr Opin Cell Biol* **20:** 650–660

Tallada VA, Tanaka K, Yanagida M, Hagan IM (2009) The *S. pombe* mitotic regulator Cut12 promotes spindle pole body activation and integration into the nuclear envelope. *J Cell Biol* **185:** 875–888

Tanaka K, Petersen J, MacIver F, Mulvihill DP, Glover DM, Hagan IM (2001) The role of Plo1 kinase in mitotic commitment and septation in *Schizosaccharomyces pombe*. *EMBO J* **20:** 1259–1270

Tran EJ, Wente SR (2006) Dynamic nuclear pore complexes: life on the edge. *Cell* **125:** 1041–1053

Vardy L, Toda T (2000) The fission yeast γ-tubulin complex is required in G_1 phase and is a component of the spindle assembly checkpoint. *EMBO J* **19:** 6098–6111

West RR, Vaisberg EV, Ding R, Nurse P, McIntosh JR (1998) *cut11*$^+$: a gene required for cell cycle-dependent spindle pole body anchoring in the nuclear envelope and bipolar spindle formation in *Schizosaccharomyces pombe*. *Mol Biol Cell* **9:** 2839–2855

Yoder TJ, McElwain MA, Francis SE, Bagley J, Muller EG, Pak B, O'Toole ET, Winey M, Davis TN (2005) Analysis of a spindle pole body mutant reveals a defect in bi-orientation and illuminates spindle forces. *Mol Biol Cell* **16:** 141–152

Zhang J, Megraw TL (2007) Proper recruitment of γ-tubulin and D-TACC/Msps to embryonic *Drosophila* centrosomes requires centrosomin motif 1. *Mol Biol Cell* **10:** 4037–4049

Zimmerman WC, Sillibourne J, Rosa J, Doxsey SJ (2004) Mitosis-specific anchoring of γ-tubulin complexes by pericentrin controls spindle organization and mitotic entry. *Mol Biol Cell* **15:** 3642–3657

Supplementary Information

Fission yeast Pcp1 links polo kinase-mediated mitotic entry to γ-tubulin-dependent spindle formation

Chii Shyang Fong, Masamitsu Sato and Takashi Toda

Supplementary Note 1:

As *pcp1-15* and *pcp1-18* show distinct defects, namely the failure in recruitment of the γ-TuC and Plo1, respectively, to the mitotic SPB, one might expect these two alleles display intragenic complementation. To address this point, we constructed various types of diploid strains that contain heterozygous (*pcp1-15/pcp1-18*) or homozygous *pcp1* alleles (*pcp1-15/pcp1-15, pcp1-15/pcp1*$^{+}$, *pcp1-18/pcp1-18* or *pcp1-18/pcp1*$^{+}$) and examined temperature sensitivity of each diploid. It was found that *pcp1-15* and *pcp1-18* mutations are recessive but no intragenic complementation was observed (Supplementary Figure S7A).

Supplementary Note 2:

Synthetic genetic interactions were examined between a *pcp1-15* or *-18* and various temperature-sensitive mutations in genes that were identified in this study. These include *alp4*, *alp6*, *plo1*, *cut11* and *cut12*. Intriguingly temperature-sensitive *cut11.1* (West et al, 1998) or *cut12.1* mutants (Bridge et al, 1998) are synthetically lethal with either of *pcp1-15* or *pcp1-18* (Supplementary Figure S7B). Furthermore although double mutants between *pcp1-15* or *pcp1-18* and *alp4-1891*, *alp6-719* (Vardy & Toda, 2000) or *plo1.ts19* (MacIver et al, 2003) were viable, their restriction temperatures were all lowered (Supplementary Figure S7C). We posit that these results substantiate our findings on roles of Pcp1 in recruitment of the γ-TuC and Plo1 to the mitotic SPB. As both γ-TuC and Plo1 are essential for cell viability, simultaneous mutants either in the same or different pathways would lead to synthetic lethality.

Supplementary Materials and Methods

Pcp1 antibody generation

Recombinant His_6-Pcp1(1-604aa) was expressed in FB810 *E. coli* host by the addition of 1 mM isopropyl β-D-1-thiogalactopyranoside (IPTG), and purified from the supernatant with HisTrap Kit according to the manufacturer's instruction (GE Healthcare Co.). The purified protein was then used to immunise rabbits.

Fluorescence signal intensity quantification

Images were merged into a single projection using maximum intensity algorithm in Deltavision-SoftWoRx (Olympus and Applied Precision Ltd.). Fluorescence signals were then quantified using maximum intensity, after subtracting background signals.

Supplementary References

Bähler J, Wu J, Longtine MS, Shah NG, McKenzie III A, Steever AB, Wach A, Philippsen P, Pringle JR (1998) Heterologous modules for efficient and versatile PCR-based gene targeting in *Schizosaccharomyces pombe. Yeast* **14:** 943-951

MacIver FH, Tanaka K, Robertson AM, Hagan IM (2003) Physical and functional interactions between polo kinase and the spindle pole component Cut12 regulate mitotic commitment in *S. pombe. Genes Dev* **17:** 1507-1523

Moreno S, Klar A, Nurse P (1991) Molecular genetic analyses of fission yeast *Schizosaccharomyces pombe. Methods Enzymol* **194:** 773-782

Sato M, Dhut S, Toda T (2005) New drug-resistant cassettes for gene disruption and epitope tagging in *Schizosaccharomyces pombe. Yeast* **22**(7)**:** 583-591

West RR, Vaisberg EV, Ding R, Nurse P, McIntosh JR (1998) *cut11*$^{+}$: a gene required for cell cycle-dependent spindle pole body anchoring in the nuclear envelope and bipolar spindle formation in *Schizosaccharomyces pombe. Mol Biol Cell* **9:** 2839-2855

Supplementary Table S1: Fission yeast strains used in this study

Strains	Genotypes	Figures used
513	*h- leu1 ura4*	1A, S2C
MS1030	*h- pcp1^{+}-HA-hph^{r} leu1 ura4*	S2A, S2C, 1C, 5B, 6F, 7A, S7C
CSF0076	*h- pcp1-15-HA-hph^{r} leu1 ura4*	1A-C, S1A, S1B, S2A, 5C, 6F, 7A, S7C
CSF0082	*h- pcp1-18-HA-hph^{r} leu1 ura4*	1A-C, S1A, S1B, S2A, 5C, 6F, 7A, S7C
CSF0148	*h- pcp1^{+}-HA-hph^{r} cut12^{+}-GFP-ura4^{+} leu1 ura4*	S2B
CSF0150	*h- pcp1-15-HA-hph^{r} cut12^{+}-GFP-ura4^{+} leu1 ura4*	S2B
CSF0405	*h- pcp1-18-HA-hph^{r} cut12^{+}-GFP-ura4^{+} leu1 ura4*	S2B
CSF0363	*h- pcp1^{+}-HA-hph^{r} sid4^{+}-mRFP-nat^{r} aur^{r}-pnda3-GFP-atb2^{+} leu1 ura4*	1D, 3B
CSF0364	*h- pcp1-15-HA-hph^{r} sid4^{+}-mRFP-nat^{r} aur^{r}-pnda3-GFP-atb2 leu1 ura4*	1D, 2B
CSF0365	*h- pcp1-18-HA-hph^{r} sid4^{+}-mRFP-nat^{r} aur^{r}-pnda3-GFP-atb2^{+} leu1 ura4*	1D, 2B
CSF0511	*h- pcp1^{+}-HA-hph^{r} cdc7^{+}-GFP-kan^{r} sfi1^{+}-mRFP-nat^{r} aur^{r}-pnda3-mCh-atb2^{+} leu1 ura4 ade6-M210*	2A
CSF0513	*h- pcp1-15-HA-hph^{r} cdc7^{+}-GFP-kan^{r} sfi1^{+}-mRFP-nat^{r} aur^{r}-pnda3-mCh-atb2^{+} leu1 ura4*	2A
CSF0515	*h- pcp1-18-HA-hph^{r} cdc7^{+}-GFP-kan^{r} sfi1^{+}-mRFP-nat^{r} aur^{r}-pnda3-mCh-atb2^{+} leu1 ura4*	2A
CSF0395	*h- pcp1^{+}-HA-hph^{r} alp4^{+}-GFP-kan^{r} sfi1-mRFP-nat^{r} leu1 ura4*	3A, 3B, 4B
CSF0397	*h- pcp1-15-HA-hph^{r} alp4^{+}-GFP-kan^{r} sfi1^{+}-mRFP-nat^{r} leu1 ura4*	3A, 3B, 4B
CSF0399	*h- pcp1-18-HA-hph^{r} alp4^{+}-GFP-kan^{r} sfi1^{+}-mRFP-nat^{r} leu1 ura4*	3A, 3B

CSF0346	*h- pcp1^{+}-HA-hph^{r} alp6^{+}-GFP-kan^{r} leu1 ura4*	S3
CSF0348	*h- pcp1-15-HA-hph^{r} alp6^{+}-GFP-kan^{r} leu1 ura4*	S3
CSF0350	*h- pcp1-18-HA-hph^{r} alp6^{+}-GFP-kan^{r} leu1 ura4*	S3
CSF0466	*h- pcp1^{+}-HA-hph^{r} alp6^{+}-GFP-kan^{r} leu1 ura4 +pREP1*	3C, 3D
CSF0468	*h- pcp1^{+}-HA-hph^{r} alp6^{+}-GFP-kan^{r} leu1 ura4 +pREP1-alp4^{+}*	3C, 3D
CSF0470	*h- pcp1-15-HA-hph^{r} alp6^{+}-GFP-kan^{r} leu1 ura4 +pREP1*	3C, 3D
CSF0472	*h- pcp1-15-HA-hph^{r} alp6^{+}-GFP-kan^{r} leu1 ura4 +pREP1-alp4^{+}*	3C, 3D
CSF0338	*h- pcp1^{+}-HA-hph^{r} leu1 ura4 +pREP1*	3E
CSF0339	*h- pcp1^{+}-HA-hph^{r} leu1 ura4 +pREP1-alp4^{+}*	3E
CSF0340	*h- pcp1-15-HA-hph^{r} leu1 ura4 +pREP1*	3E
CSF0341	*h- pcp1-15-HA-hph^{r} leu1 ura4 +pREP1-alp4^{+}*	3E
CSF0342	*h- pcp1-18-HA-hph^{r} leu1 ura4 +pREP1*	3E
CSF0343	*h- pcp1-18-HA-hph^{r} leu1 ura4 +pREP1-alp4^{+}*	3E
CSF0257	*h- pcp1-15-HA-hph^{r} leu1 ura4 +pSK-pcp1^{+}*	5A, 6B
CSF0276	*h- pcp1-15-HA-hph^{r} leu1 ura4 +pSK*	5A, 6B
CSF0555	*h- pcp1-15-HA-hph^{r} leu1 ura4 +pSK-cut11^{+}*	5A
CSF0556	*h- pcp1-15-HA-hph^{r} leu1 ura4 +pSK-pom152^{+}*	5A
CSF0269	*h- pcp1-18-HA-hph^{r} leu1 ura4 +pSK-pcp1^{+}*	5A, 6B
CSF0282	*h- pcp1-18-HA-hph^{r} leu1 ura4 +pSK*	5A, 6B
CSF0284	*h- pcp1-18-HA-hph^{r} leu1 ura4 +pSK-cut11^{+}*	5A
CSF0285	*h- pcp1-18-HA-hph^{r} leu1 ura4 +pSK-pom152^{+}*	5A
CSF0490	*h- pom152^{+}-GFP-kan^{r} cut11^{+}-4mRFP-nat^{r} leu1 ura4*	S4
CSF0474	*h- pcp1^{+}-HA-hph^{r} aur^{r}-pnda3-mCh-atb2^{+} cut11^{+}-GFP-ura4^{+} leu1 ura4*	6A
CSF0476	*h- pcp1-15-HA-hph^{r} aur^{r}-pnda3-mCh-atb2^{+} cut11^{+}-GFP-ura4^{+} leu1 ura4*	6A
CSF0478	*h- pcp1-18-HA-hph^{r} aur^{r}-pnda3-mCh-atb2^{+} cut11^{+}-GFP-ura4^{+} leu1 ura4*	6A
CSF0277	*h- pcp1-15-HA-hph^{r} leu1 ura4 +pSK-cut12^{+}*	6B
CSF0283	*h- pcp1-18-HA-hph^{r} leu1 ura4 +pSK-cut12^{+}*	6B

CSF0448	*h- pcp1^{+}-HA-hph^{r} cut12^{+}-GFP-ura4^{+} sid4^{+}-mRFP-nat^{r} leu1 ura4*	6C
CSF0450	*h- pcp1-15-HA-hph^{r} cut12^{+}-GFP-ura4^{+} sid4^{+}-mRFP-nat^{r} leu1 ura4*	6C
CSF0452	*h- pcp1-18-HA-hph^{r} cut12^{+}-GFP-ura4^{+} sid4^{+}-mRFP-nat^{r} leu1 ura4*	6C
CSF0517	*h? pcp1^{+}-HA-hph^{r} plo1^{+}-GFP-HA-kan^{r} sfi1^{+}-mRFP-nat^{r} aur^{r}-pnda3-mCh-atb2^{+} leu1 ura4*	6D, 6E
CSF0519	*h? pcp1-15-HA-hph^{r} plo1^{+}-GFP-HA-kan^{r} sfi1^{+}-mRFP-nat^{r} aur^{r}-pnda3-mCh-atb2^{+} leu1 ura4*	6D, 6E, S5
CSF0521	*h? pcp1-18-HA-hph^{r} plo1^{+}-GFP-HA-kan^{r} sfi1^{+}-mRFP-nat^{r} aur^{r}-pnda3-mCh-atb2^{+} leu1 ura4*	6D, 6E, S5
CSF0523	*h- pcp1^{+}-HA-hph^{r} cut12.s11 leu1 ura4*	6F
CSF0525	*h- pcp1-15-HA-hph^{r} cut12.s11 leu1 ura4*	6F
CSF0527	*h- pcp1-18-HA-hph^{r} cut12.s11 leu1 ura4*	6F
CSF0200	*h- pcp1^{+}-HA-hph^{r} plo1^{+}-GFP-HA-kan^{r} leu1 ura4*	S5, 6G, 6H, 7B
CSF0585	*h- pcp1^{+}-HA-hph^{r} plo1^{+}-GFP-HA-kan^{r} cut12,s11 leu1 ura4*	6G, 6H
CSF0208	*h- pcp1-18-HA-hph^{r} plo1^{+}-GFP-HA-kan^{r} leu1 ura4*	S5, 6G, 6H, 7B
CSF0586	*h- pcp1-18-HA-hph^{r} plo1^{+}-GFP-HA-kan^{r} cut12.s11 leu1 ura4*	6G, 6H
CSF0587	*h- pcp1^{+}-HA-hph^{r} plo1^{+}-GFP-HA-kan^{r} leu1 ura4 +pSK*	S6A, S6B
CSF0588	*h- pcp1^{+}-HA-hph^{r} plo1^{+}-GFP-HA-kan^{r} leu1 ura4 +pSK-cut11^{+}*	S6A, S6B
CSF0589	*h- pcp1-18-HA-hph^{r} plo1^{+}-GFP-HA-kan^{r} leu1 ura4 +pSK*	S6A, S6B
CSF0590	*h- pcp1-18-HA-hph^{r} plo1^{+}-GFP-HA-kan^{r} leu1 ura4 +pSK-cut11^{+}*	S6A, S6B
CSF0549	*h- pcp1^{+}-HA-hph^{r} wee1-50 leu1*	7A
CSF0551	*h- pcp1-15-HA-hph^{r} wee1-50 leu1*	7A
CSF0553	*h- pcp1-18-HA-hph^{r} wee1-50 leu1*	7A
CSF0204	*h- pcp1-15-HA-hph^{r} plo1^{+}-GFP-HA-kan^{r} leu1 ura4*	7B
CSF0579	*h-/h+ leu1/leu1 ura4/ura4 ade6-210/ade6-216*	S7A

	his2/his2^{+}	
CSF0580	*h-/h+ pcp1-15-HA-hph*^{r}*/pcp1*$^{+}$ *leu1/leu1 ura4/ura4 ade6-210/ade6-216 his7/his7*$^{+}$	S7A
CSF0581	*h-/h+ pcp1-18-HA-hph*^{r}*/pcp1*$^{+}$ *leu1/leu1 ura4/ura4 ade6-210/ade6-216 his7/his7*$^{+}$	S7A
CSF0582	*h-/h+ pcp1-15-HA-hph*^{r}*/pcp1-15-HA-hph*^{r} *leu1/leu1 ura4/ura4 ade6-210/ade6-216 his2/his2*$^{+}$	S7A
CSF0583	*h-/h+ pcp1-18-HA-hph*^{r}*/pcp1-18-HA-hph*^{r} *leu1/leu1 ura4/ura4 ade6-210/ade6-216 his2/his2*$^{+}$	S7A
CSF0584	*h-/h+ pcp1-15-HA-hph*^{r}*/pcp1-18-HA-hph*^{r} *leu1/leu1 ura4/ura4 ade6-210/ade6-216 his7/his7*$^{+}$	S7A
alp4-1891	*h+ alp4-1891 leu1 ura4 his2*	S7C
CSF0557	*h- pcp1-15-HA-hph*^{r} *alp4-1891 leu1 ura4*	S7B, S7C
CSF0558	*h+ pcp1-18-HA-hph*^{r} *alp4-1891 leu1 ura4 his2*	S7B, S7C
alp6-719	*h+ alp6-719 leu1 ura4 his2*	S7C
CSF0559	*h- pcp1-15-HA-hph*^{r} *alp6-719 leu1 ura4*	S7B, S7C
CSF0560	*h- pcp1-18-HA-hph*^{r} *alp6-719 leu1 ura4*	S7B, S7C
IH1636	*h- plo1.ts19-ura4*$^{+}$ *leu1 ura4 ade6-210*	S7C
CSF0563	*h- pcp1-15-HA-hph*^{r} *plo1.ts19-ura4*$^{+}$ *leu1 ura4*	S7B, S7C
CSF0564	*h+ pcp1-18-HA-hph*^{r} *plo1.ts19-ura4*$^{+}$ *leu1 ura4 his2*	S7B, S7C

All strains are created in this study, except for 513, MS1030, alp4-1891 and alp6-719 (our stock), and IH1636 (obtained from Dr. Iain Hagan).

Supplementary Figures

Figure S1: Fong *et al.*

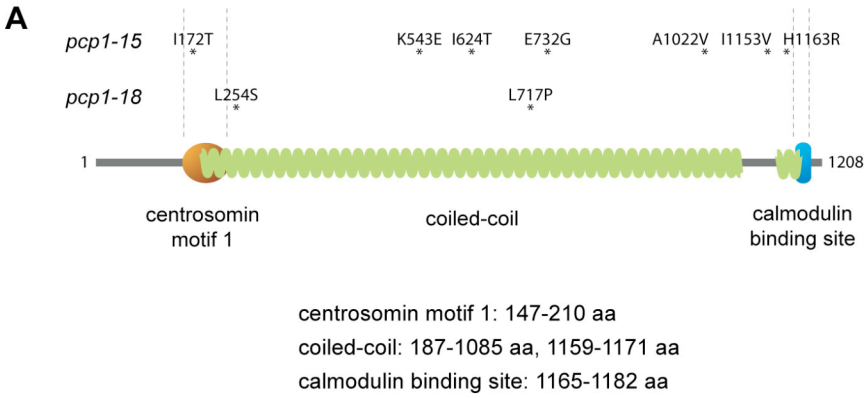

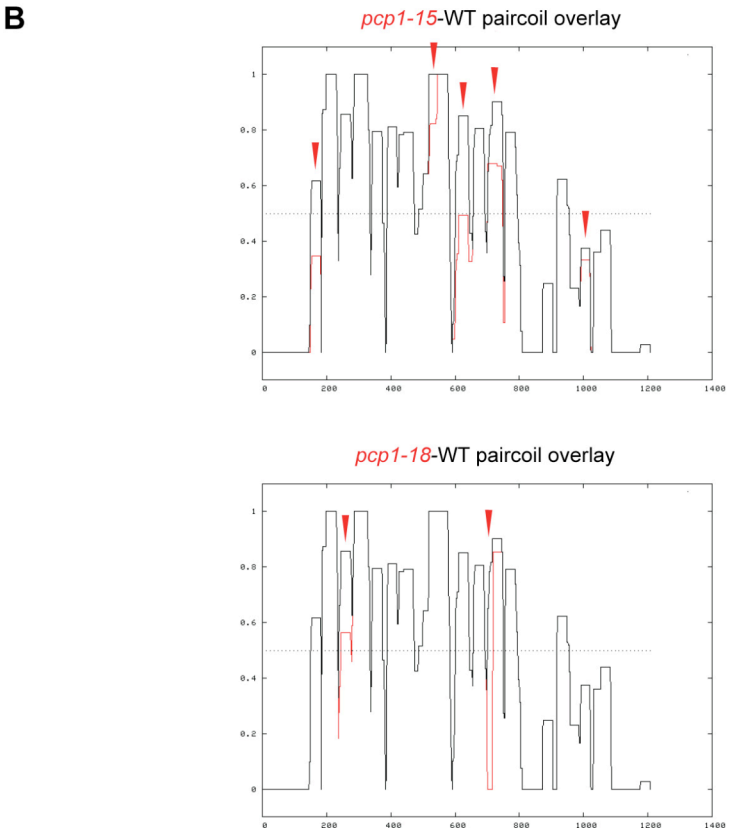

Figure S1: Mutation sites in the *pcp1* mutants

(A) Seven mutations were detected in *pcp1-15*, while two were found in *pcp1-18*. The majority of the mutations (five out of nine) affect either leucine or isoleucine, which are important amino acid (aa) residues for coiled-coil function. Notably, *pcp1-15* also carries a mutation in centrosomin motif 1. Centrosomin motif 1 (147-210 aa), Coiled-coil (187-1085 aa, 1159-1171 aa) and calmodulin binding site (1165-1182 aa) are shown in orange (oval), green (wavy box) and blue (rectangular box) respectively.

(B) Coiled-coil scores are shown in wild type Pcp1 (black) and Pcp1-15 (left, red) or Pcp1-18 (right, red). Positions of amino acid replacements in *pcp1* mutants (see A) are shown with arrowheads.

Figure S2: Fong *et al.*

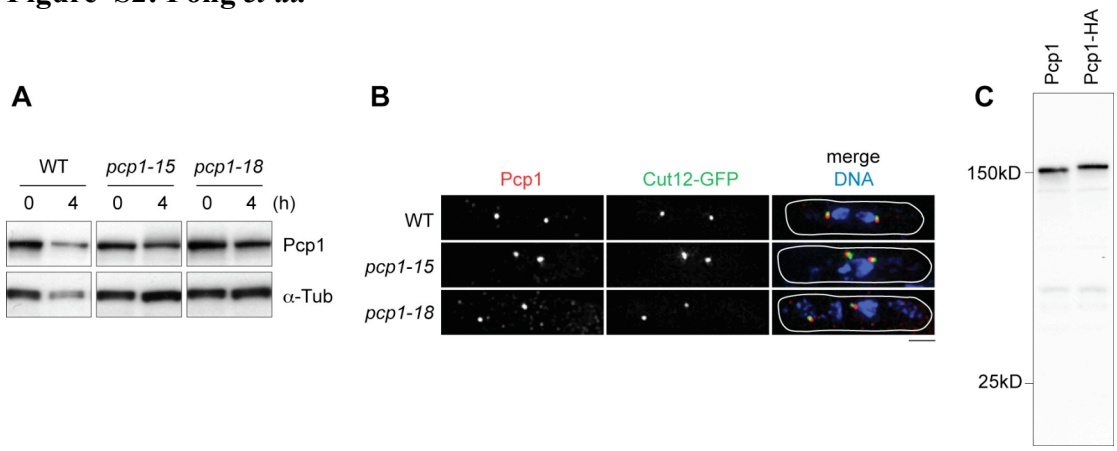

Figure S2: Pcp1 protein levels and SPB localisation are unaffected

(A) Immunoblotting analyses of Pcp1 levels. Strains contain Pcp1-HA, and anti-HA antibody was used for immunoblotting. Tubulin (anti-α-tubulin antibody) acts as a loading control.

(B) Immunofluorescence images showing localisation of Pcp1 after 4 h incubation at 36°C. Anti-Pcp1 antibody (see Supplementary Materials and Methods) was used. Cut12-GFP is a marker of the SPB. $n > 100$. Scale bar, 2 μm.

(C) Immunoblotting of Pcp1 with anti-Pcp1. Antibody was affinity-purified from serum with Pcp1 antigen, and used at 1:5000 dilution. Note that due to HA-tagging (3 copies), The size of Pcp1-HA is increased.

Figure S3: Fong *et al.*

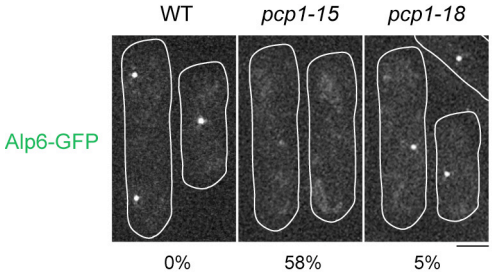

Figure S3: γ-TuC component Alp6 delocalises from the SPB in *pcp-15*, but not *pcp1-18*

Fluorescence images of fixed cells showing Alp6-GFP localisation after 2 h incubation at 36°C. $n > 100$. The percentage indicates the proportion of cells displaying Alp6-GFP delocalisation from the SPB. Scale bar, 2 μm.

Figure S4: Fong *et al.*

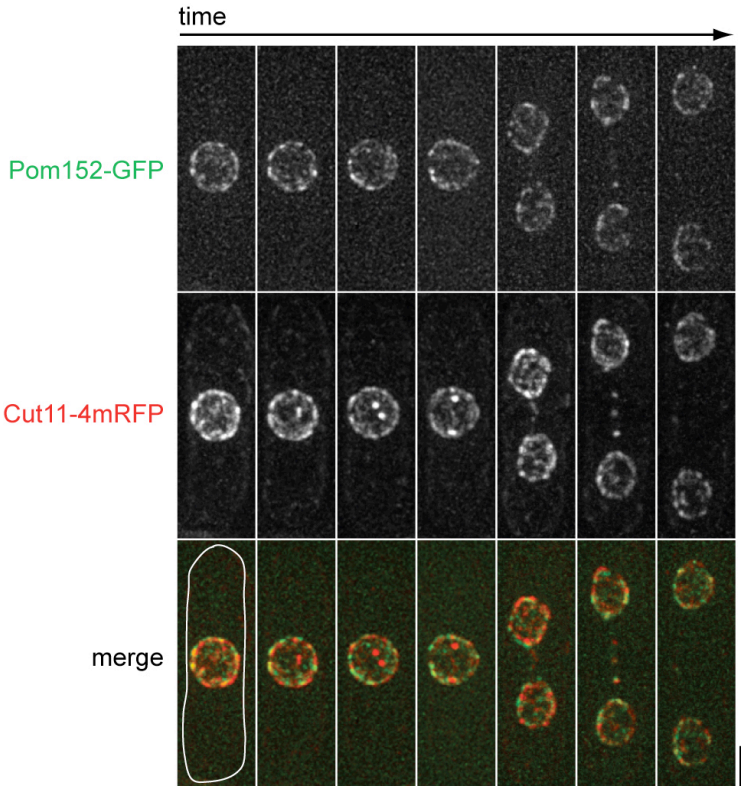

Figure S4: Pom152 does not exhibit SPB-specific localisation in mitosis
Live analysis of Pom152-GFP localisation, observed concurrently with another nuclear pore complex component Cut11-4mRFP. Pom152 is C-terminally tagged with GFP at the endogenous locus, and expressed under the endogenous promoter. In contrast to Cut11-4mRFP that localises to both the SPB in early mitosis and the NE throughout the cell cycle, Pom152-GFP only localises to the NE discontinuously. n = 15. Scale bar, 2 μm.

Figure S5: Fong *et al.*

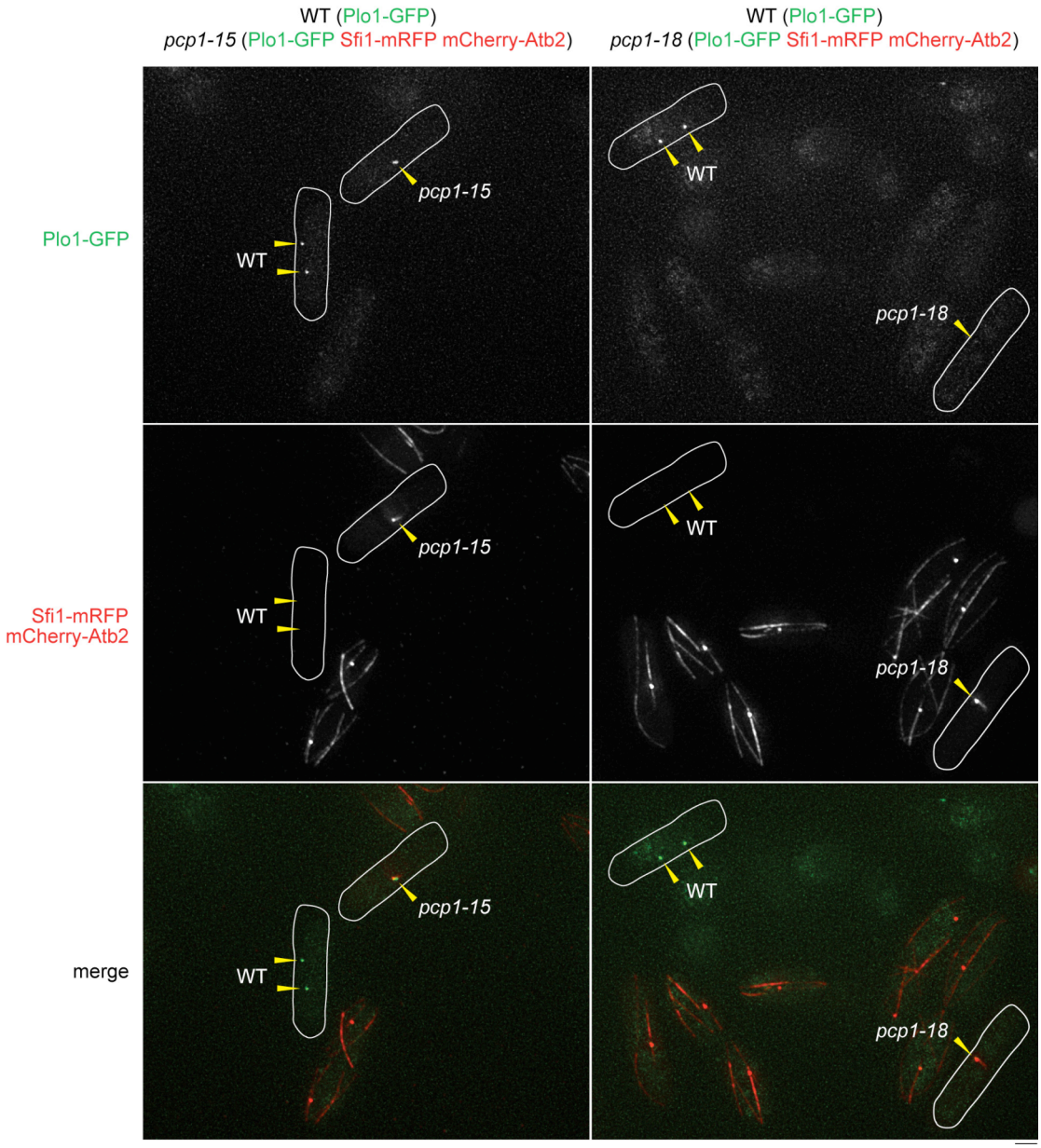

Figure S5: Plo1-GFP delocalises from the mitotic SPB specifically in *pcp1-18*.
Cells of wild type (carrying Pcp1-GFP) and *pcp1-15* (left, carrying Plo1-GFP, Sfi1-mRFP and mCherry-Atb2) or *pcp1-18* (right, carrying Plo1-GFP, Sfi1-mRFP and mCherry-Atb2) were mixed in the same culture, shifted from 27°C to 36°C and incubated for 4 h. Live images of these mixed cell populations were shown. Note that Plo1-GFP signals disappeared from SPBs only in the *pcp1-18* cells (arrowheads). $n > 25$. Scale bar, 2 μm.

Figure S6: Fong *et al.*

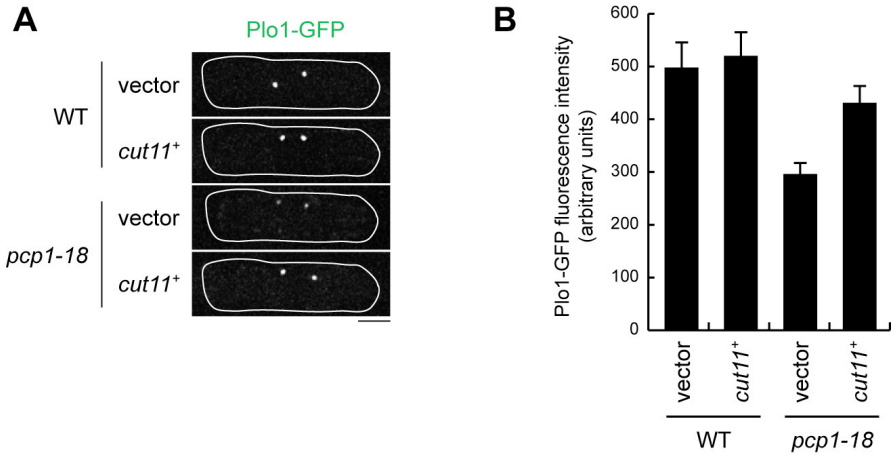

Figure S6: Plo1-GFP localisation to the SPB is restored in *pcp1-18* by introducing multicopy suppressor *cut11*$^{+}$.

(A) Plo1-GFP localisation to the SPB with or without the multicopy suppressor *cut11*$^{+}$ when incubated at 34^{o}C. Scale bar, 2 μm.

(B) Quantification of Plo1-GFP signal intensity at the SPB in A. n > 50; error bars represent standard error.

Figure S7: Fong *et al.*

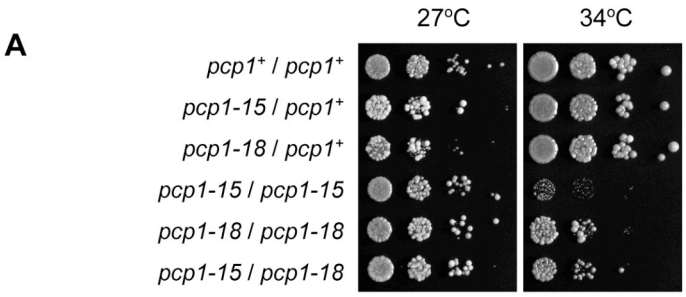

B

	synthetic lethal				
	cut11-1	*cut12.1*	*alp4-1891*	*alp6-719*	*plo1.ts19*
pcp1-15	yes	yes	*	*	*
pcp1-18	yes	yes	*	*	*

* restrictive temperature lowered (see caption)

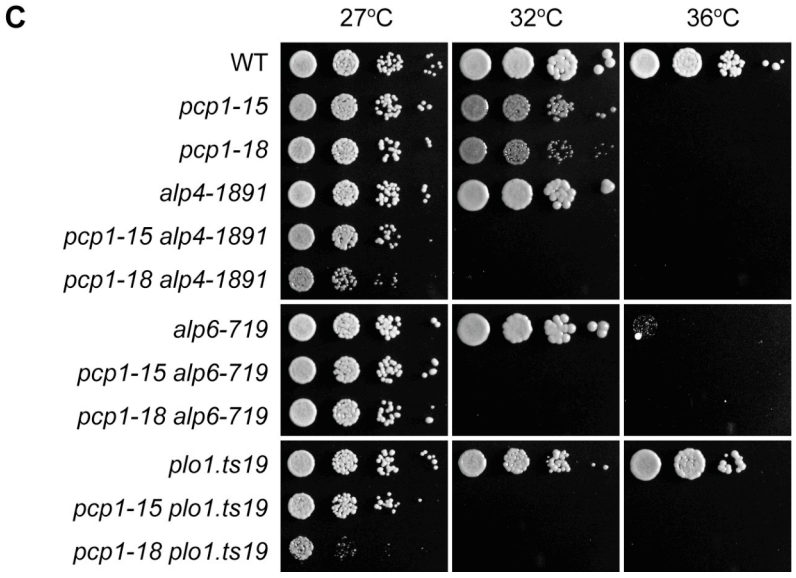

Figure S7: Synthetic genetic interactions between the *pcp1* mutants and the mutants in genes that functionally and/or physically interact with Pcp1

(A) *pcp1-15* and *pcp1-18* do not show intragenic complementation. Temperature-sensitivity of diploid containing indicated genotypes were examined. Haploid strains were also spotted as controls. Note that both *pcp1-15* and *pcp1-18 are recessive, as pcp1-15/pcp1*$^{+}$ and *pcp1-18/pcp1*$^{+}$ heterozygous diploid strains could grow at the restrictive temperature.

(B, C) Genetic interaction between *pcp1* mutants and individual mutants. *cut11.1* or *cut12.1* shows synthetic lethal interaction with both *pcp1-15* and *pcp1-18* (top). In contrast, double mutants between *alp4-1891*, *alp6-719* or *plo1.ts19* and *pcp1-15* or *-18* are viable, but their restriction temperature was lowered substantially (C). Ten-fold serial dilution assays on rich YE5S media.

Supplementary Movies

Movies S1, S2 and S3:

Mitotic progression of wild type (Movie S1, corresponding to 1D, top 3 rows), *pcp1-15* (Movie S2, corresponding to Figure 1D, middle 3 rows) and *pcp1-18* (Movie S3, bottom 3 rows). Tubulin (GFP-Atb2 in green) and SPB (Sid4-mRFP in red) are shown.